EFFECTS OF PRIOR AGING AT 274 °C IN ARGON ON THE INELASTIC DEFORMATION BEHAVIOR OF PMR-15 POLYMER AT 288 °C: EXPERIMENT AND MODELING

THESIS

Joseph A. Wahlquist, Captain, USAF
AFIT/GAE/ENY/10-D03

DEPARTMENT OF THE AIR FORCE
AIR UNIVERSITY

AIR FORCE INSTITUTE OF TECHNOLOGY

Wright-Patterson Air Force Base, Ohio

Report Documentation Page

Form Approved
OMB No. 0704-0188

1. REPORT DATE	2. REPORT TYPE	3. DATES COVERED
01 DEC 2010		**00-00-2009 to 00-00-2010**

4. TITLE AND SUBTITLE	5a. CONTRACT NUMBER
Effectsof Prior Aging at 274 ?C in Argon on Inelastic Deformation Behavior of PMR-15 Polymer at 288 ?C: Experiment and Modeling	5b. GRANT NUMBER
	5c. PROGRAM ELEMENT NUMBER
6. AUTHOR(S)	5d. PROJECT NUMBER
	5e. TASK NUMBER
	5f. WORK UNIT NUMBER
7. PERFORMING ORGANIZATION NAME(S) AND ADDRESS(ES) **Air Force Institute of Technology,2950 Hobson Way,WPAFB,OH,45433-7765**	8. PERFORMING ORGANIZATION REPORT NUMBER
9. SPONSORING/MONITORING AGENCY NAME(S) AND ADDRESS(ES)	10. SPONSOR/MONITOR'S ACRONYM(S)
	11. SPONSOR/MONITOR'S REPORT NUMBER(S)

12. DISTRIBUTION/AVAILABILITY STATEMENT
Approved for public release; distribution unlimited

13. SUPPLEMENTARY NOTES

14. ABSTRACT
This research investigates the effects of prior aging at 274 ?C on deformation behavior of PMR-15 neat resin at 288 ?C. The experimental part of this effort explored the influence of strain rate on mechanical behavior. Monotonic loading, loading followed by unloading at various constant strain rate magnitudes, recovery of strain at zero stress creep, relaxation, and strain rate jump tests were used to explore the rate-dependent inelastic behavior and to elucidate the effect of prior isothermal aging.

15. SUBJECT TERMS

16. SECURITY CLASSIFICATION OF:			17. LIMITATION OF ABSTRACT	18. NUMBER OF PAGES	19a. NAME OF RESPONSIBLE PERSON
a. REPORT **unclassified**	b. ABSTRACT **unclassified**	c. THIS PAGE **unclassified**	**Same as Report (SAR)**	**189**	

AFIT/GAE/ENY/10-D03

EFFECTS OF PRIOR AGING AT 274 °C IN ARGON ON THE INELASTIC DEFORMATION BEHAVIOR OF PMR-15 POLYMER AT 288 °C: EXPERIMENT AND MODELING

THESIS

Presented to the Faculty

Department of Aeronautics and Astronautics

Graduate School of Engineering and Management

Air Force Institute of Technology

Air University

Air Education and Training Command

In Partial Fulfillment of the Requirements for the

Degree of Master of Science in Aeronautical Engineering

Joseph A. Wahlquist, BS

Captain, USAF

December 2010

AFIT/GAE/ENY/10-D03

EFFECTS OF PRIOR AGING AT 274 °C IN ARGON ON THE INELASTIC DEFORMATION BEHAVIOR OF PMR-15 POLYMER AT 288 °C: EXPERIMENT AND MODELING

Joseph A. Wahlquist, BS
Captain, USAF

Approved:

_____//signed//_____ _____
Dr. Marina B. Ruggles-Wrenn (Chairman) date

_____//signed//_____ _____
Dr. Thomas G. Eason (Member) date

_____//signed//_____ _____
Dr. Greg A. Schoeppner (Member) date

Abstract

This research investigates the effects of prior aging at 274 °C on deformation behavior of PMR-15 neat resin at 288 °C. The experimental part of this effort explored the influence of strain rate on mechanical behavior. Monotonic loading, loading followed by unloading at various constant strain rate magnitudes, recovery of strain at zero stress, creep, relaxation, and strain rate jump tests were used to explore the rate-dependent inelastic behavior and to elucidate the effect of prior isothermal aging.

The results of these tests suggest that the deformation behavior of the PMR-15 polymer can be represented by a unified constitutive model where the inelastic strain rate depends on overstress. Experimental data was modeled using the Viscoplasticity Theory Based on Overstress for Polymers (VBOP). The VBOP was characterized using strain-controlled experiments and validated by comparing the model predictions with experimental results obtained in tests that differ in kind from those used for model characterization. To account for the effects of prior aging several VBOP model parameters were expanded into functions of prior aging duration. The model predictions were also compared with the experimental results obtained for the PMR-15 polymer subjected to 2000 h of prior aging in both strain-controlled tension to failure tests and stress-controlled creep tests. The deformation behavior of the material subjected to prior aging at 274°C was well represented by the VBOP.

Changes in material behavior due to prior aging at 274 °C were compared to changes in material behavior due to prior aging at 288 °C. The functional forms of the VBOP model parameters developed to account for the effects of prior aging at 274°C on the deformation behavior of PMR-15 at 288 °C were compared with the functional forms previously developed to account for the effects of aging at 288 °C. These results were used to qualitatively assess the effects of prior aging temperature on deformation behavior of the PMR-15 polymer.

Acknowledgements

It is a pleasure to thank my faculty advisor Dr. marina Ruggles-Wrenn. Without her mentoring, support, and hours spent in explanation and encouragement this thesis would not have been possible. The efforts of Dr. Eason and Dr. Schoeppner in making this effort possible merit my sincerest gratitude. I would also like to thank John Hixenbaugh and Barry Page for their assistance in preparation and conducting this research. Finally I would like to give my most heartfelt thanks to my wife for her listening ear and continuing support and my children for their inspiration.

Joseph A. Wahlquist

Table of Contents

Page

List of Figures

Page

List of Tables

Page

List of Symbols

Symbol	Definition
Γ	overstress
ϵ	strain
ϵ^{el}	elastic strain rate
$\dot{\epsilon}^{in}$	inelastic strain rate
η	viscosity constant
σ	stress
Ψ	shape function
A	isotropic stress
A_f	saturated value of isotropic stress
C_1, C_2, C_3, C_4	shape function parameters
C_1^*	variation of shape function parameter
E	modulus of elasticity
E_t	tangent modulus
f	kinematic stress
g	equilibrium stress
h	hours
k	viscosity function
k_1, k_2, k_3	viscosity function parameters
T_g	glass transition temperature
t	time
t_a	aging time
s	seconds

Superscript dot means time derivative (i.e. $\dot{\varepsilon} = \frac{d\varepsilon}{dt}$ = strain rate)

1. Introduction

Motivation

Since the invention of the airplane the aeronautical industry has sought materials which would be able to provide required strength while minimizing weight thus increasing performance and decrease operating costs. This quest has driven the industry to adopt engineered composite materials in both moderate and high temperature applications. Composites have increasingly become the materials of choice with both military and commercial designers incorporating more and more composites into their airframes. However, the transition to composites has not been instantaneous. Classical hesitancies about the use of composite materials have to do with their manufacturing cost and durability. To increase the use of composites in aircraft and thus realize the potential weight savings we must better understand their mechanical behavior particularly regarding long term durability and performance at elevated temperature.

Composites consist of at least two constituent materials which possess significantly different physical properties. To best understand composite behavior it is necessary to investigate the independent behavior of these constituent parts. A particularly useful category of composite materials is the polymer matrix composite. At elevated temperature many polymer matrix materials are capable of significant inelastic deformation which is not well represented by the elastic/linear viscoelastic models typically used in design today [12]. This shortfall leads to the use of excessive safety margins or the exclusion of polymer matrix composites from some of the most advantageous applications.

For applications at elevated temperature polymerization of monomeric reactants-15 (PMR-15) has become one of the most frequently used matrix materials [1]. PMR-15 has been extensively studied "in an effort to qualify the material for use in extreme conditions" [1]. Recent efforts at the Air Force Institute of Technology (AFIT) have focused on the effects of test temperature and high temperature aging on the mechanical behavior of PMR-15 [5, 10, 26, 28, 29]. It has been found that Viscoplasticity Based on Overstress for Polymers (VBOP) is capable of modeling many of the behaviors of PMR-15 at elevated temperature [5, 10, 25]. VBOP has been extended to incorporate prior aging [27] but up to this point aging temperature and test temperature have been varied jointly [5, 10, 25]. This effort will provide preliminary data necessary to begin separating the variables of aging temperature and aging duration.

Problem Statement

Polymer matrix composites are used extensively in the aerospace industry. A thorough understanding of the mechanical behavior of matrix is necessary to correctly design parts and generate accurate life predictions. Many of these applications require operation under conditions at which aging duration and operating temperature become important. It is vital for the material models used in durability analysis to accurately predict the material behavior under these conditions. In order to correctly construct and characterize a material model, experimentation must be performed at elevated temperature and under representative aging conditions.

Thesis Objective

This effort investigates the mechanical behavior at 288 °C of PMR-15 neat resin aged at 274 °C in an argon. Strain-controlled tests at 288 °C will be used to characterize VBOP for

PMR-15 aged at 274 °C. Model parameters thus determined will be validated by comparing results of numerical simulations with the experimental data. Model parameters obtained for material subjected to prior aging for 50 to 1000 hours will be used to predict behavior of specimens aged for 2000 hours. Experimental results as well as the results of modeling with the VBOP produced in this effort will be compared with the results of previous research performed on PMR-15 aged at 288 °C in order to provide a preliminary assessment of the effects of aging temperature on deformation behavior.

Methodology

The research objectives outlined above were accomplished as follows:

1. Assess specimen-to-specimen variability through room temperature modulus testing.
2. Age material samples for various durations at 274 °C in argon.
3. Assess effects of strain rate and of aging duration on stress-strain response through monotonic tensile tests.
4. Assess unloading behavior through loading and unloading tests performed at constant strain rates for specimens subjected to prior aging for various durations between 50 and 2000 hours.
5. Assess recovery of strain at zero stress preceded by loading and unloading at several constant strain rates for specimens subjected to prior aging of various durations.
6. Assess relaxation response through monotonic tests with a period of relaxation conducted at several constant strain rates on specimens subjected to prior aging of varying durations.

7. Perform creep tests preceded by strain-controlled loading to creep stress level on specimens subjected to prior aging of varying durations to determine at the effect of prior strain rate and of prior aging time on creep response.
8. Assess presence or absence of strain rate history effect through strain rate jump test performed on specimens subjected to prior aging of varying durations.
9. Determine VBOP model parameters from experimental data obtained in monotonic tensile tests and in relaxation tests on specimens subjected to prior aging for durations varying between 50 and 1000 hours.
10. Validate the determined VBOP model parameters by comparing numerical simulations and model predictions of various strain-controlled and stress-controlled loading histories with experimental results.
11. Determine and validate the VBOP model parameters for specimens subjected to prior aging for 2000 h.
12. Compare results obtained for specimen aged at 274 °C to those obtained for specimens aged at 288 °C.

2. Background

Polymer Matrix Composites

As previously discussed a composite consists of at least two materials with significantly different material properties. Typical composites have reinforcement and matrix phases. Common reinforcement materials for aerospace components include glass, carbon, aramid, or boron fibers. These materials are typically stiffer and have greater tensile strength than the matrix materials. The matrix phase serves to bind reinforcement fibers together and is responsible for material strength in the direction normal to the fibers, as well as for transmitting shear loads to the fibers and for providing additional strength in the direction of the fibers. The most common matrix phases are polymer, metal, ceramic, and carbon. Because of their low cost and relatively high strength to weight ratio polymer matrix materials are frequently used in aerospace structures. A polymer is a general term for any "macromolecule that contains many smaller groups of atoms, called monomeric units, which are covalently bonded" [30]. Polymers can further be sub-divided into three categories: elastomers, thermoplastics, and thermosets [9].

Thermosets are "polymeric materials that in their final state cannot be fused, are insoluble, and degrade before melting" [16]. Unlike elastomers and thermoplastics, thermosets retain significant strength close to their melting temperatures. Thermosets may in turn be divided into three categories: polyesters, epoxies, and polyimides. Polyimides are the only class of thermoset polymers capable of operation at high temperatures up to 370 °C [9]. PMR-15 is one of the most frequently used high-temperature thermoset polyimides today.

While thermoset polyimides are capable of operating at elevated temperature it has been found that their material properties are generally temperature dependent. For example, PMR-15

exhibits nearly glassy behavior at low to moderate temperature (25 °C to 230°C) and large inelastic deformations at higher temperatures (260 °C to 316°C) [10, 25, 29]. The property changes experienced by matrix materials at elevated temperature must be considered in the design process to make efficient and safe use of polymer matrix composites.

Polymer Aging

Over time polymers experience changes in material properties due to multiple causes. Many polymers experience degradation of bonds due to exposure to chemically reactive environments [5], material deformation [19], and thermal degradation [19, 23]. Because degradation or "aging" occurs due to multiple factors it is important to define these terms. For the present work the following definitions will be used:

- Strain aging: mechanical property or material behavior changes caused by deformation [23]
- Prior thermal aging: mechanical property/behavior changes induced by exposure to elevated temperature prior to deformation [23]

Polymers experience degradation due to prior thermal aging when their covalent bonds begin to break down. This results in polymer chain scission and additional cross linking between chains. These processes typically occur very rapidly at temperatures above the glass transition temperature, but can also occur at lower temperatures although at a slower rate [4, 6]. These effects should not be neglected as degradation even below the glass transition temperature has been shown to result in a significant change in the material properties [4, 6, 10, 25,29].

Because changes in material properties occur due to multiple factors it becomes necessary to understand how material properties are affected by each individual variable before

evaluating the synergistic effect of several variables. It is recognized that materials subjected to long-term exposures at elevated temperatures will be affected by the exposure temperature as well as by the exposure duration. Therefore to produce safe and efficient designs we must understand the changes caused by both prior aging duration and prior aging temperature before we are able to fully understand the synergistic effect of these two factors.

Previous Research: Experimental Investigations

PMR-15 – Mechanical Behavior

The behavior of PMR-15 has been studied both at ambient and elevated temperatures. Because the focus of this research centers on behavior at elevated temperature only research performed at elevated temperature will be reviewed.

PMR-15 - Mechanical Behavior at 288 °C

Westberry investigated the time-dependent material behavior of PMR-15 at 288 °C. While performing tests in load control she found that PMR-15 at 288 °C exhibited pronounced dependence on prior stress rate in both creep and recovery tests. She concluded that to accurately model the behavior of PMR-15 under these conditions it is necessary to employ rate-dependent constitutive equations [33]. Falcone also conducted load control testing of PMR-15 at 288 °C. She similarly concluded that to accurately model creep, relaxation, and monotonic loading and unloading a rate dependent model was needed [11, 12]. The dependence of creep response on prior loading rate is illustrated in Figure 2.1 and the rate dependence on loading and unloading behavior is illustrated in Figure 2.2.

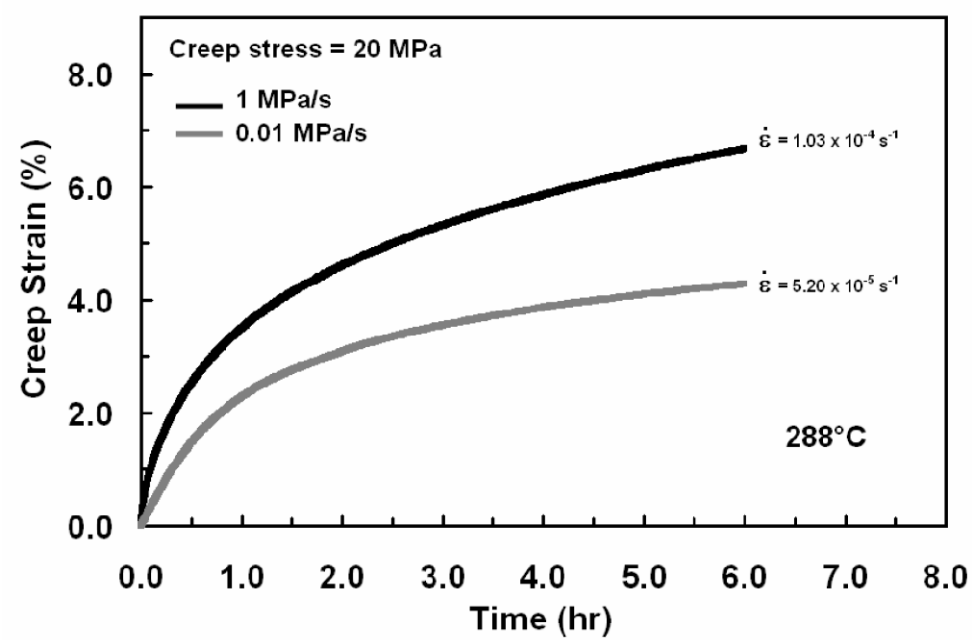

Figure 2.1: Creep Behavior of PMR-15 Following Stress Controlled Loading at 288 °C. Reproduced from Falcone [12].

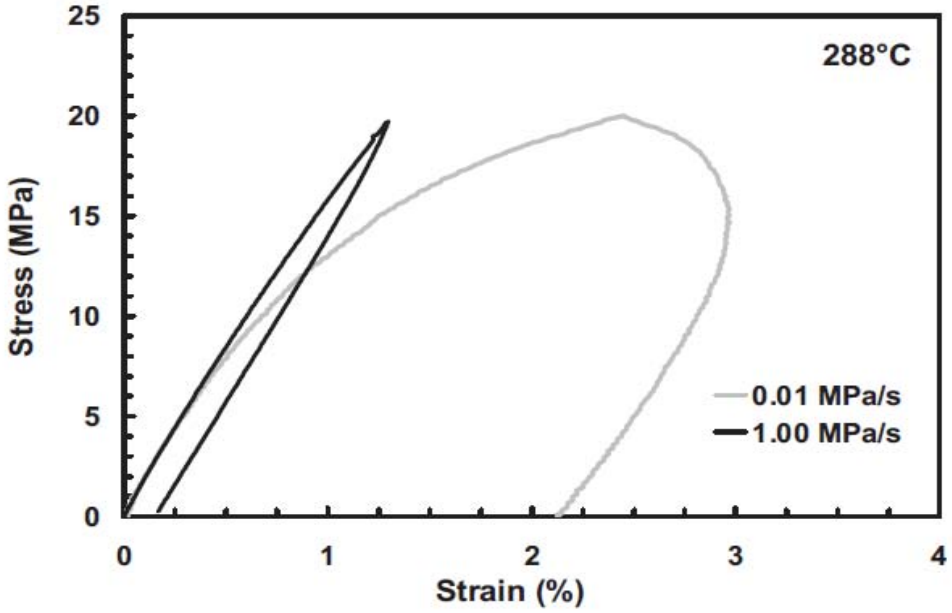

Figure 2.2: Loading and Unloading of PMR-15 at 288 °C. The Influence of Load Rate is Readily Apparent. Reproduced from Falcone [11].

McClung performed testing of PMR-15 at 288 °C under strain control. While testing at strain rates between 10^{-3} and 10^{-6} s^{-1} she made the following observations [25, 26, 27]:

1. Upon initial loading the material exhibits a linear quasi-elastic stress-strain behavior, which transitions to the region of inelastic deformation characterized by the tangent modulus.
2. PMR-15 exhibits nonlinear strain rate sensitivity in monotonic loading. Flow stress increases nonlinearly with increasing load rate.
3. Once the plastic flow is fully established, a unique stress-strain curve is obtained for a given strain rate. PMR-15 exhibits no strain rate history effect.
4. Strain recovery is strongly influenced by prior strain rate.
5. Creep behavior is strongly influenced by prior strain rate.
6. Relaxation behavior is strongly influenced by prior strain rate. Stress drop during relaxation is independent of stress and strain at the beginning of relaxation. Stress drop during relaxation depends only on time and on prior strain rate.

PMR-15 – Mechanical Behavior at 316 °C

Ozmen performed testing on PMR-15 at 316 °C in strain control at strain rates between 10^{-3} and 10^{-6} s^{-1}. Experimental observations made at 316 °C were similar to those made for PMR-15 at 288 °C [28, 29]:

1. At 316 °C PMR-15 exhibits positive nonlinear strain rate sensitivity in monotonic loading and unloading. The flow stress region is not achieved at the faster strain rates due to early failures. The flow stress level increases with strain rate.

2. At 316 °C PMR-15 exhibits no strain rate history effect.
3. Strain recovery of PMR-15 at 316°C is strongly influenced by prior strain rate. The recovery rate increases with prior strain rate.
4. Creep behavior is strongly influenced by prior strain rate. Creep rate increases with prior strain rate.
5. Relaxation behavior is strongly influenced by prior strain rate. The existence of an equilibrium stress curve is suggested.

PMR-15 – Mechanical Behavior at 260 °C

To better understand changes in the behavior of PMR-15 at temperatures below the maximum operating temperature Diedrick performed testing at 260 °C in strain control at strain rates between 10^{-3} and 10^{-6} s^{-1}. Diedrick observed the following key features of the deformation behavior at 260°C [10]:

1. Linear, quasi-elastic behavior upon initial loading.
2. Strain rate sensitivity in monotonic loading. The flow stress increases nonlinearly with increasing strain rate. A unique stress-strain curve exists for a given strain rate.
3. Fully established inelastic flow is almost never reached due to early failures.
4. Prior strain rate significantly affects recovery of strain. Recovery rate increases with prior strain rate.
5. Creep response is strongly affected by prior strain rate. An increase in prior strain rate results in an increase in creep strain accumulation.
6. Relaxation behavior is influenced by prior strain rate. Higher prior strain rates result in larger stress drops during relaxation.

Prior Aging – Effects on Mechanical Behavior

Many materials which operate at elevated temperature are exposed to those elevated temperatures for prolonged periods of time. It thus becomes necessary to understand how long-term exposure to elevated temperature affects the mechanical behavior of the material. Changes due to prior isothermal aging must be isolated from other effects to accurately understand and model the material behavior.

PMR-15- Effect of Prior Aging in Argon at 288 °C

To isolate the effects of prior isothermal aging from degradation caused by exposure in an oxidizing environment Broeckert tested specimens previously exposed to elevated temperature in both oxidizing (air) and inert (argon) environments [5]. It was concluded that significant material degradation occurs due to oxidation but that this degradation is limited to a thin layer on the exposed surface of the material. Broeckert also concluded that prior isothermal aging in an inert environment results in an increase of the elastic modulus, a decrease in the material's ability to accumulate inelastic strain, and an increase in the glass transition temperature. The effects of prior isothermal aging are seen in the creep response as illustrated in Figure 2.3.

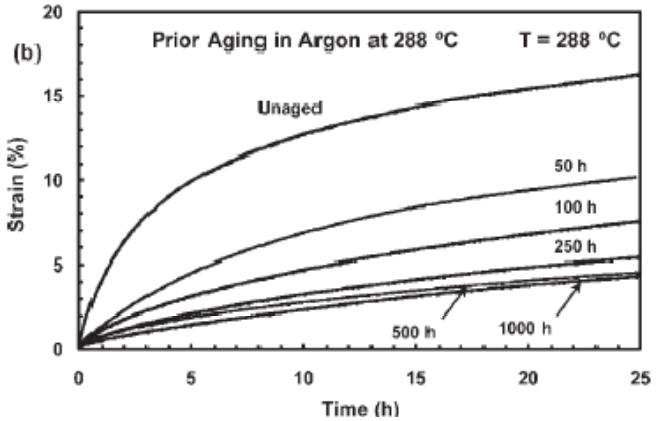

Figure 2.3: Creep Behavior at 20 MPa and 288 °C for PMR-15 Aged at 288 °C in Argon. Reproduced from Broeckert [5].

Subsequent to Broeckert's investigation, research at AFIT has focused on isolating the effects of prior isothermal aging. Hence all elevated temperature aging has been performed in an argon environment. In addition to work with unaged specimens McClung investigated deformation behaviors of PMR-15 specimens aged in argon at 288 °C for durations varying between 100 and 2000 hours [27]. McClung noted that prior isothermal aging resulted in the following changes in material response: the elastic modulus increased with increasing aging time, the tangent modulus increased with increasing aging time, the flow stress increased with increasing aging time, and departure from quasi-linear behavior was delayed. These effects of prior isothermal aging are illustrated in Figure 2.4 which shows the tensile stress-strain curves obtained for specimens loaded at a constant strain rate of 10^{-6} s^{-1} at 288 °C [27].

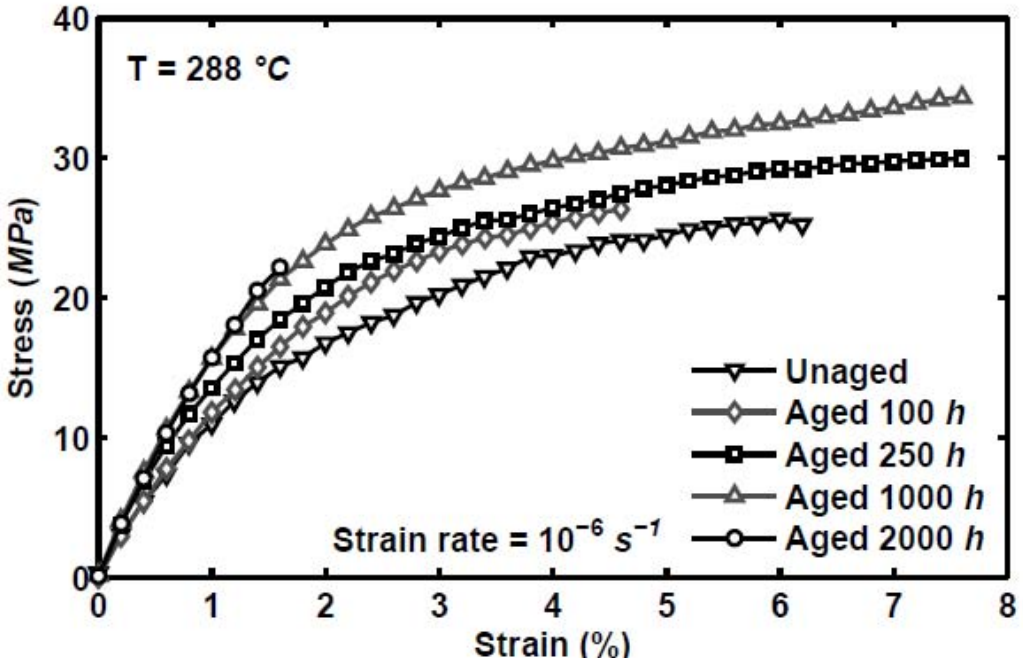

Figure 2.4: Stress-Strain Curves for PMR-15 Aged in Argon at 288 °C subjected to Tension to Failure Tests at a Strain Rate of 10^{-6} s^{-1}. Reproduced from McClung [27].

PMR-15- Effect of Prior Aging in Argon at 316 °C

Ozmen studied the effects of prior isothermal aging at 316 °C in an argon environment [29]. Ozmen noted that prior aging at 316 °C had the following effects on the material properties of the PMR-15 polymer: both the elastic modulus and the tangent modulus increased with increasing prior aging time [28]. Due to early failures it was difficult to determine the effects of prior aging on flow stress. These observations mirror those made for PMR-15 aged at 288 °C and are illustrated in Figure 2.5. Ozmen further noted that prior aging at 316 °C for durations over 100 hours resulted in a decreased ductility and early failures [29].

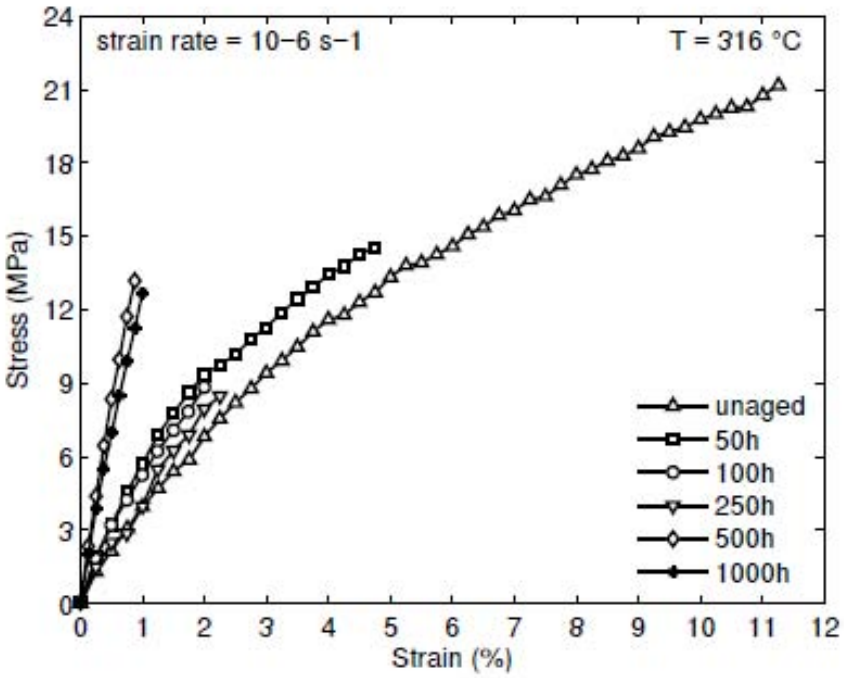

Figure 2.5: Stress-Strain Curves for PMR-15 Aged in Argon at 316 °C subjected to Tension to Failure Tests at a Strain Rate of 10^{-6} s^{-1}. Reproduced from Ozmen [28].

PMR-15- Effect of Prior Aging in Argon at 260°C

Diedrick exposed PMR-15 specimens to an argon environment at 260 °C for durations varying between 50 and 2000 hours [10], then tested the aged specimens at 260°C. Some of the experimental results obtained by Diedrick are shown in Figure 2.6. Very few of the specimens entered the flow stress region due to the relatively low test temperature. The effects of prior isothermal aging were less pronounced, but the following trends were still observed:

1. Increase in modulus of elasticity with increase in prior aging time
2. Increased brittleness with increase in prior aging time
3. Decreased strain accumulation in creep with increase in prior aging time

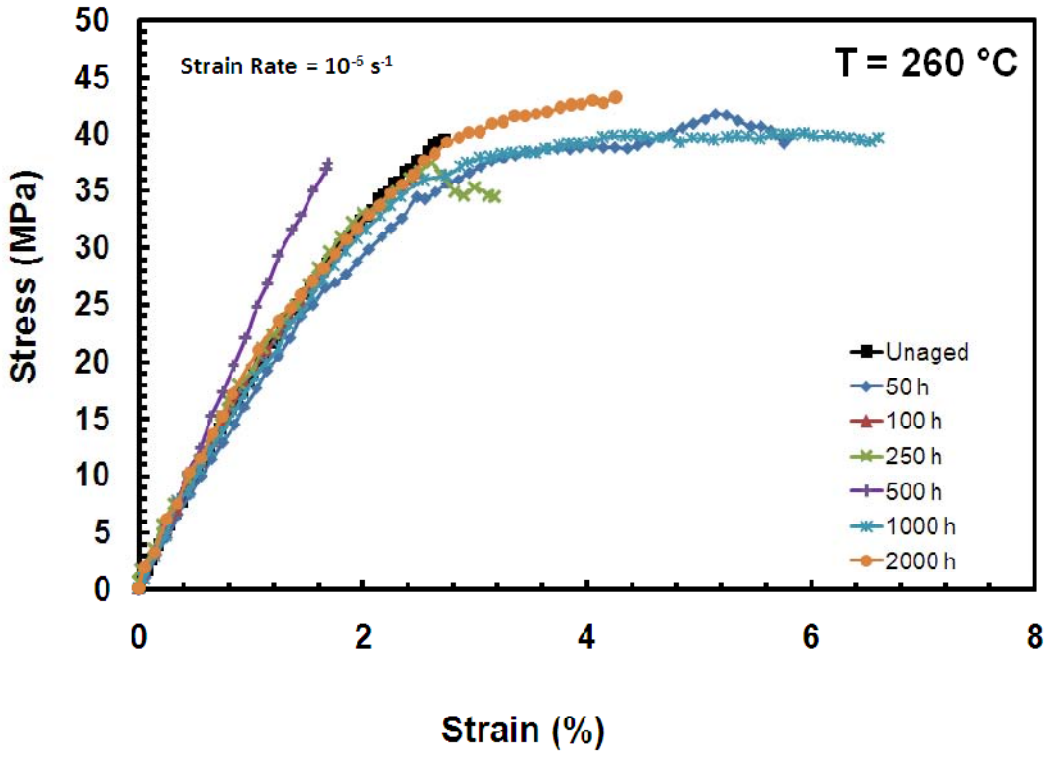

Figure 2.6: Stress-Strain Curves for PMR-15 Aged in Argon at 260 °C subjected to Tension to Failure Tests at a Strain Rate of 10^{-6} s^{-1}. Reproduced from Diedrick [10].

The following observations were reported for all prior aging temperatures [10]: The modulus of elasticity increased with prior aging time, increase in aging time results in an increasingly brittle response. It may be conjectured that if specimens aged and tested at 260 °C and at 316 °C had not experienced early failures they would likewise have demonstrated an increase in flow stress and in tangent modulus with increased aging duration.

Previous Research: Constitutive Modeling

Viscoelastic Modeling

Initial attempts to model the behavior of PMR-15 at elevated temperature employed Schapery's viscoelastic model [31]. Schapery's model has become widely used because of the existence of a systematic material characterization procedure and the models capability to represent many material behaviors [31]. Falcone found that Schapery's model did not adequately represent the rate-dependent aspects of the material behavior observed for PMR-15 [11, 12] as illustrated in Figure 2.7.

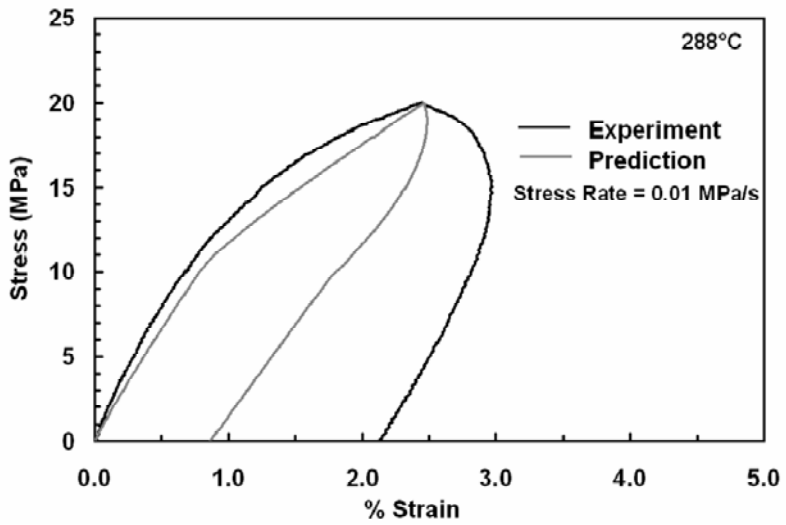

Figure 2.7: Loading and Unloading at a Constant Stress Rate for Unaged PMR-15 at 288 °C Experimentation and the Schapery's Model. Reproduced from Falcone [12].

Viscoplasticity Based on Overstress

Because a viscoelastic model was unable to accurately represent the behavior of PMR-15 at elevated temperature McClung decided to employ a viscoplastic model [27]. One key difference between viscoelastic and viscoplastic models is the capability of the viscoplastic model to account for permanent or plastic strain. This difference is shown in Figure 2.8 which depicts loading and unloading behavior followed by a period of recovery. Viscoelastic models predict recovery of all strain if given a sufficient amount of time. However, viscoplastic models predict the existence of permanent plastic strain which will not be recovered regardless of how long the material held at zero load. In addition, the viscoplastic models are capable of accounting for the effects of loading rate on the inelastic deformation behavior.

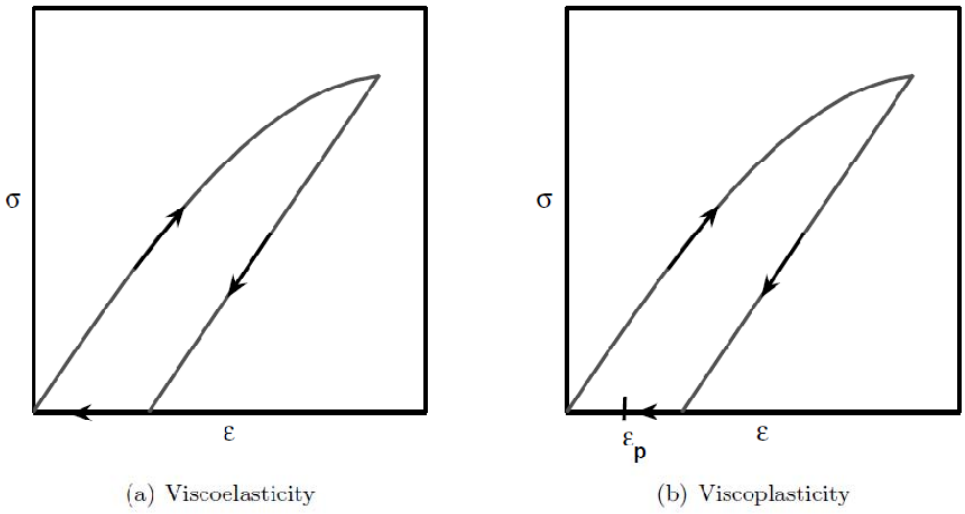

Figure 2.8: Schematic of Viscoelastic (a) and Viscoplastic (b) Behavior Exhibited in Loading and Unloading Followed by Recovery. Reproduced from McClung [25].

After considering various models McClung selected Viscoplasticity Based on Overstress (VBO) to represent the inelastic behavior of PMR-15 at 288 °C. This model was developed by Krempl and colleagues [20]. VBO is based on overstress and thus employs the concept of equilibrium stress. Equilibrium stress is the state of stress that would exist in a material if the loading rate was allowed to approach zero. Overstress is the amount of applied stress in excess of the equilibrium stress. These concepts are schematically depicted in Figure 2.9. VBO also predicts material behavior that is rate dependent as illustrated in Figure 2.9, which shows that distinct loading curves will exist for the same material loaded at different rates. We may also note the flow stress region in this same figure. Flow stress is observed for the portion of the stress-strain curve at large strain. In this region the slope of the stress strain curves becomes nearly constant. Within the VBO model the slope of the stress-strain curves at large strain is referred to as the tangent modulus. Krempel defines flow stress as the "steady inelastic flow with a tangent modulus much smaller than the elastic modulus measured at the origin" [21]

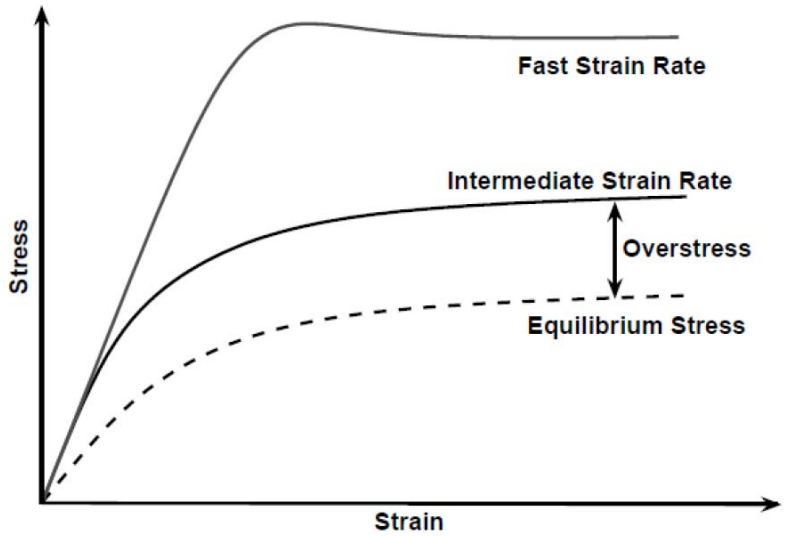

Figure 2.9: Schematic Representation of Equilibrium and Overstress Concepts. Reproduced from Ozmen [29].

It has been postulated that material behavior may be represented by a constitutive equation dependent on overstress [7]. For Viscoplasticity Based on Overstress the uniaxial constitutive equation is given in the following form [18]:

$$\dot{\epsilon} = \dot{\epsilon}^{el} + \dot{\epsilon}^{in} = \frac{\dot{\sigma}}{E} + \frac{\sigma - g}{Ek(\sigma - g)} \tag{2.1}$$

In this equation σ is engineering stress, ϵ is engineering strain, $\epsilon^{el}$is elastic strain, $\epsilon^{in}$is inelastic strain, E is the elastic modulus. The viscosity function, which governs rate dependence, is denoted as k. Equilibrium stress, the theoretical stress that would be present if all rates approached zero is denoted as g. Brackets represent "function of" and the quantity $(\sigma - g)$ represents the stress in excess of the equilibrium stress and is called the overstress. A detailed discussion of the mathematical formulation of the VBO is given in chapter 3.

Viscoplasticity Based on Overstress for Polymers

VBO was originally created to model the behavior of engineering alloys and was shown to be capable of representing many of the observed behaviors. The merits of this model in representing the behaviors of SAE 1020, HY-80, and Aer-Met steels as well as those of tantalum-titanium alloys was demonstrated by Krempl [21]. However, VBO was not able to adequately represent all of the material behavior observed for some polymers. These polymers exhibited high relaxation rates, increased strain recovery after loading followed by unloading to zero stress, curved unloading in stress control, reduced rate dependence during unloading, merging of the stress-strain curves produced at different strain rates, and relaxation or creep rate reversal (change of sign of stress rate during relaxation or strain rate during creep) on unloading [2, 3, 17]. To account for these behaviors Ho introduced Viscoplasticity Based on Overstress for

Polymers (VBOP) [13]. It was demonstrated that VBOP predicted the behavior of various polymers better than the standard VBO [13, 17, 27].

McClung tested PMR-15 at 288 °C and observed behaviors, as noted earlier in this chapter, which led her to select VBOP to model the deformation behavior this material [27]. Additionally, she developed a systematic characterization procedure for VBOP and applied that procedure to the experimental data obtained for PMR-15 at 288 °C. McClung was able to accurately model the material behavior (1) for several loading scenarios used for model characterization (tension to failure, relaxation) and (2) for loading histories used for model validation (load unload followed by recovery, creep, strain rate jump test). Figure 2.10 clearly shows that the model predicts rate-dependence of tensile stress-strain behavior. Furthermore, predictions compare well with the experimental data.

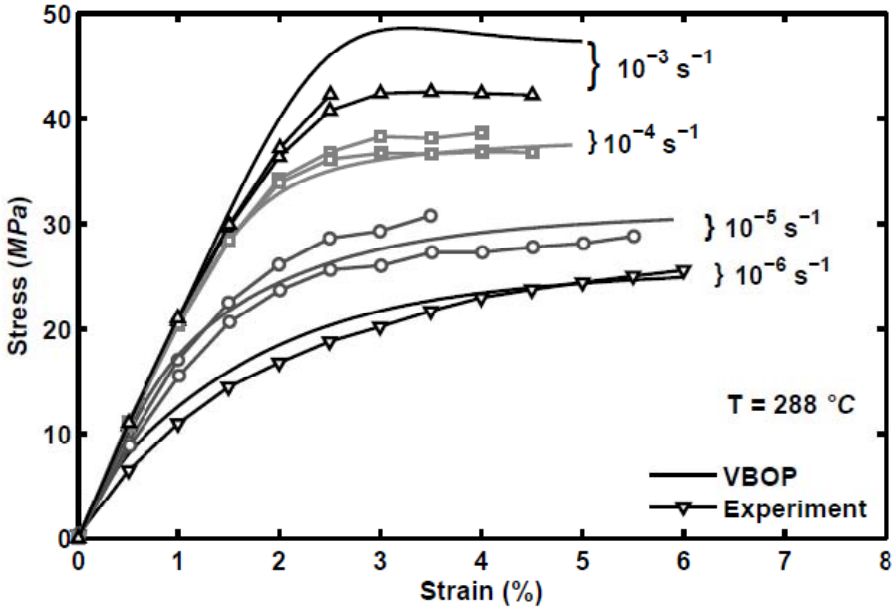

Figure 2.10: Stress-Strain Behavior of Unaged PMR-15 at 288 °C in Monotonic Tension to Failure Tests Described by Experimentation and VBOP. Reproduced from McClung [25].

Relaxation behavior is also modeled well by VBOP (see Figure 2.11).

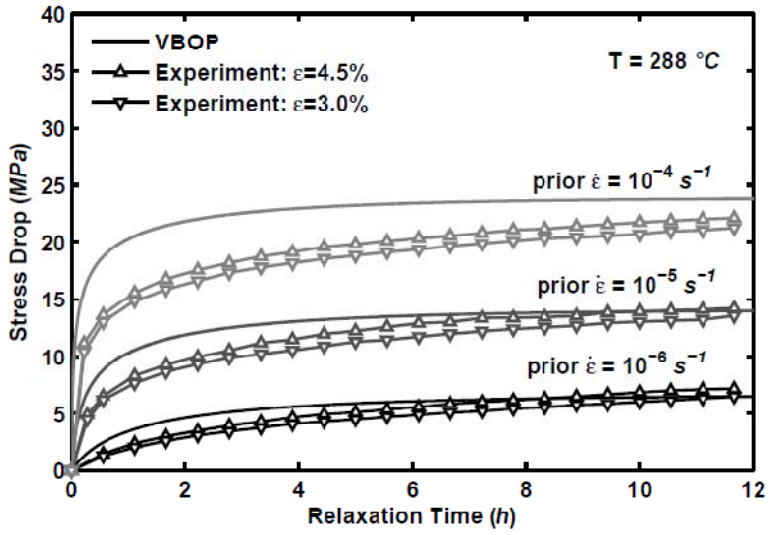

Figure 2.11: Relaxation Behavior of Unaged PMR-15 at 288 °C Described by Experimentation and the VBOP. Reproduced from McClung [25].

Figure 2.12 shows that the model accurately predicts the stress-strain behavior produced in a strain rate jump tests.

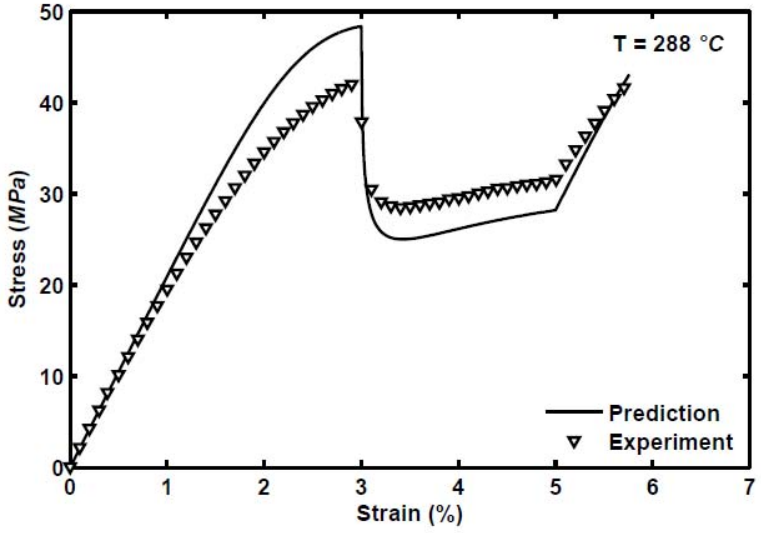

Figure 2.12: Stress-Strain Behavior of Unaged PMR-15 at 288 °C in the Strain Rate Jump Test Described by Experimentation and the VBOP. Reproduced from McClung [25].

The capacity of VBOP to model curved unloading is demonstrated in Figure 2.13.

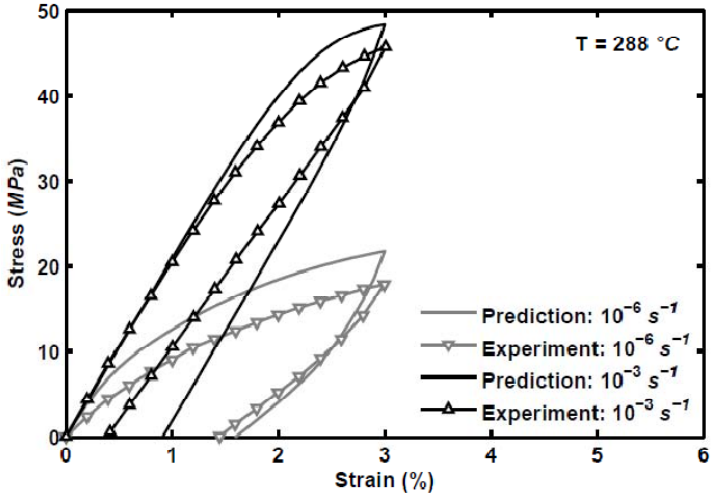

Figure 2.13: Stress-Strain Behavior of Unaged PMR-15 at 288 °C in Loading Followed by Unloading Described by Experimentation and the VBOP. Reproduced from McClung [25].

McClung also notes the aptitude of VBOP to model the effects of prior strain rate on creep behavior as depicted in Figure 2.14.

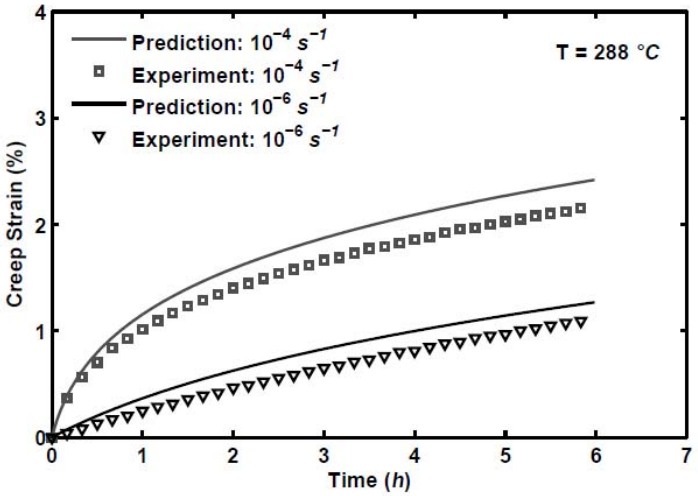

Figure 2.14: Creep Behavior of Unaged PMR-15 at 288 °C Described by Experimentation and the VBOP. Reproduced from McClung [25].

Following the procedure established by McClung [27], Ozmen characterized the VBO model parameters to represent the behavior of PMR-15 at 316 °C [28, 29]. Ozmen used creep, load-unload, and strain rate jump test histories to validate the model. Comparisons of the experimental results with model predictions are shown in Figure 2.15 through Figure 2.17.

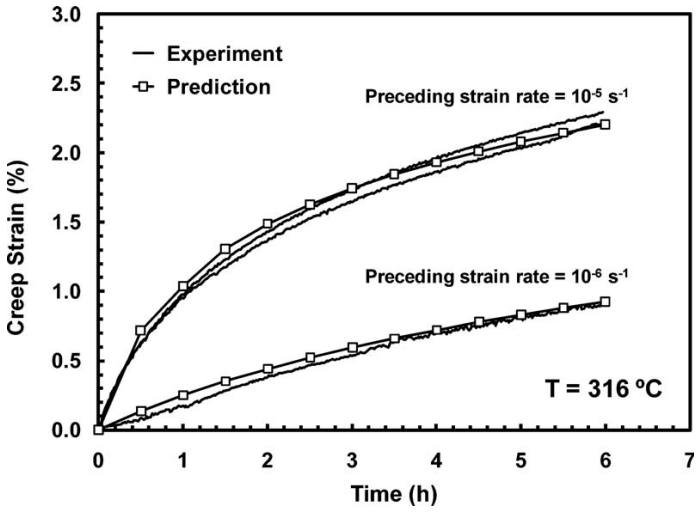

Figure 2.15: Creep Behavior of Unaged PMR-15 at 316 °C. Experimental results and VBOP model predictions. Reproduced from Ozmen[29].

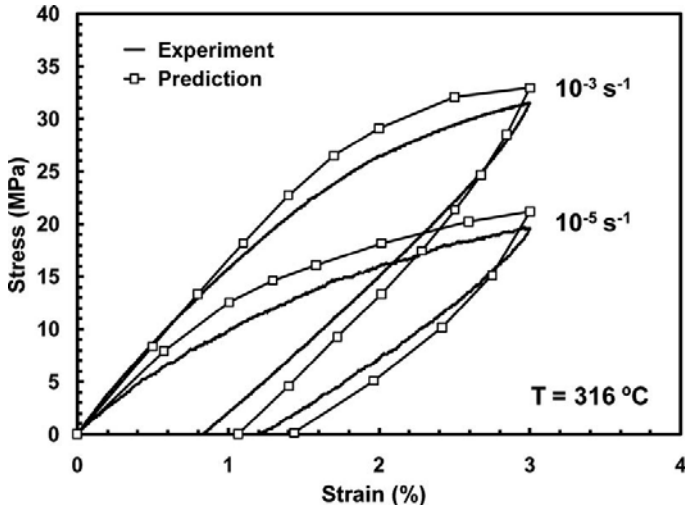

Figure 2.16: Stress-Strain Behavior of Unaged PMR-15 at 316 °C in Loading and Unloading Tests. Experimental results and VBOP model predictions. Reproduced from Ozmen [29].

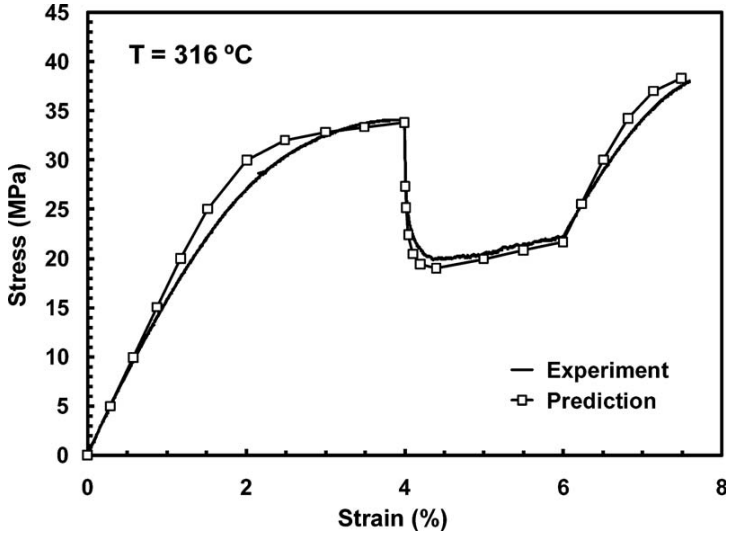

Figure 2.17: Stress-Strain Behavior of Unaged PMR-15 at 316 °C in the Strain Rate Jump Test. Experimental results and VBOP model predictions. Reproduced from Ozmen [29].

Diedrick also modeled the behavior of PMR-15 at 260 °C using VBOP. To characterize the model he followed the procedures established by McClung employing tension to failure and relaxation tests. Modeling of the deformation behavior produced at this temperature became difficult because very few specimens entered the flow stress region. It has been proposed that the deformation behavior of PMR-15 at this temperature is outside of the domain of validity for VBOP, and that simpler models may be able to adequately represent the material behavior. Results of Diedrick's testing and modeling are shown in Figure 2.18 through Figure 2.20

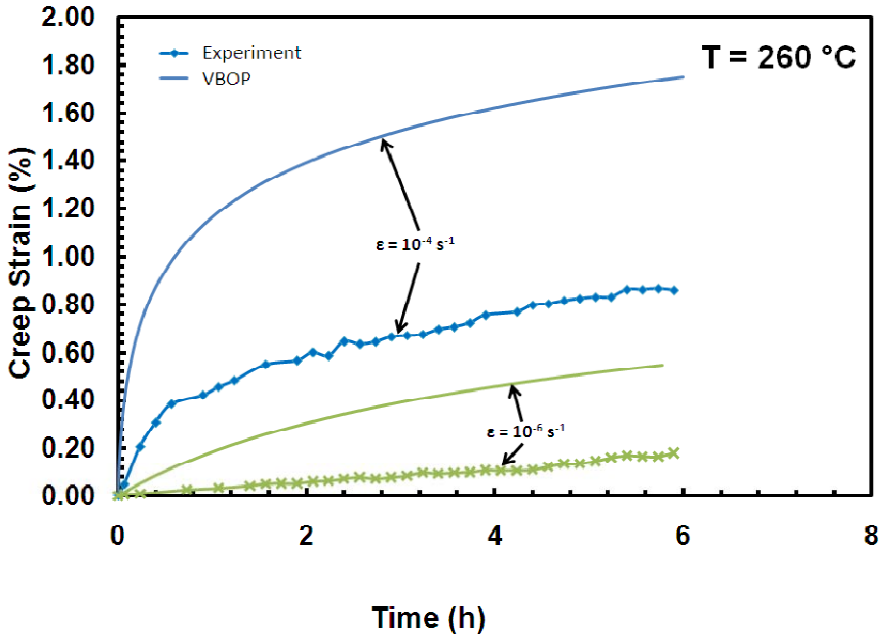

Figure 2.18: Creep Behavior of Unaged PMR-15 at 260 °C. Experimental results and VBOP model predictions. Reproduced from Diedrick[10].

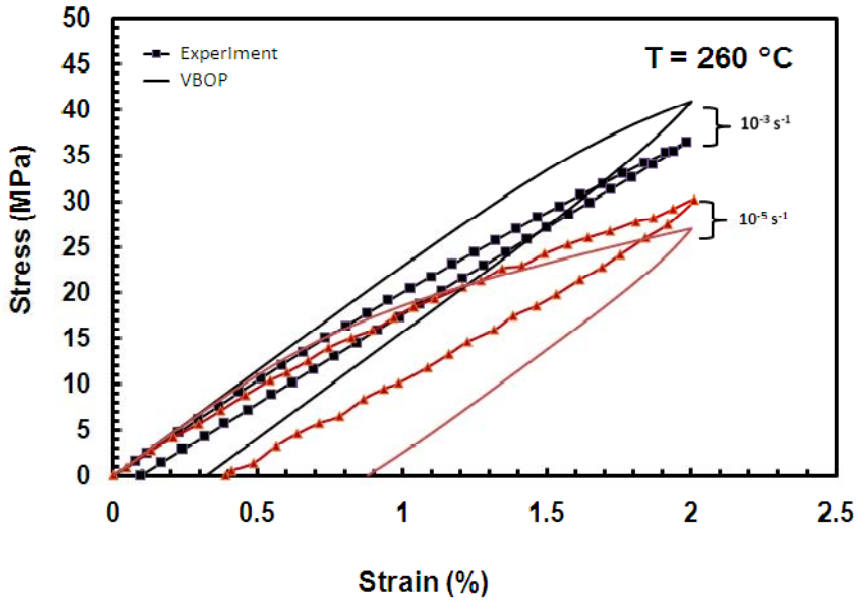

Figure 2.19: Stress-Strain Behavior of Unaged PMR-15 at 260 °C in Loading Followed by Unloading. Experimental results and VBOP model predictions. Reproduced from Diedrick [10].

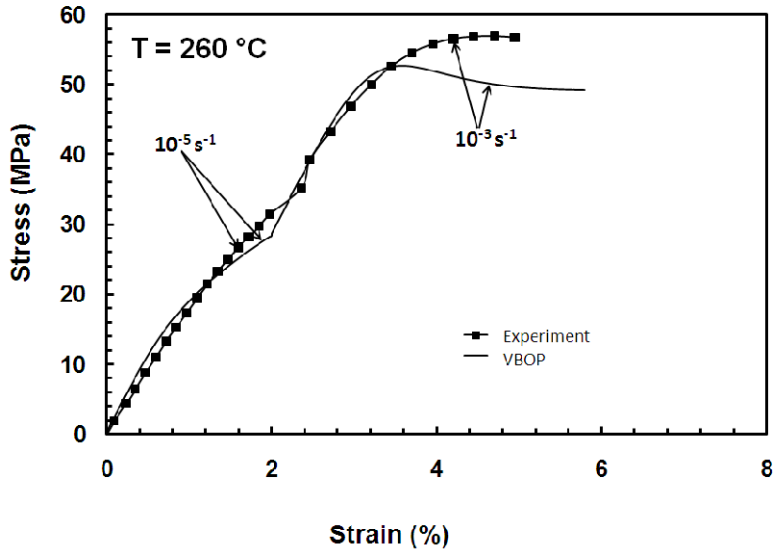

Figure 2.20: Stress-Strain Behavior of Unaged PMR-15 at 260 °C in the Strain Rate Jump Test. Experimental results and VBOP model predictions. Reproduced from Diedrick [10].

Viscoplasticity Based on Overstress for Polymers with Prior Aging

It is recognized that polymer deformation behavior changes with prior isothermal aging. McClung analyzed such changes and developed an analytical capability within the VBOP model to represent the effects of prior aging time on the deformation behavior. As noted previously McClung observed that prior aging has the following effects on the deformation behavior [27]:

1. Initial slope of stress-strain curve increases with prior aging time.
2. Final slope of stress-strain curve increases with prior aging time.
3. Flow stress increases with prior aging time.
4. Departure from quasi-linear behavior is delayed with prior aging time.

McClung modeled the aforementioned effects of prior aging on deformation behavior in VBOP by expanding the following model parameters into functions of prior aging time [27]:

1. Elastic modulus, E
2. Tangent modulus, E_t.
3. Isotropic stress, A.
4. Shape parameter, C_2.

McClung used the data collected for specimens aged at 288 °C for durations varying between 0 and 1000 hours to establish these model parameters as functions of aging duration. It was found that power law functions were well suited for this purpose. The developed power law relationships were used to predict the material behavior of PMR-15 aged at 288 °C for 2000 hours. Figure 2.21 and Figure 2.22 demonstrate the ability of the VBOP with the model parameters established as functions of prior aging time to accurately predict the material behavior of specimen aged for 2000 hours.

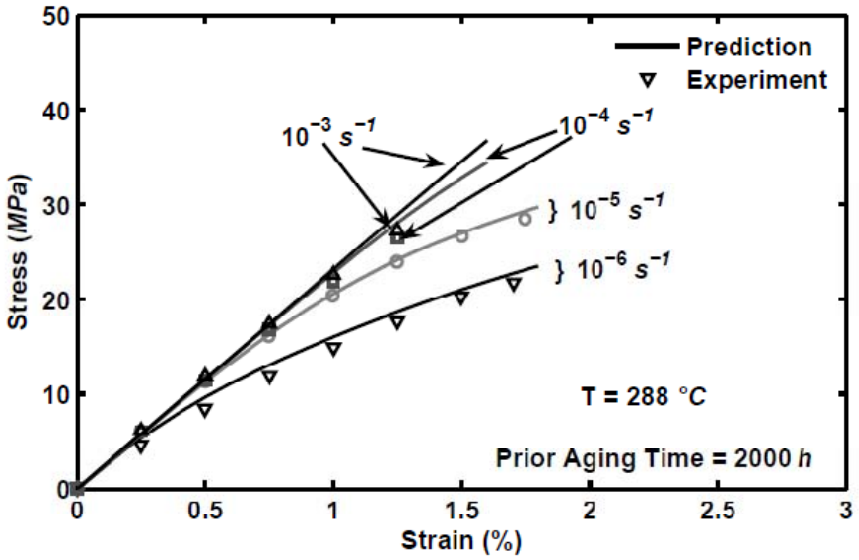

Figure 2.21: Comparison Between Experimental and Predicted Stress-Strain Curves Obtained in Tensile Test for PMR-15 Aged at 288 °C for 2000 h. Reproduced from McClung [27].

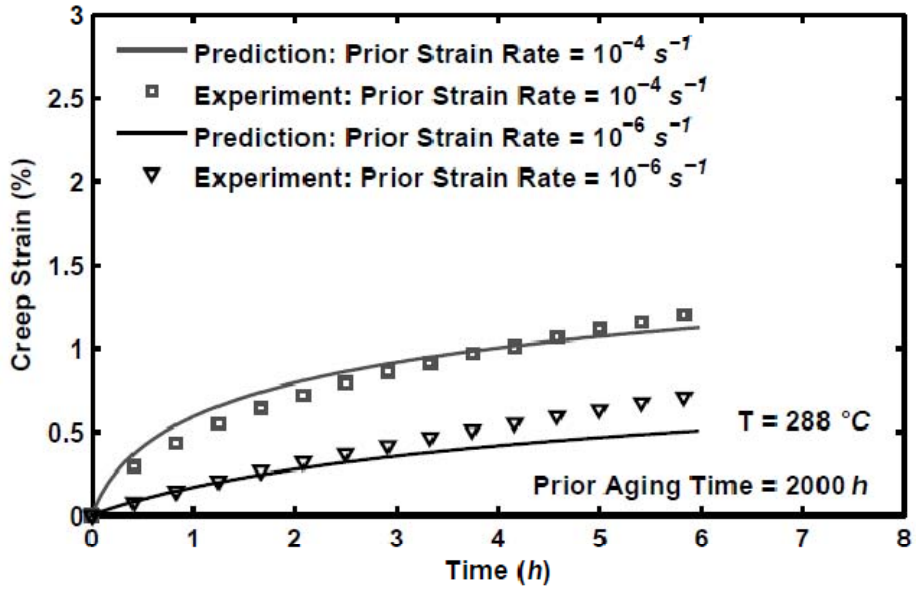

Figure 2.22: Comparison Between Experimental and Predicted Creep Strain vs. Time Curves Obtained at 21 MPa for PMR-15 Aged at 288 °C for 2000 h. Reproduced from McClung [27].

Using the power law form proposed by McClung, Diedrick made the VBOP model parameters dependent on the duration of prior aging at 260 °C. Diedrick used test data obtained for specimen aged for 0, 100, and 200 hours to expand the model parameters as functions of prior aging time. The augmented VBOP was employed to predict material behavior for specimen aged at 260°C for 500, 1000, and 2000 hours. Results of this effort were mixed. In the case of tension to failure tests, predictions agreed with experimental results reasonably well (see Figure 2.23). However, in the case of relaxation and creep tests, predictions did not agree with experimental results equally well (see Figure 2.24 and Figure 2.25).

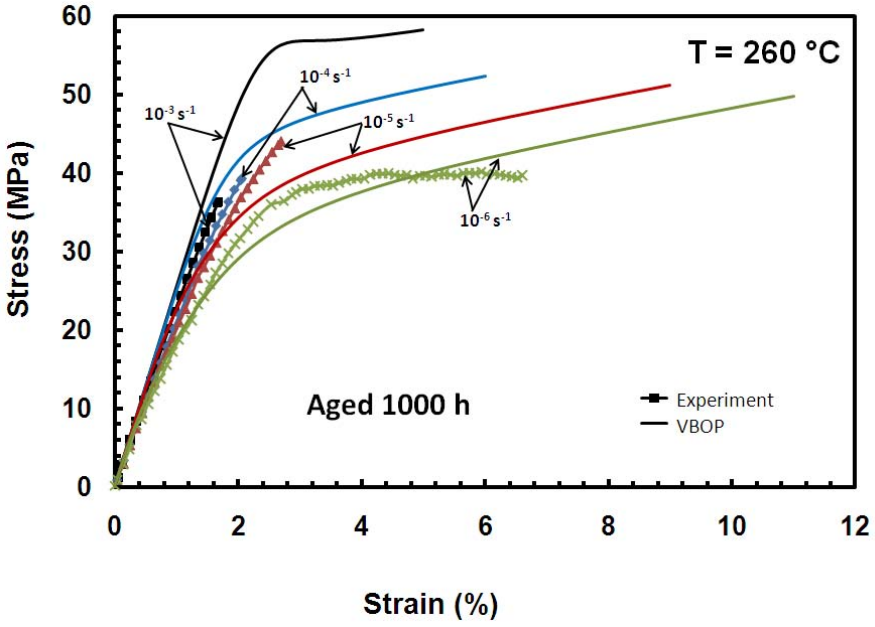

Figure 2.23: Experimental and Predicted Stress-Strain Curves Obtained in Monotonic Tension at 260 °C for PMR-15 Aged in Argon at 260 °C for 1000 h. Reproduced from Diedrick [10].

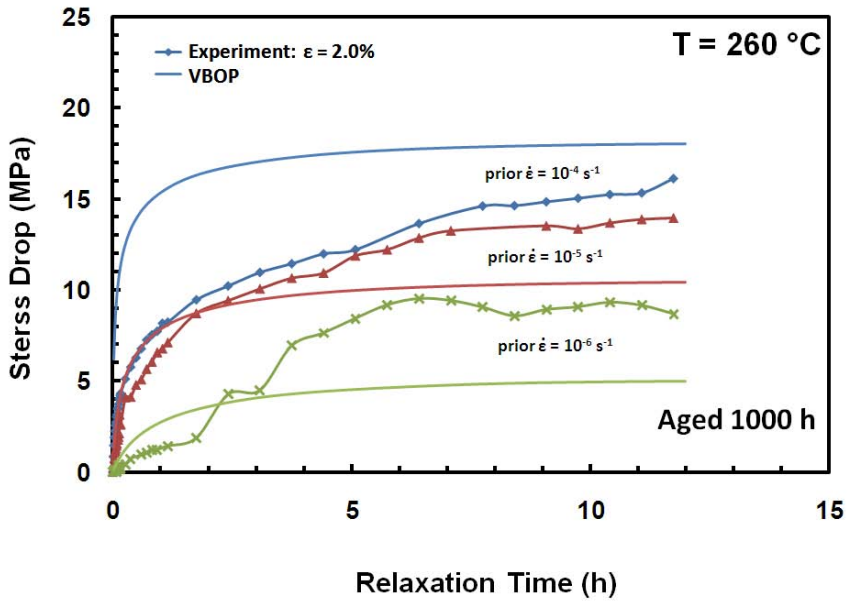

Figure 2.24: A Comparison Between Experimental and Predicted Stress Drop vs. Relaxation Time Curves Obtained at 260 °C for the PMR-15 Polymer Aged in Argon at 260 °C for 1000 h. Reproduced from Diedrick [10].

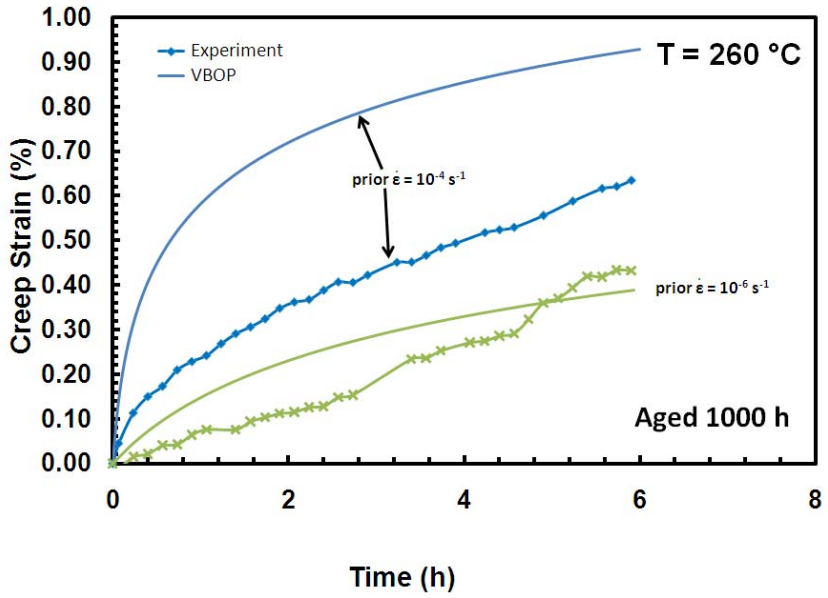

Figure 2.25: A Comparison Between Experimental and Predicted Creep Strain vs Time Curves Obtained at 25 MPa and at 260 °C for PMR-15 Polymer Aged in Argon at 260 °C for 1000 h. Reproduced from Diedrick [10].

3. Theoretical Formulation of Viscoplasticity Based on Overstress for Polymers

To predict the mechanical behavior of PMR-15 aged at 274 °C and tested at 288 °C a constitutive model must be selected. The model which will be used in this research is Viscoplastisity Based on Overstress for Polymers (VBOP). This is a unified constitutive model capable of representing many of the material behaviors exhibited by PMR-15. This chapter discusses the theoretical development of Viscoplasticity Based on Overstress including the model extension to account for the effects of prior aging.

Basis of Viscoplasticity Based on Overstress – Standard Linear Solid

The origin of Viscoplasticity Based on Overstress (VBO) may be traced to the standard liner solid [22]. The Standard Linear Solid (SLS) consists of a linear spring connected in series with a Kelvin-Voigt element, which is composed of a linear spring and a linear dashpot. A schematic representation of the SLS is presented in Figure 3.1. A key feature of SLS is that it is capable of representing both creep and relaxation [22].

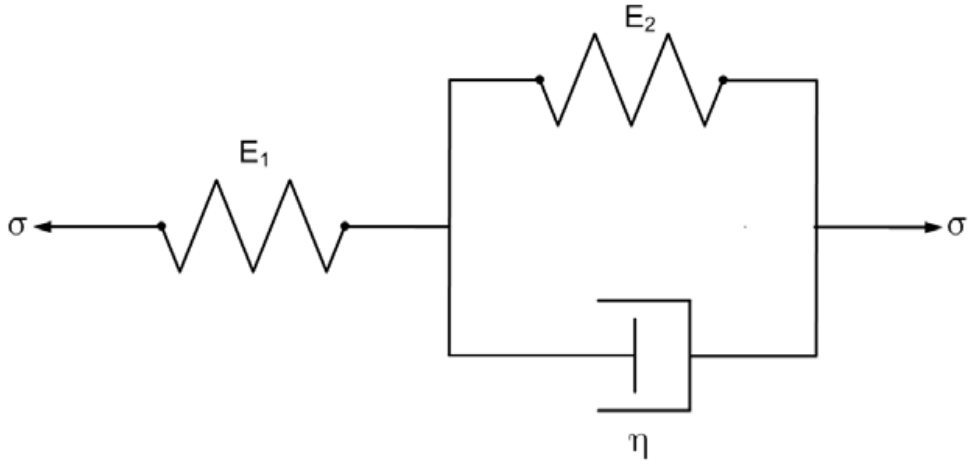

Figure 3.1: Standard Linear Solid. Reproduced From Falcone [12]

The SLS may be represented mathematically in the following standard form:

$$\dot{\epsilon} + \frac{E_2}{\eta}\epsilon = \frac{\dot{\sigma}}{E_1} + \left(\frac{E_1 + E_2}{E_1}\right)\frac{\sigma}{\epsilon} \tag{3.1}$$

In this constitutive equation strain is denoted by ϵ, stress is denoted by σ, the elastic spring constants are E_1 and E_2, and the viscosity coefficient of the dashpot is denoted by η.

Viscoplasticity Based on Overstress

It is convenient to rearrange the constitutive equation for the SLS by isolating the strain rate term on the left side of the equation. This allows the division of the strain response into elastic $\dot{\epsilon}^{el}$ and inelastic $\dot{\epsilon}^{in}$ components.

$$\dot{\epsilon} = \dot{\epsilon}^{el} + \dot{\epsilon}^{in} = \frac{\dot{\sigma}}{E_1} + \frac{\sigma - aE_2\epsilon}{a\eta} \tag{3.2}$$

where

$$a = \frac{E_1}{E_1 + E_2} \tag{3.3}$$

The numerator of the inelastic component of the response, $-aE_2\epsilon$, is called the overstress. The stress which the model would predict as all rates approach zero is called the equilibrium stress and is represented as g where

$$g = aE_2\epsilon \tag{3.4}$$

Making this substitution the constitutive equation for the standard linear solid in overstress form becomes:

$$\dot{\epsilon} = \frac{\dot{\sigma}}{E_1} + \frac{\sigma - g}{a\eta} \tag{3.5}$$

The standard linear solid predicts different material responses for different applied loading rates. At an infinitely slow loading rate the model predicts behavior characteristic of the two springs in series as given by ——. At an infinitely fast loading rate the dashpot is unable to produce a strain response and model behavior is governed only by E_1. Thus elastic stress-strain behavior is produced. Intermediate loading rates produce responses which vary between these two bounds as depicted in Figure 3.2.

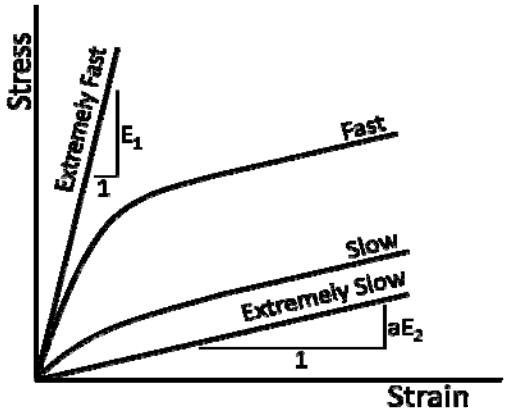

Figure 3.2: Schematic of SLS Response to Monotonic Loading. Reproduced From Krempl [22].

In order to better represent material behavior it is desirable to replace the linear spring in the Kelvin-Voigt element E_2 with a nonlinear function of strain and allow the viscosity of the dashpot to vary as a function of overstress incorporating the former constant into this function [22]. To account for hysteretic behavior the equilibrium stress must be allowed to change and become a function of overstress [20].

The governing equation for VBO now becomes:

– —— (3.6)

where $\dot{\epsilon}$ is the strain rate, E is the elastic modulus, g is the equilibrium stress, and k is the viscosity function.

The equilibrium stress is a function of overstress given as:

$$\dot{g} = \Psi \frac{\dot{\sigma}}{E} + \frac{\Psi}{E}\left[\frac{\sigma - g}{k} - \frac{g - f}{A}\frac{(\sigma - g)}{k}\right] + \left(1 - \frac{\Psi}{E}\right)\dot{f} \tag{3.7}$$

where Ψ is the shape function, f is the rate dependent or kinematic stress, and A is the rate independent or isotropic stress.

The viscosity function is dependent on overstress and is written as [20]:

$$k = k_1\left(1 + \frac{|\sigma - g|}{k_2}\right)^{-k_3} \tag{3.8}$$

where k_1, k_2, and k_3 are material constants.

The isotropic stress A is the difference between the equilibrium stress g and the kinematic stress f in the region of fully established plastic flow. Variation in isotropic stress is the repository for modeling cyclic work hardening or softening [14, 20].

$$\dot{A} = A_c[A_f - A]\left|\frac{\sigma - g}{Ek}\right| \tag{3.9}$$

where A_c and A_f are constants which control the rate of hardening (A_c) and represents the final value of A once saturation is reached (A_f).

Kinematic or rate dependent stress f governs the region of fully established inelastic flow as given by:

$$\dot{f} = E_t \frac{(\sigma - g)}{Ek} \tag{3.10}$$

This function includes the tangent modulus E_t which is defined as the slope of the stress-strain curve in region of fully established plastic flow.

The shape function is responsible for modeling the transition from the initial quasi elastic behavior to fully established inelastic flow. The effect of the shape functions is most readily apparent in its influence on the shape of the "knee" of the stress strain diagram.

$$\Psi = C_1 + (C_2 - C_1)e^{-C_3|\epsilon^{in}|} \tag{3.11}$$

where the shape function parameters C_1, C_2, and C_3 are material constants.

The VBO model does not produce a purely elastic response because inelastic strain, even if extremely small, is always present [20]. For this reason the model does not employ a yield surface. There are several versions of VBO in existence which attempt to represent various material behaviors under specific conditions. However, all of these models employ a flow law and the state variables for equilibrium stress g, isotropic stress A, and kinematic stress f. Because PMR-15 (a high temperature polymer) is the material used in this research the VBO formulation known as Viscoplasticity Based on Overstress for Polymers (VBOP) has been selected.

Viscoplasticity Based on Overstress for Polymers

Bordonaro and Krempl observed that some polymer deformation behaviors were not adequately modeled by the standard VBO [2, 3]. In order to represent these behaviors Ho and Krempl formulated VBOP [13]. VBOP was subsequently used to model the deformation behaviors of various polymers including PMR-15 [27]. The governing equation of VBOP retains the same form as that of the VBO:

$$\dot{\epsilon} = \frac{\dot{\sigma}}{E} + \frac{\sigma - g}{Ek} \tag{3.12}$$

The evolution of equilibrium stress g is modified by the addition of the term dependent on overstress rate, $\frac{\Psi}{E}(\dot{\sigma} - \dot{g})n$. This term influences equilibrium stress which in turn alters the relaxation rate. With the addition of this term the growth law for equilibrium stress becomes:

$$\dot{g} = \Psi\frac{\dot{\sigma}}{E} + \frac{\Psi}{E}\left[\frac{\sigma-g}{k} - \frac{g-f}{A}\frac{(\sigma-g)}{k} + (\dot{\sigma} - \dot{g})n\right] + \left(1 - \frac{\Psi}{E}\right)\dot{f} \qquad (3.13)$$

Here n is a material constant which controls relaxation rate and varies from 0 to 1. McClung found that setting n=0 produced optimal results for PMR-15. Following McClung, this research uses a value of n=0, returning the growth law for equilibrium stress to the form given in Equation 3.7.

The viscosity function for polymers is modified as follows:

$$k = k_1\left[1 + \left(1 + \frac{A_0 - A}{A_0 - A_f}\right)\frac{\Gamma}{k_2}\right]^{-k_3} \qquad (3.14)$$

where

$$\Gamma = |\sigma - g| \qquad (3.15)$$

and A_0 is the initial value of isotropic stress and A_f is the final value of isotropic stress. The addition of these terms allows the stress-strain curves produced at various rates to merge.

The evolution equation for the isotropic stress remains the same as in the standard VBO:

$$\dot{A} = A_c[A_f - A]\left|\frac{\sigma-g}{Ek}\right| \qquad (3.16)$$

For a cyclically neutral material A_C=0 which results in A=const. Near cyclically neutral behavior has been reported for various polymers and A=const has been used to effectively model their behavior [15, 17]. McClung assumed that PMR-15 at 288 °C was also a cyclically neutral material and has demonstrated that a constant value of isotropic stress produced acceptable

results [27]. If cyclically neutral behavior is assumed the viscosity function for VBOP is the same as the viscosity function for VBO, as given in Equation 3.8.

For VBOP the evolution of the kinematic stress is modified to take the form:

$$\dot{f} = \left(\frac{|\sigma|}{\Gamma+|g|}\right) E_t \frac{(\sigma-g)}{Ek} \tag{3.19}$$

This is different than the formulation used for standard VBO in its addition of the term $\left(\frac{|\sigma|}{\Gamma+|g|}\right)$, which was introduced to model increased strain recovery at zero stress. McClung determined that including this term improved the ability of VBOP to accurately represent the behavior of PMR-15 at 288 °C [27].

For VBOP the shape function takes the form:

$$\Psi = C_1^* + (C_2 - C_1^*)e^{-C_3|\epsilon^{in}|} \tag{3.17}$$

where

$$C_1^* = C_1\left[1 + C_4\left(\frac{|g|}{A+|f|+\Gamma^2}\right)\right] \tag{3.18}$$

C_1, C_2, C_3 , and C_4 are material constants and C_1^* is a function of equilibrium stress, isotropic stress, kinematic stress, and overstress. McClung observed that for PMR-15 at 288 °C the shape function given in the standard VBO formulation produced more accurate results than this modified shape function [27]. Based on McClung's finding the shape function given in Equation 3.11 will be used for this research. Note that that this is equivalent to setting the constant C_4=0 in equation (3.18).

Previous research has found that VBOP is capable of accurately representing many of the behaviors exhibited by PMR-15 at elevated temperature [10, 27, 28, 29]. A summary of the VBOP formulation used in this research is as follows:

Uniaxial Flow Law

$$\dot{\epsilon} = \dot{\epsilon}^{el} + \dot{\epsilon}^{in} = \frac{\dot{\sigma}}{E} + \frac{\sigma - g}{Ek} \tag{3.20}$$

Evolution of Equilibrium Stress

$$\dot{g} = \Psi \frac{\dot{\sigma}}{E} + \frac{\Psi}{E}\left[\frac{\sigma - g}{k} - \frac{g - f}{A}\left|\frac{(\sigma - g)}{k}\right|\right] + \left(1 - \frac{\Psi}{E}\right)\dot{f} \tag{3.21}$$

Evolution of Kinematic Stress

$$\dot{f} = \left(\frac{|\sigma|}{\Gamma + |g|}\right) E_t \frac{(\sigma - g)}{Ek} \tag{3.22}$$

Shape Function

$$\Psi = C_1 + (C_2 - C_1)e^{-C_3|\epsilon^{in}|} \tag{3.23}$$

Viscosity Function

$$k = k_1\left[1 + \frac{\Gamma}{k_2}\right]^{-k_3} \tag{3.24}$$

where the stress invariant is defined as

$$\Gamma = |\sigma - g| \tag{3.25}$$

and A is assumed to be constant. The key difference between VBOP as used in this research and the standard VBO formulation is the inclusion of the term $\left(\frac{|\sigma|}{\Gamma + |g|}\right)$ in the evolution of the kinematic stress.

Extension of VBOP to Account for Effects of Prior Aging Time

McClung modified the VBOP by adding the capability to account for changes in deformation behavior due to prior isothermal aging [27]. It was found that some model parameters varied with prior aging duration and could be modeled as functions of prior aging time using power law relationships. The elastic modulus, E, tangent modulus, E_t, isotropic

stress, A, and the shape function parameter, C_2, were developed as functions of prior aging time. These relationships do not change the established formulation of VBOP, but instead add the analytical capability to predict model parameters for aging durations not investigated experimentally.

4. Material and Test Specimen

This section discussed the material studied during this research, the test specimen geometry, and test specimen preparation.

PMR-15 (Polymerization of Monomeric Reactants – 15) Solid Polymer

The material selected for this research was PMR-15 which was developed by the NASA Lewis Research Center in the 1970's. It has a long term use temperature of 288°C and a glass transition temperature T_g between 331°C [6] and 347°C [4]. PMR-15 is a widely used matrix material for high temperature polymer matrix composites and has become the "leading polymer matrix resin for carbon-fiber-reinforced composites used in aircraft engines" [8]. The PMR-15 neat resin panels were supplied and postcured by HyComp Inc. (Cleveland, OH). The details of the free-standing postcure cycle are shown in Table 4-1. Panels were cut into 152 mm x 23 mm rectangular blanks and delivered to AFIT.

Table 4-1: Freestanding PostCure Cycle

Step	Description
1	Heat to 204 °C in 2 h and hold for 1 h
2	Heat to 260 °C in 1 h and hold for 1 h
3	Heat to 316 °C in 2 h and hold for 16 h
4	Cool to room temperature at a rate of 1 °C/min

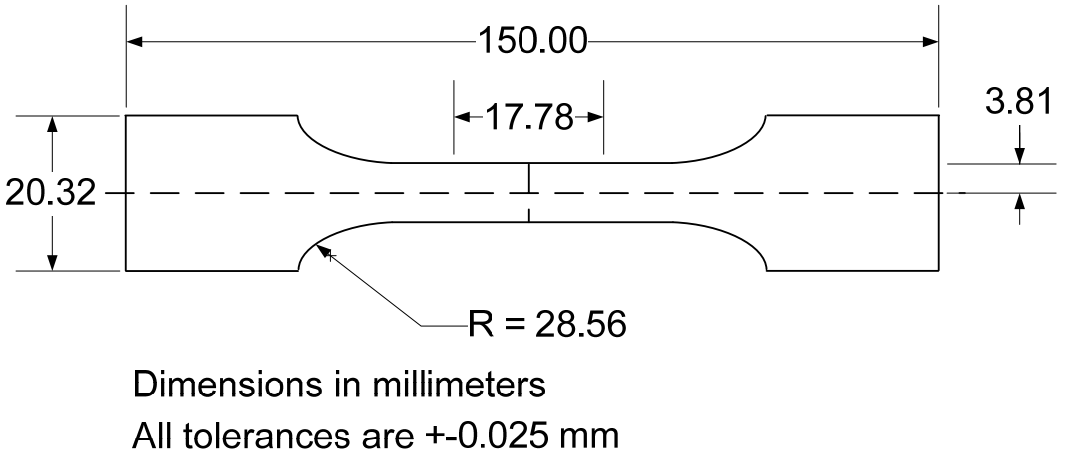

Figure 4.1: Nominal Test Specimen Geometry

Specimen Geometry

In order to ensure failure occurred within the gage section of the test specimen, standard dogbone-shaped specimens shown in Figure 4.1 were employed in this research effort Specimen thickness varied between 2.85mm and 4.38 mm with an average thickness of 3.70 mm.

Specimen Preparation

Upon receipt of the material each blank was visually inspected for uniformity and absence of defects. Test specimens were machined to specifications in Figure 4.1 using diamond grinding in order to minimize surface defects [6]. Some of the material was left as rectangular blanks and used to assess the weight loss due to aging. The test specimens and the rectangular blanks were washed in a solution consisting of 2% micro 90 soap and distilled water, then dried in a Isotemp Model 282A vacuum oven at 105° at a pressure of 6 kPa. Due to space constraints the drying was accomplished in two batches. A sample group from each batch was periodically weighed to determine when they were "dry." Each batch's weight loss stabilized in less than 10

days as shown in shown in Figure 4.2, at which time the specimens and the blanks were removed from the drying oven and stored at room temperature in a desiccator maintained at about 10% relative humidity.

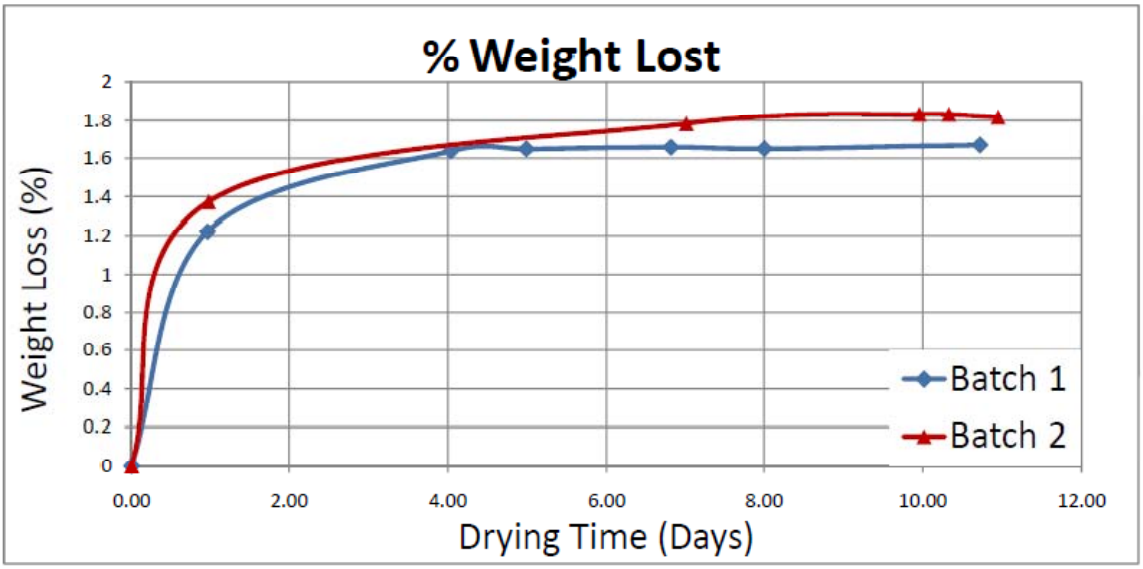

Figure 4.2: Specimen Weight Loss during Drying

In order to mount the extensometer on the specimen and avoid slippage, two small dimples were made in each specimen using a hammer and a punch provided by Material Test Systems (MTS). Dimple depth was kept to a minimum to avoid fracture initiation at the dimple. To avert slipping and to prevent the textured surface of the griping wedges from damaging the specimen small fiberglass tabs were bonded to the gripping portion of each specimen using M-bond 200, a room temperature cure epoxy.

5. Experimental Setup and Testing Procedures

This section describes the mechanical testing equipment and the test procedures used in this research.

Mechanical Testing Equipment

Room temperature modulus measurements were carried out on a vertically configured model 810 MTS servo-hydraulic testing machinewith a 15 kN (3.3 kip) load cell with . MTS hydraulic wedge grips, model 647.02B, were used with a grip pressure of 8 MPa. Strain was measured using an MTS model 632.53E-14 serial number 10184989B axial extensometer with a 12.5-mm gage section.

Elevated-temperature testing was performed on a vertically configured model 810 MTS servo-hydraulic testing machine with a 25 kN (5.5 kip) load cell. MTS hydraulic water-cooled wedge grips, model 647.02, were used with a grip pressure of 8 MPa. These grips were continuously cooled with 15°C water supplied by a Neslab RTE7chiller. A two zone MTS 653 furnace and MTS 409.83 Temperature Controllers were used for elevated temperature testing . Strain was measured using an MTS high-temperature low contact force axial extensometer, model 632.53E-14, with a 12.7-mm gage section The 25 kN (5.5 kip) hydraulic testing machine, furnace, and extensometer are depicted in Figure 5.1.

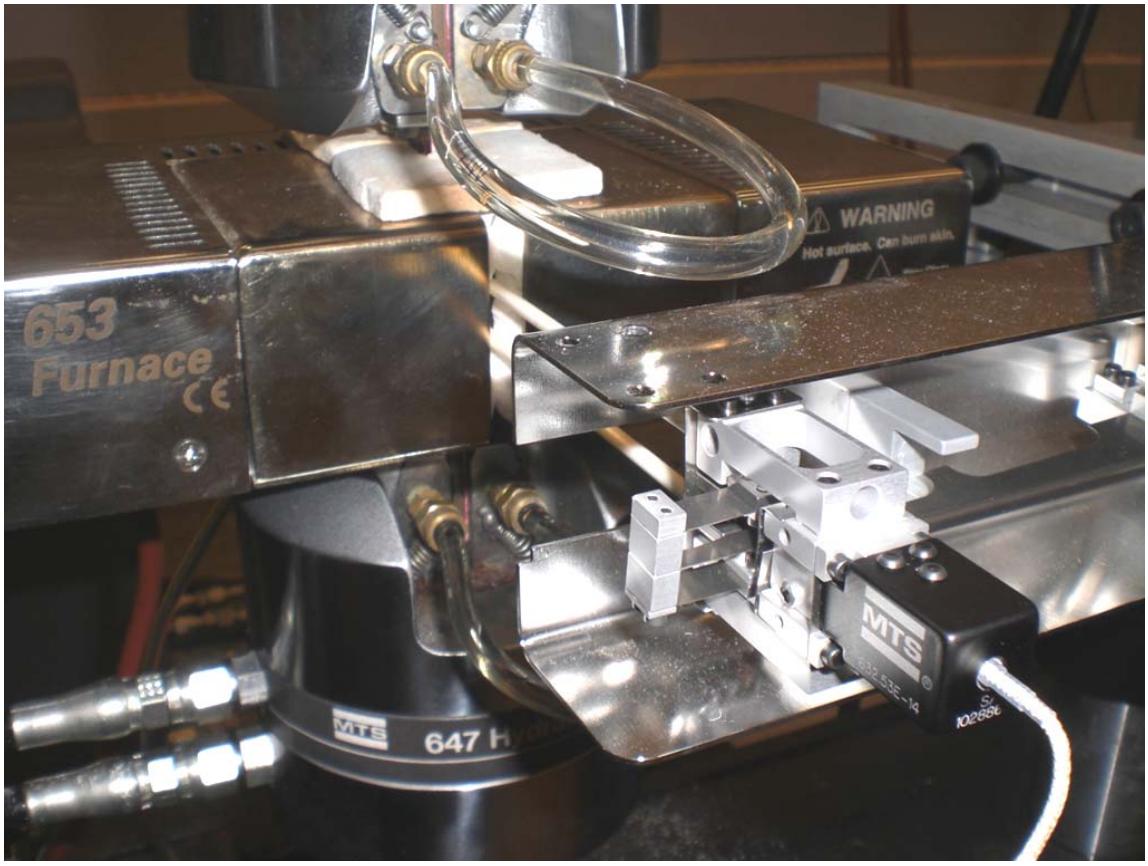

Figure 5.1: Mechanical Test Equipment Setup

Data acquisition and input signal generation were accomplished via a Flex Test 40 digital controller. MTS station builder release 5.2B was used to create a configuration file and the station manager interface was used to perform routine operations. This software enables the development of procedures which will both run the desired test and save requested data. The following signals were recorded for each test: time, zone 1 temperature, zone 2 temperature, displacement, force, strain, and the commanded. Timed data acquisition was carried out at rates sufficient to ensure that desired behavior was appropriately captured and later filtering could be performed to reduce signal noise.

Temperature Calibration and Controller Tuning

Temperature Calibration

In order to determine the temperature controller settings required to obtain a specimen temperature of 288°C a specimen was instrumented with two type K thermocouples. One thermocouple was attached to each side of the specimen using high temperature gasket material and was held firmly against the specimen with a piece of metallic wire separated from the specimen by a piece of high temperature insulation as illustrated in the cross section view shown in Figure 5.2. The size of the gasket material and insulation were kept as small as possible in order to minimize the area where the specimen was not directly exposed to heat. This mounting technique provides good contact between the thermocouple and the specimen.

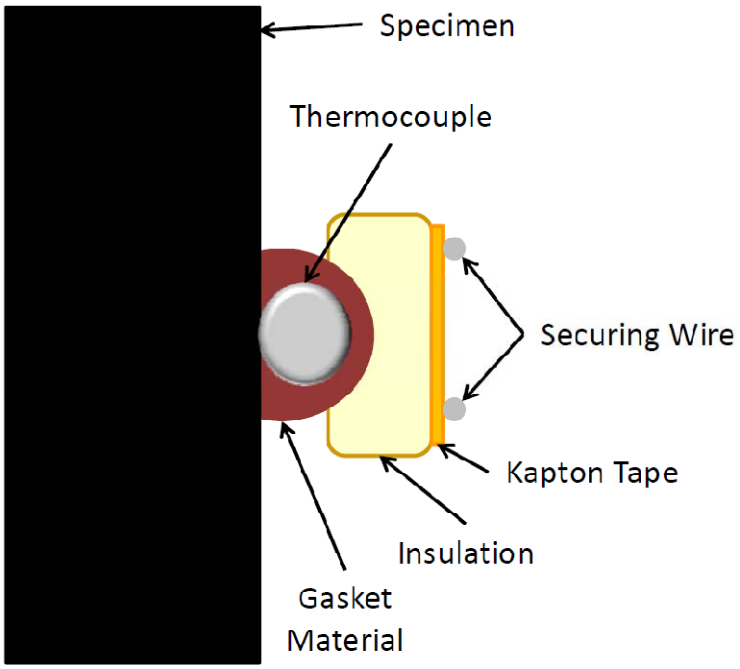

Figure 5.2: Thermocouple Mounting Schematic (Only Right Side Shown)

The temperature controller settings were adjusted until the desired temperature was obtained on the specimen. A temperature controller set point of 257°C was found to produce a specimen temperature of 288°C. It was also found that the ~3°C temperature overshoot had dissipated and thermal strain had stabilized in less than 45 minutes. The determined temperature controller settings were validated by allowing the furnace to cool to room temperature, increasing the temperature controller set point to 257°C at the rate of 2°C/min, then holding the temperature constant. Temperature was checked 45 later minutes then held constant for an additional 3 hours. It was found that the furnace maintained a specimen temperature of 288°C ±2°C during the three hours over which temperature was monitored. Thermal strain accumulated between room temperature and 288°C was found to be approximately 1.5% which is consistent with previous research [6, 12].

Tuning of the Flex Test 40 Digital Controller

Prior to testing the Flex Test 40 digital controller had to be adjusted for the PMR-15 test specimens. This calibration process is called “tuning”. Tuning involves minimizing the error between the command signal and the feedback signal. Initial tuning for the displacement control mode was performed using the controller auto tune function. As a result the following gain values were established: Proportional (P)=36.273 and Integral (I)=7.255. These gain values were verified by using the function generator in Flex Text 40 and specifying a square wave form with 5-mm amplitude and a frequency ranging from 0.1 to 1.0 Hz for the command signal. The selected values of P and I gains produced a good agreement between the command and feedback signals. Next the force control mode was tuned using an aluminum alloy specimen at room temperature and a square wave form of 1.3kN ±1.1kN at frequencies between 0.1 and 1 Hz for the command signal. The gain

values P = 6.2 and I = 3.0 were found to give good results. Finally the strain control mode was tuned using an aluminum alloy specimen and a sinusoidal wave form of 0.5% ± 0.2% strain. The gain values P = 2100 and I = 21 produced good results.

Once rough tuning had been accomplished on an aluminum alloy specimen at room temperature, final tuning using a PMR-15 specimen was carried out. The gain settings determined with the aluminum alloy specimen produced good results at room temperature. Further tuning of the load and strain control modes was performed using a PMR-15 specimen at 288°C. Tuning of the load control mode was performed using the auto tune function for a load varying between 350 N and 50 N, yielding the gain values P = 32.139 and I = 6.4279. These gain values were verified using the function generator and a square wave of 200N ±150N at frequencies between 0.1 and 1 Hz. The strain control mode was also tuned manually using the function generator and a sinusoidal wave form of 0.5% ± 0.3% strain at frequencies between 0.1 and 1 Hz. The gain values P = 2400 and I = 400 were found to produce good agreement between the command and the feedback signals. These gain settings were further verified using the function generator and a triangular wave form of 0.5% ± 0.3% strain at frequencies up to 1.0 Hz.

Isothermal Aging in Argon

All specimens used in this research were aged at 274°C in argon in a Blue M model 7780 oven. High purity argon gas (99.999% pure) was supplied to the Blue M oven from a liquid argon tank. When specimens were taken out for periodic inspection and/or testing, the oven was opened without cooling and closed immediately. Then the oven automatically entered the 28-min purge cycle to flush out any ambient air that had entered the chamber. The flow rate of argon was ~30 SCFH during the steady state operation and 150 SCFH during the purge cycle. Once specimens were removed from the Blue

M oven they were stored in the desiccator to prevent moisture absorption. In previous research efforts the aging temperature was the same as the test temperature. McClung aged and tested PMR-15 specimens at 288°C [25, 26, 27]. Ozmen investigated the aging/test temperature of 316°C [28, 29] and Diedrick considered the aging/test temperature of 260°C [10]. McClung [25, 26, 27], Ozmen [28, 29] and Diedrick [10] focused on exploring the effects of prior aging time on deformation behavior of the PMR-15 polymer at elevated temperature. The current research aims to assess the effect of prior aging temperature on the inelastic behavior of PMR-15. Therefore in this effort, the PMR-15 specimens were aged at 274°C then tested at 288°C. A group of specimens was aged at 274°C for each of the following durations: 50, 100, 250, 500, 1000 and 2000 h.

Weight Measurements

Five rectangular samples were included with each group of test specimens aged for a given duration with the purpose of monitoring weight change with aging time. The aged rectangular samples were removed from the oven, allowed to cool in the desiccator for at least 20 minutes, then weighed on a Voyager Pro VP214CN scale with an accuracy of 0.1 mg.

Mechanical Test Procedures

Room Temperature Elastic Modulus Measurements

To assess specimen-to-specimen variability room temperature elastic modulus of each specimen was measured by loading the specimen to a stress of 3 MPa at a stress rate of 1 MPa/s then unloading to zero stress at the same stress rate magnitude. These measurements were

performed on the 15 kN (3.3 kip) load frame. Previous research has shown that stress levels below 3 MPa produce nearly linear response and do not result in permanent strain [6].

Monotonic Tensile Test at Constant Strain Rate

Monotonic tensile tests to failure were conducted at 288°C and at constant strain rates of 10^{-3}, 10^{-4}, 10^{-5}, and 10^{-6} s^{-1}. Specimens from each aging group were tested. Results from these tests provided information needed to establish the initial "elastic" modulus, tangent modulus, and flow stress. These tests further served to inform the decision as to the strain level which would be selected for use in the load/unload, relaxation, and strain rate jump tests and the stress level selected for the creep tests. Testing at various constant strain rates allows the rate dependence of the material response to be evaluated. Typical strain rate dependence is schematically illustrated in Figure 5.3.

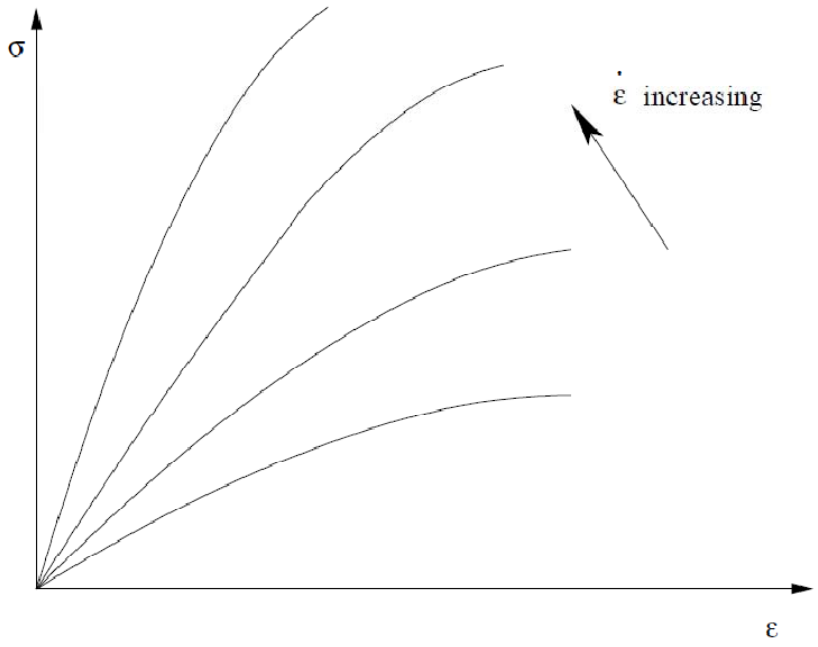

Figure 5.3: Schematic of a Set of Monotonic Tensile Tests at Various Strain Rates. Reproduced from McClung [27]

Constant Strain Rate Test with a Period of Relaxation

Specimens from each aging group were subjected to monotonic tension tests with a 12-h period of relaxation at the strain of 3%. These tests were conducted at constant strain rates of 10^{-3}, 10^{-4}, 10^{-5}, and 10^{-6} s^{-1}. Previous research has shown that a 12-h relaxation period is sufficiently long to allow stress to approach the asymptotic value [10, 27, 28]. Following the relaxation period the specimens were loaded to failure at the same constant strain rate. Within the framework of the VBOP the stress level measured at the end of a sufficiently long relaxation period is at the equilibrium stress. The results of these tests provide the data necessary to estimate the equilibrium stress at a given strain. A depiction of stress drop during relaxation is shown in Figure 5.4.

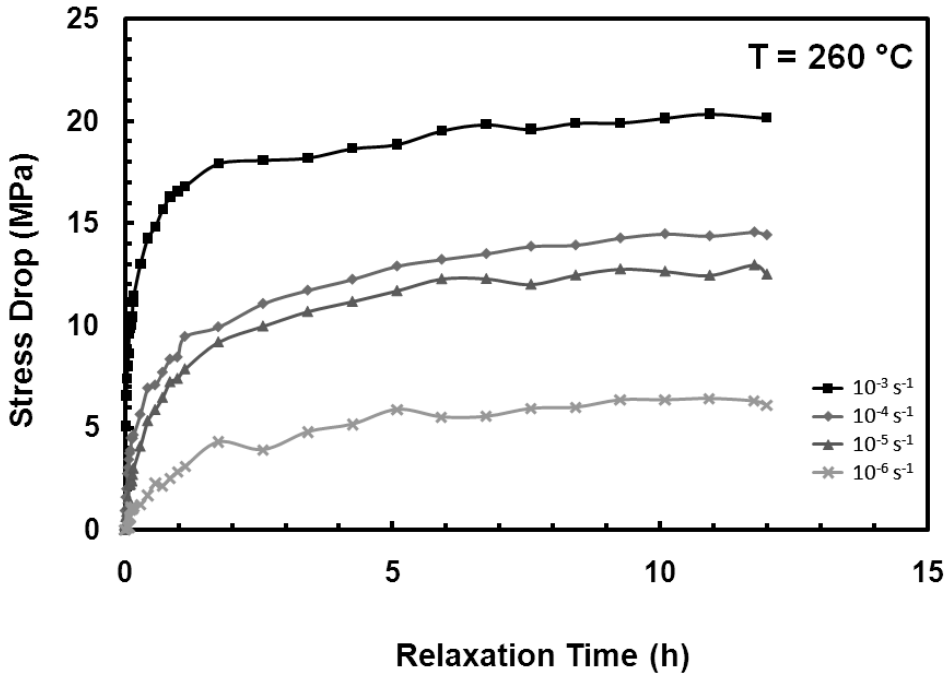

Figure 5.4: Stress Decrease vs. Relaxation Time for the Un-aged PMR-15 at 260 °C. Reproduced from Diedrick [10]

Loading / Unloading Test at Constant Strain Rate

Specimens from each aging group were also subjected to loading at a constant strain rate to the strain of 3% followed by unloading to zero stress at the same strain rate magnitude. Loading and unloading were performed at each of the following strain rate magnitudes: 10^{-3}, 10^{-4}, 10^{-5}, and 10^{-6} s^{-1}. This test is designed to reveal the effect of strain rate on the unloading behavior of PMR-15 at 288°C, In addition the effects of prior aging will be elucidated. An example of stress-strain curves obtained in a loading/unloading test performed for un-aged material at 288°C is shown in Figure 5.5.

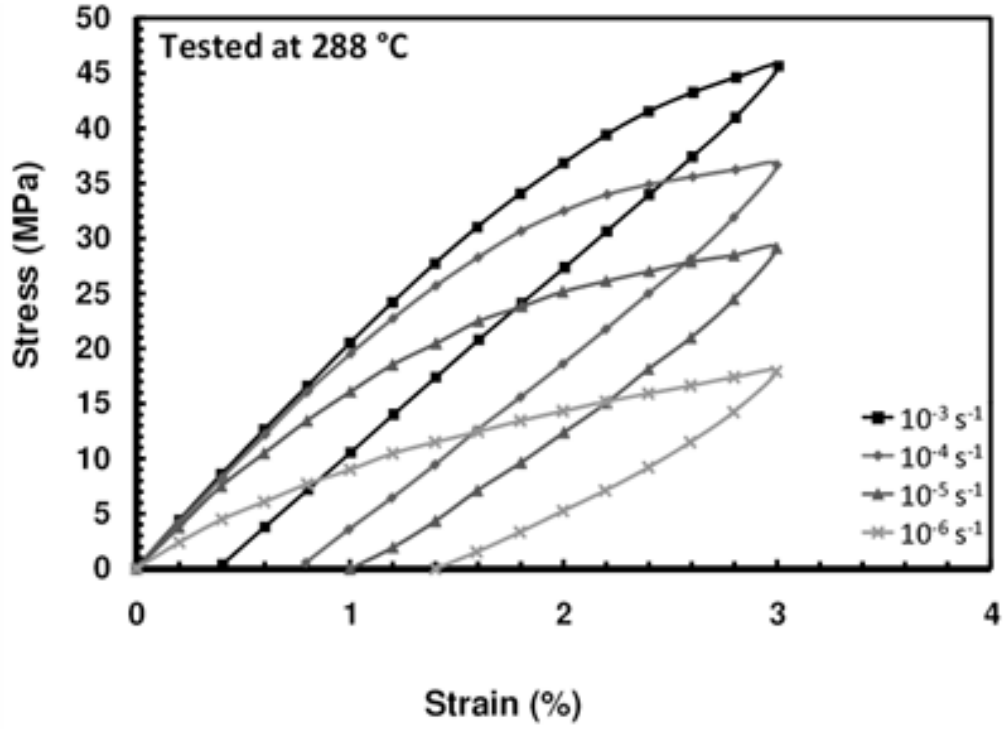

Figure 5.5: Stress-Strain Curves Obtained for PMR-15 in Loading/Unloading Tests at 288 °C. Experimental Data from McClung[27].

Recovery of Strain at Zero Stress

Immediately following the unloading portion of the loading/unloading test described above, the control mode was switched to load and the specimens were held at zero stress for a minimum of 6 h to assess the influence of prior strain rate magnitude on the recovery of strain. While zero load was maintained the change in strain was observed and recorded. The test continued until the strain approached an asymptotic solution. Recovery tests were performed for each aging group following loading/unloading at strain rate magnitudes of 10^{-3}, 10^{-4}, 10^{-5}, and 10^{-6} s^{-1}. An example of the results obtained in a recovery test is shown in Figure 5.6, where the recovered strain is presented as a percentage of the inelastic strain value measured immediately after reaching zero stress.

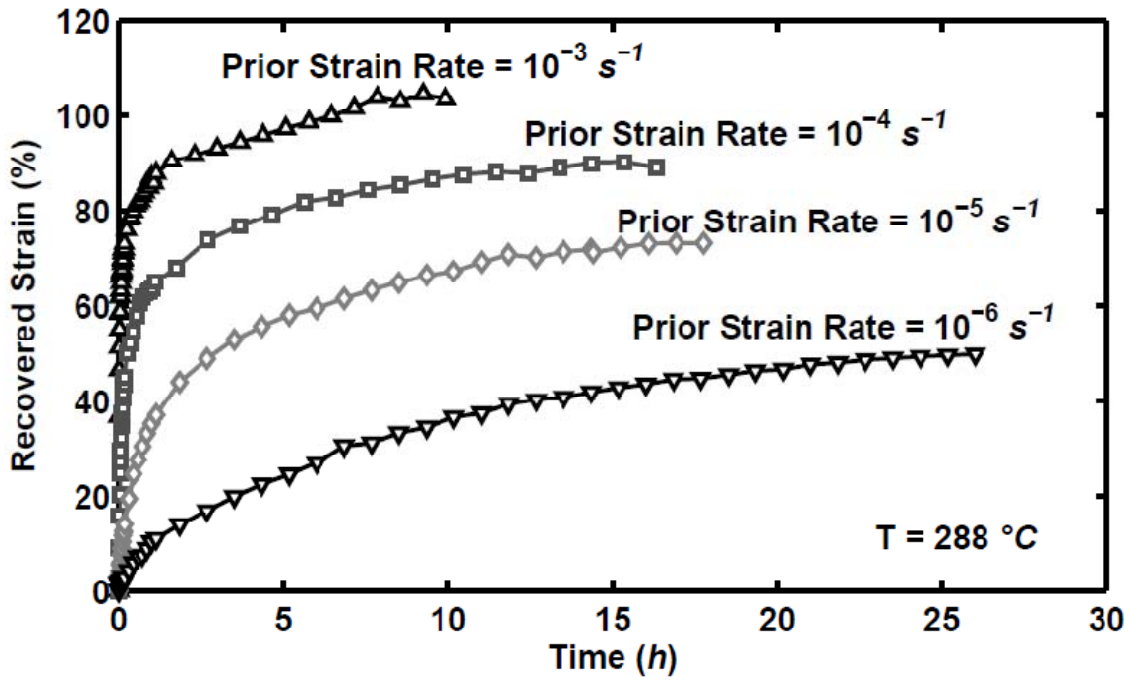

Figure 5.6: Recovery at Zero Stress Following Loading/Unloading of un-aged PMR-15 at 288 °C. Recovered Strain as Percentage of Strain Immediately After Reaching Zero Stress. Reproduced from McClung and Ruggles-Wrenn [26].

Creep Test

Specimens from each aging group were subjected to monotonic loading at strain rates of 10^{-4} and 10^{-6} s^{-1} up to a stress of 21 MPa. Once this stress level was reached the control mode was switched to load and a creep test of 6-h duration was performed. After the end of the creep period, straining resumes at the given strain rate and continues to specimen failure. These tests are designed to elucidate the influence of prior strain rate on creep behavior. Results of these tests are also used to validate the VBOP by comparing the model predictions with the experimental data. A sample of the results obtained from a creep tests are shown in Figure 5.7.

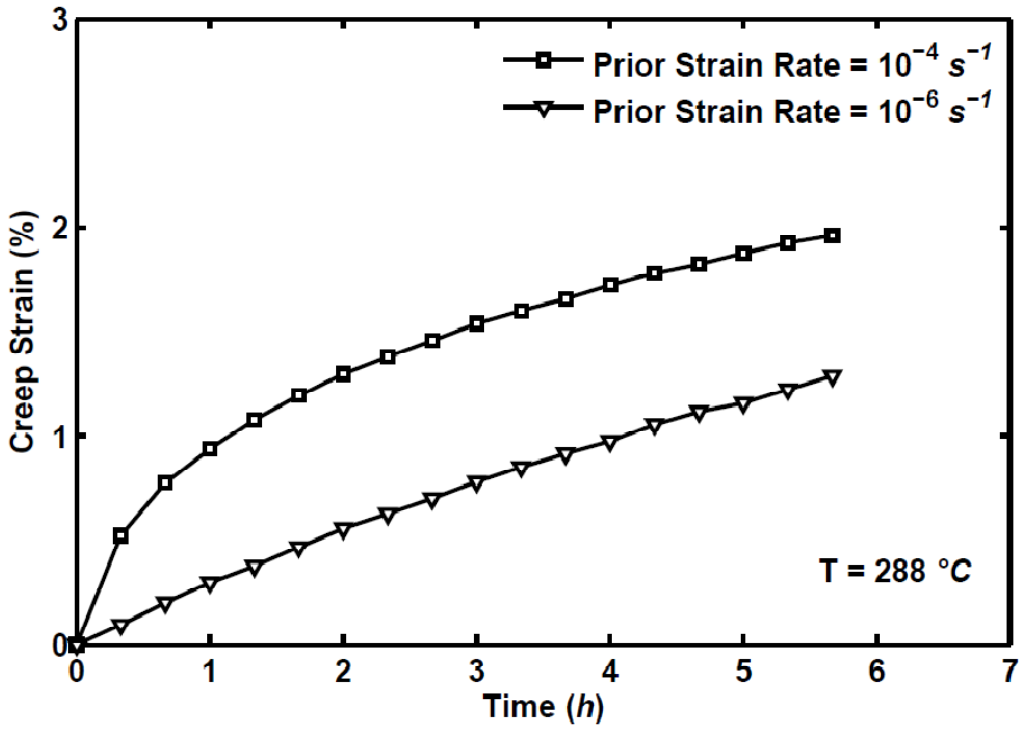

Figure 5.7: Creep Strain vs. Time for Un-aged PMR-15 at 21 MPa and 288 °C. Reproduced from McClung [26].

Strain Rate Jump Test

The strain rate jump test was employed in order to determine whether PMR-15 polymer exhibits the strain rate history effect (SRHE). The strain rate jump test consisting of segments of monotonic loading at two different strain rates test is shown schematically in Figure 5.8. Strain rates of 10^{-3} and 10^{-5} s^{-1} were employed. Specimens from each aging group were tested. Due to limited ductility of the PMR-15 polymer at 288°C, only a single strain rate jump was performed at the strain of 3.0%. The results of these tests can be compared to the stress-strain curves produced in monotonic tension tests performed at 10^{-3} and 10^{-5} s^{-1} to determine whether the material exhibits the SRHE.

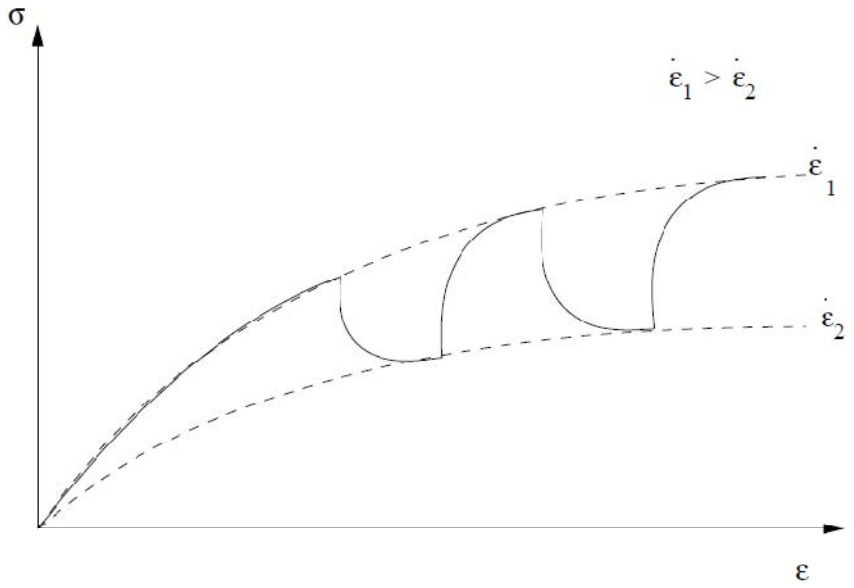

Figure 5.8: Schematic of a Strain Rate Jump Test. Reproduced from McClung [27]

6. Experimental Observations

Assessment of Specimen-to-Specimen Variability

Because each PMR-15 specimen exhibits slightly different characteristics it is necessary to quantify those differences to avoid drawing false conclusions from specimens which display atypical mechanical behavior. To accomplish this assessment of specimen-to-specimen variability room temperature modulus of each specimen was measured prior to. During these measurements the stresses were maintained below 3 MPa. Previous testing has also shown that PMR-15 at room temperature exhibits nearly linear elastic behavior below this stress level [5, 10,12, 27, 29]. To eliminate data scatter observed at very low stress levels and potential differences between the loading and unloading path a linear best fit was computed using data gathered only during loading and at stresses above 0.5 MPa. Because these tests were run in stress control and scatter is principally in strain it is proper to use a linear best fit value for compliance and then invert this value to find the modulus. This was accomplished via the MATLAB ‘polyfit’ command which performed a linear fit based on least squares of the error. The average room temperature modulus for this batch of material was 3.63 GPa with a standard deviation of 0.20 GPa. No specimens produced an anomalous value of the room-temperature elastic modulus. Hence all specimens were used in elevated temperature testing. The distribution of the room temperature elastic modulus is depicted in Figure 6.1.

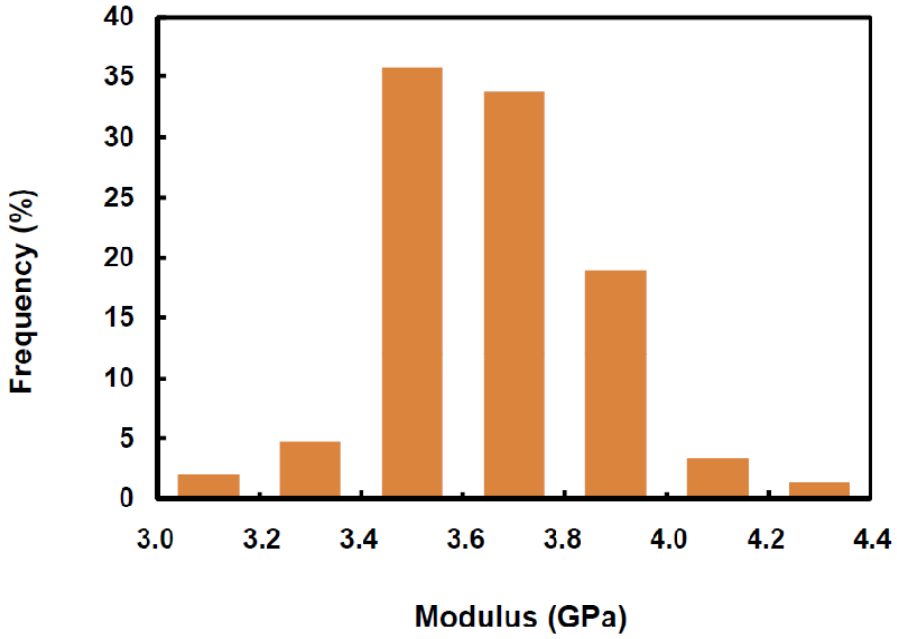

Figure 6.1: Room Temperature Elastic Modulus for the PMR-15 Polymer

Weight Loss Measurements

When polymers are exposed to elevated temperature chain scission and additional cross linking occurs [6]. This chemical degradation results in the release of light weight volatiles. The rectangular samples included with each aging group were weighed as described in Chapter 5. Changes in weight were small but measurable and a general trend of increasing weight loss with increasing aging temperature may be observed in Figure 6.2. For samples aged at 274 °C the rate of weight loss is pronounced initially, then slows down and stabilizes between 1000 and 2000 hours of aging time with samples showing very little change in weight. This stop in weight loss may be attributed to saturation in chain scission at this temperature as suggested by Broeckert [6]. It may be noted that weight loss observed for specimens aged at 260 °C appears to exceed weight loss observed for specimen aged at 274 °C for aging durations of 1000 and 2000

hours. This is likely due to specimen-to-specimen variability as only a single rectangular sample was weighed for each 260 °C aging group.

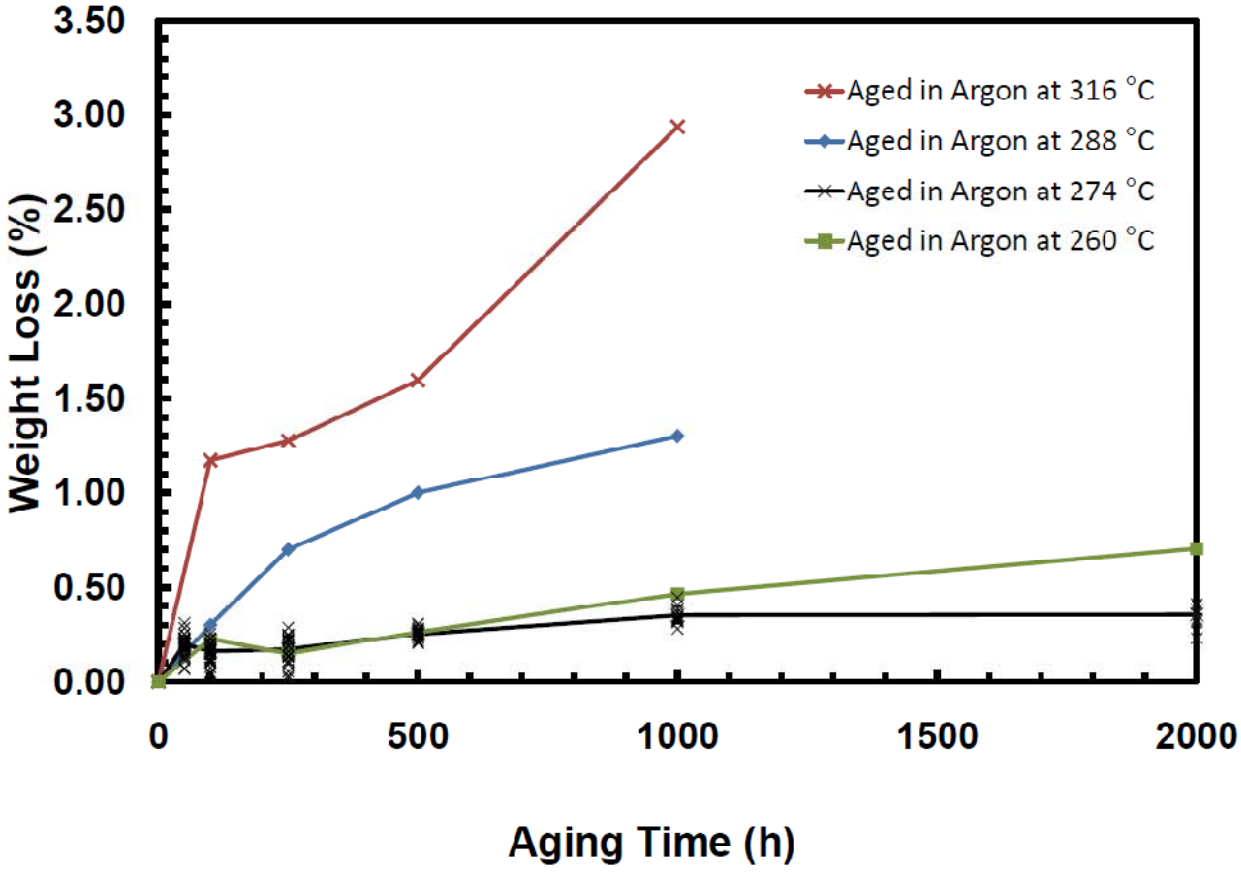

Figure 6.2: Comparison of Percent Weight Loss for PMR-15 Neat Resin Aged in Argon at 260 °C, 274 °C, 288 °C, and 316 °C. Data at 260 °C from Diedrick [10]. Data at 288 °C from Broeckert [6]. Data at 316 °C from Ozmen[28].

Thermal Expansion

Previous research has suggested that the coefficient of thermal expansion is not strongly influenced by prior aging [6, 32]. While the objectives of this research did not include a rigorous validation of this assumption, the thermal strain accumulated as the temperature increased from room temperature (24 °C) to test temperature (288 °C) was recorded for each specimen. The

coefficients of thermal expansion determined in this effort were in agreement with those reported previously [6, 12, 32]. Figure 6.3 shows an average thermal strain produced at 288 °C as a function of the duration of prior aging at 274° C in argon. The standard deviation of each sample group is represented by the vertical bars at each data point. While it appears that there is some change in average thermal strain with prior aging time it should be noted that specimen-to-specimen variability plays a much larger role. In fact, variation of average thermal strain fits well within the standard deviation of thermal strains measured for any aging group.

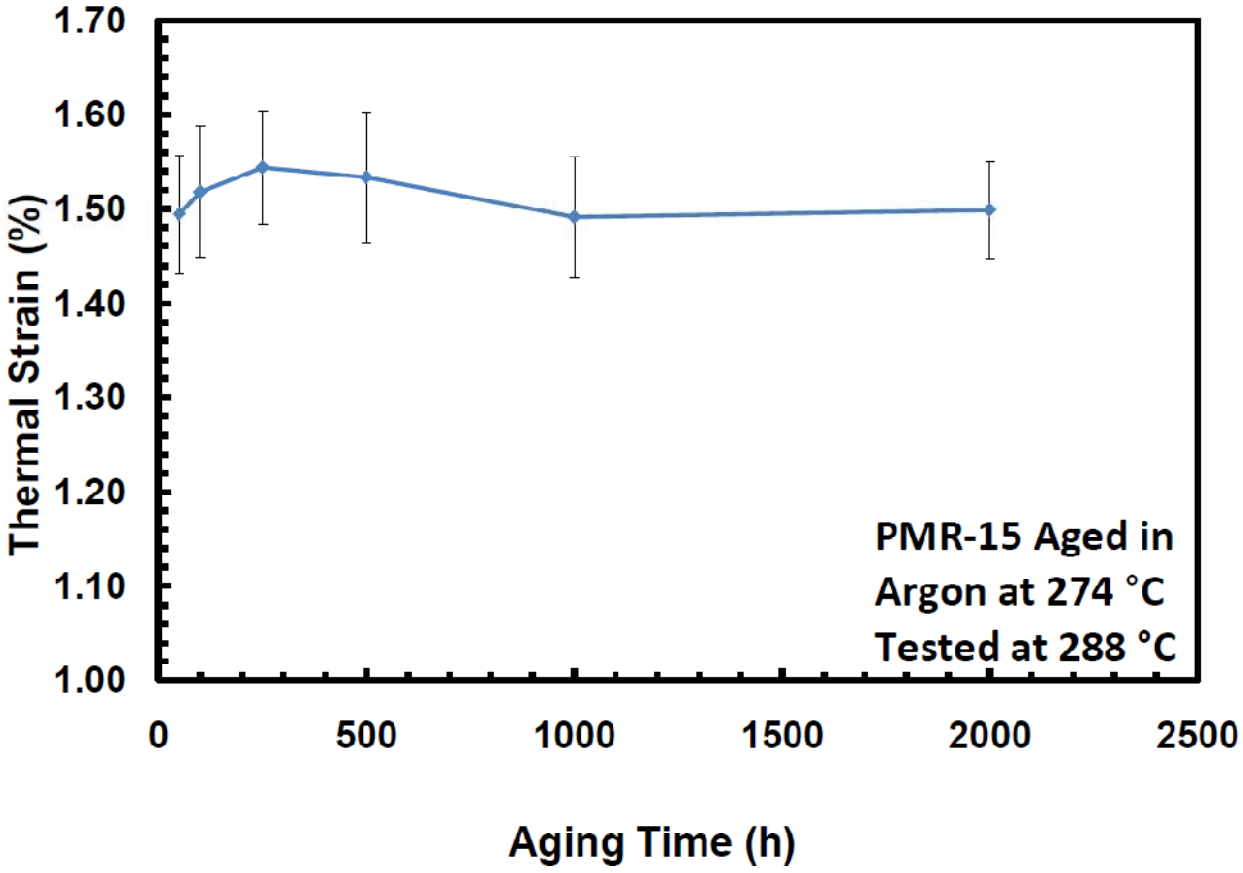

Figure 6.3: Thermal Strain at 288 °C vs. Duration of Aging in Argon at 274 °C for PMR-15 Neat Resin.

Deformation Behavior at 288 °C of PMR-15 Subjected to Prior Aging in Argon at 274 °C

To understand the effects of aging at 274 °C on the mechanical behavior of PMR-15 at 288 °C the exploratory tests outlined in Chapter 5 were carried out. The results of these tests will be organized by test type. For every test type results produced by each aging group will be reviewed, then compared to the results obtained for other aging groups. Because no un-aged specimens were tested as a part of this effort, data from experiments performed by McClung [27] will be presented in aging comparison charts.

Monotonic Tension to Failure

Specimens from each aging group were subjected to monotonic tension to failure tests at 10^{-3}, 10^{-4}, 10^{-5}, and 10^{-6} s^{-1}. For all aging durations the material exhibits no distinctly linear region as the slope of the stress strain curve diminishes gradually with increasing strain. However, in all cases the stress-strain curves exhibit nearly linear behavior in the small region immediately upon leaving the origin In this region the slope of the stress-strain curve does not exhibit a large dependence on strain rate with the average difference between the fastest (10^{-3} s^{-1}) and slowest (10^{-6} s^{-1}) loading rates being less than 0.4 GPa.

For the 50 h aging aging group the initial quasi-elastic modulus for all strain rates is 1.8 GPa. Due to unavailability of the 25 kN (5.5 kip) testing machine, monotonic tests at strain rates of 10^{-3}, 10^{-5}, and 10^{-6} s^{-1} were performed on the 15 kN (3.3 kip) testing machine. Poor alignment of this caused early failures of two specimens. Yet, even with this limited data it is seen that the strain rate has a prominent effect on the monotonic stress-strain behavior (see Figure 6.4). Increasing strain rate results in higher flow stress and a delayed departure from nearly linear stress-strain

behavior. This delayed departure from nearly linear behavior results in a more pronounced "knee" of the stress-strain curves obtained at faster strain rates.

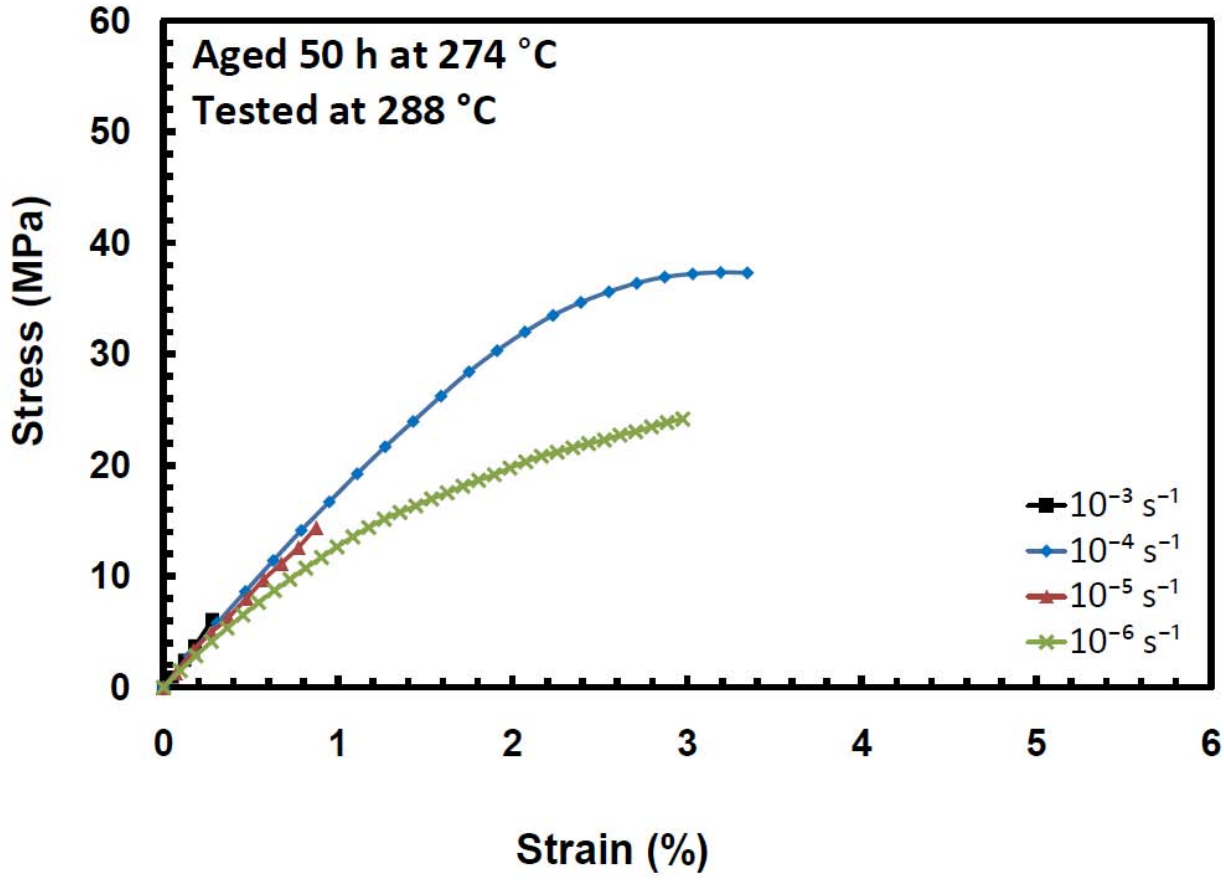

Figure 6.4: Stress-Strain Curves for PMR-15 Specimens Aged for 50 h at 274 °C in Argon Obtained in Monotonic Tension to Failure Tests Conducted at Constant Strain Rates of 10^{-3}, 10^{-4}, 10^{-5}, and 10^{-6} s^{-1} at 288 °C.

Specimens aged for 100 hours produced much larger strains in monotonic tension tests. Hence the results provide more insight into the strain rate dependence of the material behavior. Results produced at 10^{-4} and 10^{-6} sec^{-1} reveal that the flow stress increases with increasing strain rate (see Figure 6.5). Each of these tests also demonstrates that the departure from nearly linear behavior is delayed as strain rate is increased. Strain rate also has a strong effect on the shape of

the “knee” of the stress-strain curve; the “knee” becomes more pronounced with increasing strain rate. These results also demonstrate that strain rate has little effect on the tangent modulus. The stress-strain curves produced at 10^{-4} s^{-1} and at 10^{-6} s^{-1} exhibit similar slopes in the region of fully established plastic flow.

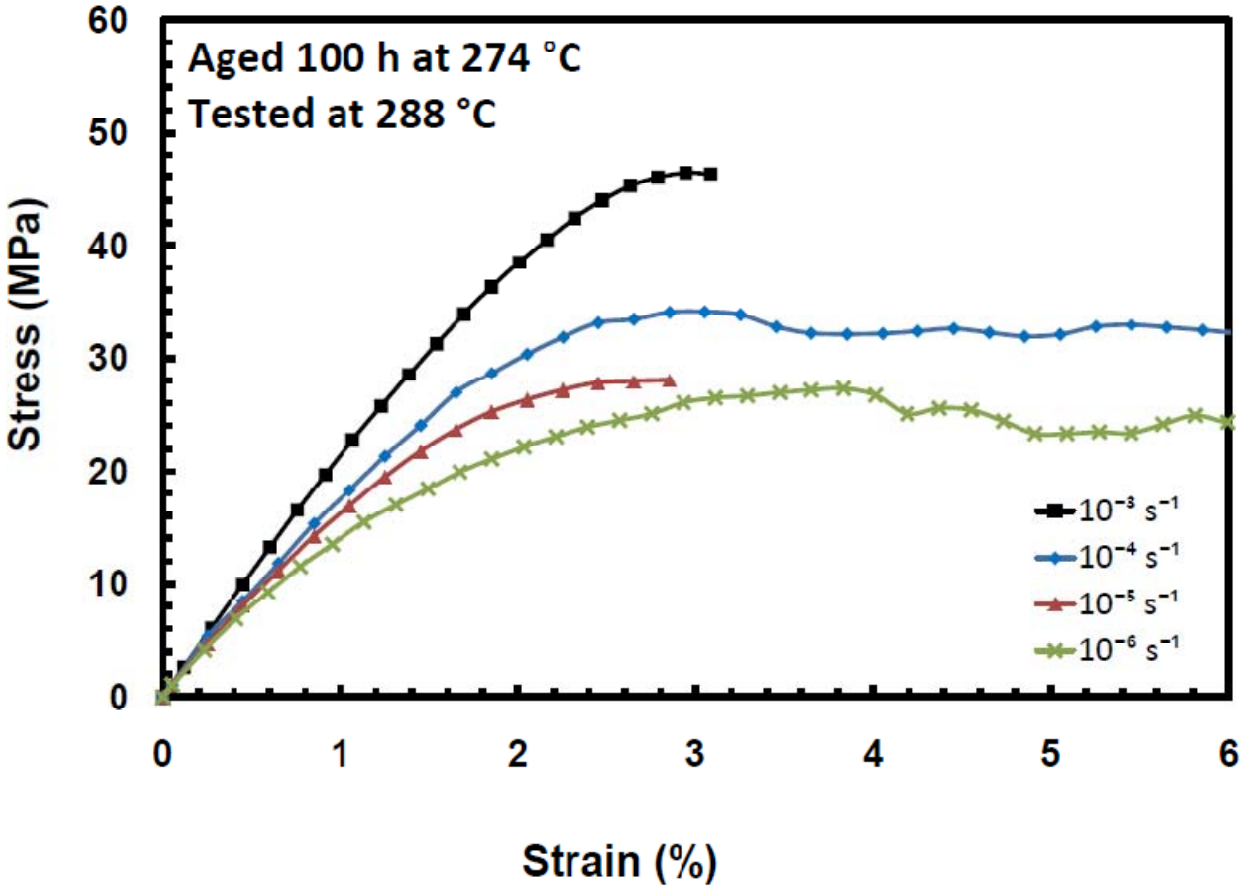

Figure 6.5: Stress-Strain Curves for PMR-15 Specimens Aged for 100 h at 274 °C in Argon Obtained in Monotonic Tension to Failure Tests Conducted at Constant Strain Rates of 10^{-3}, 10^{-4}, 10^{-5}, and 10^{-6} s^{-1} at 288 °C.

Some of the specimens aged for 250 hours exhibited the expected strain rate dependence as shown in Figure 6.6. However, the specimen tested at 10^{-4} s^{-1} produced non typical results with stress-strain curve lying very close to the test performed at a strain rate of 10^{-5} s^{-1}. This

behavior is likely attributable to specimen-to-specimen variability. Additionally the specimen tested at 10^{-4} s^{-1} exhibited an anomalous stress drop following the knee which is not consistent with other testing.

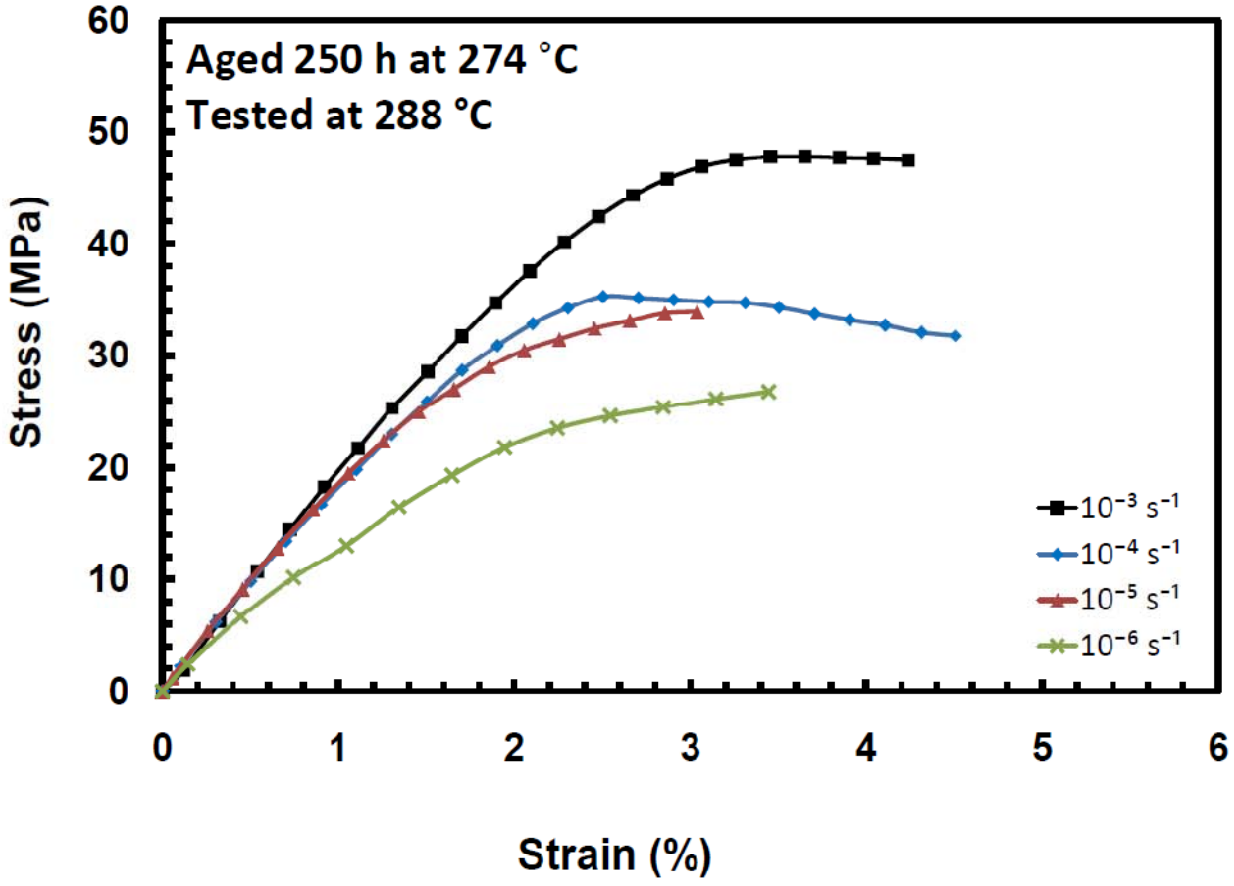

Figure 6.6: Stress-Strain Curves for PMR-15 Specimens Aged for 250 h at 274 °C in Argon Obtained in Monotonic Tension to Failure Tests Conducted at Constant Strain Rates of 10^{-3}, 10^{-4}, 10^{-5}, and 10^{-6} s^{-1} at 288 °C.

Figure 6.7 shows the stress-strain behavior for specimen subjected to 500 h of aging in argon at 274°C. The strain rate dependence is again evident. Note that the specimen loaded at 10^{-5} s^{-1} exhibits a higher tangent modulus than that exhibited by specimens subjected to prior

aging of shorter duration. Results in Figure 6.7 also demonstrate a more pronounced “knee” is produced at higher strain rates.

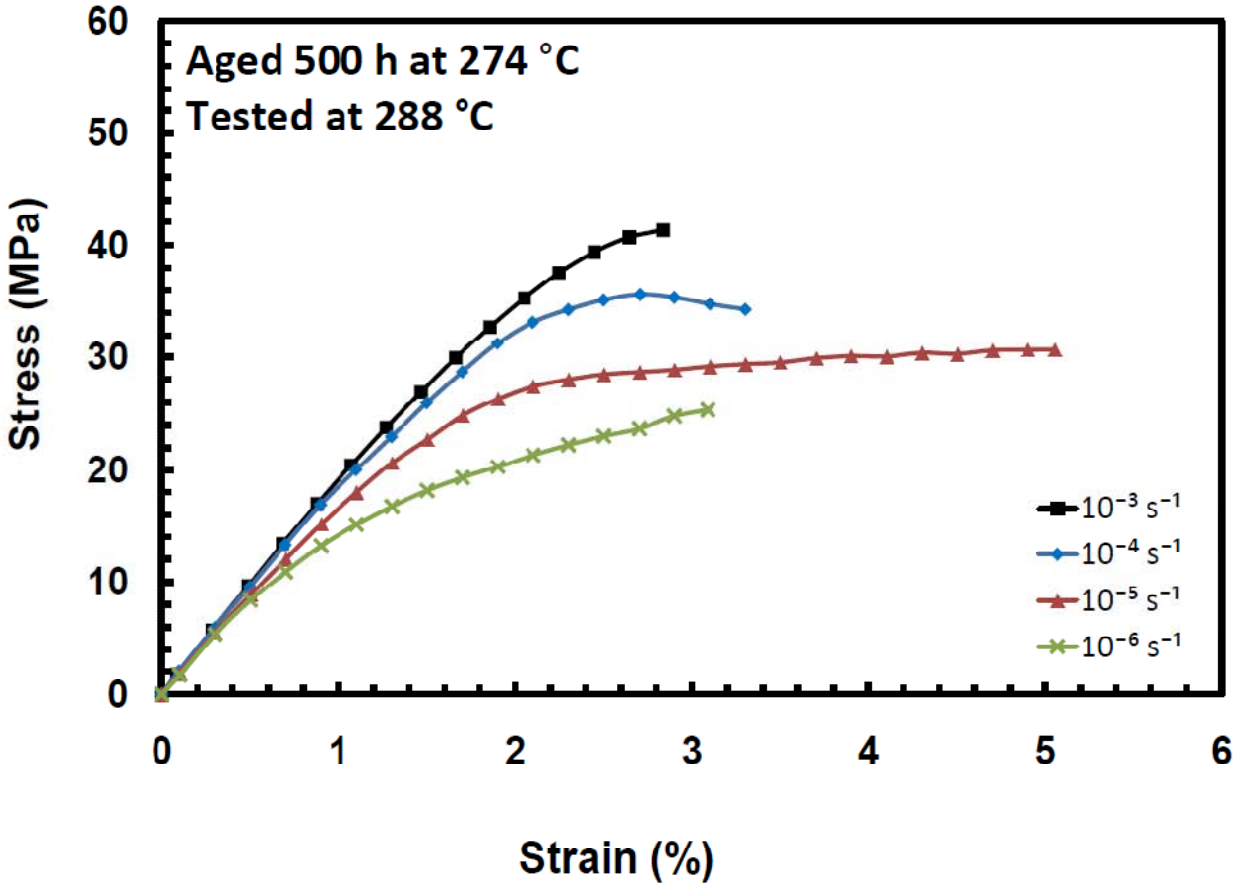

Figure 6.7: Stress-Strain Curves for PMR-15 Specimens Aged for 500 h at 274 °C in Argon Obtained in Monotonic Tension to Failure Tests Conducted at Constant Strain Rates of 10^{-3}, 10^{-4}, 10^{-5}, and 10^{-6} s^{-1} at 288 °C.

All specimens subjected to 100 h of prior aging entered the flow stress region during monotonic tension to failure tests (Figure 6.8). Results obtained at 10^{-3}, 10^{-4}, and 10^{-6} s^{-1} clearly demonstrate that departure from nearly linear behavior is strongly influenced by strain rate (Figure 6.8). Note that the stress-strain curve produced at a strain rate of 10^{-5} s^{-1} departs from nearly liner behavior sooner, and exhibits lower flow stress levels than expected.

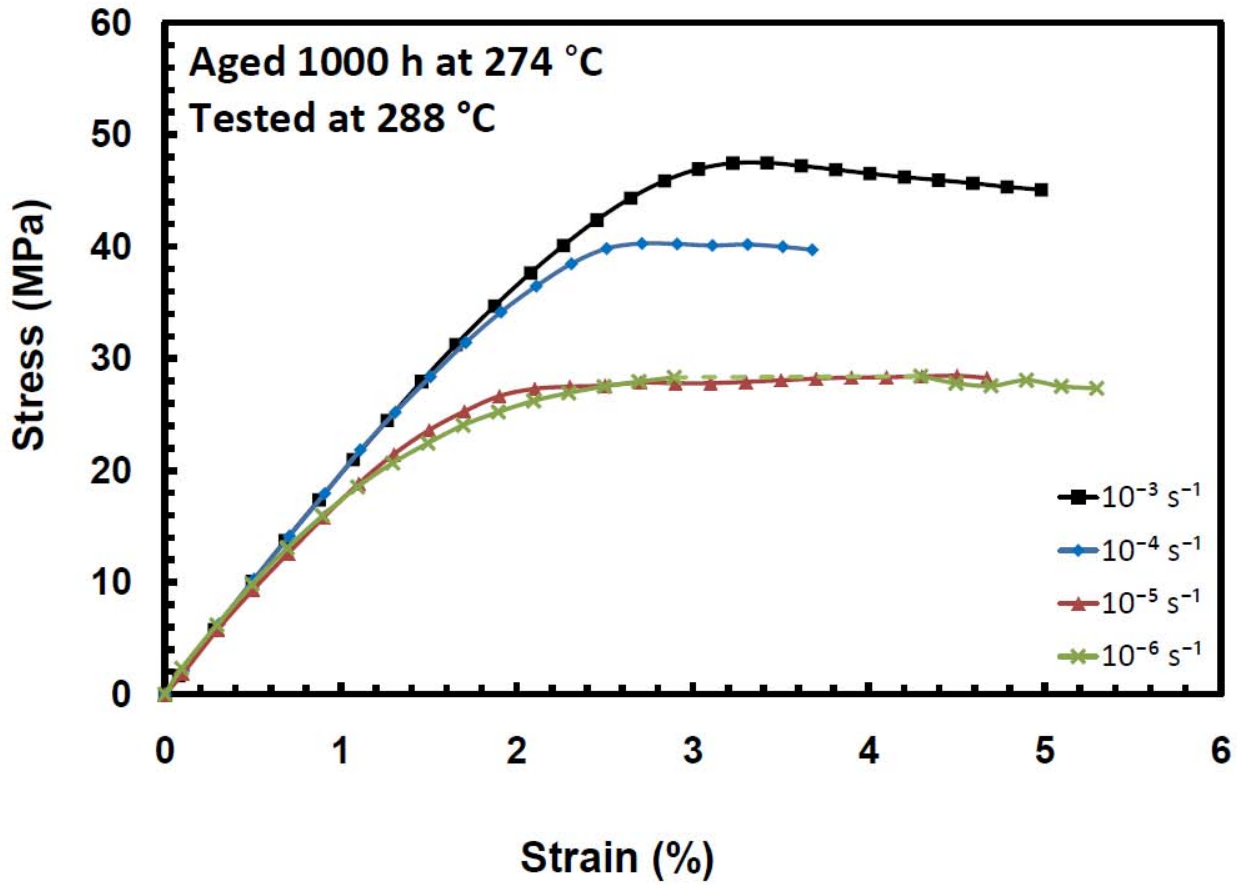

Figure 6.8: Stress-Strain Curves for PMR-15 Specimens Aged for 1000 h at 274 °C in Argon Obtained in Monotonic Tension to Failure Tests Conducted at Constant Strain Rates of 10^{-3}, 10^{-4}, 10^{-5}, and 10^{-6} s^{-1} at 288 °C.

Results of the monotonic tension to failure tests obtained for specimens aged for 2000 h are depicted in Figure 6.9. The specimens tested at 10^{-3} s^{-1} and at 10^{-4} s^{-1} failed before reaching the flow stress region, however specimens loaded at slower strain rates produced deformations well beyond the nearly liner region. All stress-strain curves exhibit nearly identical slopes at or near maximum strain, confirming McClung's assertion that tangent modulus is nearly independent of strain rate [27]. Note that the stress-strain curve obtained at a strain rate of 10^{-6} s^{-1} exhibits a negative slope at about 4.25% strain. A careful review of the recorded test data

revealed a marked increase in test temperature at this point in time. This increase in temperature was observed in other tests conducted in both load and strain control. Monitoring the ambient temperature in the laboratory revealed a ~5 °C increase in average ambient temperature between 9:00 pm and 4:00 am, when the building air conditioning system is inactive. It is conjectured that the change in the thermal profile of the specimen is caused by the change in the ambient temperature.

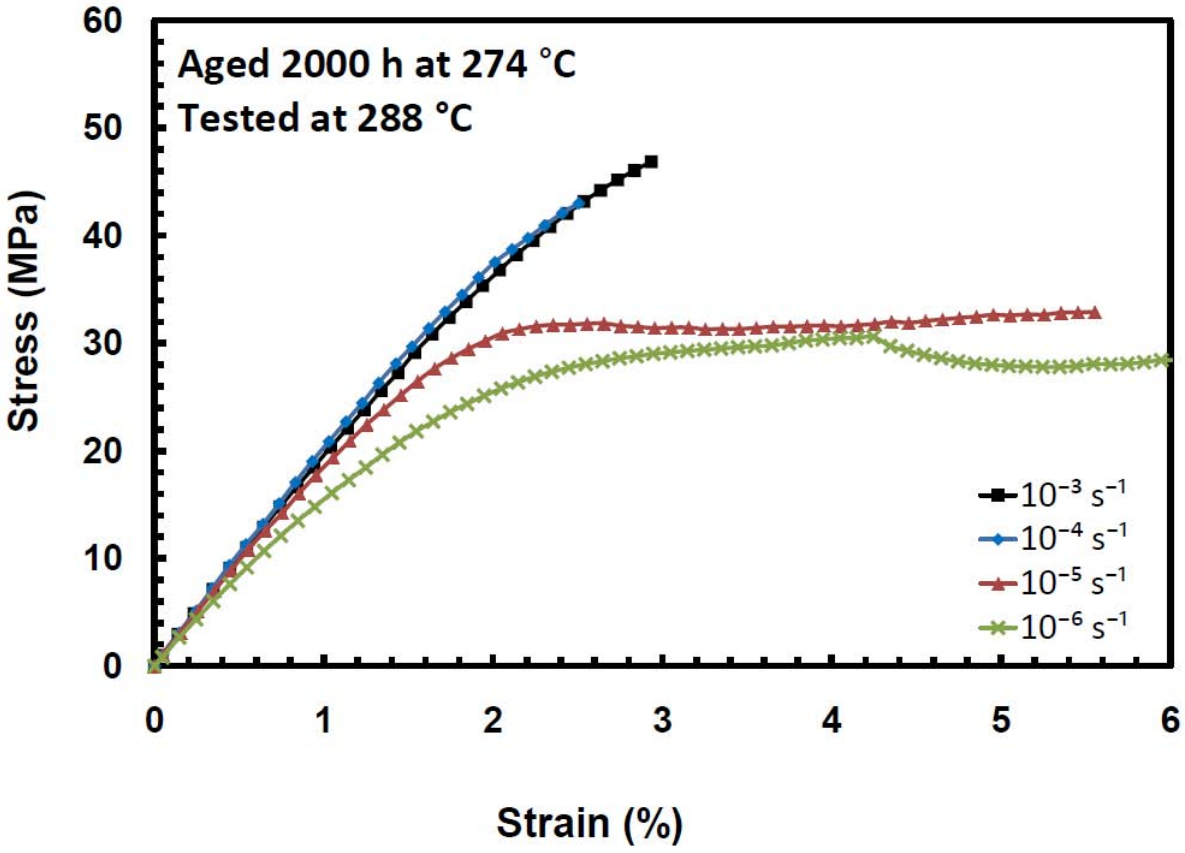

Figure 6.9: Stress-Strain Curves for PMR-15 Specimens Aged for 2000 h at 274 °C in Argon Obtained in Monotonic Tension to Failure Tests Conducted at Constant Strain Rates of 10^{-3}, 10^{-4}, 10^{-5}, and 10^{-6} s^{-1} at 288 °C.

To elucidate changes in deformation behavior due to aging, results of the monotonic tensile tests obtained at a given strain rate for specimens in different aging groups are presented

together in Figure 6.10 through Figure 6.13. Figure 6.10 presents the stress-strain curves produced at a strain rate of 10^{-3} s^{-1}. The effects of aging duration on both the flow stress and the knee of the stress-strain curve are readily seen. Increasing aging duration produces a higher flow stress and causes a more pronounced knee. Additionally, the slope of the stress-strain curve immediately upon leaving the origin increases with increasing aging duration.

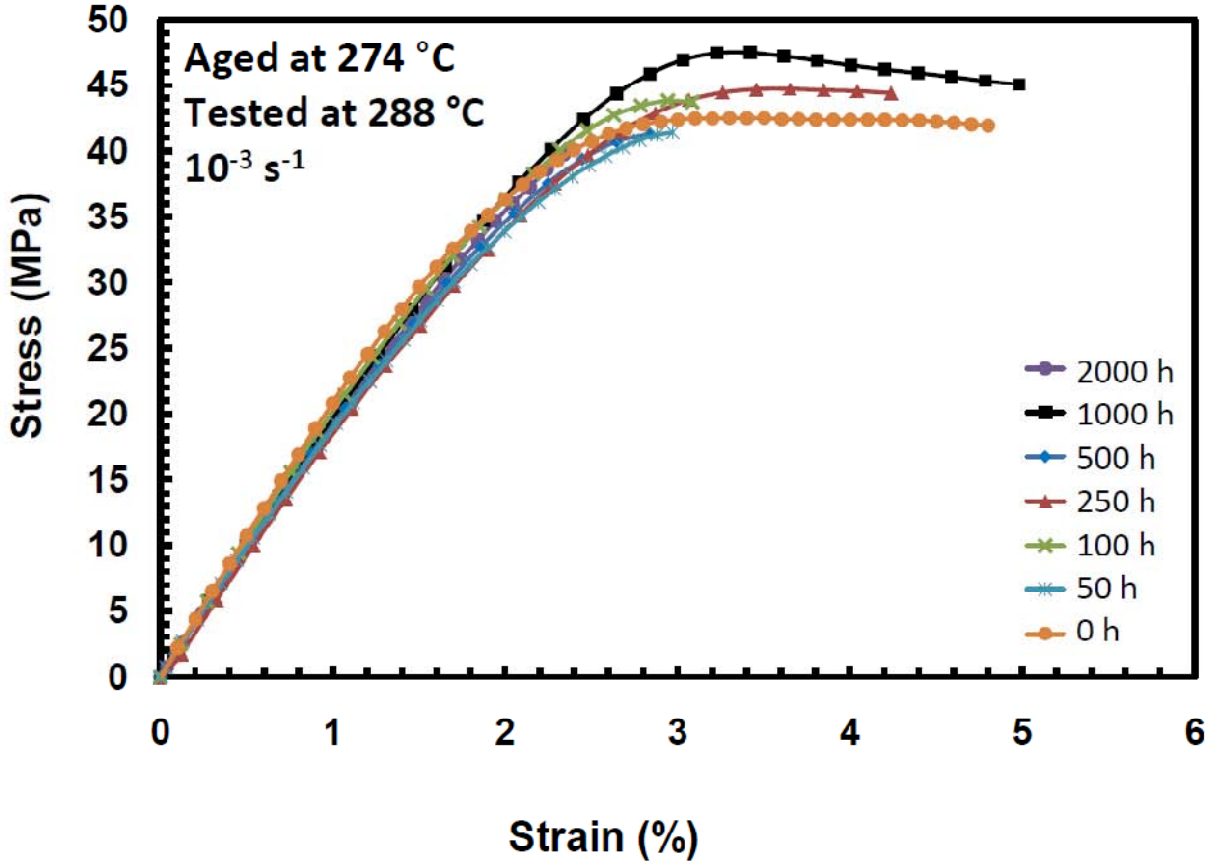

Figure 6.10: Stress-Strain Curves Obtained in Monotonic Tensile Tests at a Strain Rate of 10^{-3} s^{-1} at 288 °C for PMR-15 Aged at 274 °C for 0 to 2000 h. Data for the Un-aged Material from McClung[27].

The results of tests performed at a strain rate of 10^{-4} s^{-1} are in displayed in Figure 6.11. The effects of prior aging are more pronounced at this lower strain rate. The specimen subjected

to 50 hours of prior aging exhibited higher stress than was typical for this strain rate. Specimens subjected to prior aging for 0, 100, and 250 h show only minor changes in behavior. Specimens aged for 500, 1000, and 2000 h showed delayed departure from nearly linear behavior with increasing aging duration. The specimens aged for 500 and 1000 h also produced stress-strain curves with the increasingly pronounced knee and higher flow stress levels. These results illustrate the effects of prior aging on tensile stress-strain behavior.

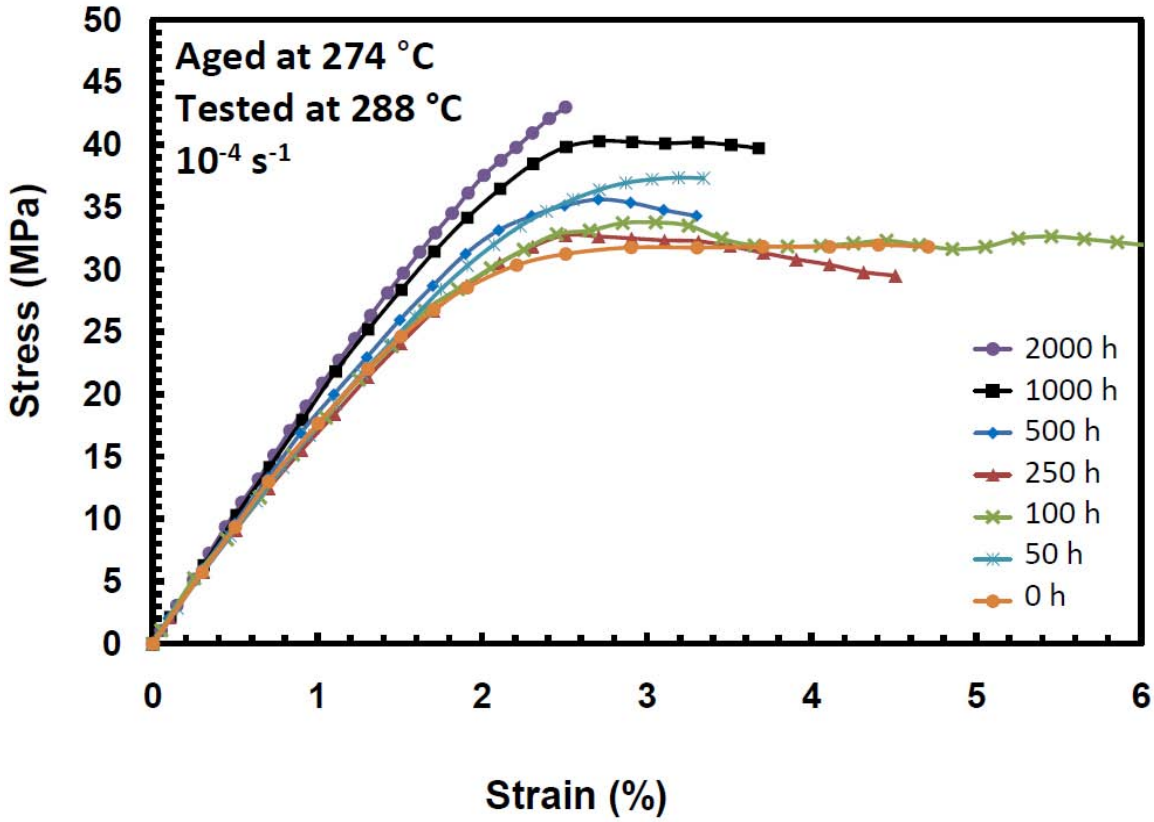

Figure 6.11: Stress-Strain Curves Obtained in Monotonic Tensile Tests at a Strain Rate of 10^{-4} s^{-1} at 288 °C for PMR-15 Aged at 274 °C for 0 to 2000 h. Data for the Un-aged Material from McClung[27].

Figure 6.12 shows the results produced at a strain rate of 10^{-5} s^{-1}. At this strain rate the specimens attain much larger strains, hence the changes in flow stress are easier to observe.

Specimens aged for 0, 50, and 100 h show very little difference in behavior. Specimens subjected to longer aging durations show delayed departure from nearly linear behavior. The knee of the stress-strain curve also becomes more pronounced, with the 2000 h specimen exhibiting a "stress overshoot." Flow stress increases with aging duration. Although difficult to observe in Figure 6.12, computed tangent modulus also increases with aging duration.

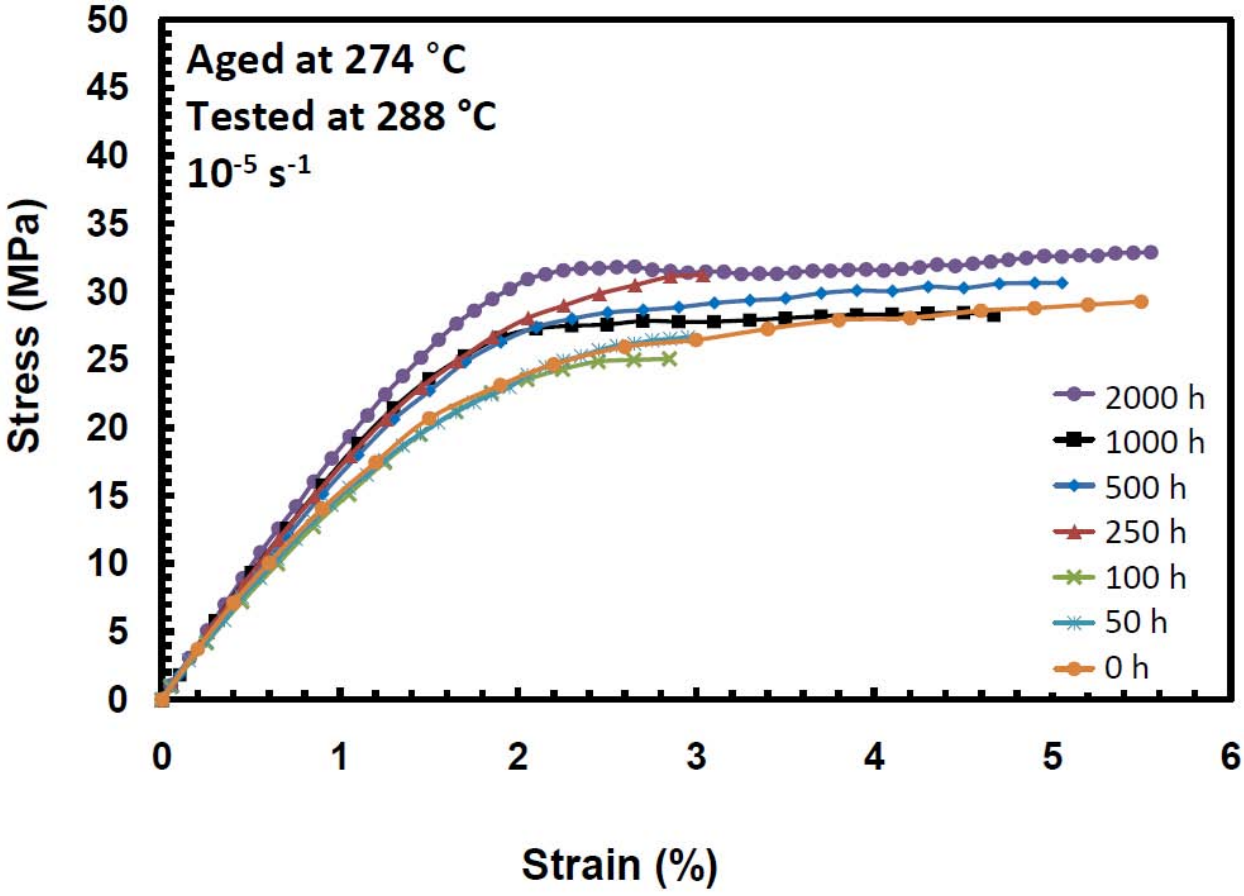

Figure 6.12: Stress-Strain Curves Obtained in Monotonic Tensile Tests at a Strain Rate of 10^{-5} s^{-1} at 288 °C for PMR-15 Aged at 274 °C for 0 to 2000 h. Data for the Un-aged Material from McClung[27].

At the slowest strain rate of 10^{-6} s^{-1} the effects of high temperature aging are most pronounced. The response of the un-aged specimen appears significantly "softer" than that of

the specimen subjected to even short aging durations. This may be due to material batch variability. However, at slow strain rates significant changes in material behavior of the specimens aged for short durations may also be observed in data reported by McClung [27]. The weight loss data in Figure 6.2, results in Figure 6.13, and results of experiments conducted at slow strain rates reported by McClung [27] suggest that the changes in material behavior occur rapidly during the initial hours of aging then approach some slower constant rate for subsequent hours of aging.

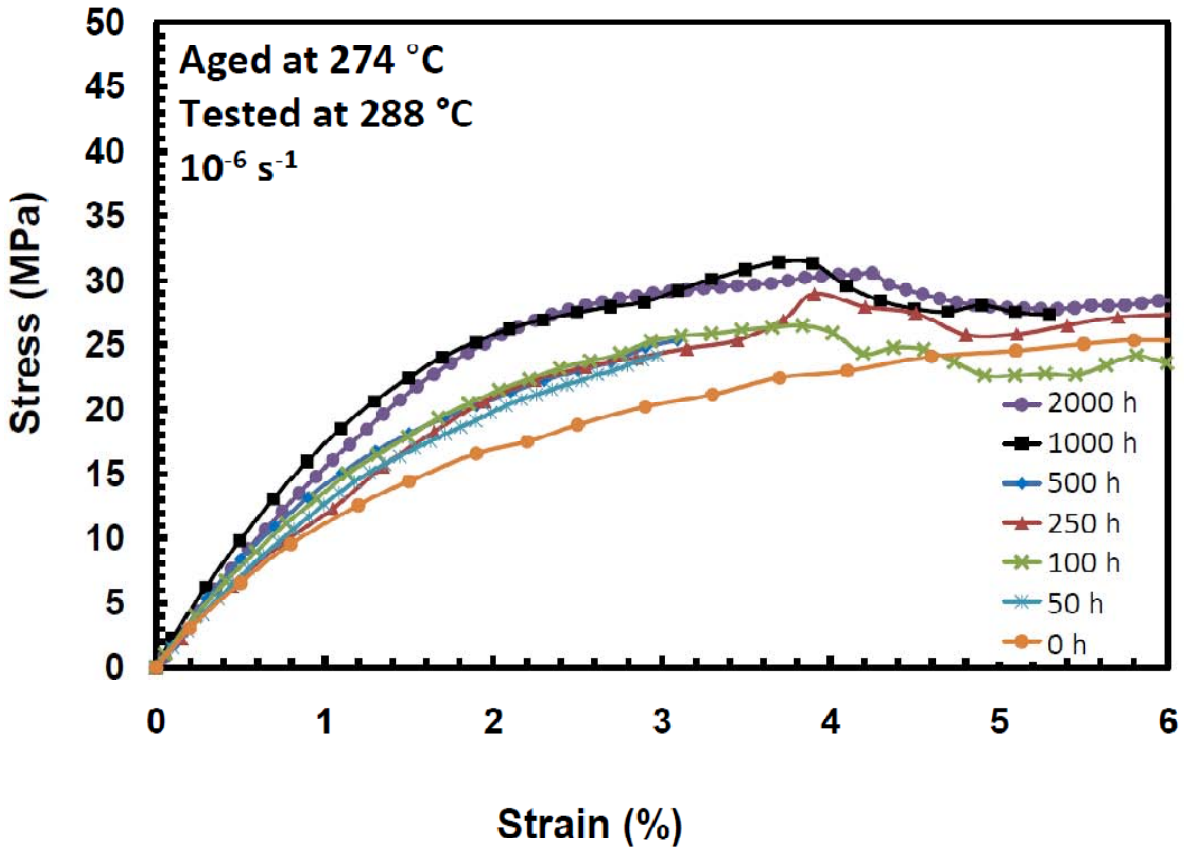

Figure 6.13: Stress-Strain Curves Obtained in Monotonic Tensile Tests at a Strain Rate of 10^{-3} s^{-1} for PMR-15 Aged at 274 °C for 0 to 2000 h, Tested at 288 °C Un-aged Experimental Data from McClung[27].

Constant Strain Rate Test with a Period of Relaxation

To characterize VBOP relaxation tests must be performed. In a relaxation test the strain is held constant while and the load is allowed to vary with time. To accurately characterize the VBOP model the relaxation test should be performed in the region of fully established plastic flow. Results in Figure 6.6 show that the specimens in the 250-h aging group subjected to monotonic tension to failure tests at 10^{-3} s^{-1} achieve fully established plastic flow only at strains $\geq$ 3.5%. Therefore, the relaxation test should be performed at a strain greater than 3.5%. However, because a large percentage of the specimens failed at strains < 3.5% a strain of 3% was selected for relaxation tests. Specimens were loaded at constant strain rate to the strain of 3%, where a 12-h relaxation test was performed. The strain rates of 10^{-3}, 10^{-4}, 10^{-5}, and 10^{-6} s^{-1} were employed. It was found that 12 hours was sufficient for the stress to reach asymptotic values during relaxation. Following relaxation each specimen was loaded to failure at the strain rate used in the initial loading of the specimen.

A figure depicting the stress-strain behavior of material aged for 50 hours at 274°C is shown in Figure 6.14. It is seen that the increasing strain rate results in delayed departure from nearly linear behavior, a more pronounced knee of the stress-strain curve, and increasing flow stress. Note that the monotonic stress-strain behavior produced at the strain rate of 10^{-4} s^{-1} during initial strain-controlled loading is very similar to that produced at 10^{-5} s^{-1}. This observation suggests that the scatter in the monotonic stress-strain response due to specimen-to-specimen variability is comparable to the difference in the stress-strain response caused by an order of magnitude change in strain rate. The results in Figure 6.10 also reveal that a nearly equal stress level was reached by all specimens at the end of the relaxation test, regardless of the prior strain

rate. After the relaxation test, straining resumed at the strain rate used during initial loading. It is seen in Figure 6.10 that during this latter part of the test flow stress levels characteristic of a given strain rate were reached in all tests.

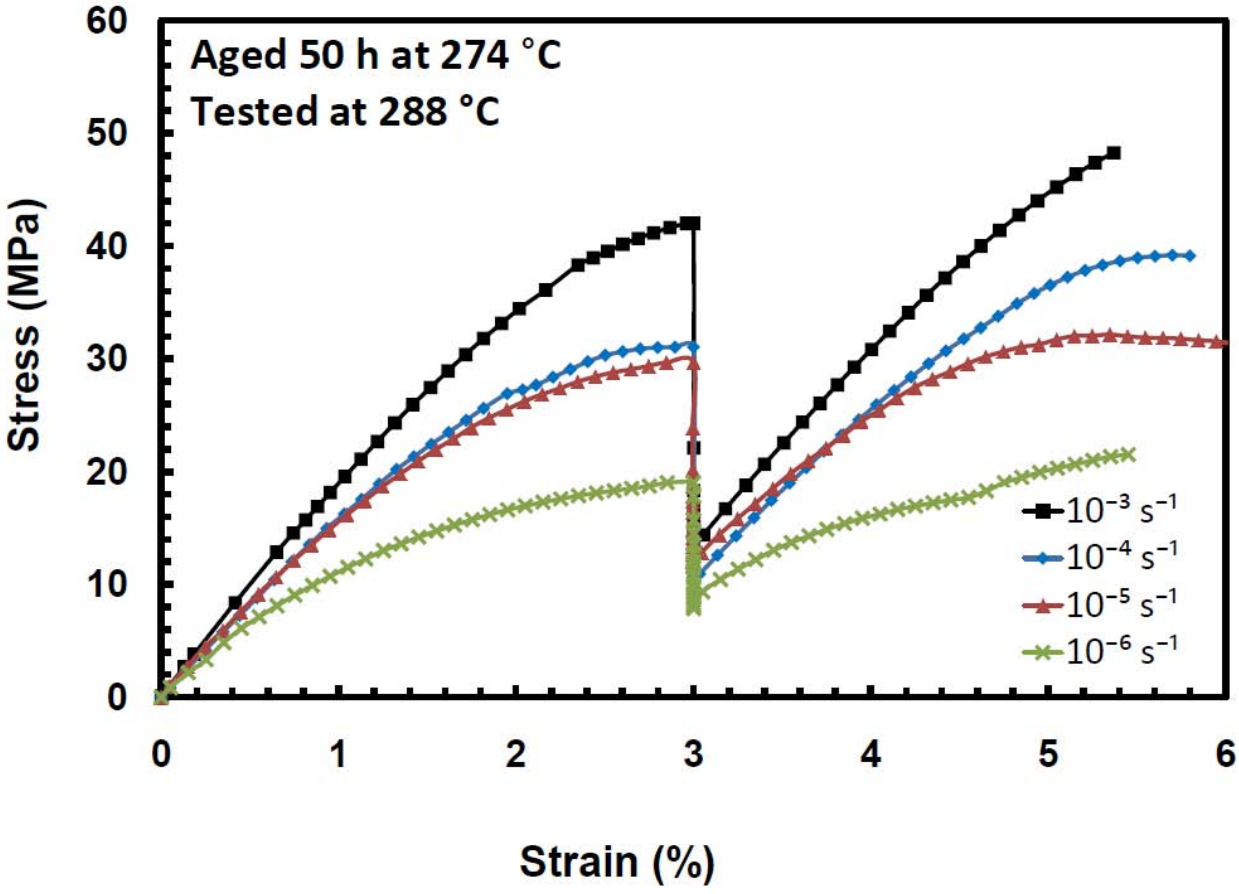

Figure 6.14: Stress-Strain Curves for PMR-15 Specimens Aged for 50 h at 274 °C in Argon Obtained in Constant Strain Rate Tests with a Period of Relaxation Conducted at Constant Strain Rates of 10^{-3}, 10^{-4}, 10^{-5}, and 10^{-6} s^{-1} at 288 °C.

Stress-strain response obtained for specimens in the 100-h aging group is depicted in Figure 6.15. The results in this figure demonstrate delayed departure from nearly linear behavior, a more pronounced knee of the stress-strain curve, and increasing flow stress with increasing loading rate. As was the case for the specimens in the 50-h aging group, the monotonic stress-

strain curves produced at strain rates of 10^{-4} and 10^{-5} s^{-1} are nearly the same. At the end of the relaxation test, most specimens produced the same stress level. However, the specimen strained at 10^{-5} s^{-1} before the relaxation test, produced an uncharacteristically high stress level at the end of relaxation. Straining resumed after the relaxation test was complete produced flow stress levels characteristic of the strain rate employed. The specimen tested with the strain rate of 10^{-5} s^{-1} represents an exception. In this case the stress levels were uncharacteristically high.

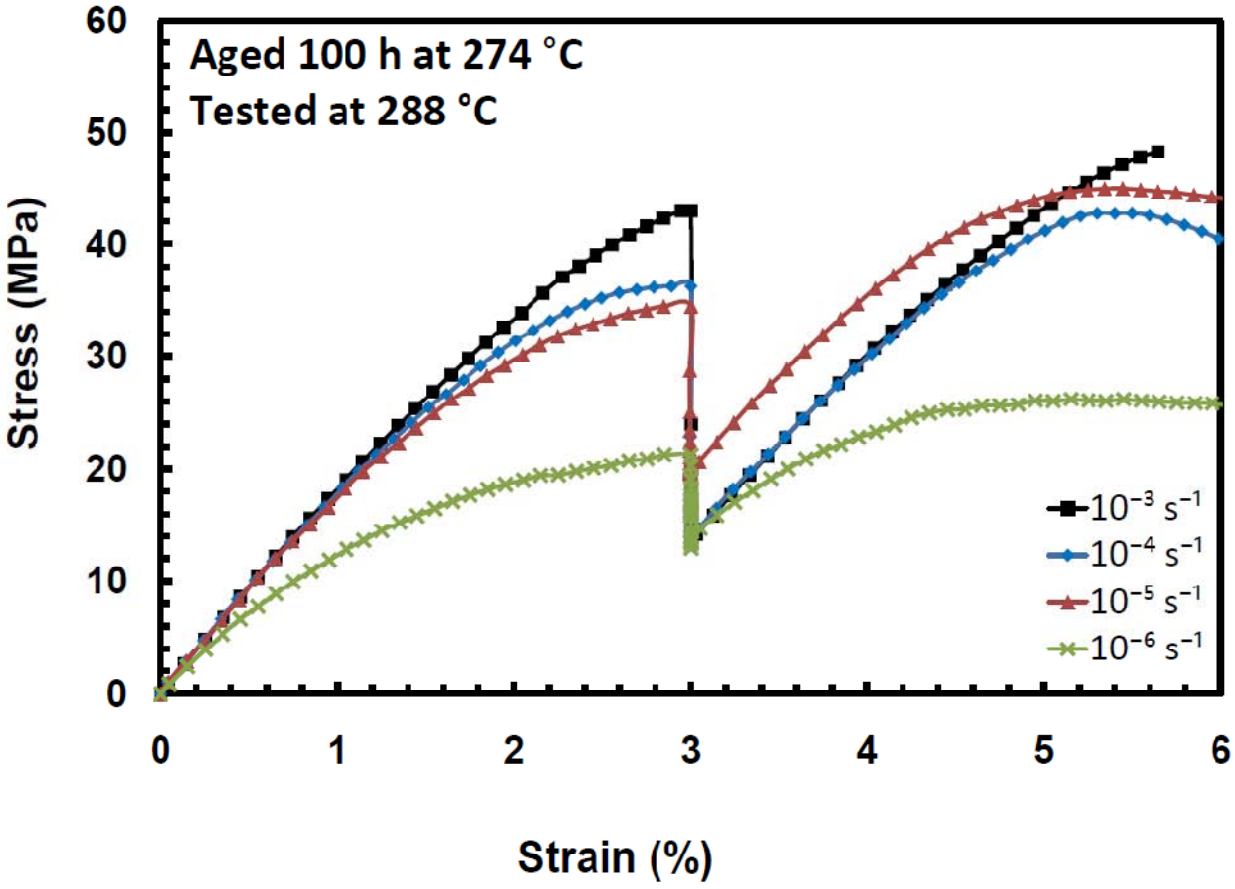

Figure 6.15: Stress-Strain Curves for PMR-15 Specimens Aged for 100 h at 274 °C in Argon Obtained in Constant Strain Rate Tests with a Period of Relaxation Conducted at Constant Strain Rates of 10^{-3}, 10^{-4}, 10^{-5}, and 10^{-6} s^{-1} at 288 °C.

Figure 6.16 shows the results obtained for specimens which had previously been aged for 250 h. Again, the stress-strain curves produced at strain rates of 10^{-4} and 10^{-5} s^{-1} before relaxation are nearly identical. The specimens previously loaded at faster strain rates reached lower stress levels at the end of relaxation than those previously loaded at slower rates. As the straining at a given strain rate resumed after the relaxation test all specimens produced flow stress levels characteristic of the given strain rate.

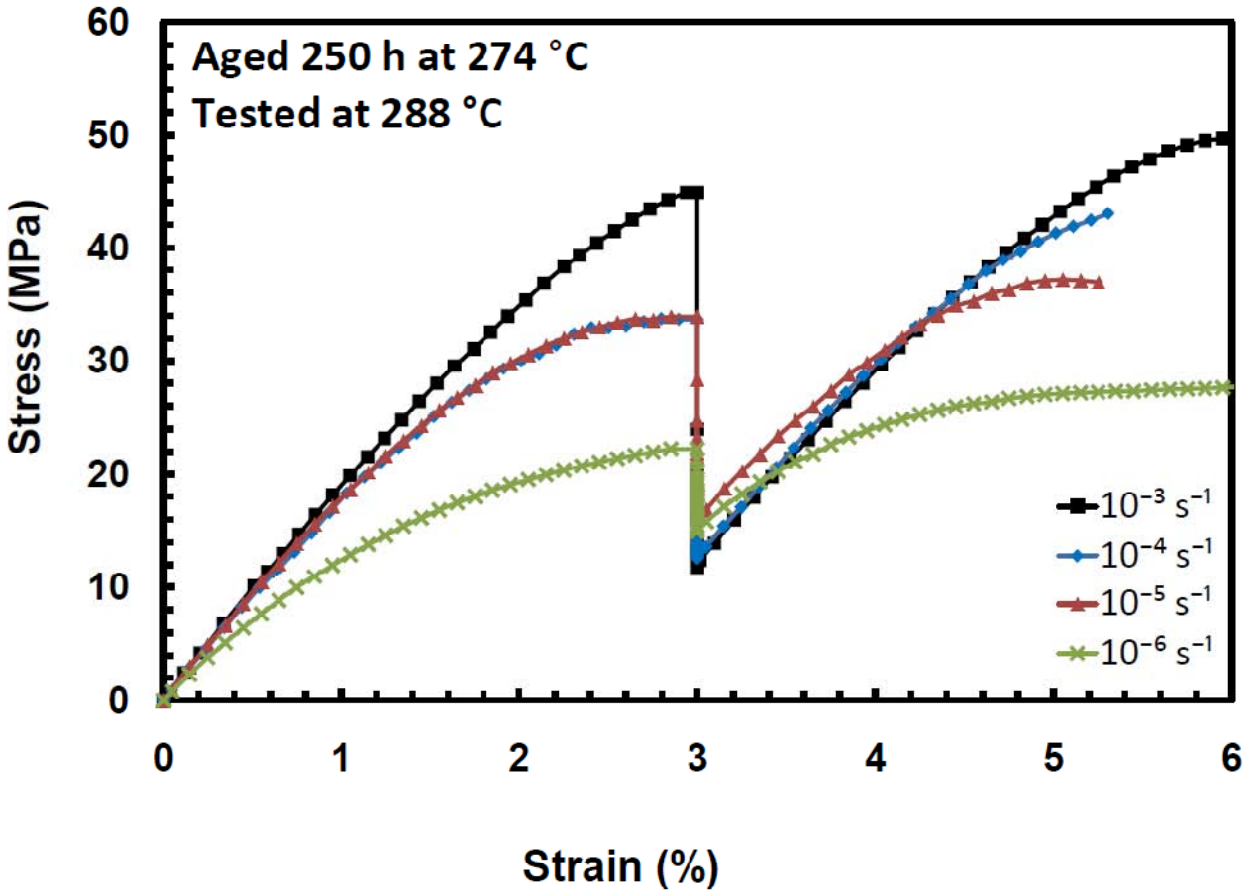

Figure 6.16: Stress-Strain Curves for PMR-15 Specimens Aged for 250 h at 274 °C in Argon Obtained in Constant Strain Rate Tests with a Period of Relaxation Conducted at Constant Strain Rates of 10^{-3}, 10^{-4}, 10^{-5}, and 10^{-6} s^{-1} at 288 °C.

Results of the monotonic tests with a period of relaxation obtained for specimen aged for 500 hours, are depicted in Figure 6.17. In this case distinctly different stress-strain curves were produced during monotonic loading at 10^{-4} and 10^{-5} s^{-1}. However, for this aging group, similar stress-strain curves were obtained at strain rates of 10^{-5} and 10^{-6} s^{-1}. This result again suggests that data scatter due to specimen-to-specimen variability may cloud the behavior changes caused by a tenfold increase or decrease in strain rate.

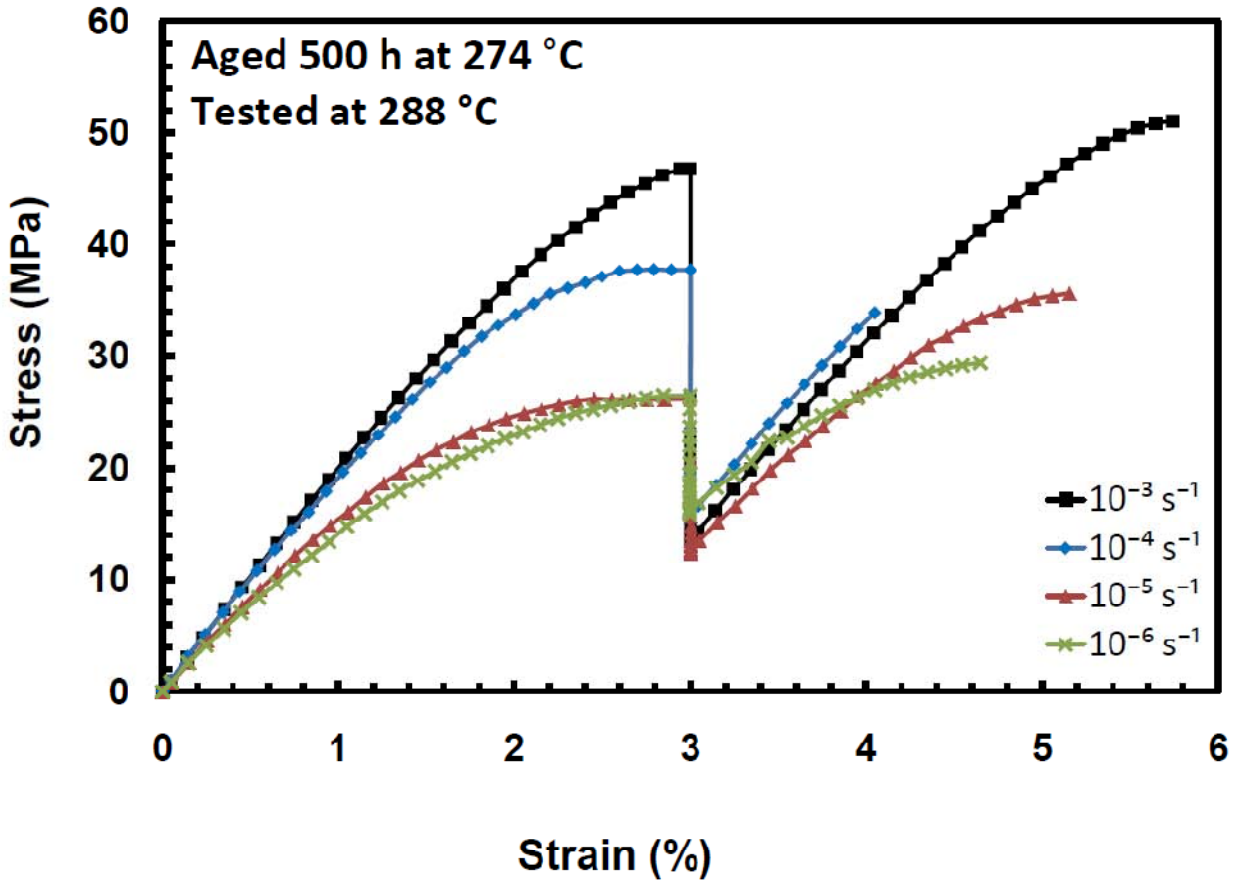

Figure 6.17: Stress-Strain Curves for PMR-15 Specimens Aged for 500 h at 274 °C in Argon Obtained in Constant Strain Rate Tests with a Period of Relaxation Conducted at Constant Strain Rates of 10^{-3}, 10^{-4}, 10^{-5}, and 10^{-6} s^{-1} at 288 °C.

Specimens subjected to aging at 274 °C for 1000 hours or longer exhibited increased embrittlement. Multiple tests were attempted at a strain rate of 10^{-3} s^{-1},. However, all specimens failed before reaching the strain of 3%. Specimen strained at all three slower strain rates reached the strain of 3%, where a 12-h period of relaxation was introduced. The results of these tests are shown in Figure 6.18. Strain rate dependence of the monotonic stress-strain response is evident. As the straining was resumed after relaxation the specimen tested at 10^{-6} s^{-1} reached a flow stress that was slightly higher than that characteristic of this strain rate. All other specimens failed prior to reaching the flow stress region.

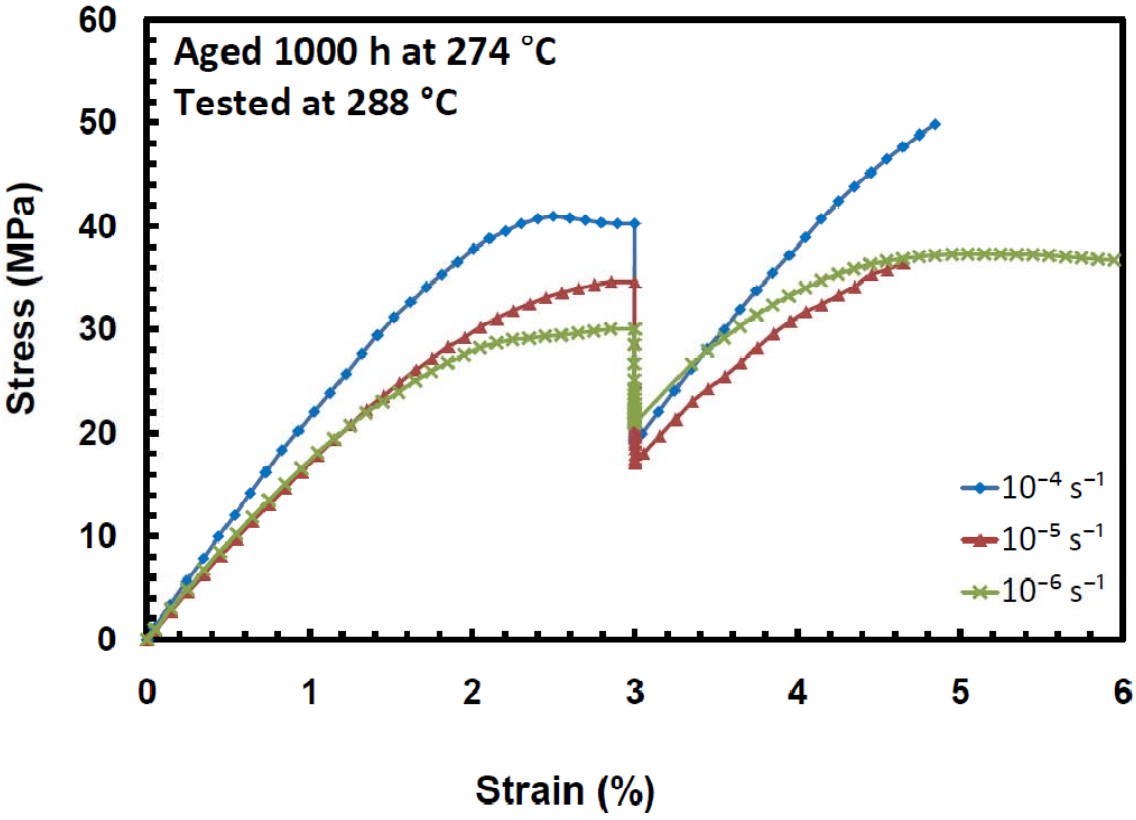

Figure 6.18: Stress-Strain Curves for PMR-15 Specimens Aged for 1000 h at 274 °C in Argon Obtained in Constant Strain Rate Tests with a Period of Relaxation Conducted at Constant Strain Rates of 10^{-4}, 10^{-5}, and 10^{-6} s^{-1} at 288 °C.

A marked increase in brittleness is observed for specimens aged for 2000 hours. Most specimens failed before reaching the strain of 3%. Remarkably the specimen tested at the fastest strain rate of 10^{-3} s^{-1} attained the strain of 3% as did the specimen tested at 10^{-6} s^{-1}. Hence only these two specimens were subjected to relaxation at the strain of 3%. Results are presented in Figure 6.19.

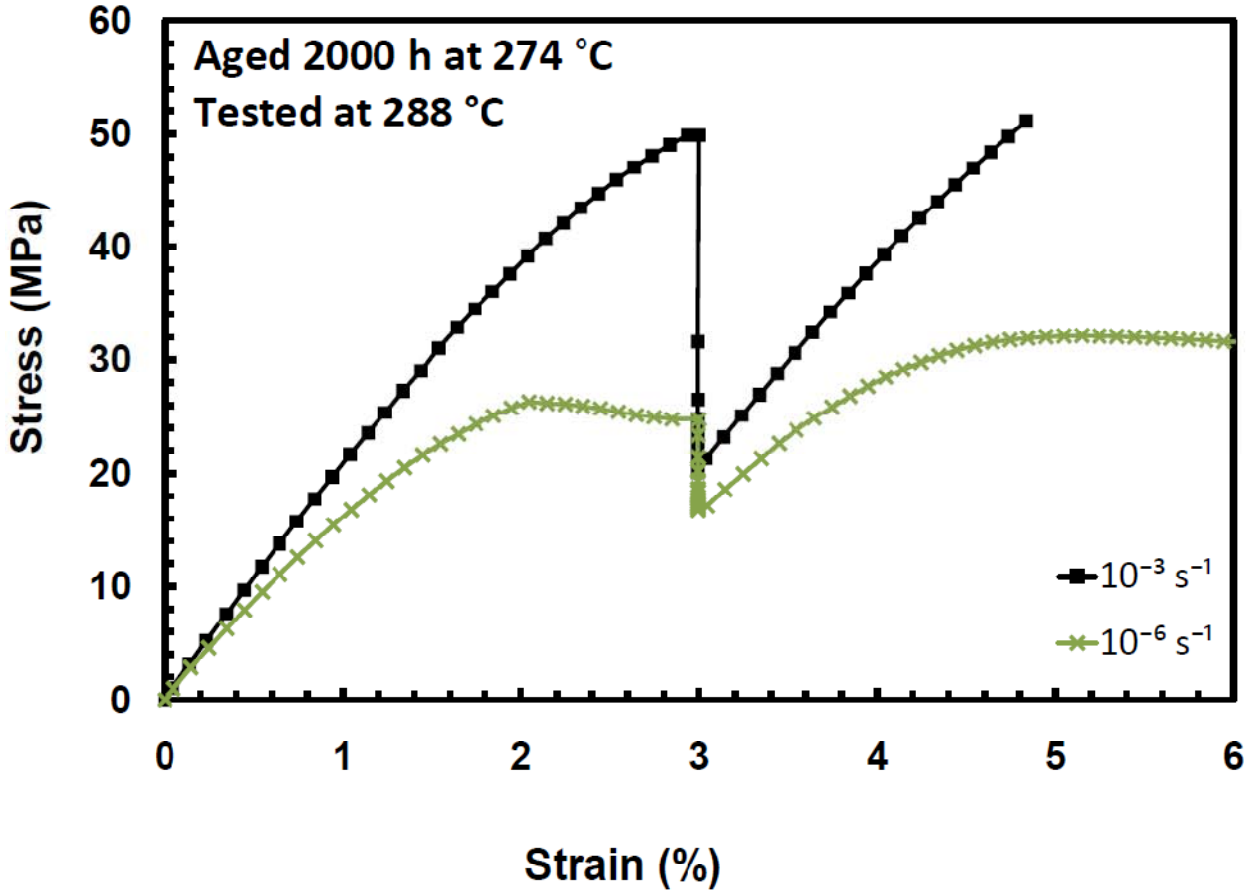

Figure 6.19: Stress-Strain Curves for PMR-15 Specimens Aged for 2000 h at 274 °C in Argon Obtained in Constant Strain Rate Tests with a Period of Relaxation Conducted at Constant Strain Rates of $10^{-3}$and 10^{-6} s^{-1} at 288 °C.

When specimens are held at a constant strain during the relaxation test the stress decreases. Stress drop during relaxation is plotted vs relaxation time in Figure 6.20 through

Figure 6.25. The majority of stress drop occurs during the first few hours of relaxation. The rate of stress decrease immediately at the beginning of relaxation is a strongly influenced by prior strain rate. Specimens strained at faster strain rates produce a more rapid initial stress drop and approach asymptotic stress values more quickly. In most tests the stress has reached an asymptotic value after about 10 h of relaxation. Hence it is reasonable to assume that little additional stress drop would occur if relaxation test were extended beyond 12 hours. Several marked "jumps" can be seen in the stress drop vs. relaxation time curves. For example, see the stress drop vs. relaxation time curve obtained for the specimen in the 50-h aging group strained with a prior strain rate of 10^{-5} s^{-1}. Note a "jump" in that curve occurring at 5.5 h of relaxation. It is believed that these changes in stress levels occur due to changes in the ambient laboratory temperature caused by the inactivity of the air conditioning system as previously discussed. These jumps in stress level may also be observed in the relaxation curves obtained for (1) the specimens in the 100-h age group strained at prior strain rates of 10^{-3}, 10^{-5}, and 10^{-6} s^{-1}, (2) the specimens in the 250-h age group strained at prior strain rates of 10^{-3}, 10^{-5}, and 10^{-6} s^{-1}, (3) and the specimens in the 500-h age group strained at prior strain rates of 10^{-3} and 10^{-6} s^{-1}.

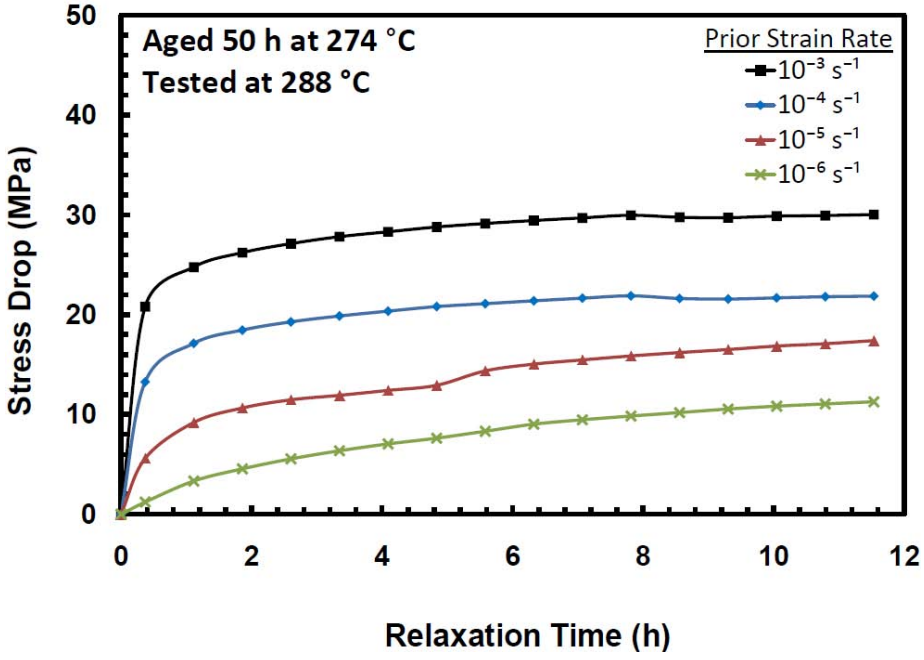

Figure 6.20: Stress Decrease vs. Relaxation Time obtained at 288 °C for PMR-15 Aged in Argon for 50 h at 274 °C.

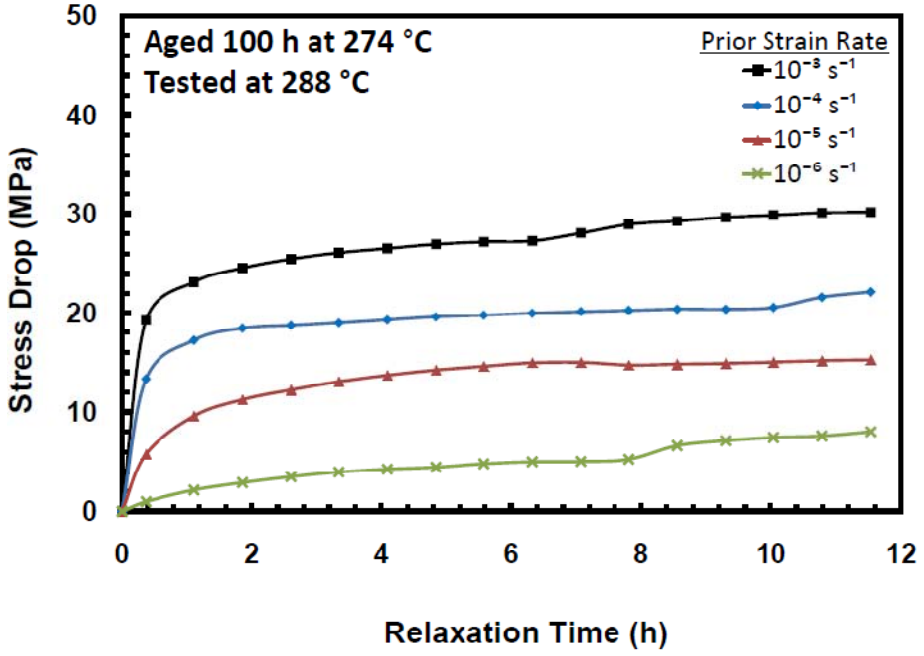

Figure 6.21: Stress Decrease vs. Relaxation Time obtained at 288 °C for PMR-15 Aged in Argon for 100 h at 274 °C.

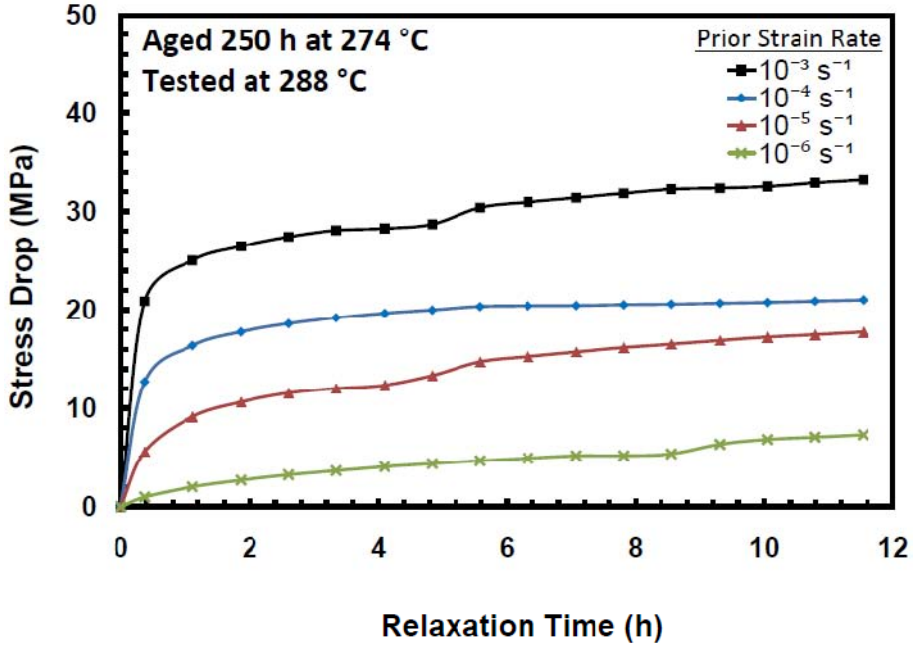

Figure 6.22: Stress Decrease vs. Relaxation Time obtained at 288 °C for PMR-15 Aged in Argon for 250 h at 274 °C.[1]

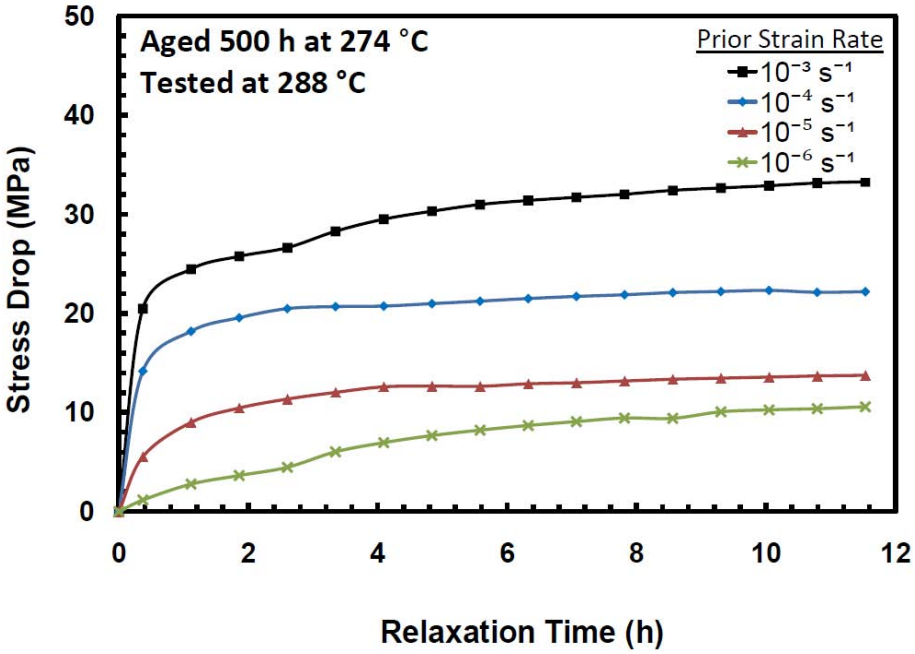

Figure 6.23: Stress Decrease vs. Relaxation Time obtained at 288 °C for PMR-15 Aged in Argon for 500 h at 274 °C.

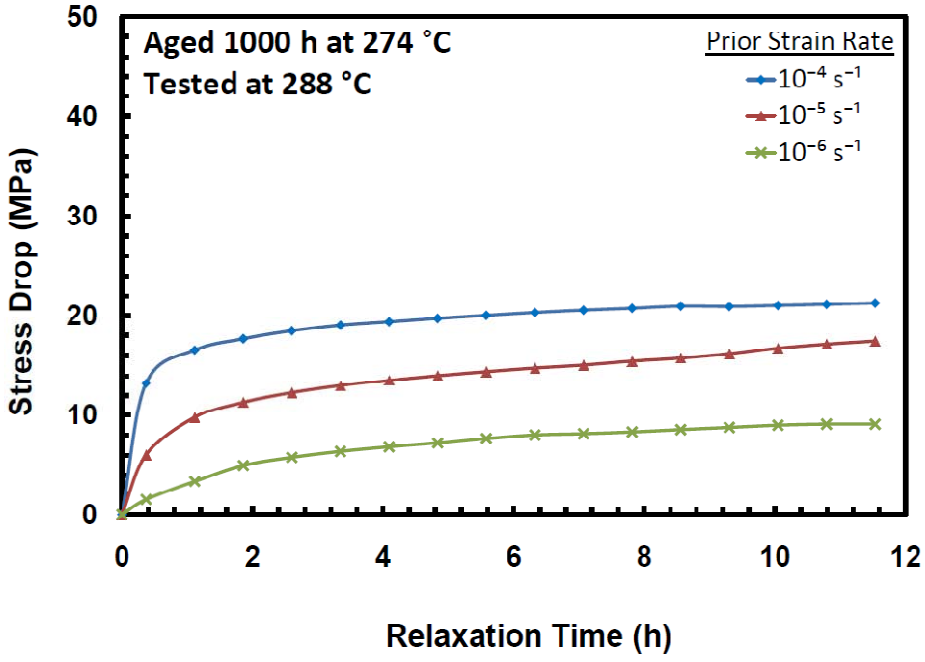

Figure 6.24: Stress Decrease vs. Relaxation Time obtained at 288 °C for PMR-15 Aged in Argon for 1000 h at 274 °C.

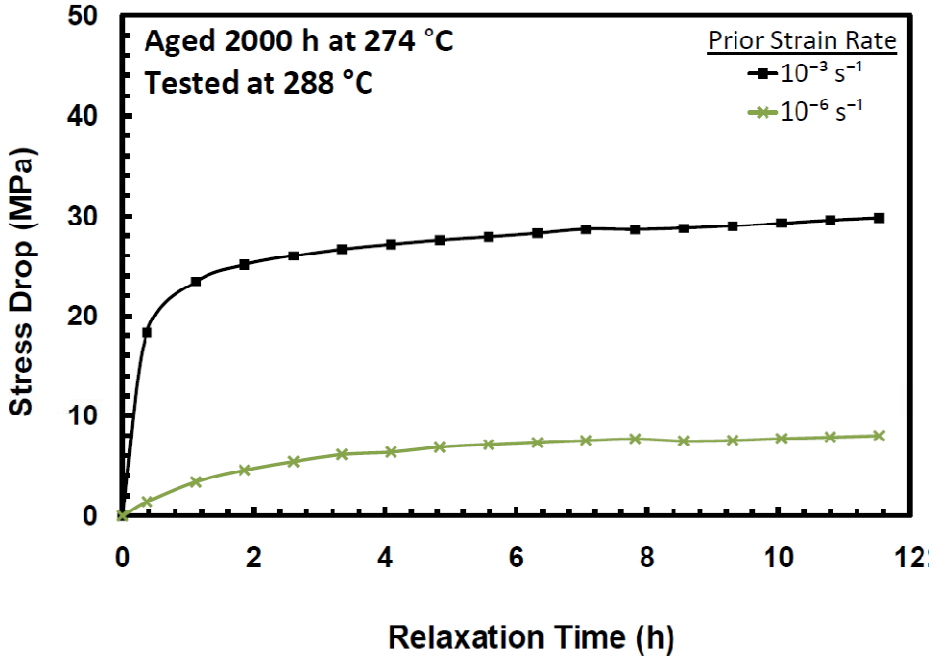

Figure 6.25: Stress Decrease vs. Relaxation Time obtained at 288 °C for PMR-15 Aged in Argon for 2000 h at 274 °C.

A key observation made by other researchers suggests that the relaxation behavior is little affected by prior isothermal aging [10, 27, 28]. The results of relaxation tests performed at 288 °C on specimens subjected to prior aging at 274 °C are shown in Figure 6.26 through Figure 6.29. Results in Figures 6.26-6.29 demonstrate that prior aging at 274°C has little effect on the relaxation response. The amount of stress drop during relaxation neither increases nor decreases with increasing prior aging duration, all differences in behavior are due to experimental scatter.

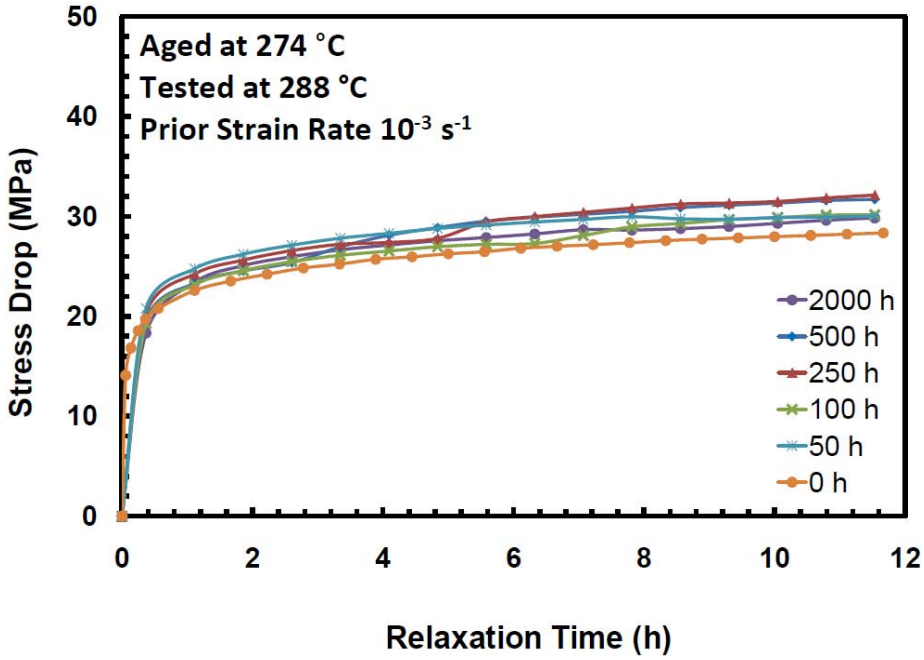

Figure 6.26: Stress Drop During Relaxation at 288 °C for PMR-15 Specimens Aged at 274 °C. Data for the Un-aged Material from McClung[27].

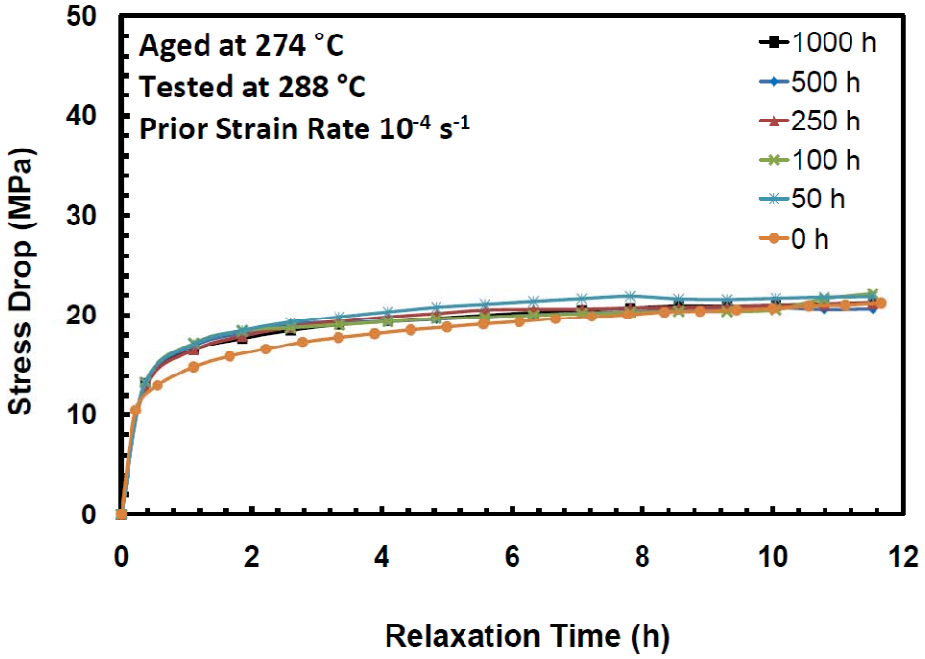

Figure 6.27: Stress Drop During Relaxation at 288 °C for PMR-15 Specimens Aged at 274 °C. Data for the Un-aged Material from McClung[27].

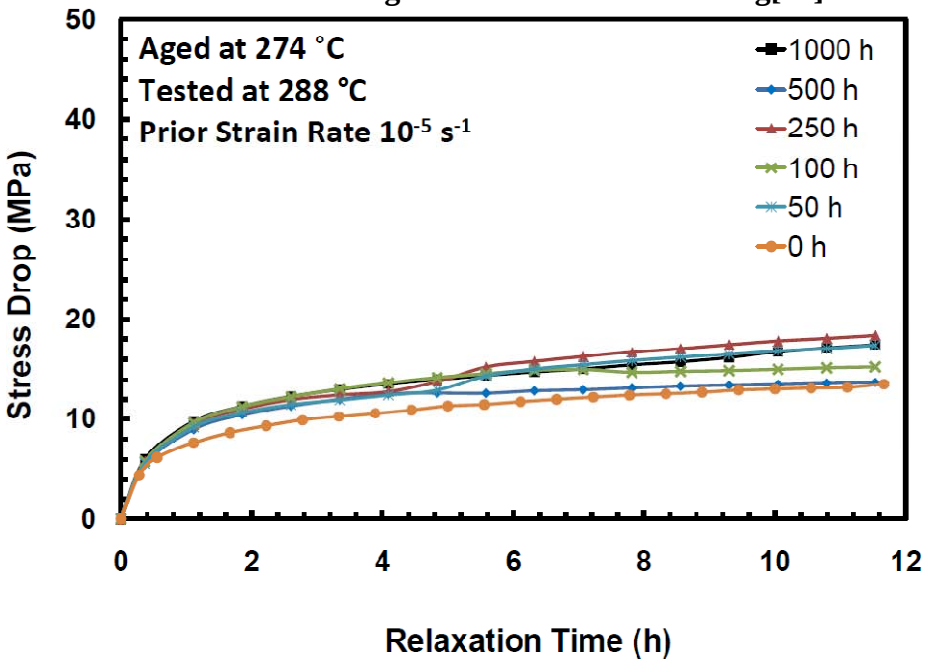

Figure 6.28: Stress Drop During Relaxation at 288 °C for PMR-15 Specimens Aged at 274 °C. Data for the Un-aged Material from McClung[27].

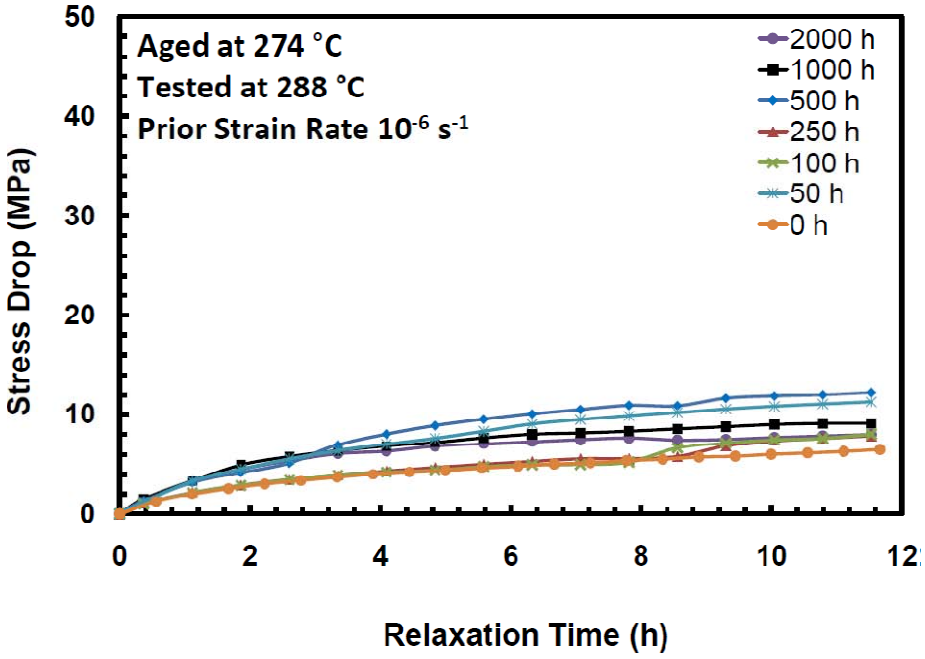

Figure 6.29: Stress Drop During Relaxation at 288 °C for PMR-15 Specimens Aged at 274 °C. Data for the Un-aged Material from McClung[27].

Loading / Unloading Test at Constant Strain Rate

The PMR-15 specimens from each aging group were loaded at constant strain rates of 10^{-3}, 10^{-4}, 10^{-5}, and 10^{-6} s^{-1} to a strain of 3% then unloaded to zero stress at the same strain rate magnitude. The results of these tests are presented together with the results of the monotonic tension to failure tests in Figure 6.30 through Figure 6.35. The effects of strain rate on the stress-strain behavior are readily apparent on both the loading and the unloading paths.

The results of loading/unloading tests for specimens aged for 50 hours at 274 °C are shown in Figure 6.30. Because specimen tested in tension to failure at 10^{-3} and 10^{-5} s^{-1} failed at very small strains Figure 6.30 includes the stress-strain curves produced during loading at 10^{-3} and 10^{-5} s^{-1} in the monotonic tests with a relaxation period. As previously reported [10, 27, 28] the specimens exhibited curved unloading, which is more pronounced at slower loading rates.

The strain measured immediately upon reaching zero stress at the end of unloading increases with decreasing strain rate, except in the case of the specimen tested at 10^{-5} s^{-1} which produced the same strain (1.2% strain) as did the specimen tested at 10^{-6} s^{-1}.

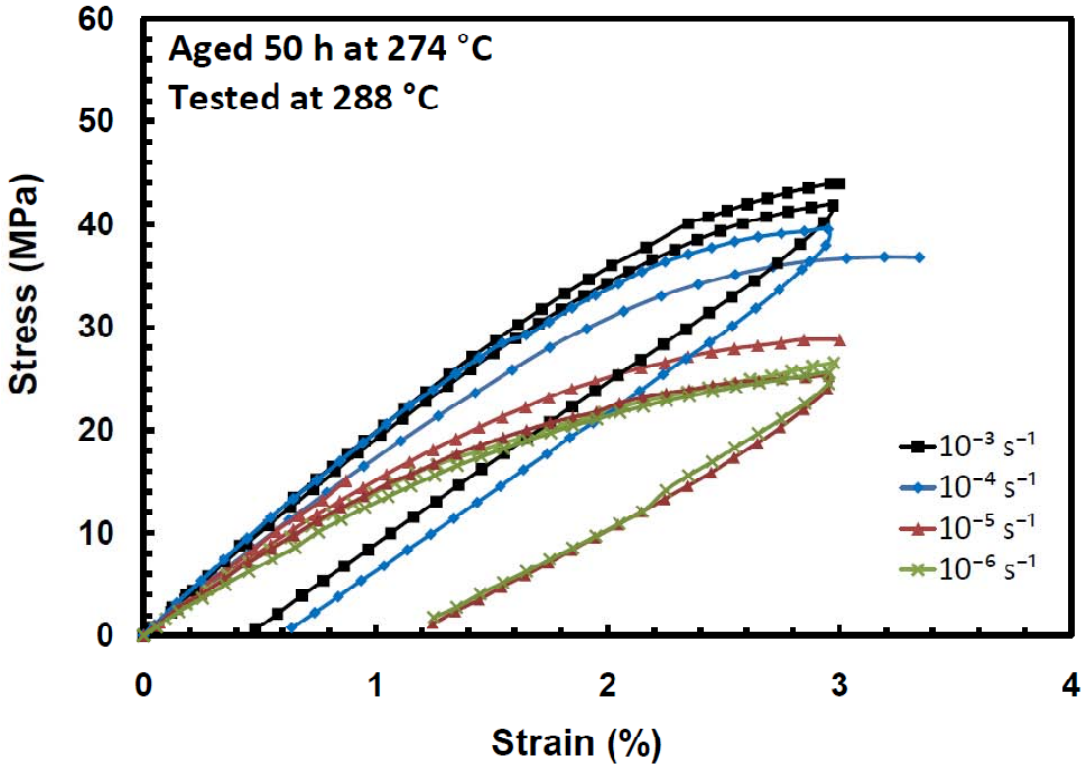

Figure 6.30: Stress-Strain Curves Obtained at 288 °C for PMR-15 Specimens Aged for 50 h at 274 °C in Argon in Monotonic Tensile Tests and in Loading/Unloading Tests at Strain Rates of 10^{-3}, 10^{-4}, 10^{-5}, and 10^{-6} s^{-1}.

Figure 6.31 shows the stress-strain behavior of the specimens which were subjected to 100 h of aging at 274 °C. All specimens in this aging group exhibited loading behavior consistent with the results of prior testing. The curvature of the unloading path is most pronounced in the case of the specimens loaded at slower strain rates. The strain measured immediately upon reaching zero stress at the end of unloading increases with decreasing strain rate.

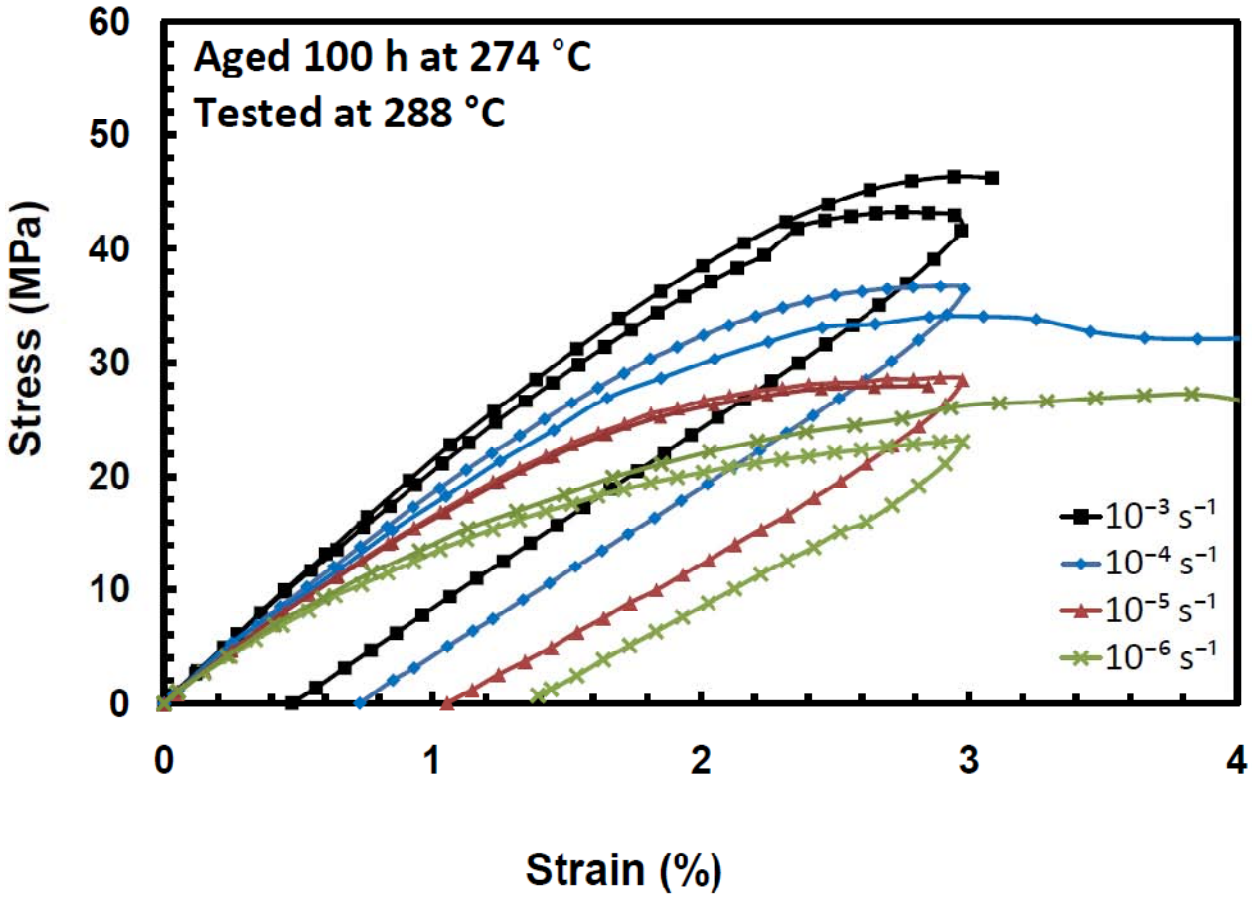

Figure 6.31: Stress-Strain Curves Obtained at 288 °C for PMR-15 Specimens Aged for 100 h at 274 °C in Argon in Monotonic Tensile Tests and in Loading/Unloading Tests at Strain Rates of 10^{-3}, 10^{-4}, 10^{-5}, and 10^{-6} s^{-1}.

For specimens aged for 250 hours, close agreement between the results of the monotonic tensile to failure and the results produced during loading portion of the loading/unloading tests was observed for three of the four strain rates used (see Figure 6.32). The stress-strain curve obtained for the specimen tested at a strain rate of 10^{-4} s^{-1} departs from nearly linear behavior sooner and produces lower stresses than the stress-strain curve obtained at that strain rate in monotonic tension. Furthermore, the unloading stress-strain curve produced at the strain rate magnitude of 10^{-4} s^{-1} exhibited more curvature than that produced at the strain rate magnitude of

10^{-5} s^{-1}. Results in Figure 6.32 also demonstrate that the strain measured immediately upon reaching zero stress increases with decreasing strain rate magnitude.

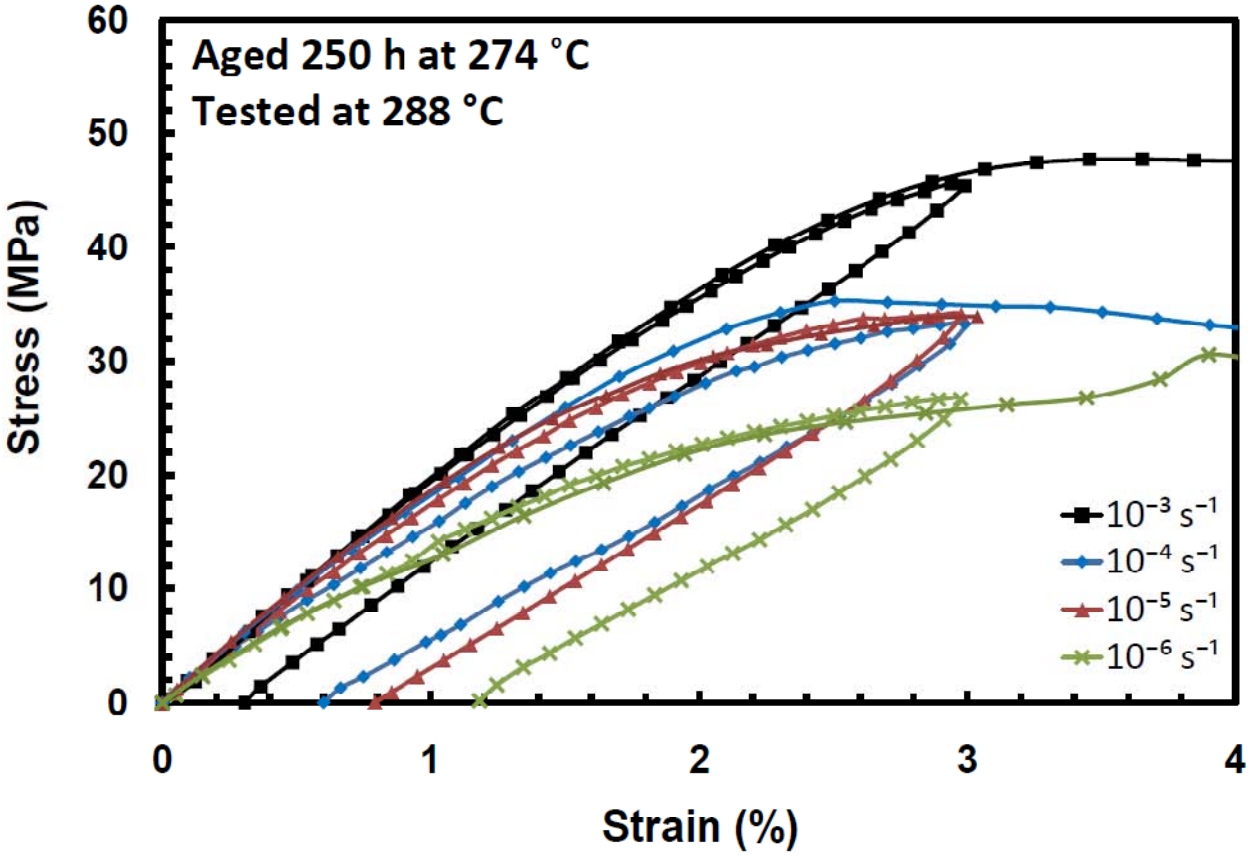

Figure 6.32: Stress-Strain Curves Obtained at 288 °C for PMR-15 Specimens Aged for 250 h at 274 °C in Argon in Monotonic Tensile Tests and in Loading/Unloading Tests at Strain Rates of 10^{-3}, 10^{-4}, 10^{-5}, and 10^{-6} s^{-1}.

The results obtained for specimens aged for 500 h are shown in Figure 6.33. Strain rate dependence is prominent in the three fastest tests. However, the loading/unloading test performed at 10^{-6} s^{-1} produced stresses that were about 15% higher than the stresses produced in the monotonic tensile test conducted at the same strain rate. In fact, stresses produced in loading/unloading at 10^{-6} s^{-1} were s similar to those produced in loading/unloading at a strain rate

of 10^{-5} s^{-1}. Note that the strain measured immediately upon reaching zero stress at the end of unloading decreases with increasing strain rate for all specimens except the specimen tested at the slowest strain rate.

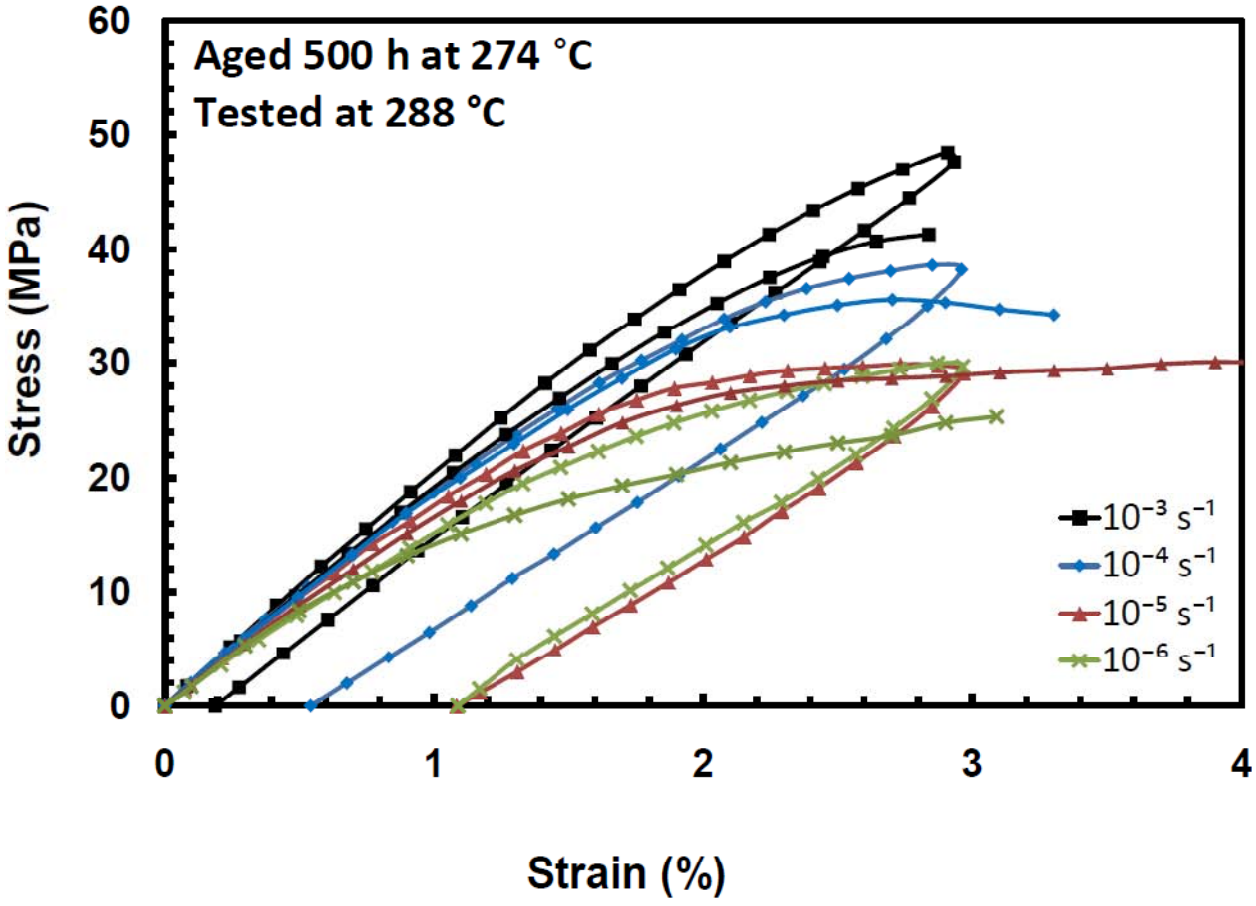

Figure 6.33: Stress-Strain Curves Obtained at 288 °C for PMR-15 Specimens Aged for 500 h at 274 °C in Argon in Monotonic Tensile Tests and in Loading/Unloading Tests at Strain Rates of 10^{-3}, 10^{-4}, 10^{-5}, and 10^{-6} s^{-1}.

Loading/unloading tests performed on specimens in the the 1000-h aging group produced results consistent with those previously reported. Stress-strain behavior is affected by strain rate with decreasing strain rate producing lower stresses during loading and a more curved

unloading stress-strain path. Results in Figure 6.34 also show that the monotonic tension to failure test performed at 10^{-5} s^{-1} produced stress levels lower than those produced in the corresponding loading/unloading test.

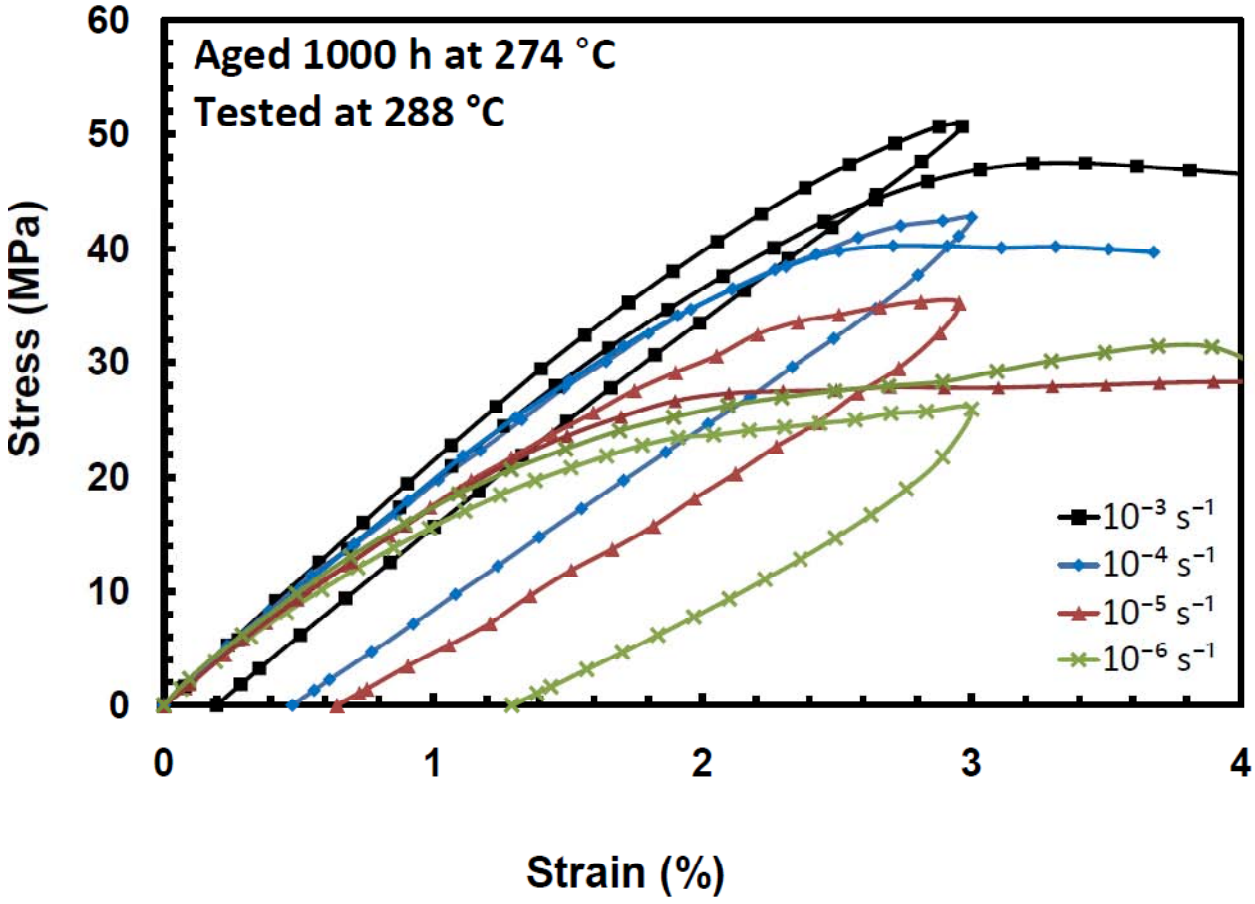

Figure 6.34: Stress-Strain Curves Obtained at 288 °C for PMR-15 Specimens Aged for 1000 h at 274 °C in Argon in Monotonic Tensile Tests and in Loading/Unloading Tests at Strain Rates of 10^{-3}, 10^{-4}, 10^{-5}, and 10^{-6} s^{-1}.

Specimens subjected to 2000 h of aging at 274 °C exhibited increased embrittlement. Therefore the specimen tested at a strain rate of 10^{-3} s^{-1} failed before reaching the strain of 3%. The results of the other loading/unloading tests obtained for the 2000-h aging group are presented in Figure 6.35. It is seen in Figure 6.35 that higher stress levels were produced in the

loading/unloading test performed at a strain rate magnitude of 10^{-6} s^{-1} than in the monotonic tension test conducted at the same strain rate. Note that the results produced in loading/unloading test conducted at10^{-5} s^{-1} are close to those produced in loading/unloading at 10^{-6} s^{-1}.

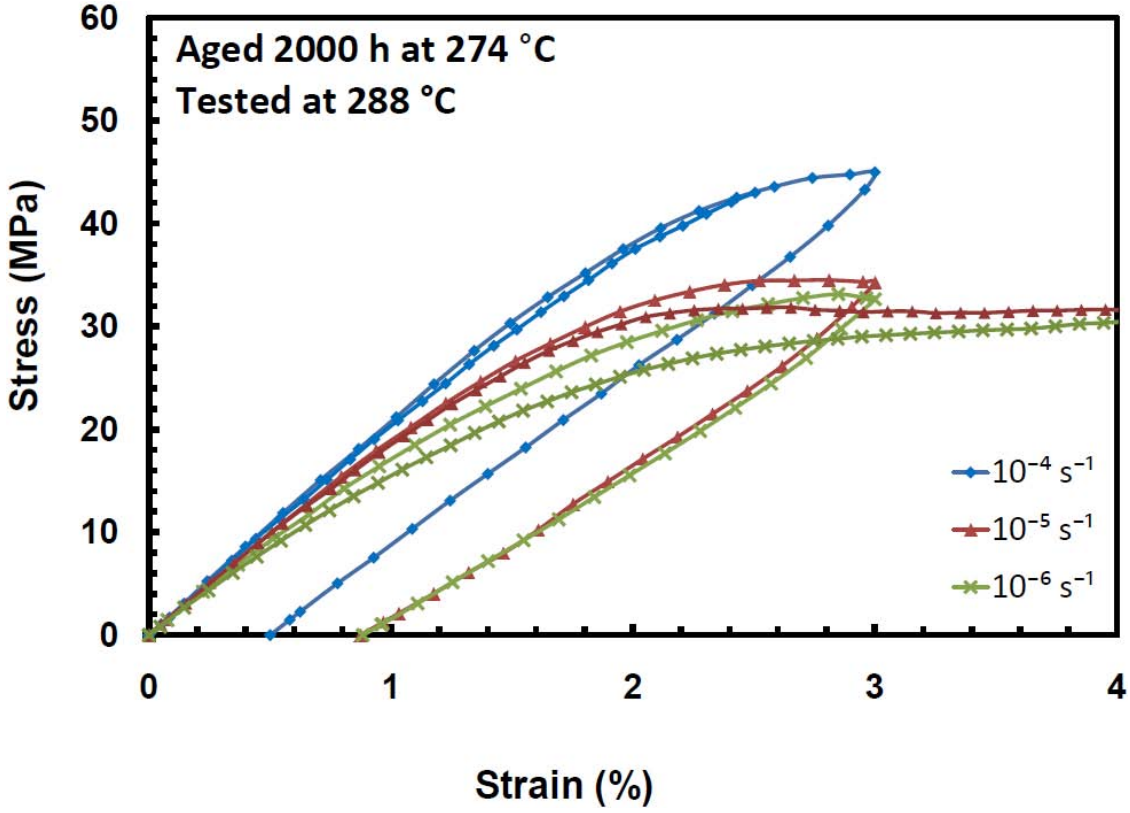

Figure 6.35: Stress-Strain Curves Obtained at 288 °C for PMR-15 Specimens Aged for 2000 h at 274 °C in Argon in Monotonic Tensile Tests and in Loading/Unloading Tests at Strain Rates of 10^{-4}, 10^{-5}, and 10^{-6} s^{-1}.

Recovery of Strain at Zero Stress

Immediately after completion of loading/unloading test, the control mode was switched to load and the specimens were held at zero stress in order to evaluate the recovery of strain . The results of these tests are displayed in Figure 6.36 through Figure 6.41 where recovered strain is shown as a percentage of the inelastic strain value measured immediately after reaching zero

stress. There were multiple instances within these tests where the recorded strain experienced an abrupt “jump”. Typically the strain would later return to values consistent with the initial portion of the strain recovery curve. These “jumps” in strain data are concurrent with changes in the ambient laboratory observed consistently from 9:00 pm to 4:00 am and at other occasions when the lab door was left open. These effects were observed while operating in both strain and load control. The portions of the data where these “jumps” in strain data occurred have been replaced with dashed lines in the figures to display results believed to be more representative of true material behavior.

The prior strain rate has a dramatic effect on the percentage of strain recovered at zero stress. For specimens tested with slower prior strain rates the strain measured after unloading is larger and the percentage of this strain recovered is smaller than those for specimens loaded and unloaded at faster strain rates. For the three fastest strain rates the majority of strain was recovered in less than 10 h regardless of prior aging duration. Whereas, specimens loaded at a strain rate of 10^{-6} s^{-1} continued to recover measurable strain for roughly 30 h after unloading to zero stress. Specimens loaded at the two slower strain rates did not recover 100% of the strain, yet the strains measured during recovery approached asymptotic values. While some specimens loaded at slower prior strain rates were allowed to recover for durations in excess of 100 h the majority of the strain was recovered in the first 30 h. Based on these observations permanent strain can be reasonably assumed.

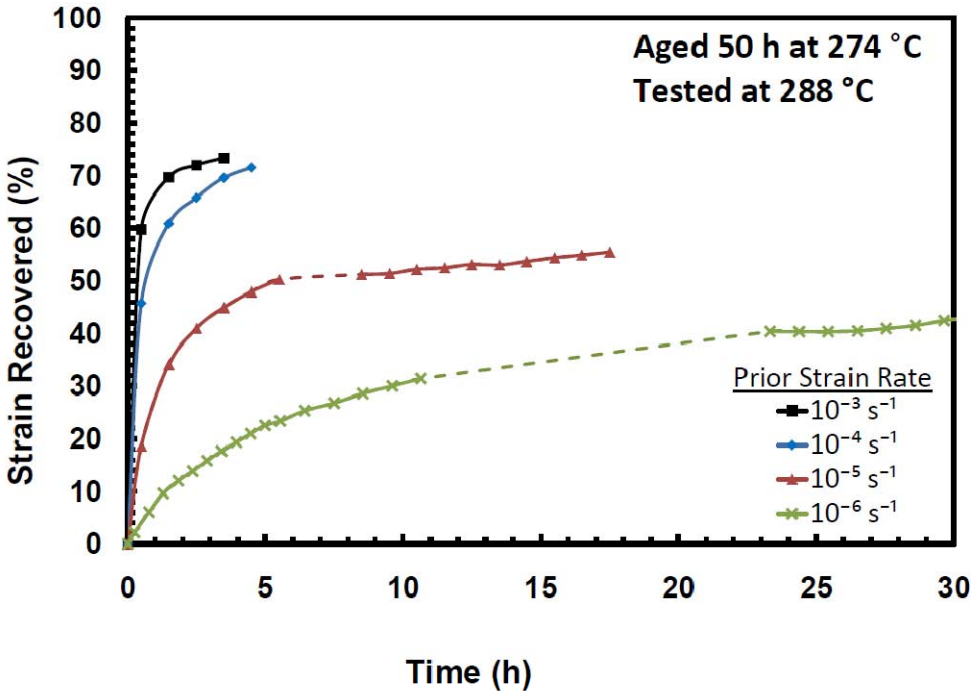

Figure 6.36: Recovery at Zero Stress at 288 °C Following Loading and Unloading for PMR-15 Aged for 50 h at 274 °C. Recovered Strain is shown as a Percentage of the Inelastic Strain Value Measured Immediately After Reaching Zero Stress.

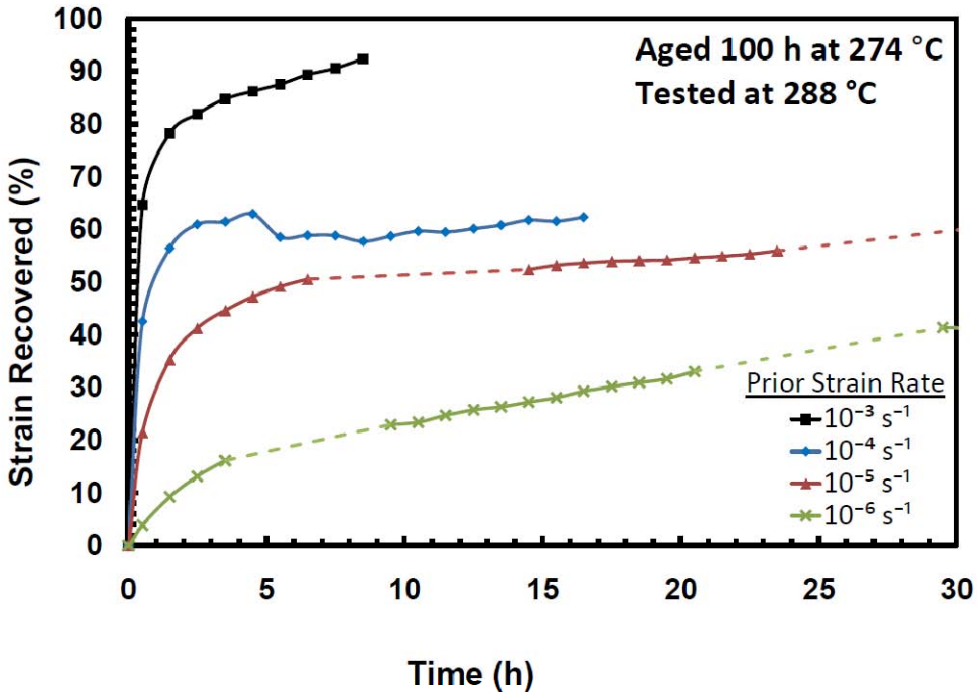

Figure 6.37: Recovery at Zero Stress at 288 °C Following Loading and Unloading for PMR-15 Aged for 100 h at 274 °C. Recovered Strain is shown as a Percentage of the Inelastic Strain Value Measured Immediately After Reaching Zero Stress.

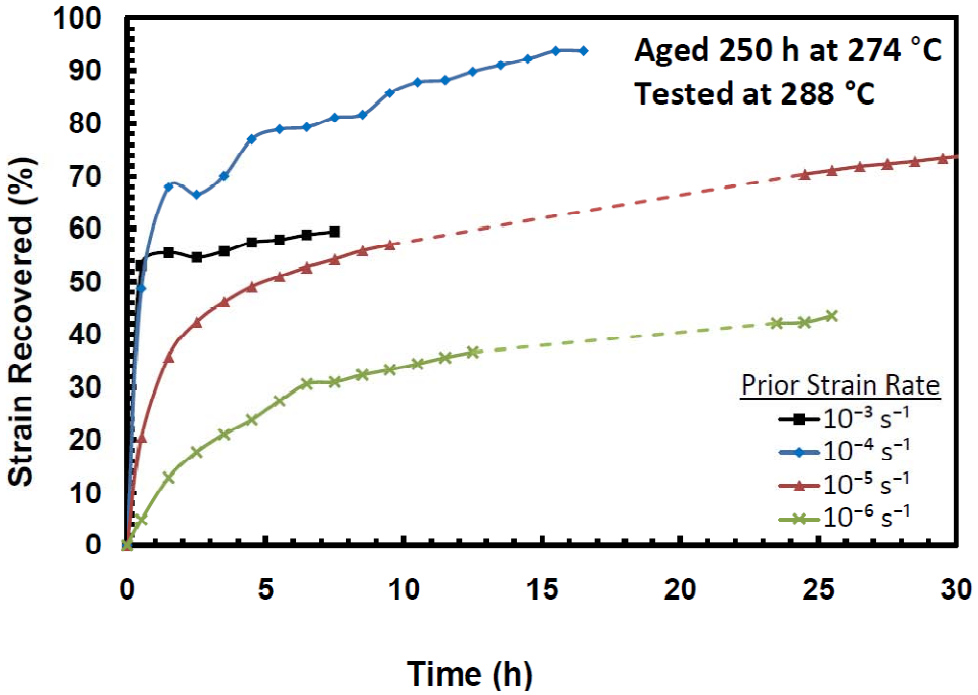

Figure 6.38: Recovery at Zero Stress at 288 °C Following Loading and Unloading for PMR-15 Aged for 250 h at 274 °C. Recovered Strain is shown as a Percentage of the Inelastic Strain Value Measured Immediately After Reaching Zero Stress.

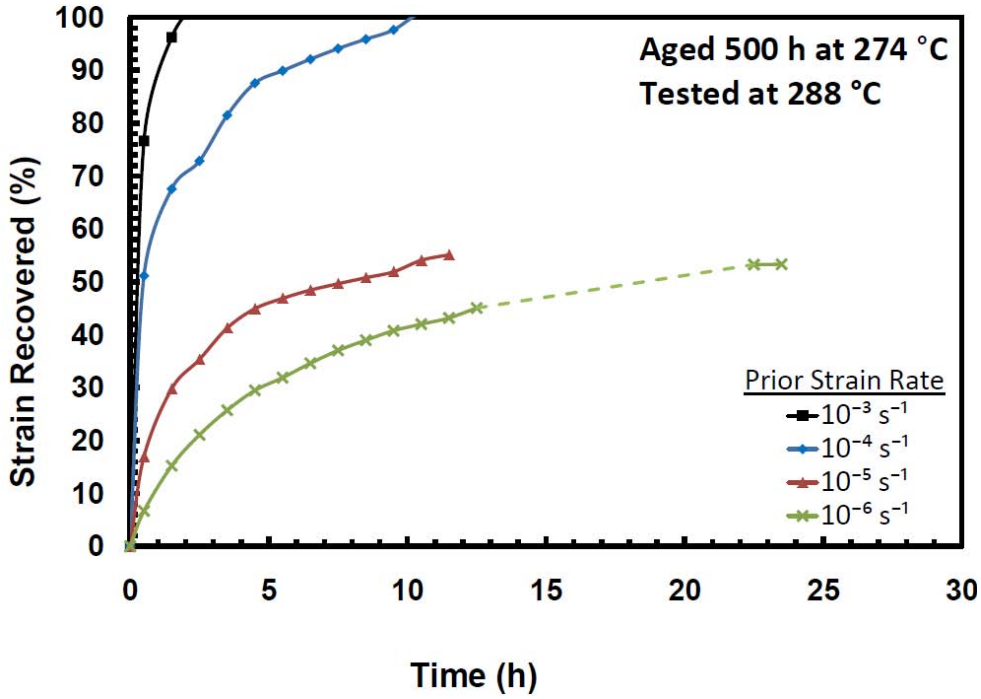

Figure 6.39: Recovery at Zero Stress at 288 °C Following Loading and Unloading for PMR-15 Aged for 500 h at 274 °C. Recovered Strain is shown as a Percentage of the Inelastic Strain Value Measured Immediately After Reaching Zero Stress.

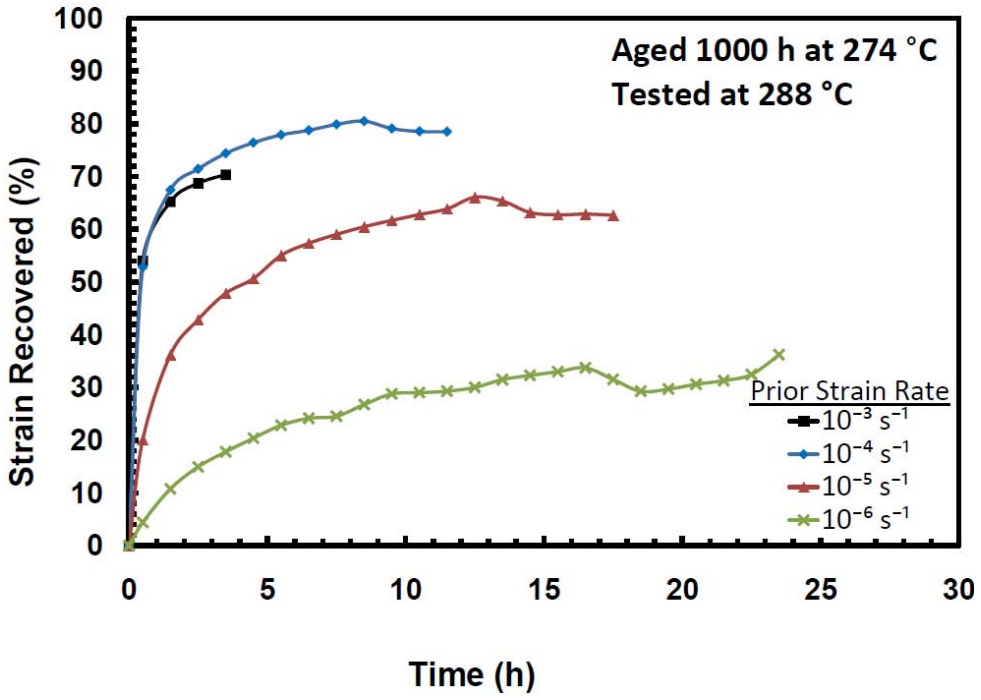

Figure 6.40: Recovery at Zero Stress at 288 °C Following Loading and Unloading for PMR-15 Aged for 1000 h at 274 °C. Recovered Strain is shown as a Percentage of the Inelastic Strain Value Measured Immediately After Reaching Zero Stress.

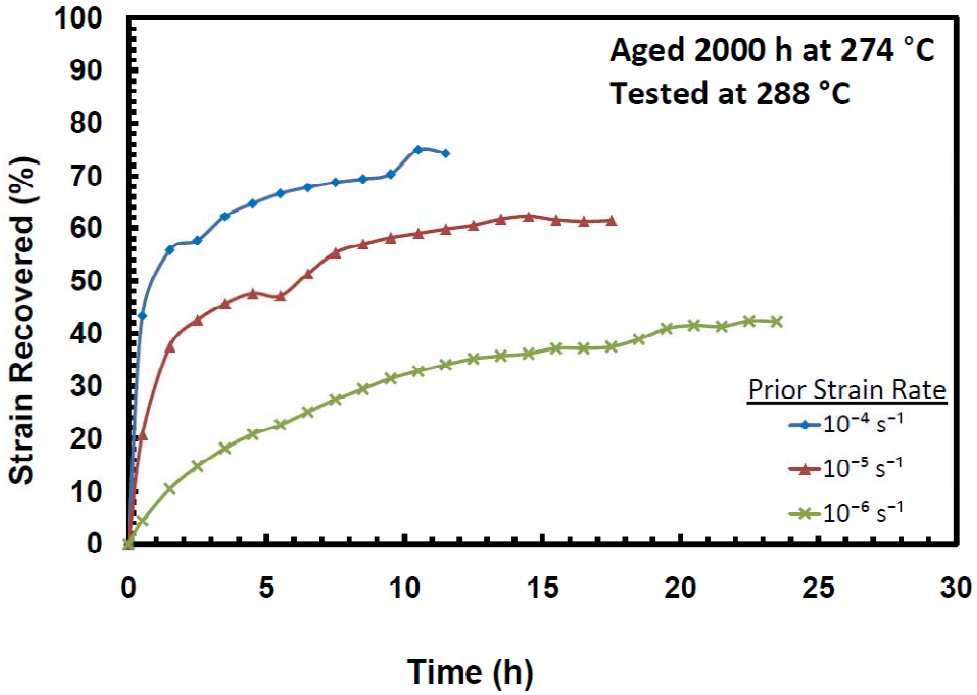

Figure 6.41: Recovery at Zero Stress at 288 °C Following Loading and Unloading for PMR-15 Aged for 2000 h at 274 °C. Recovered Strain is shown as a Percentage of the Inelastic Strain Value Measured Immediately After Reaching Zero Stress.

Creep Test

Specimens from each aging group were loaded at constant strain rates of 10^{-4} and 10^{-6} s^{-1} to a load of 21 MPa. Then the control mode was then switched to load and a 6-h creep test was performed. The results of these tests are presented in Figure 6.42 through Figure 6.47 as the creep strain vs. creep time curves. Influence of prior strain rate on creep behavior is readily seen. For all aging groups the specimens loaded to creep stress at a faster strain rate accumulated more creep strain. Both primary and secondary creep was observed in all tests.

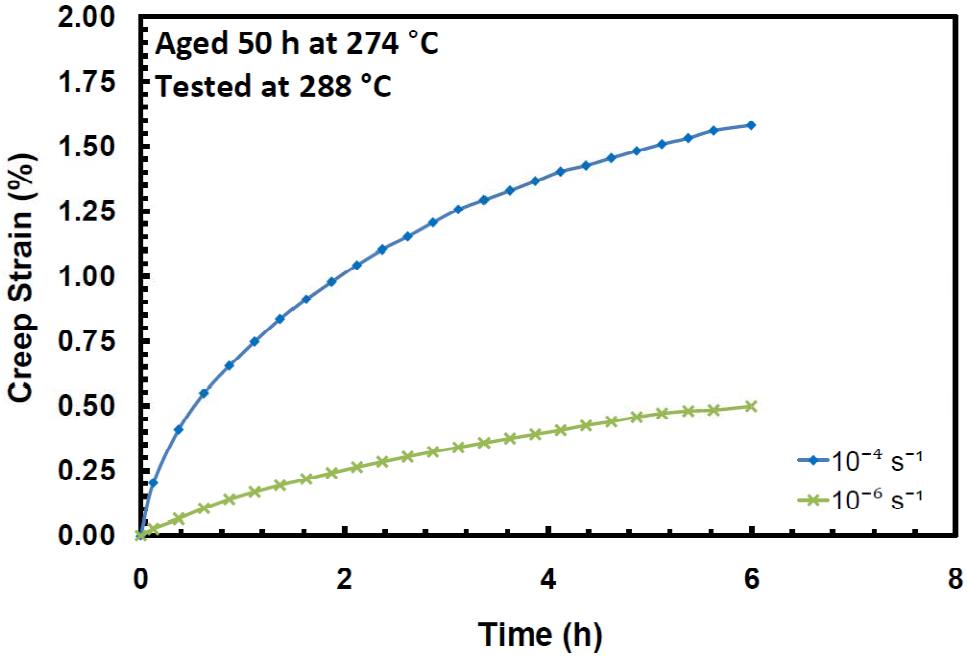

Figure 6.42: Creep Strain vs. Time Curves Obtained at 288 °C and 21 MPa for PMR-15 Aged for 50 h at 274 °C. Prior Strain Rates of 10^{-4} and 10^{-6} s^{-1}.

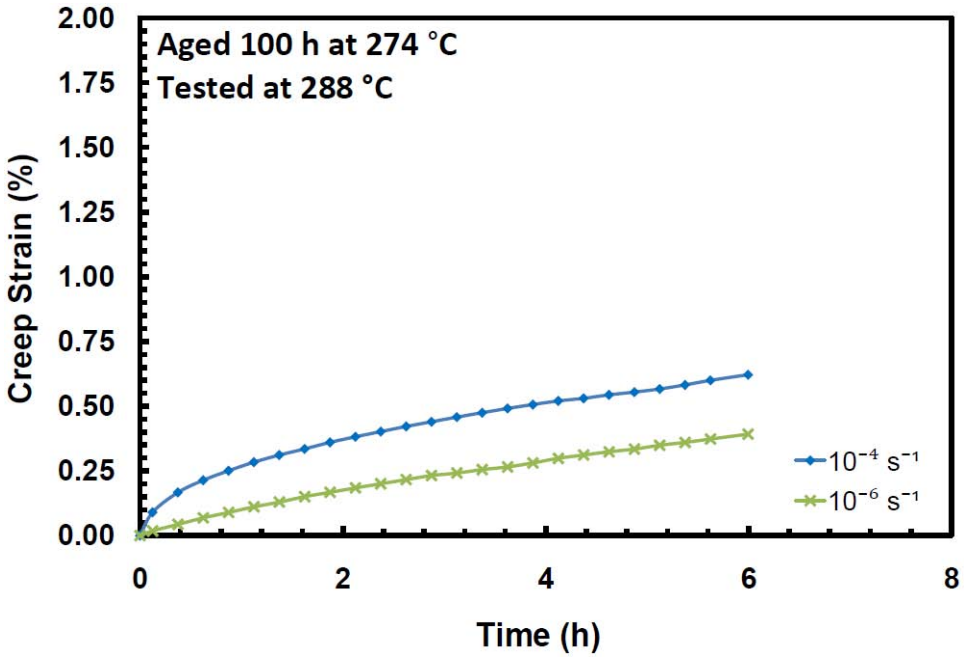

Figure 6.43: Creep Strain vs. Time Curves Obtained at 288 °C and 21 MPa for PMR-15 Aged for 100 h at 274 °C. Prior Strain Rates of 10^{-4} and 10^{-6} s^{-1}.

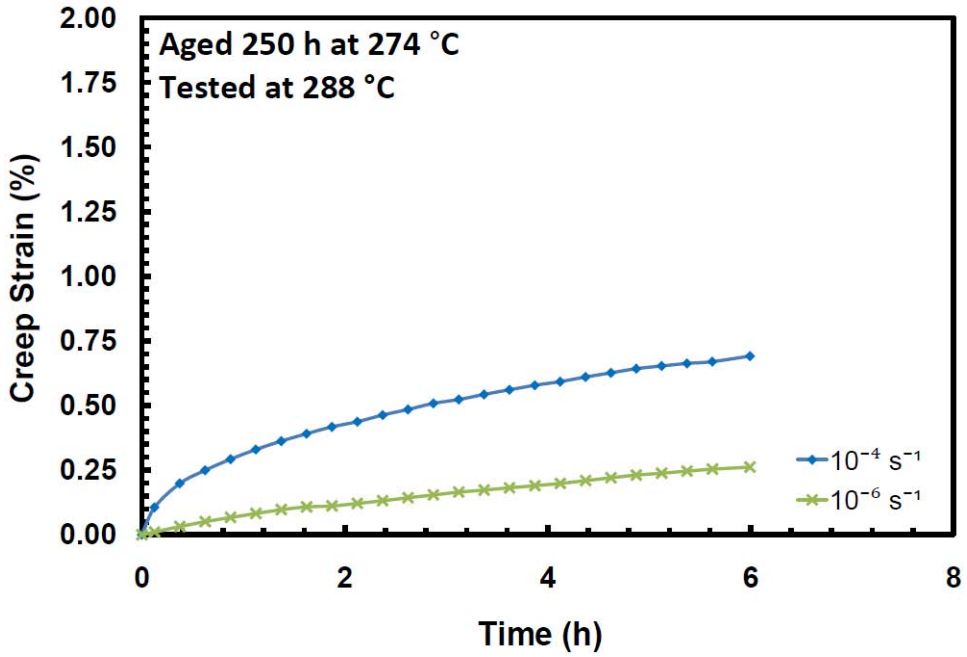

Figure 6.44: Creep Strain vs. Time Curves Obtained at 288 °C and 21 MPa for PMR-15 Aged for 250 h at 274 °C. Prior Strain Rates of 10^{-4} and 10^{-6} s^{-1}.

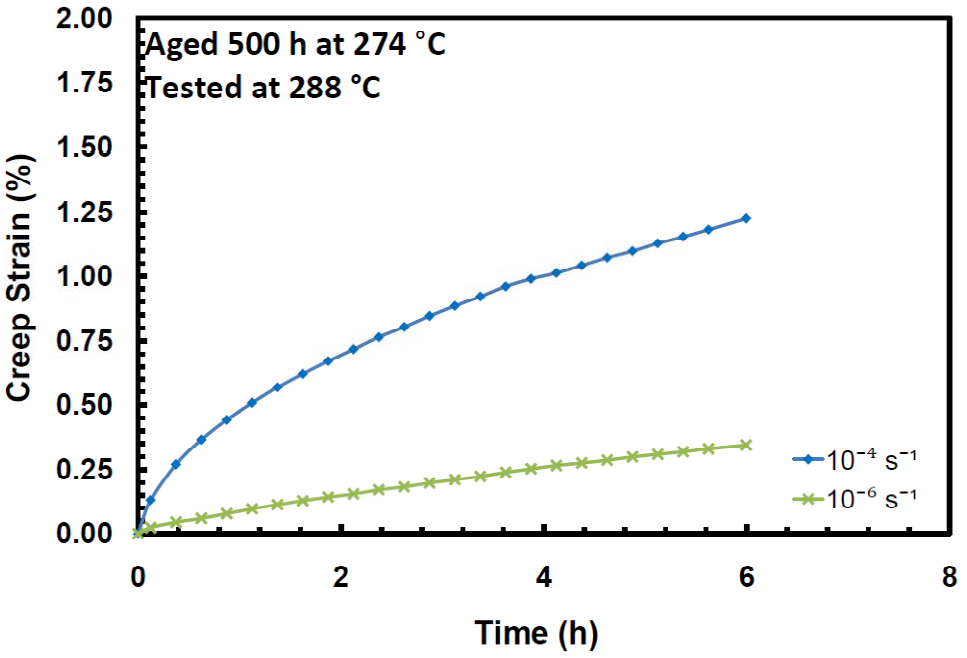

Figure 6.45: Creep Strain vs. Time Curves Obtained at 288 °C and 21 MPa for PMR-15 Aged for 500 h at 274 °C. Prior Strain Rates of 10^{-4} and 10^{-6} s^{-1}.

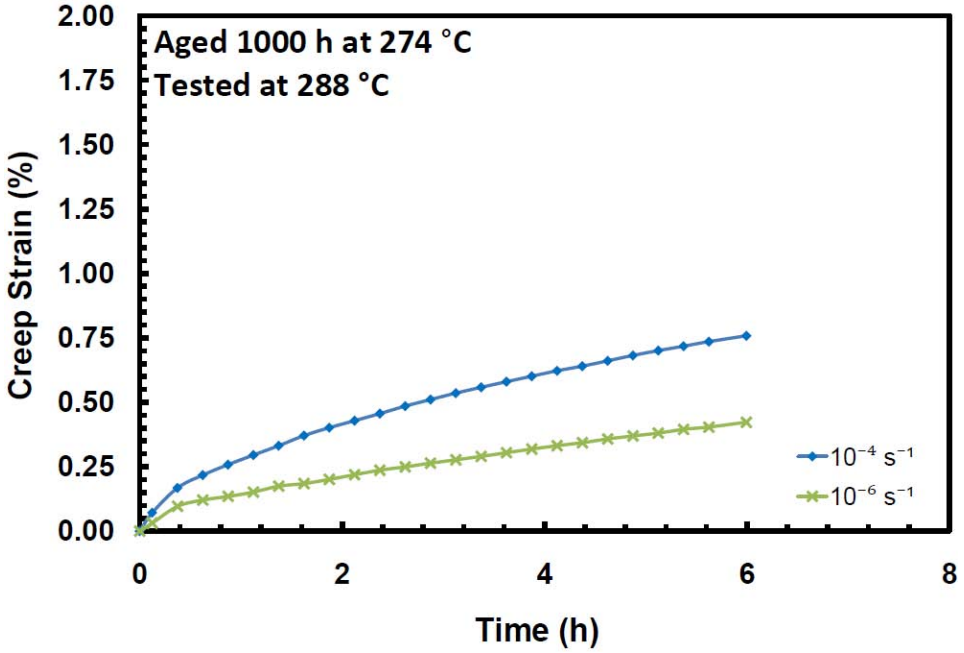

Figure 6.46: Creep Strain vs. Time Curves Obtained at 288 °C and 21 MPa for PMR-15 Aged for 1000 h at 274 °C. Prior Strain Rates of 10^{-4} and 10^{-6} s^{-1}.

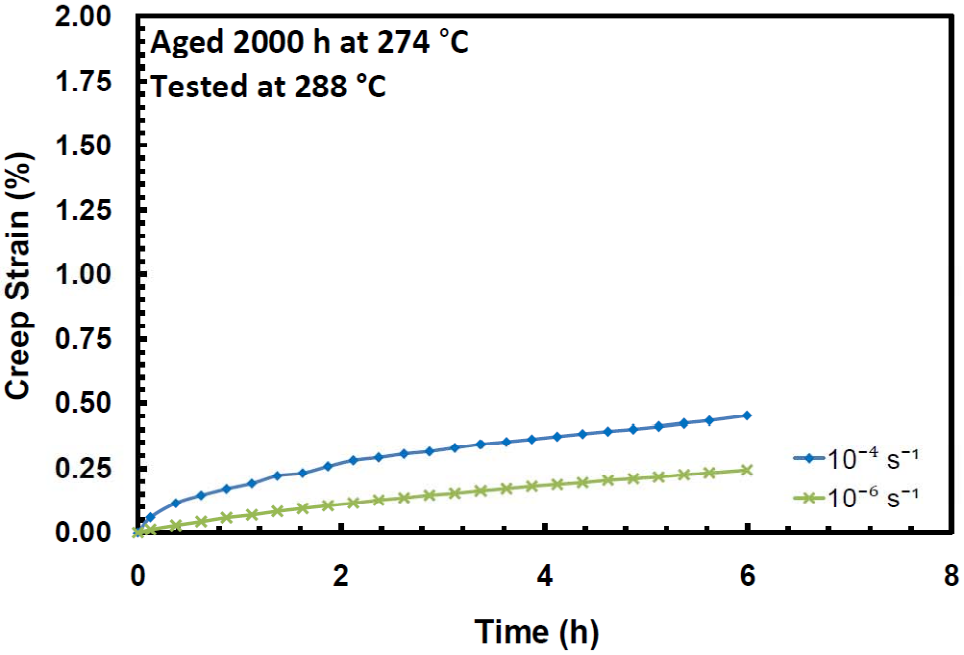

Figure 6.47: Creep Strain vs. Time Curves Obtained at 288 °C and 21 MPa for PMR-15 Aged for 2000 h at 274 °C. Prior Strain Rates of 10^{-4} and 10^{-6} s^{-1}.

Effects of prior aging at 274 °C on creep response may be assessed by comparing creep strains accumulated by specimens from different aging groups. The results of the creep tests are shown in Figure 6.48 and in Figure 6.49 for the prior strain rates of 10^{-4} s^{-1} and 10^{-6} s^{-1}, respectively. A general trend of decreasing creep strain accumulation with increasing aging duration may be observed. The most dramatic changes in creep strain accumulation are seen for specimens subjected to prior aging of shorter duration. For both prior strain rates the un-aged material accumulated the most creep strain and specimens aged for 2000 h accumulated the least creep strain.

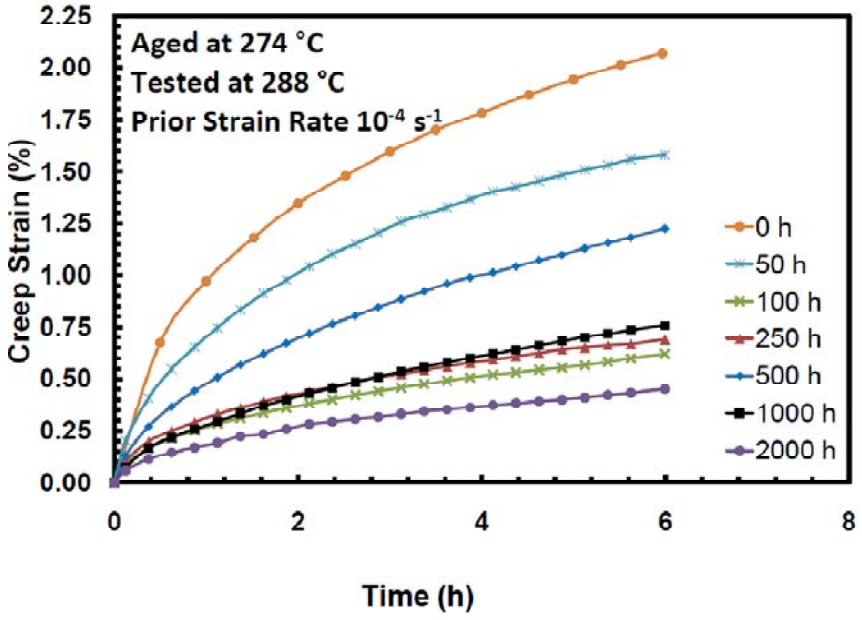

Figure 6.48: Creep Strain vs. Time Curves Obtained at 288 °C and 21 MPa for PMR-15 Aged at 274 °C. Prior strain rate is 10^{-4} s^{-1}. Data for the Un-aged Material from McClung[27].

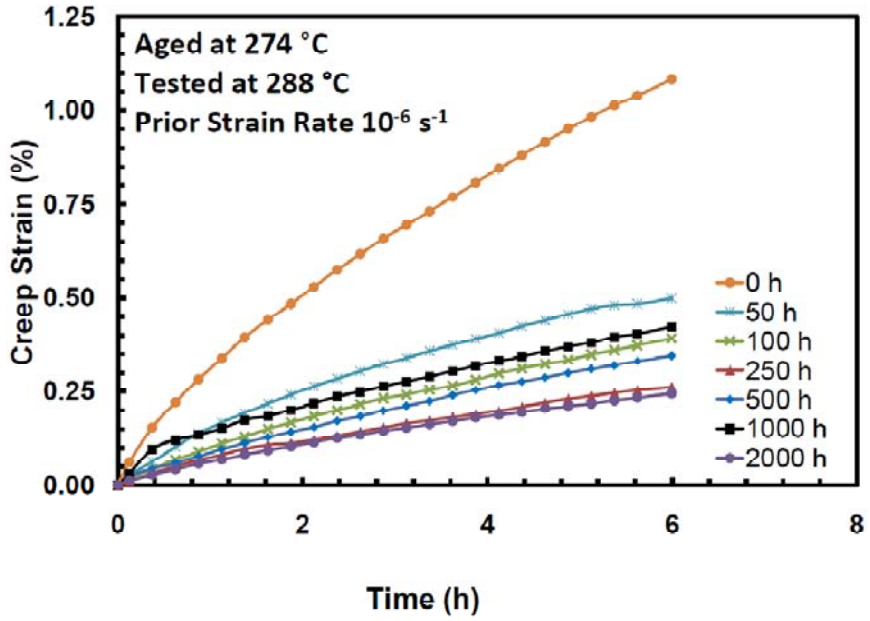

Figure 6.49: Creep Strain vs. Time curves obtained at 288 °C and 21 MPa for PMR-15 Aged at 274 °C. Prior strain rate is 10^{-6} s^{-1}. Data for the unaged material from McClung[27].Strain Rate Jump Test

The strain rate jump test is performed in order to assess whether the material exhibits the strain rate history effect (SRHE). The specimens were loaded to a strain of 3% at 10^{-5} s^{-1} where the strain rate was changed to 10^{-3} s^{-1}. A second set of tests were performed where specimens were loaded to a strain of 3% at 10^{-3} s^{-1} where the strain rate was changed to 10^{-5} s^{-1}.

Results of the strain rate jump tests obtained for specimens aged for 50 h are shown in Figure 6.50. It is seen that the stress-strain curve produced at 10^{-5} s^{-1} by the specimen initially loaded at a strain rate of 10^{-3} s^{-1} is consistent with the stress-strain curve produced by the specimen initially loaded at 10^{-5} s^{-1}. The specimen tested first at 10^{-5} s^{-1} then at 10^{-3} s^{-1} failed before the transient effects following the change in strain rate could diminish. However, it appears that the stress-strain curve produced after the strain rate was increased from 10^{-5} s^{-1} to

10^{-3} s^{-1} would have approached the curve expected in monotonic loading at an equal rate. This result suggests that the material does not exhibit SRHE. A unique stress-strain curve is obtained for a given strain rate. When the strain rate changes the stress "returns" to the stress-strain curve characteristic for that strain rate.

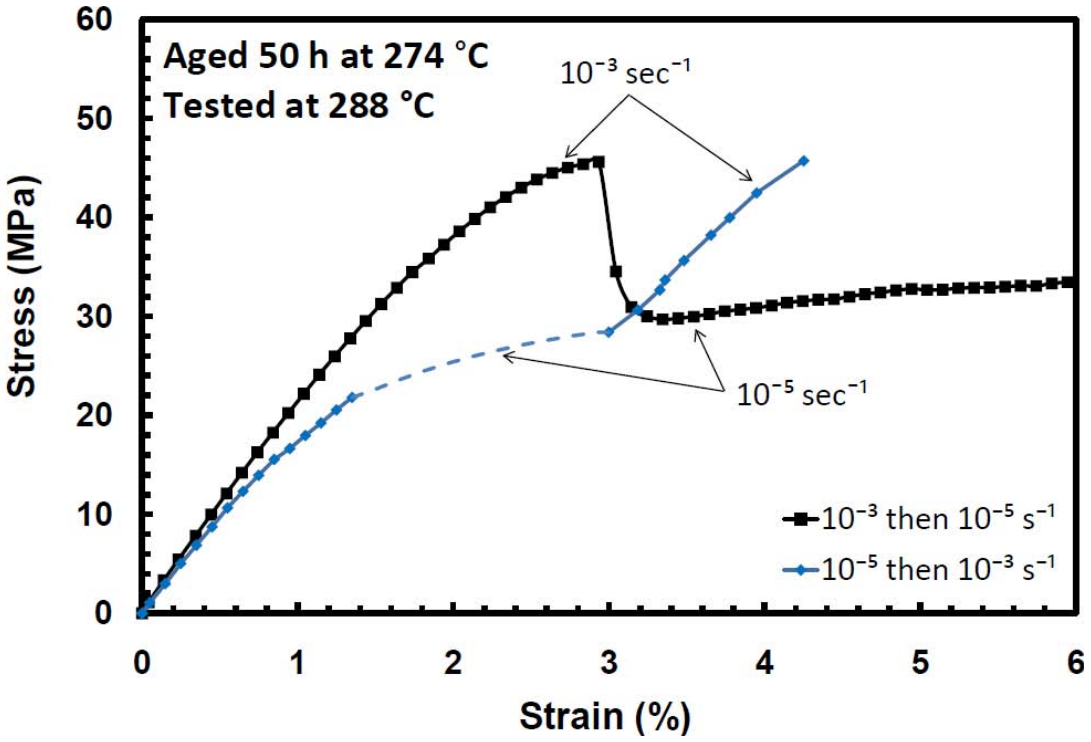

Figure 6.50: Stress-Strain Curves Obtained in Strain Rate Jump Tests for PMR-15 Aged 50 h at 274 °C Tested at 288 °C.

Only one of the two specimens aged for 100 h reached the strain of 3% where the strain rate was changed. As seen in Figure 6.51 the specimen subjected to the strain rate jump test produced higher flow stress at a strain rate of 10^{-5} s^{-1} than the specimen subjected to monotonic tension at that strain rate. Due to early failure of the specimen strained at 10^{-3} s^{-1} it is difficult to

draw any conclusions regarding the SRHE. However, the stress produced at 10^{-3} s^{-1} in the strain rate jump test appears to be consistent with the flow stress expected at this strain rate.

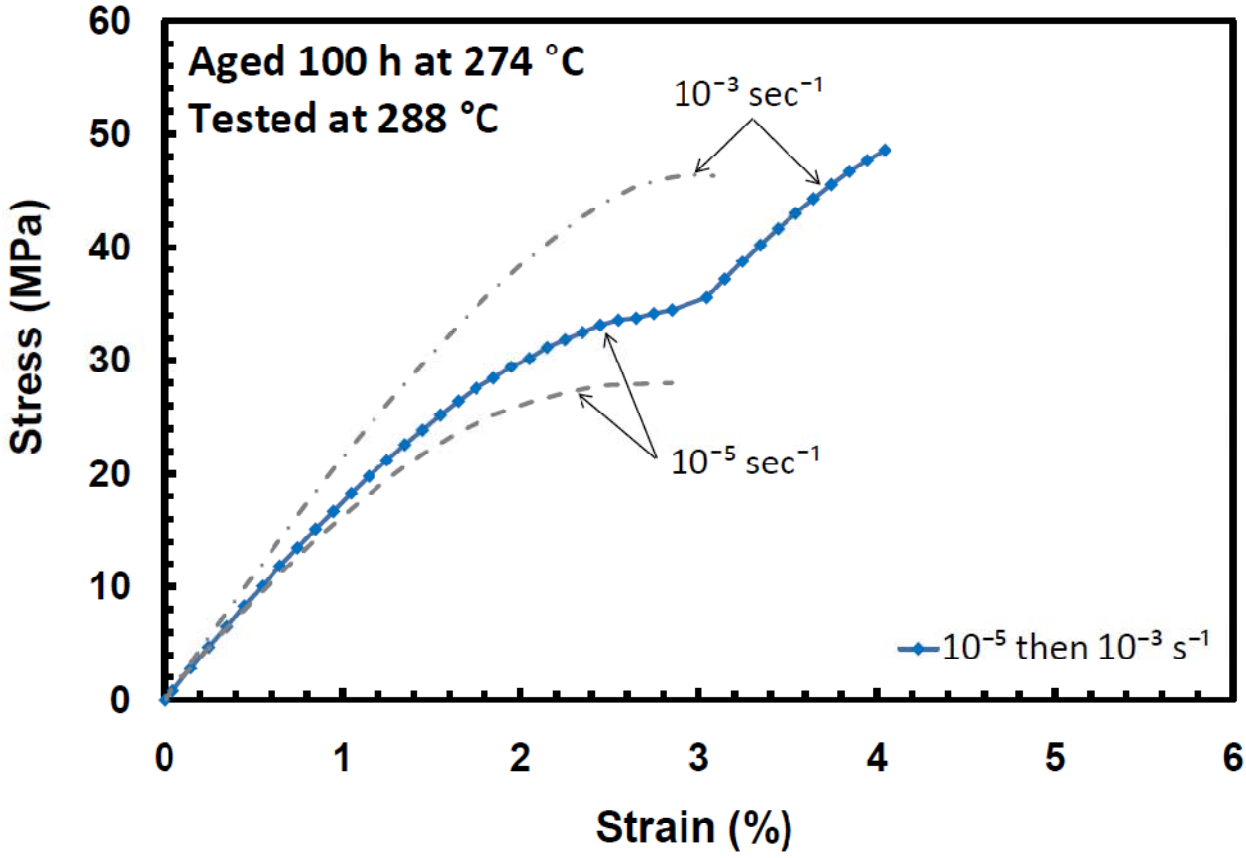

Figure 6.51: Stress-Strain Curves Obtained in Strain Rate Jump Test and Monotonic Tensile Tests for PMR-15 Aged 100 h at 274 °C Tested at 288 °C.

Results of the strain rate jump tests obtained for the specimens in the 250-h aging group provide some of the most valuable data in evaluating whether the material exhibits the strain rate history effect. As shown in Figure 6.52, the stress levels produced after the change in strain rate by both specimens quickly approach the flow stress levels characteristic for that particular strain

rate. These results support the assertion that PMR-15 does not exhibit SRHE at 288 °C.

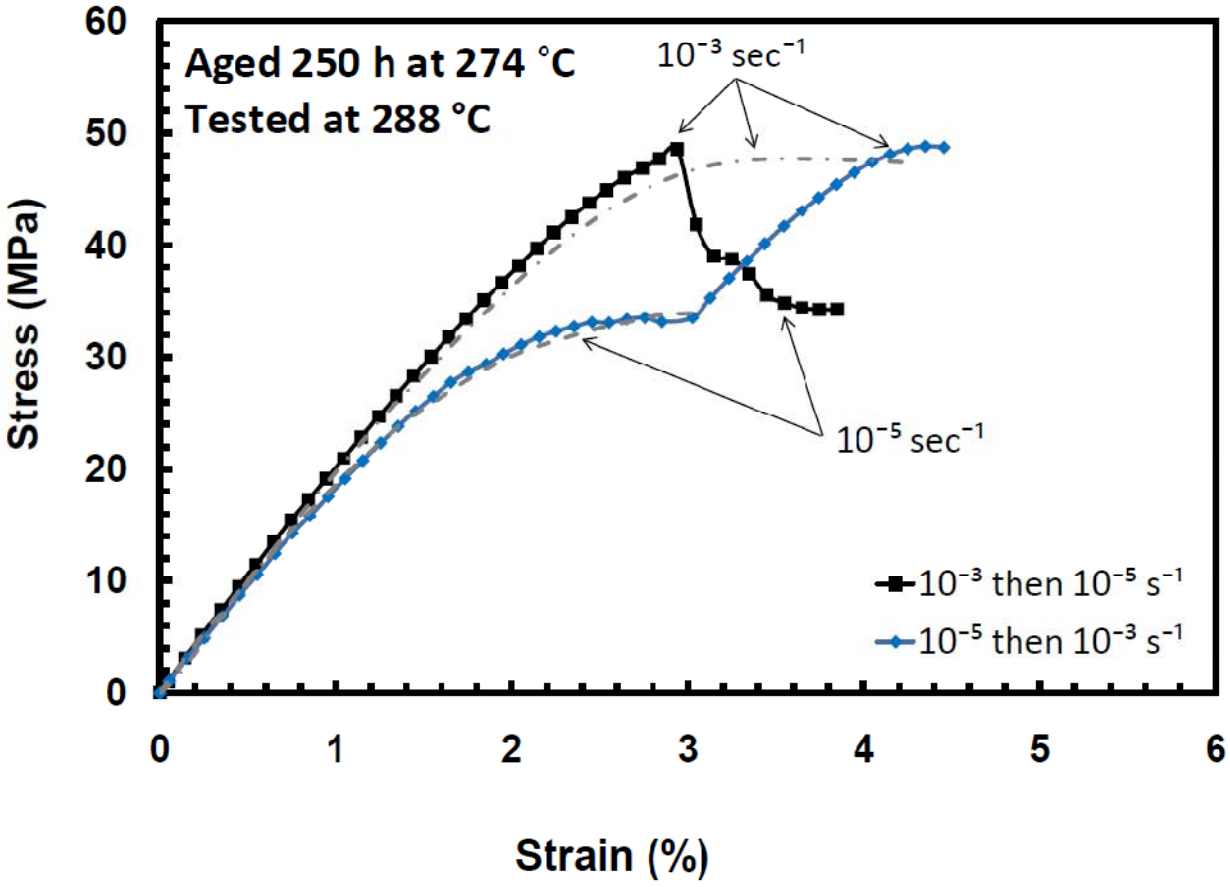

Figure 6.52: Stress-Strain Curves Obtained at 288 °C in Strain Rate Jump Test and in Monotonic Tensile Tests for PMR-15 Aged 250 h at 274 °C.

Results of the strain rate jump tests obtained for specimens aged for 500, 1000, and 2000 h are shown in Figure 6.53 through Figure 6.55. For all of these ageing groups, the specimens initially loaded at a strain rate of 10^{-3} s^{-1} failed before reaching the strain of 3%. Specimens initially loaded at the slower strain rate of 10^{-5} s^{-1} achieved the strain of 3% but produced stress levels that were higher than those produced in monotonic tension tests conducted at that strain rate. These specimens exhibited a rapid increase in stress following the strain rate jump.

However, specimen failures occurred shortly after the strain rate jump. Therefore only limited insight into the SRHE could be gained from these tests. McClung also noted difficulty in performing strain rate jump tests for specimens which had been exposed to long aging durations due to failures occurring at small strains [27].

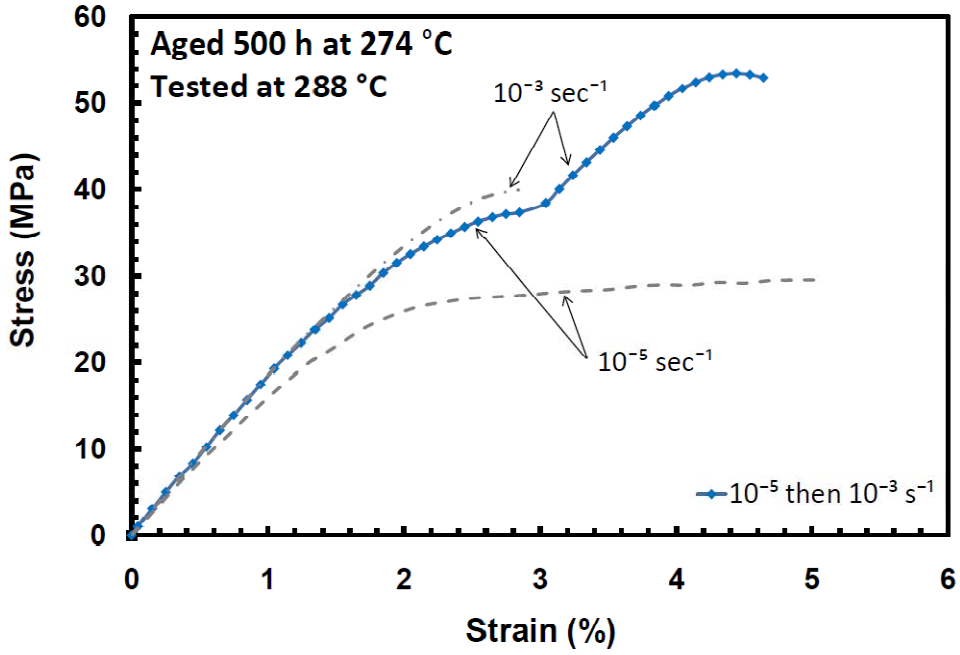

Figure 6.53: Stress-Strain Curves Obtained at 288 °C in Strain Rate Jump Test and in Monotonic Tensile Tests for PMR-15 Aged 500 h at 274 °C.

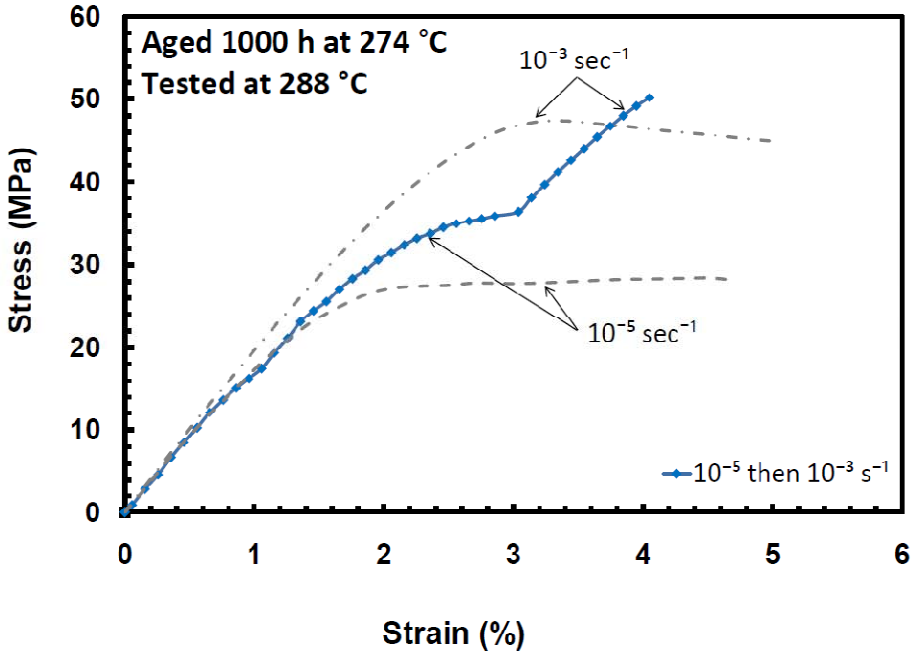

Figure 6.54: Stress-Strain Curves Obtained at 288 °C in Strain Rate Jump Test and in Monotonic Tensile Tests for PMR-15 Aged 1000 h at 274 °C.

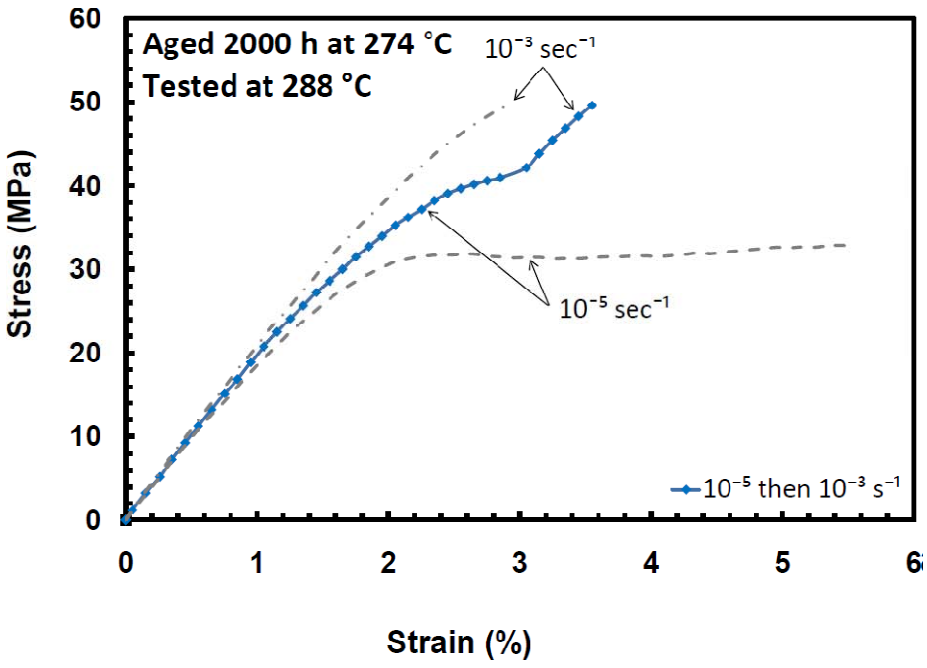

Figure 6.55: Stress-Strain Curves Obtained at 288 °C in Strain Rate Jump Test and in Monotonic Tensile Tests for PMR-15 Aged 2000 h at 274 °C.

Summary of Key Effects of Prior Aging in Argon at 274 °C on Deformation Behavior at 288 °C

This section summarizes the effects of prior aging at 274 °C on the mechanical deformation behavior of PMR-15 at 288 °C. Key effects of prior aging are listed below:

- Increase in quasi elastic modulus with increase in prior aging time
- Increasingly pronounced knee of the tensile stress-strain curve with increased prior aging time
- Increase in flow stress with increasing prior aging time
- Increase in tangent modulus with increasing prior aging time
- Decreasing creep strain accumulation with increase in prior aging time
- Increased brittleness with increase in prior aging time
- Prior aging has no discernible effect on stress drop during relaxation
- PMR-15 does not exhibit the strain rate history effect irrespective of prior aging history

Comparison of the Effects of Prior Aging in Argon at 274 °C with the Effects of Prior Aging at 288 °C

Previous research assessed the effects of prior aging at 288°C in argon on deformation behavior of PMR-15 at 288 °C [25, 26, 27]. The focus of prior work [25, 26, 27] was not on the effect of prior aging temperature on deformation behavior, but rather on the effect of prior aging time. Hence the aging and test temperature were the same (i. e. 288 °C). The current research aims to assess the effects of prior aging temperature on the deformation behavior. Therefore the effects of prior aging at 274°C on the deformation behavior at 288 °C were identified. Next the

effects of prior aging at 274°C on the deformation behavior at 288 °C will be compared to the effects of aging at 288 °C on the deformation behavior at 288 °C. By evaluating the deformation behavior at a single temperature (i. e. 288 °C) of the material with two different aging histories (the first involves aging at 274 ° while the second involves aging at 288°C) we aim to isolate and identify the effects of prior aging temperature. Specimens aged at these two different temperatures produced the following qualitatively similar features of deformation behavior:

- Increase in quasi elastic modulus with increase in prior aging time
- Increasingly pronounced knee of the tensile stress-strain curve with increased prior aging time
- Increase in flow stress with prior aging time
- Increase in tangent modulus with increasing aging time
- Decreasing creep strain accumulation with increase in prior aging time
- Increased brittleness with increase in prior aging time

Many of the observed behaviors are not only qualitatively similar but quantitatively comparable. The quantitative features of the material behavior will be further discussed in chapter 7. A notable difference in the effects of aging at these two temperatures is seen in the weight loss measurements presented in Figure 6.2.

In prior research efforts PMR-15 specimens were aged at 260 °C and at 316 °C [10, 27, 28]. In these efforts testing was performed at temperatures which were equal to the aging temperature. Despite these differences in aging/testing temperature the following common effects of prior aging may still be noted:

- Quasi-elastic modulus increased with prior aging time

- Increasingly pronounced knee of the tensile stress-strain curve with increasing prior aging time
- The flow stress increases with prior aging time at 274 °C and at 288 °C. (Specimens aged at 316 °C experienced failures before reaching the flow stress region)
- Increase in aging time (at all aging temperatures) results in an increasingly brittle response of the material

7. Constitutive Modeling

This chapter describes characterization of the VBOP model for PMR-15 subjected to prior aging at 274° C in argon. The VBOP has been successfully used to predict the mechanical behavior of PMR-15 aged and tested at 260 °C, 288 °C, and 316°C [10, 27, 28]. The effects of prior isothermal aging on deformation behavior have been modeled by making the VBOP model parameters dependent on prior aging time as suggested by McClung [27]. Based on test data from the current research the VBOP model parameters will be expanded into functions of prior aging time at 274 °C using the power law form recommended by McClung and employed to predict the behavior of PMR-15 specimen subjected to 2000 hours of aging at 274 °C.

Phenomenological Aspects of Deformation Behavior and Implications for Modeling

The results of experiments performed at 288 °C on PMR-15 subjected to prior aging at 274 °C has revealed the following characteristics:

1. Nearly linear elastic behavior upon initial loading
2. Nonlinearly increasing flow stress with increasing strain rate
3. Existance of a unique stress-strain curve for each strain rate
4. The rate of recovery of strain at zero stress increases with prior strain rate.
5. Increasing prior strain rate results in increasing creep strain.
6. Faster prior strain rates result in increased stress drop during relaxation.

The same trends were observed and modeled with the VBOP for both aged and un-aged PMR-15 polymer by Deidrick [10] at 260 °C, by McClung [27] at 288 °C, and by Ozmen [28] at 316 °C. In all prior research efforts the temperature of prior aging was the same as the

temperature, at which the deformation behavior was evaluated. The focus was on elucidating and modeling the effect of prior aging time on deformation behavior. This effort will also use the VBOP model to model the deformation behavior of PMR-15. However, the current research addresses the deformation behavior at 288 °C of the material subjected to prior aging at 274 °C. Now the focus is on elucidating and modeling the effect of prior aging temperature on deformation behavior.

Implications for Modeling the Effects of Prior Aging in Argon at 274 °C on Deformation Behavior at 288 °C

The key effects of prior isothremal aging on the deformation behavior of PMR-15 may be related to changes in specific VBOP model parameters:

1. As aging time increased the slope of the stress-strain curve immediately upon leaving the origin also increased. This can be accounted for in the VBOP model by changing the elastic modulus.
2. The increasingly pronounced knee of the stress-strain curve seen with longer aging times can be modeled by modifying parameter C_2 of the shape function as recommended by McClung [X].
3. The slope of the stress-strain curve in the region of the fully established inelastic flow increases with increasing prior aging duration. The VBOP model accounts for this variation by modifying the tangent modulus.
4. Increases in the flow stress level due to prior aging are readily observed. Flow stress levels are affected by tangent modulus, however changes in tangent modulus alone are

not sufficient to account for the observed changed in flow stress. The remaining difference may be accounted for within the VBOP framework by modifying the isotropic stress.

5. Due to the relative insensitivity of relaxation behavior to changes in prior aging history we may conclude that the VBOP viscosity function remains unchanged with prior aging duration.

Review of VBOP Model Formulation

A full explanation of the VBOP model formulation used to represent the behavior of PMR-15 at 288 °C subject to prior aging at 274 °C is provided in Chapter 3. For convenience this is reproduced here [27].

The uniaxial flow law is a combination of the elastic and inelastic strain rates

$$\dot{\epsilon} = \dot{\epsilon}^{el} + \dot{\epsilon}^{in} = \frac{\dot{\sigma}}{E} + \frac{\sigma - g}{Ek} \qquad (7.1)$$

The growth law of the equilibrium stress is

$$\dot{g} = \Psi \frac{\dot{\sigma}}{E} + \Psi \left[\frac{\sigma - g}{Ek} - \frac{g - f}{A}\left|\frac{\sigma - g}{Ek}\right|\right] + [1 - \frac{\Psi}{E}]\dot{f} \qquad (7.2)$$

The kinematic stress has the form

$$\dot{f} = \left[\frac{|\sigma|}{\Gamma + |g|}\right] E_t \frac{(\sigma - g)}{Ek} \qquad (7.3)$$

The overstress invariant is defined as

$$\Gamma = |\sigma - g| \qquad (7.4)$$

The isotropic stress evolution for polymers remains the same as that in the standard VBO

$$\dot{A} = A_c[A_f - A]\left|\frac{\sigma - g}{Ek}\right| \qquad (7.5)$$

Equation 7.5 is simplified for PMR-15 at 288 °C by setting $A_c = 0$ thus A is constant.

The shape function has the form

$$\Psi = C_1 + (C_2 - C_1)e^{-C_3|\epsilon^{in}|} \qquad (7.6)$$

Since A is constant, the viscosity function for polymers reduces to

$$k = k_1\left[1 + \frac{\Gamma}{k_2}\right]^{-k_3} \qquad (7.7)$$

Where k_1, k_2, and k_3 are material constants.

This formulation of VBOP was used in previous research accomplished for PMR-15 at 260 °C [10], 288 °C [27], and 316 °C [28]. Based upon experimental observations made at 288 °C for PMR-15 subjected to prior aging at 274 °C this formulation of VBOP is appropriate.

Model Characterization Procedures

Before a model may be employed to predict mechanical behavior it must be characterized for a given material. A systematic VBOP model characterization procedure was developed by McClung [27]. This research will follow the model characterization approach outlined in [27]:

1. Determine elastic modulus and tangent modulus from monotonic tensile data
2. Determine the equilibrium stress from relaxation data
3. Determine the isotropic stress from the equilibrium stress and the tangent modulus
4. Assess the viscosity function using results of the relaxation tests
5. Determine the shape function parameters from monotonic tensile test data

Elastic Modulus and Tangent Modulus

Because the initial loading portion of both the monotonic tension to failure and relaxation tests are identical both tests may be used to determine the initial quasi-elastic modulus. For

PMR-15 aged at 274 °C and tested at 288 °C a small portion of the stress-strain curve immediately after leaving the origin exhibits a nearly constant the slope. For strains below ~0.1% the slope of the stress-strain curve shows only modest dependence on strain rate. Thus, experimental data from both monotonic tension to failure tests and relaxation tests for all strain rates at strains below 0.1% were used to determine the elastic modulus used in the VBOP model.

To calculate the tangent modulus only tests which exhibit fully established inelastic flow should be used. Determining tangent modulus was difficult because many of the specimens failed before plastic flow was fully established. When experimental data provided the opportunity to calculate multiple measures of tangent modulus for an aging group the average of these measurements was used.

Equilibrium Stress and Isotropic Stress

The isotropic stress can be determined in the region of fully established plastic flow by taking the difference between the kinematic stress, f, and the equilibrium stress, g. The relationships between the kinematic stress, f, isotropic stress, A, equilibrium stress, g, and overstress, (σ-g), are shown in Figure 7.1. Kinematic stress is defined as $f = E_t\epsilon$ and may be determined using the tangent modulus already calculated. After determining kinematic stress the isotropic stress can be determined from the equation $A = \{g - E_t\epsilon\}$.

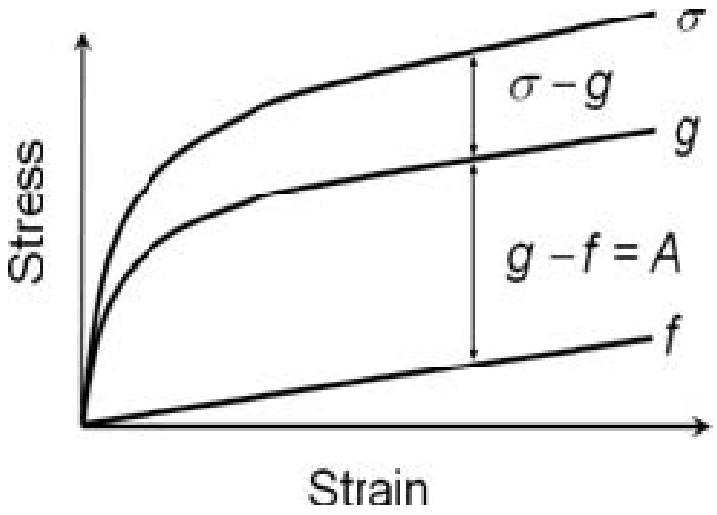

Figure 7.1: Schematic of a stress-strain path generated by the VBOP. The equilibrium stress, g, and kinematic stress, f, curves are also shown.

In the VBOP model stress present at the end of a sufficiently long period of relaxation is expected to approach the equilibrium stress-strain curve. It should be noted that the VBOP model predicts diminishing equilibrium stress during relaxation, thus the equilibrium stress present at the end of relaxation at a given strain is not equal to the equilibrium stress present during loading at that same strain. The fact that equilibrium stress evolves during relaxation complicates the computation of isotropic stress. McClung [27] and Diedrick [10] found that assuming that equilibrium stress did not change during relaxation resulted in unacceptably low values of isotropic stress. McClung [27] proposed iteratively estimating a value for isotropic stress and comparing the results to monotonic tension to failure experiments until acceptable results are obtained. This process was successfully followed by Diedrick [10] and is used in this research. McClung [27] states that once a value of isotropic stress has been found that produces good results for a particular material we may calculate the isotropic stress for the same material subjected to other prior aging durations from relaxation data.

In addition, the numerical VBOP simulations of the monotonic tension tests to failure together with the optimization techniques were employed to determine the isotropic stress. The isotropic stress computed using this method was higher than that produced by measuring stress at the end of relaxation. However, when this value of isotropic stress was used to model monotonic tension to failure it was found that it was still too low to produce good agreement with experimental data. For example, in the case of specimens in the 50-h aging group, stress at the end of the relaxation test was 10.8 MPa, isotropic stress generated by using numerical simulations and optimization was 17 MPa, and isotropic stress that produced satisfactory simulations of the monotonic tension to failure data was 22 MPa. It is believed that if relaxation tests were performed in the region of fully established plastic flow the agreement between the isotropic stress found through numerical simulation and optimization and the isotropic stress determined from experimental results would be improved.

Alternately, stress levels in the region of fully established flow could be used to solve for isotropic stress if viscosity function parameters were simultaneously established. An improved method of finding isotropic stress may entail optimizing viscosity function parameters and isotropic stress simultaneously using experimental relaxation data obtained in the flow stress region. This method was not applied in this research due to lack of experimental data in the flow stress region.

Viscosity Function

Rate dependence of the VBOP is controlled by the viscosity function given in Equation 7.7. McClung [27] concluded that the viscosity function parameters do not change with prior isothermal aging. McClung [27] investigated the deformation behavior of PMR-15 at 288°C as

did this effort. Hence the viscosity function parameters obtained in this research should be nearly equal to those obtained by McClung [26]. Experimental results of relaxation tests obtained for the 50-h aging group for prior strain rates of 10^{-3}, 10^{-4}, 10^{-5}, and 10^{-6} s^{-1} and a least squares optimization routine in MATLAB were used to determine the values of the viscosity function parameters k_1, k_2, and k_3. McClung [26] reported that using values of stress drop produced during the entire relaxation period resulted in viscosity function parameters that did not match monotonic tension to failure data. For this reason only experimental data obtained in the last two hours of relaxation were used to determine the viscosity function parameters.

Note that the viscosity function parameters established in this research differ from those determined by McClung [27]. These differences, although measureable cause only minor changes in relaxation behavior. Recall that McClung [26] determined the viscosity function parameters from relaxation tests performed at the strain of 4.5%, where the inelastic flow was fully established. In the case of present research, the relaxation tests were performed at the strain of 3.0%, where at some strain rates the inelastic flow was not fully established. Due to limited ductility and early failures of the material in the current study, the relaxation tests could not be performed at larger strain values and in some cases the relaxation data had to be collected before the inelastic flow was fully established. Using relaxation data collected outside the flow stress region as well as the variability in the material is likely behind the difference between the values of the viscosity function parameters produced in this research and those reported by McClung [26].

Shape Function

The shape function is responsible for the shape of the stress-strain curve during the transition from quasi-elastic to inelastic behavior and is given in Equation 7.6. A MATLAB optimization program and experimental data from monotonic tension to failure tests at strain rates of 10^{-3}, 10^{-4}, 10^{-5}, and 10^{-6} s^{-1}were used to determine the values of the shape function parameters C_1, C_2, and C_3. For the 50-h aging group the shape function parameters were $C_1 = 100$ MPa, $C_2 = 1.02e + 03$ MPa, and $C_3 = 9.00e - 4$. Note that the value of C_3 is significantly lower than the value $C_3 = 10$ reported by McClung [26]. Furthermore, McClung [26] points out that C_3 is not affected by prior isothermal aging. Further investigation revealed that C_3 did not strongly influence the shape of the stress-strain curve. By carrying out the MATLAB optimization with C_3=10 new shape function parameters $C_1 = 100$ MPa and $C_2 = 1.00e + 03$ MPa were obtained. The stress-strain curves generated by using VBOP with these two sets of shape function parameters are shown in Figure 7.2. Note that increasing the value of C_3 by more than four orders of magnitude has little effect on the shape of the stress-strain curve. Inspection of the shape function Equation 7.6 reveals that parameter C_3 appears as a coefficient multiplying the inelastic strain. As the amount of the inelastic strain is rather small, parameter C_3 has little influence. To maintain consistency with previous research the value $C_3 = 10$ will be used in this study.

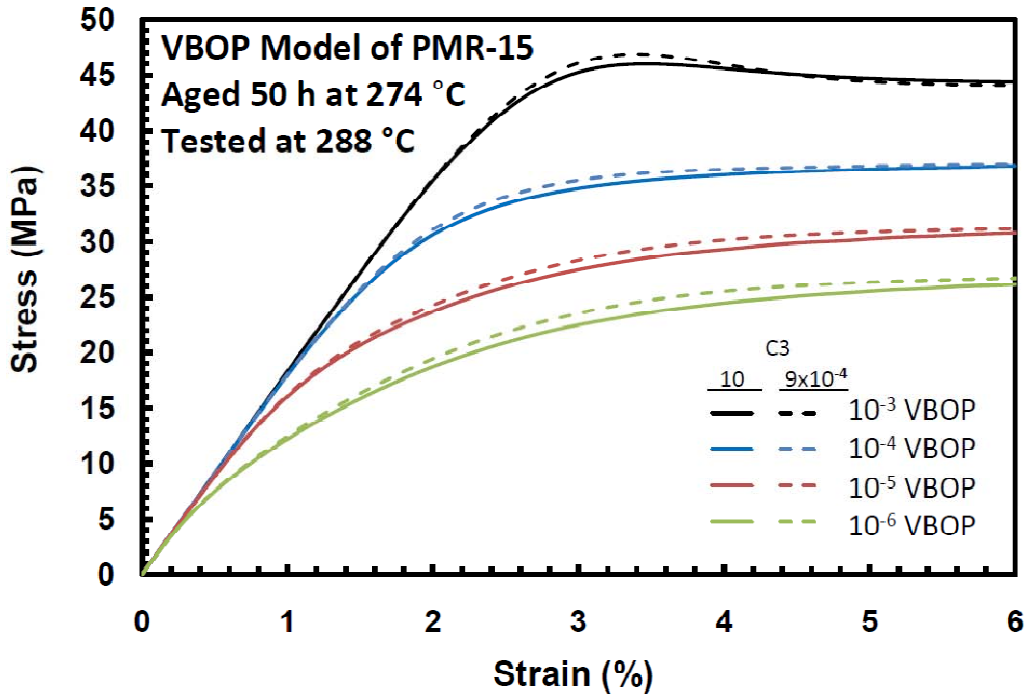

Figure 7.2: Simulated Stress-Strain Curves Generated Using VBOP with Different Values of the Shape Function Parameter C_3

Characterization of Model Parameters for PMR-15 Neat Resin Subjected to Prior Aging in Argon at 274 °C

The model characterization procedure outlined in the previous section was applied to PMR-15 aged in argon at 274 °C for 50, 100, 250, 500, and 1000 h. The parameters which are not affected by prior isothermal aging (k_1, k_2, k_3, C_1, and C_3) were determined from experimental results obtained for the 50-h aging group and then used for all other aging groups. Modeling efforts for each aging group are discussed below.

Prior Aging for 50 h

The VBOP model parameters obtained at 288 ° for PMR-15 aged for 50 h at 274 °C in argon are summarized in Table 7-1.

Table 7-1: VBOP Model Parameters at 288 °C for PMR-15 Neat Resin Subjected to 50 h of Prior Aging at 274 °C in Argon.

Moduli	E = 1830 MPa, E_t = 16.6 MPa
Isotropic Stress	A = 22.0 MPa
Viscosity Function	k_1 = 1.15e+04 s, k_2 = 29.8 MPa, k_3 = 12.7
Shape Function	C_1 = 100 MPa, C_2 = 1000 MPa, C_3 = 10.0

The experimental results used to characterize the model for this aging group are compared with the VBOP simulations in Figure 7.3 and Figure 7.4. The VBOP simulations of the stress-time behavior during relaxation slightly over predict the stress drop for the fastest prior strain rate in the early stages of relaxation. The model simulations give a very good representation of the stress-time behavior during relaxation for the two intermediate prior strain rates. The VBOP under predicts stress drop late in the relaxation period for the specimen loaded at the slowest prior strain rate. Because of early failures only monotonic tensile tests conducted at strain rates of 10^{-4} and 10^{-6} s^{-1} provide useful experimental data beyond the initial quasi-elastic regime. For all specimens tested, the model accurately simulates the experimental results up to failure (see Figure 7.4).

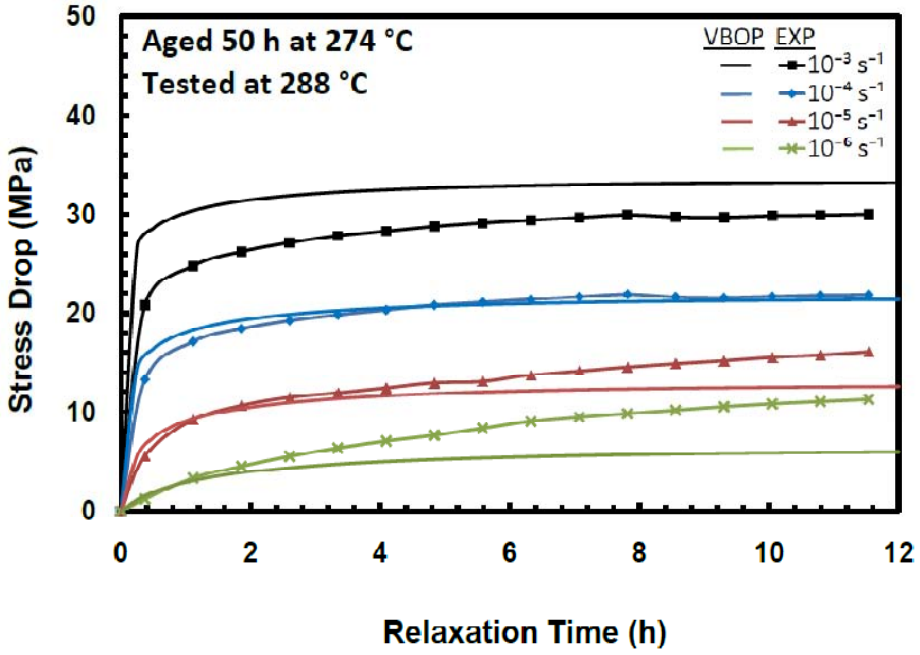

Figure 7.3: A Comparison of Experimental and Simulated Stress Decrease vs. Relaxation Time Curves Obtained at 288 °C for PMR-15 Aged for 50 h at 274 °C in Argon.

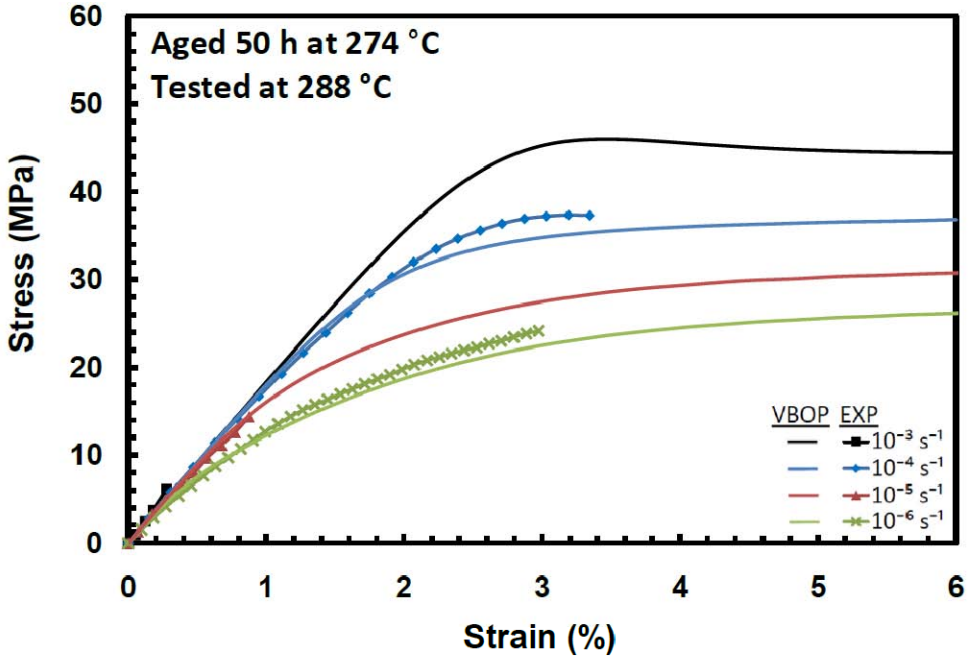

Figure 7.4: A Comparison of Experimental and Simulated Monotonic Tensile Stress-Strain Curves Obtained at 288 °C for PMR-15 Aged for 50 h at 274 °C in Argon.

It is seen that the simulations of strain-controlled monotonic loading (Figure 7.4) and simulations of the relaxation response (Figure 7.3) are in good agreement with experimental data. Next the VBOP constitutive model and the model parameters determined in the characterization procedure at 288 °C for PMR-15 aged for 50 h at 274 °C in argon must be validated by comparing the model predictions with experimental results that differ in kind from those used for model characterization. Three types of tests have been selected for validation: loading and unloading at a constant strain rate magnitudes, creep tests, and strain rate jump tests. These tests are described in greater detail in Chapter 5. Predictions of the loading and unloading at constant strain rates of 10^{-3} and 10^{-5} s^{-1} are compared with experimental results in Figure 7.5. The strain rate sensitivity of the material during loading is well represented for both strain rates. The unloading behavior predicted by the VBOP model does not match the behavior observed in experiments. The model qualitatively predicts increased curvature of the unloading stress-strain curve with decreasing strain rate. Yet in all cases the VBOP over predicts the strains measured immediately upon reaching zero stress. Failure of the VBOP to accurately predict unloading behavior has been noted by both McClung [27] and Diedrick [10]. To produce quantitatively accurate predictions of the unloading behavior the model formulation would have to be modified.

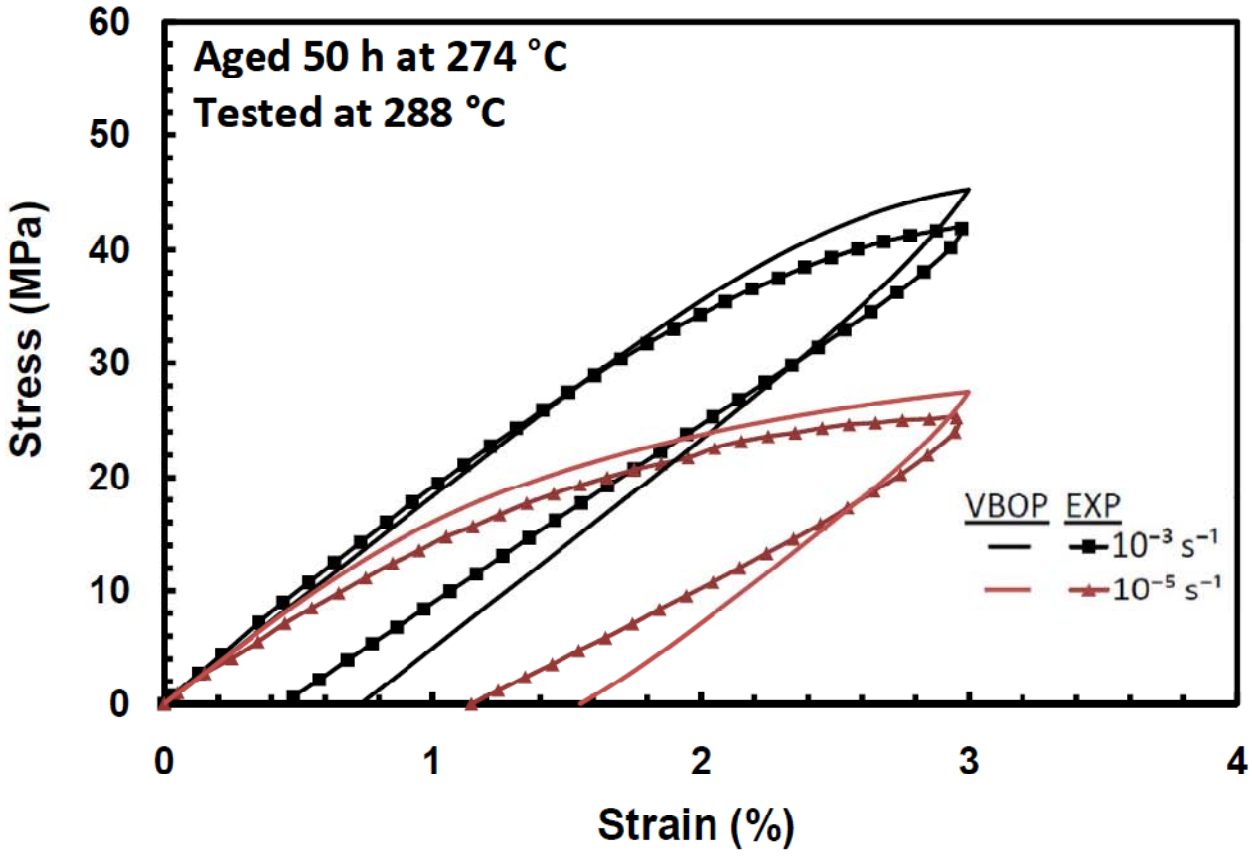

Figure 7.5 A Comparison of Experimental and Predicted Stress-Strain Curves Obtained in Loading and Unloading at Two Constant Strain Rates at 288 °C for PMR-15 Aged for 50 h at 274 °C in Argon.

The model characterization procedure employs strain-controlled experiments. Therefore prediction of the stress-controlled experiments represents a more rigorous validation of the VBOP and of the model characterization procedure. Figure 7.6 compares predictions with the experimental results produced in creep tests of 6-h duration conducted at 21 MPa, preceded by strain-controlled loading at 10^{-6} s^{-1} and 10^{-4} s^{-1}. The qualitative effect of prior strain rate is predicted well, higher prior strain rate results in larger creep strain. However, the quantitative predictions are inadequate. The VBOP model over predicts the creep strain for both prior strain

rates. Diedrick reported similar discrepancies when modeling creep behavior at 260°C [10]. Because strain rate dependence is governed by the viscosity function, the results of creep tests could be used to characterize the viscosity function parameters of the VBOP. However Diedrick noted that because calibration of the model based on relaxation data failed to produce quantitatively accurate predictions of creep response, characterization of the model based on creep data would likely result in inaccurate predictions of relaxation behavior.

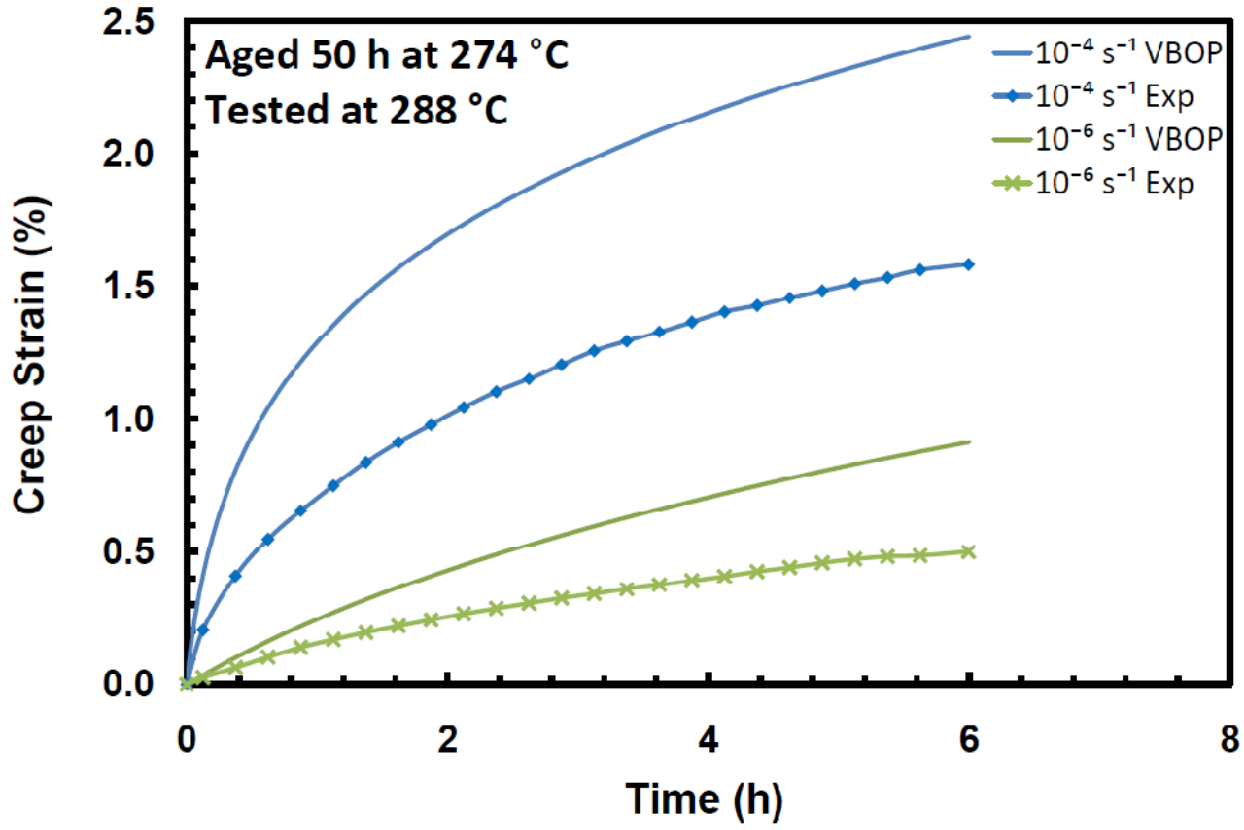

Figure 7.6: A Comparison of Experimental and Predicted Creep Strain vs. Time Curves Obtained at 21 MPa and 288 °C for PMR-15 Aged for 50 h at 274 °C in Argon.

Predictions of the strain rate jump tests performed in strain control with the strain rates of 10^{-3} then 10^{-5} s^{-1} are presented together with the experimental data in Figure 7.7. The VBOP successfully predicts the stress response during all stages of the test. The model predictions are in excellent agreement with experimental results.

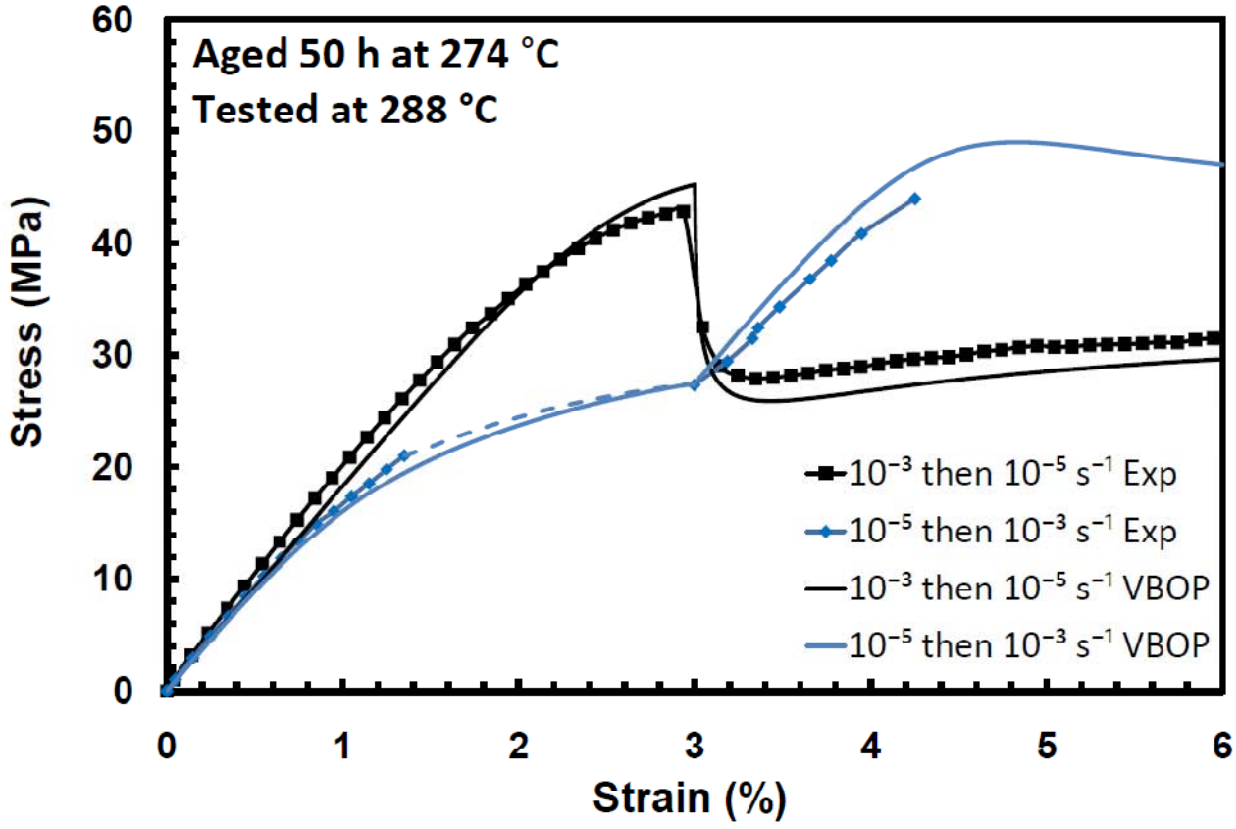

Figure 7.7: A Comparison of Experimental and Predicted Stress-Strain Curves Obtained in Strain Rate Jump Tests at 288 °C for PMR-15 Aged for 50 h at 274 °C in Argon.

Prior Aging for 100 h

The VBOP model parameters obtained at 288 ° for PMR-15 aged for 100 h at 274 °C in argon are summarized in Table 7-2.

Table 7-2: VBOP Model Parameters at 288 °C for PMR-15 Neat Resin Subjected to 100 h of Prior Aging at 274 °C in Argon.

Moduli	E = 1920 MPa, E_t = 36.4 MPa
Isotropic Stress	A = 23.0 MPa
Viscosity Function	k_1 = 1.15e+04 s, k_2 = 29.8 MPa, k_3 = 12.7
Shape Function	C_1 = 100 MPa, C_2 = 1030 MPa, C_3 = 10.0

The VBOP simulations of the relaxation behavior are compared with the experimental data in Figure 7.8. Simulations generated for prior strain rates of at 10^{-4} then 10^{-6} s^{-1} are in excellent agreement with experimental results. For strain rates of at 10^{-3} then 10^{-5} s^{-1} the model simulations are in reasonable agreement with the data.

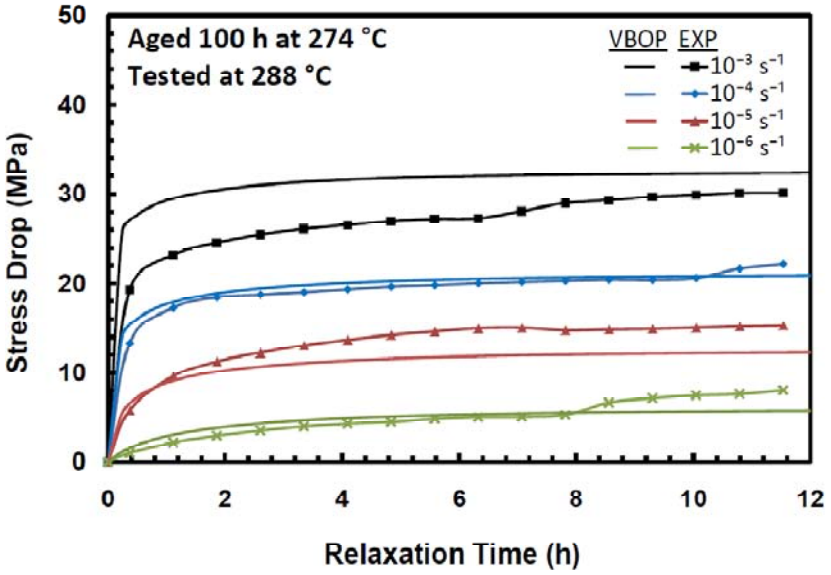

Figure 7.8: A Comparison of Experimental and Simulated Stress Decrease vs. Relaxation Time Curves Obtained at 288 °C for PMR-15 Aged for 100 h at 274 °C in Argon.

The simulations of the strain-controlled monotonic loading are compared with the results of the tensile tests in Figure 7.9. Stress-strain behavior is well represented by the VBOP with the experimental and simulated stress-strain curves showing little divergence for strains < 3.5%. In the flow stress region the model predicts higher stress levels than those measured in experiments. This may be caused by a fairly high isotropic stress value determined for this aging group.

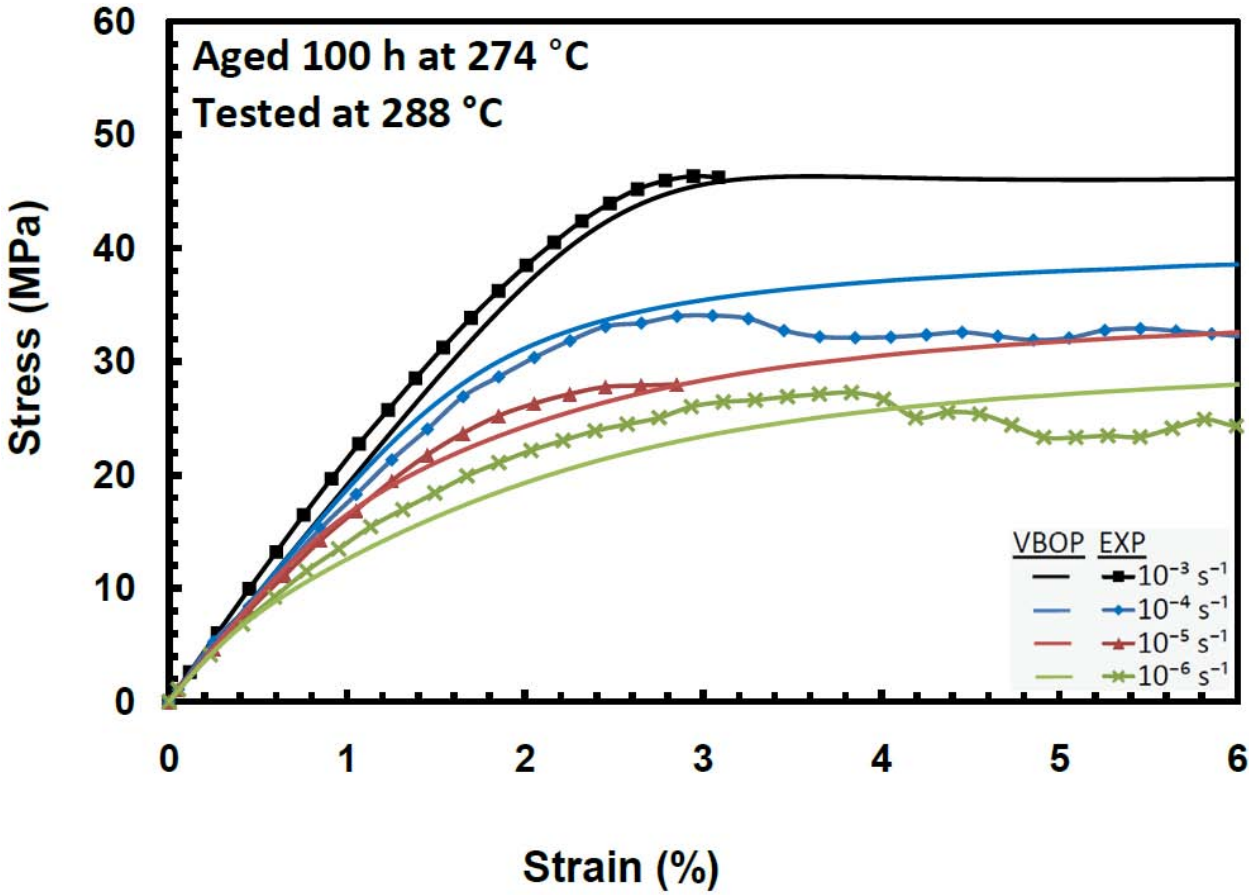

Figure 7.9: A Comparison of Experimental and Simulated Monotonic Tensile Stress-Strain Curves Obtained at 288 °C for PMR-15 Aged for 100 h at 274 °C in Argon.

To validate the model parameters calculated for the 100-h aging group, predictions of strain-controlled loading and unloading at several strain rate magnitudes were generated with the

VBOP and compared with experimental data (see Figure 7.10). The stress-strain behavior on the loading path is predicted very well for all strain rates. The stress-strain behavior on the unloading path is predicted accurately only in the case of the slowest strain rate.

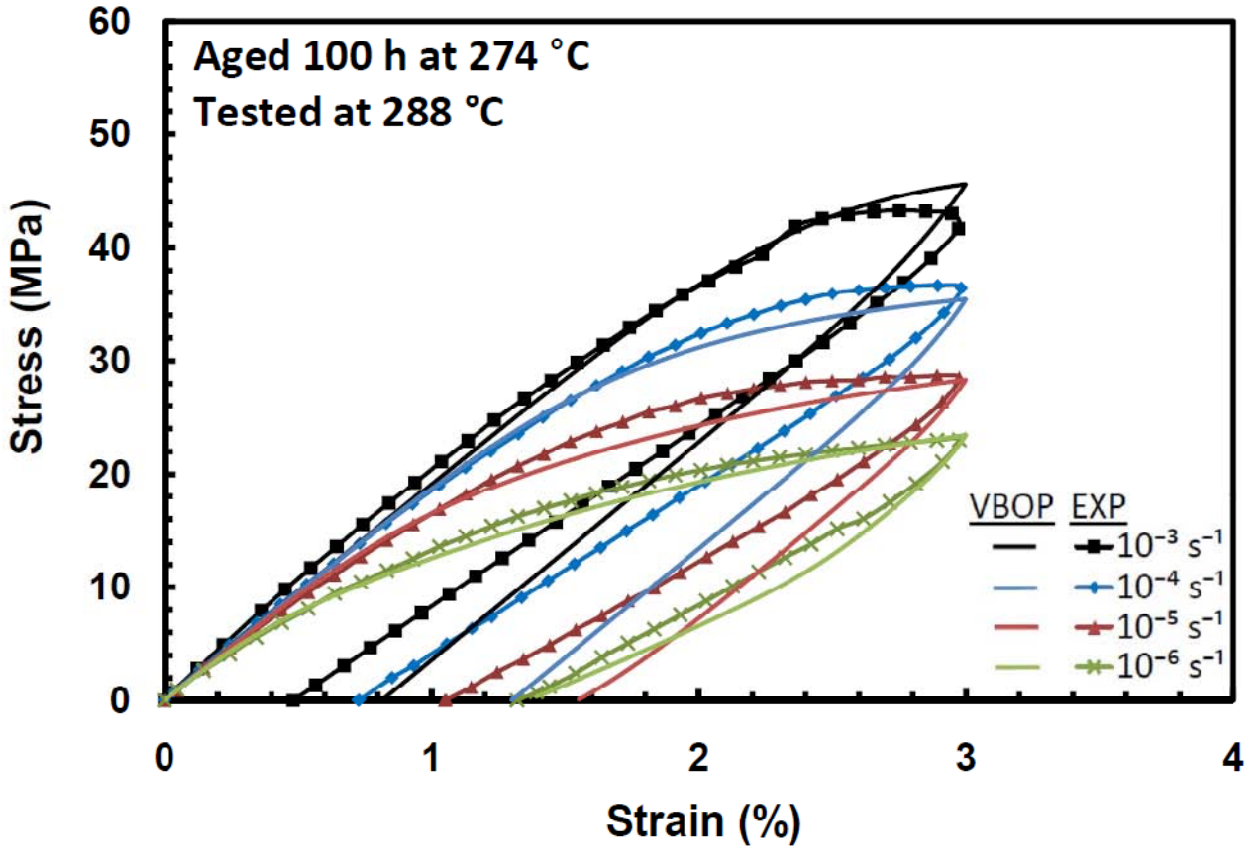

Figure 7.10: A Comparison of Experimental and Predicted Stress-Strain Curves Obtained in Loading and Unloading at 288 °C for PMR-15 Aged for 100 h at 274 °C in Argon.

Figure 7.11 compares predictions with the experimental results produced in creep tests of 6-h duration conducted at 21 MPa, preceded by strain-controlled loading at 10^{-6} s^{-1} and 10^{-4} s^{-1}. The VBOP considerably over predicts creep strains. However, it should be noted that the specimen loaded to the creep stress at a strain rate of 10^{-4} s^{-1} produced an exceptionally low creep strain. In fact, the only specimen that produced less creep strain under the same test

conditions in the current study was the specimen subjected to 2000 h of prior aging. It is likely that additional specimens in the 100-h aging group (if such were available) would have produced larger creep strains under the given test condition.

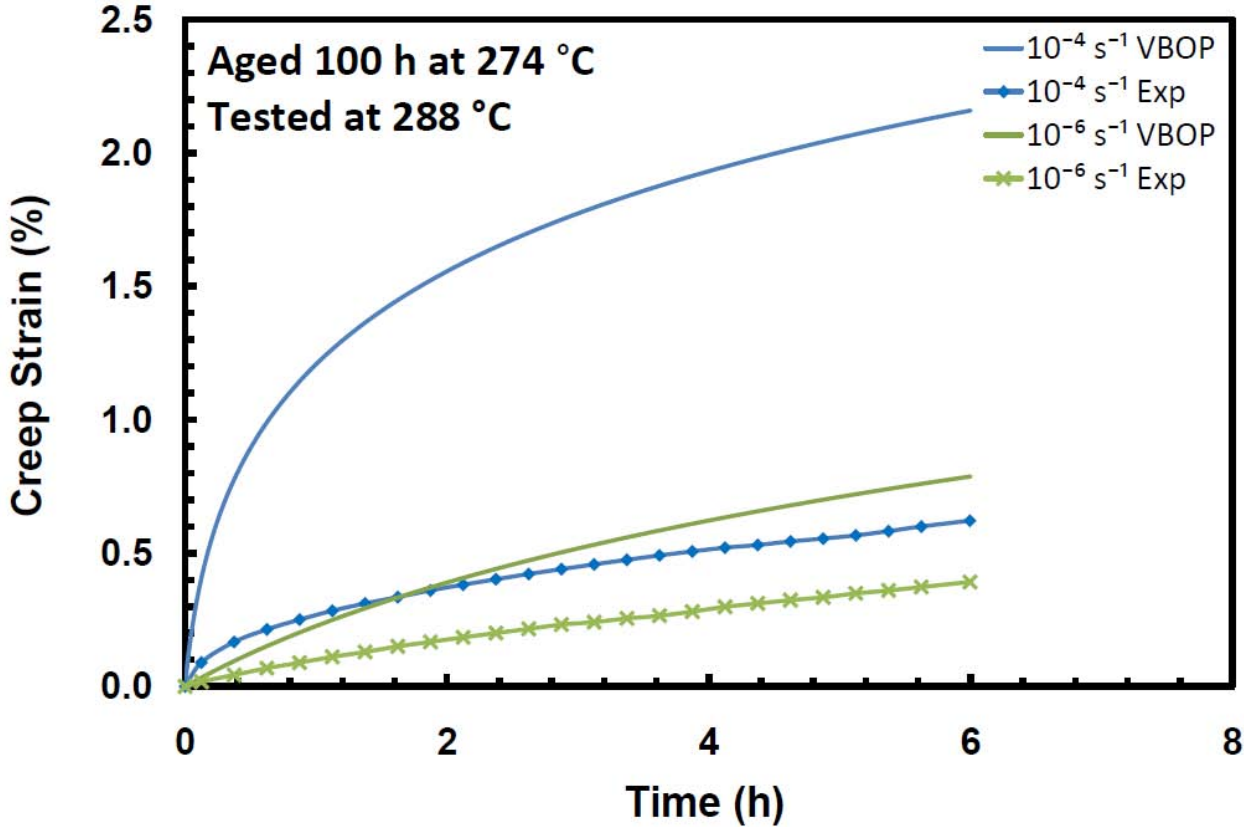

Figure 7.11: A Comparison of Experimental and Predicted Creep Strain vs. Time Curves Obtained at 21 MPa and 288 °C for PMR-15 Aged for 100 h at 274 °C in Argon.

The VBOP prediction of the strain rate jump test is compared with the experimental results in Figure 7.12. Note that during the initial loading at a strain rate of 10^{-3} s^{-1} the specimen produced higher stress levels than were typical for this aging group. Consequently the experimental stress levels exceeded the predicted ones. After the strain rate change the prediction was in better agreement with the experimental data.

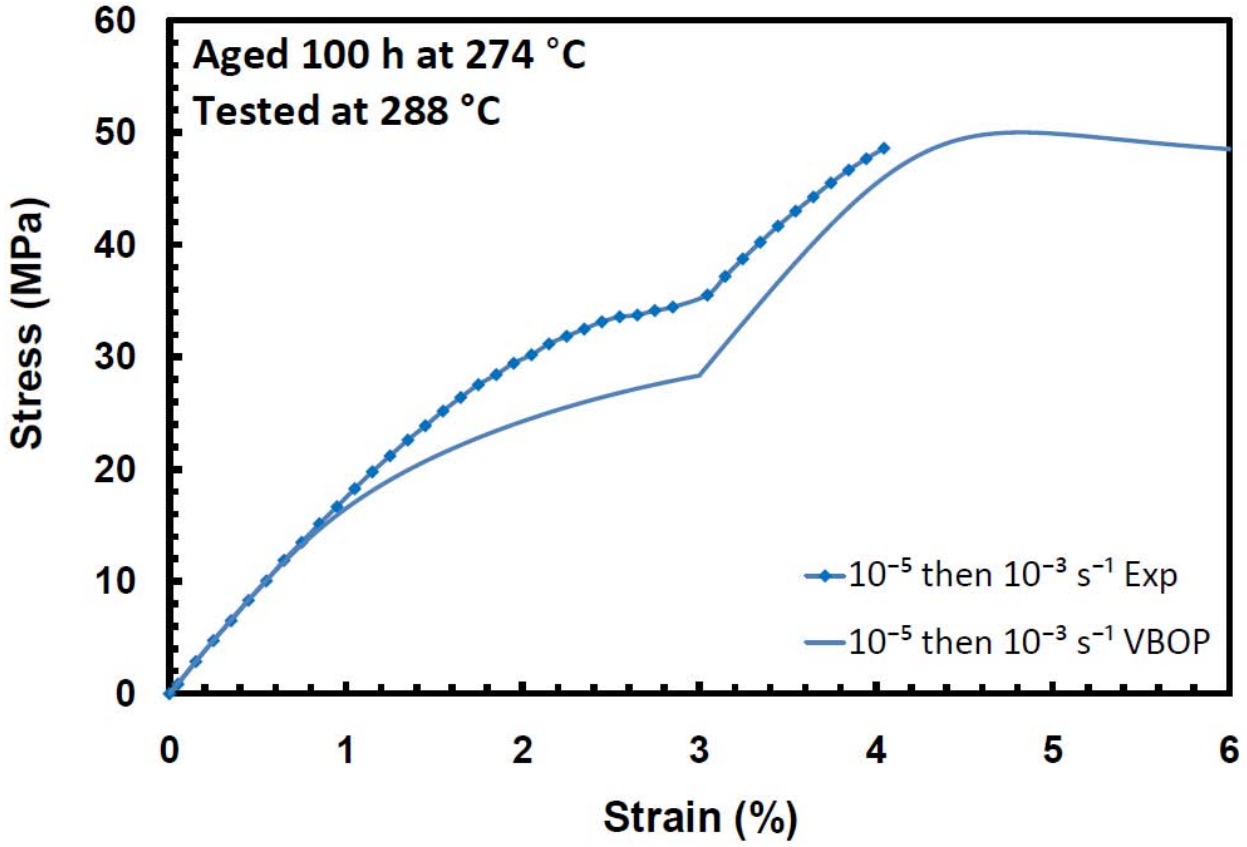

Figure 7.12: A Comparison of Experimental and Predicted Stress-Strain Curves Obtained in Strain Rate Jump Tests at 288 °C for PMR-15 Aged for 100 h at 274 °C in Argon.

Prior Aging for 250 h

The VBOP model parameters obtained at 288 ° for PMR-15 aged for 250 h at 274 °C in argon are summarized in Table 7-3.

Table 7-3: VBOP Model Parameters at 288 °C for PMR-15 Neat Resin Subjected to 250 h of Prior Aging at 274 °C in Argon.

Moduli	E = 1910 MPa, E_t = 58.0 MPa
Isotropic Stress	A = 23.9 MPa
Viscosity Function	k_1 = 1.15e+04 s, k_2 = 29.8 MPa, k_3 = 12.7
Shape Function	C_1 = 100 MPa, C_2 = 1090 MPa, C_3 = 10.0

Simulations of the relaxation behavior are compared with the experimental data in Figure 7.13. In the case of the three slowest prior strain rates, the simulations of the relaxation response agree well with the experimental results. In the case of fastest prior strain rate, the model over predicts the stress drop in the early stages of the relaxation. Yet after about 5 h of relaxation, model simulation and experimental results begin to converge.

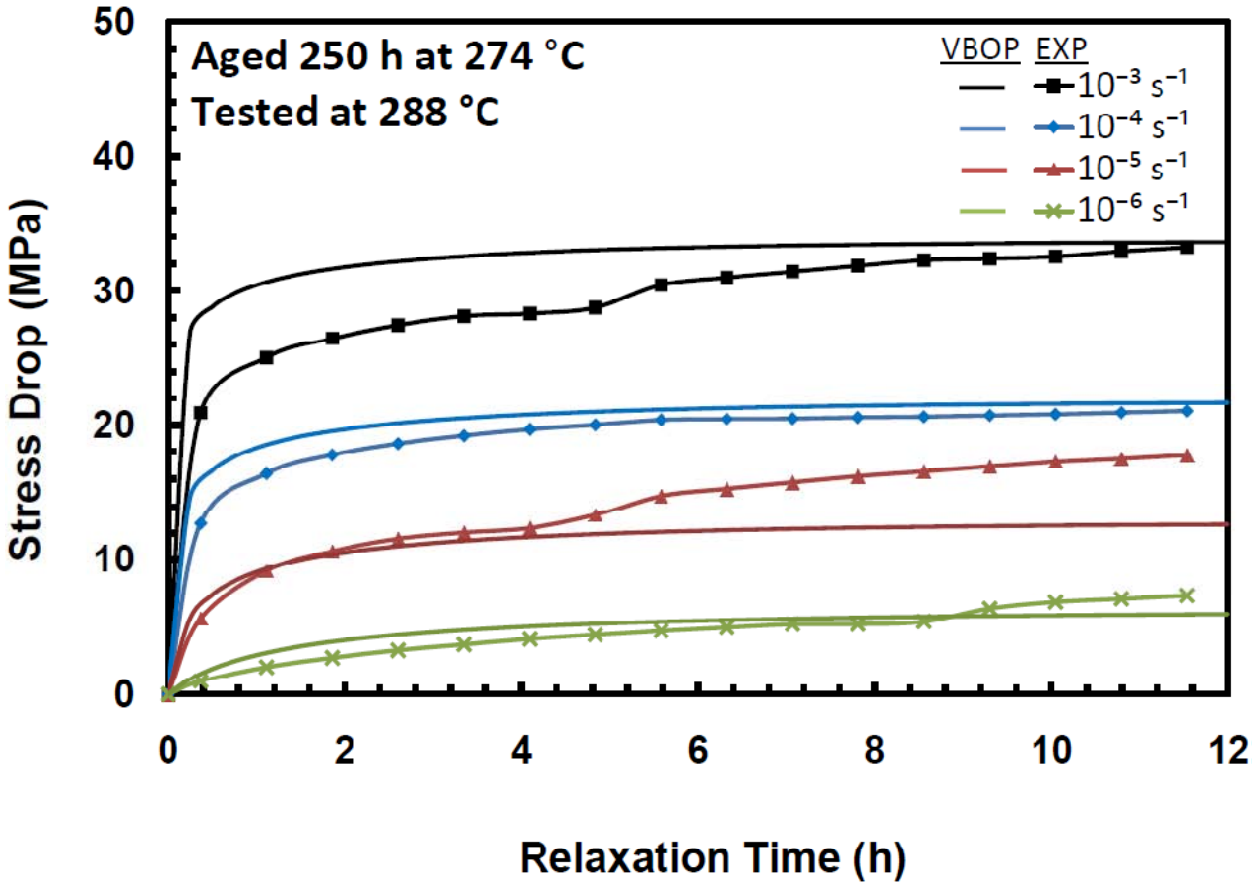

Figure 7.13: A Comparison of Experimental and Simulated Stress Decrease vs. Relaxation Time Curves Obtained at 288 °C for PMR-15 Aged for 250 h at 274 °C in Argon.

A comparison of the simulations and experimental results for monotonic tension to failure at various strain rates is presented in Figure 7.14. At the strain rates of 10^{-3} s^{-1} and 10^{-6} s^{-1} the simulations are in excellent agreement with the experimental data. The stress-strain behavior produced at a strain rate of 10^{-4} s^{-1} was well modeled by the VBOP for strains < 2.5%, where experiment exhibited a sudden decrease in stress. Unfortunately due to a limited number of specimens additional tests could not be performed. The specimen tested at10^{-5} s^{-1} produced higher than average stress levels and failed before plastic flow was fully established.

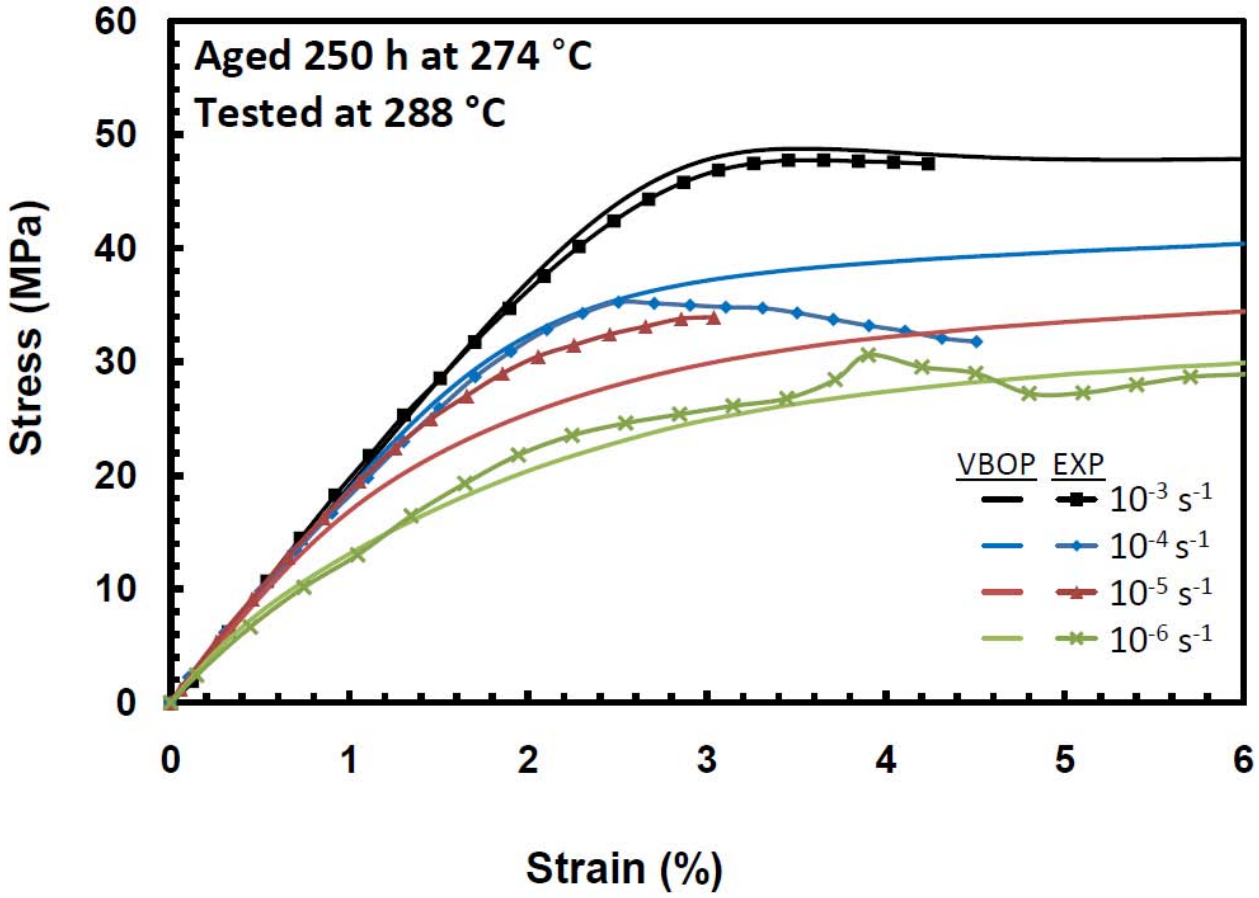

Figure 7.14: A Comparison of Experimental and Simulated Monotonic Tensile Stress-Strain Curves Obtained at 288 °C for PMR-15 Aged for 250 h at 274 °C in Argon.

To validate the model, predictions of strain-controlled loading and unloading were compared with experimental results (see Figure 7.15). In the case of loading at the two fastest strain rates, predictions are in good agreement with experimental results. However, the model under predicts the stress levels produced during loading at the slower strain rates. As was the case with other aging groups, the model does not accurately represent unloading stress-strain behavior at faster strain rates. Conversely at 10^{-6} s^{-1}, the unloading stress-strain behavior is well represented by the VBOP.

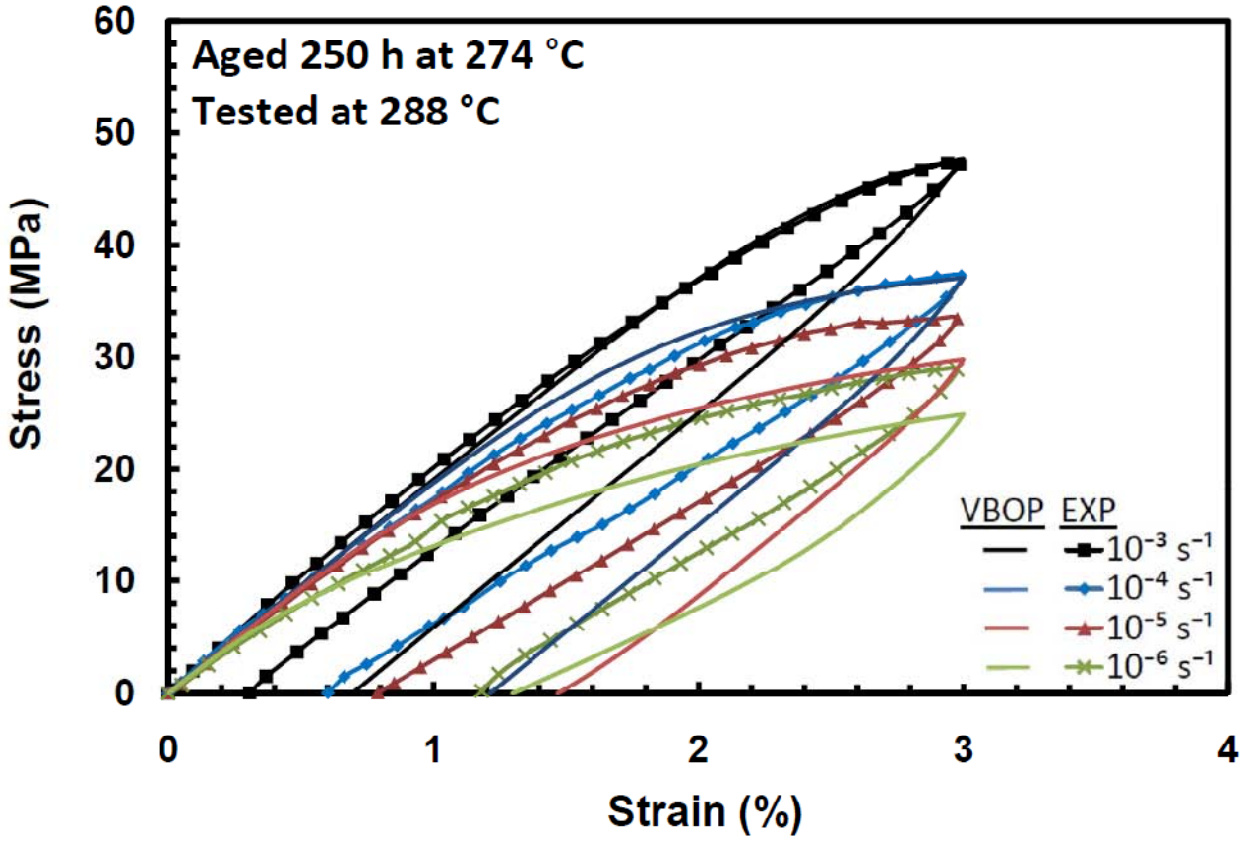

Figure 7.15: A Comparison of Experimental and Predicted Stress-Strain Curves Obtained in Loading and Unloading at 288 °C for PMR-15 Aged for 250 h at 274 °C in Argon.

Figure 7.16 compares prediction with the experimental results obtained in 6-h creep tests at 21 MPa, preceded by strain-controlled loading at 10^{-6} s^{-1} and at 10^{-4} s^{-1}. As was the case for other aging groups, the VBOP qualitatively captures dependence of creep response on prior strain rate, but over predicts the creep strain.

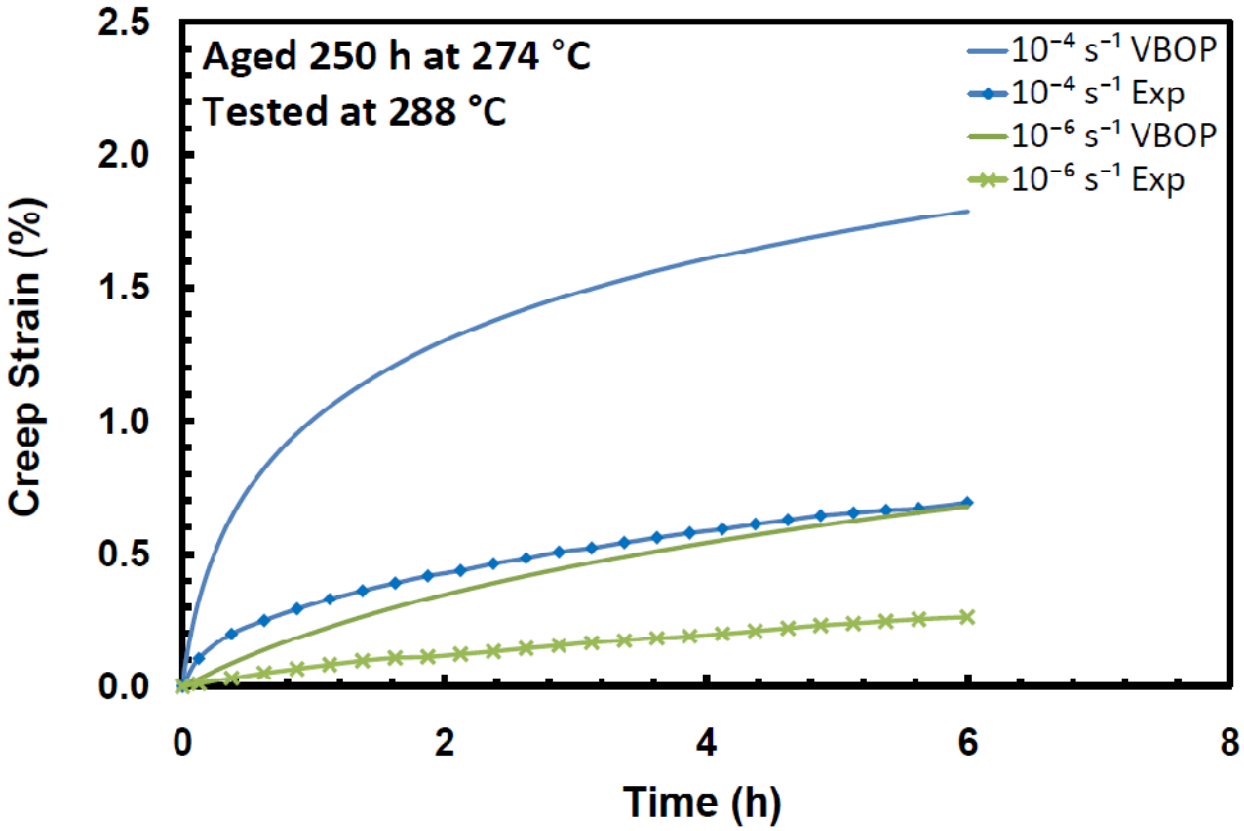

Figure 7.16: A Comparison of Experimental and Predicted Creep Strain vs. Time Curves Obtained at 21 MPa and 288 °C for PMR-15 Aged for 250 h at 274 °C in Argon.

Predictions of the strain rate jump test are compared with experimental results in Figure 7.17. Note that both specimens in this aging group subjected to the strain rate jump tests accumulated over 3% strain. Overall, the VBOP predicts the behavior observed in the strain rate jump test well.

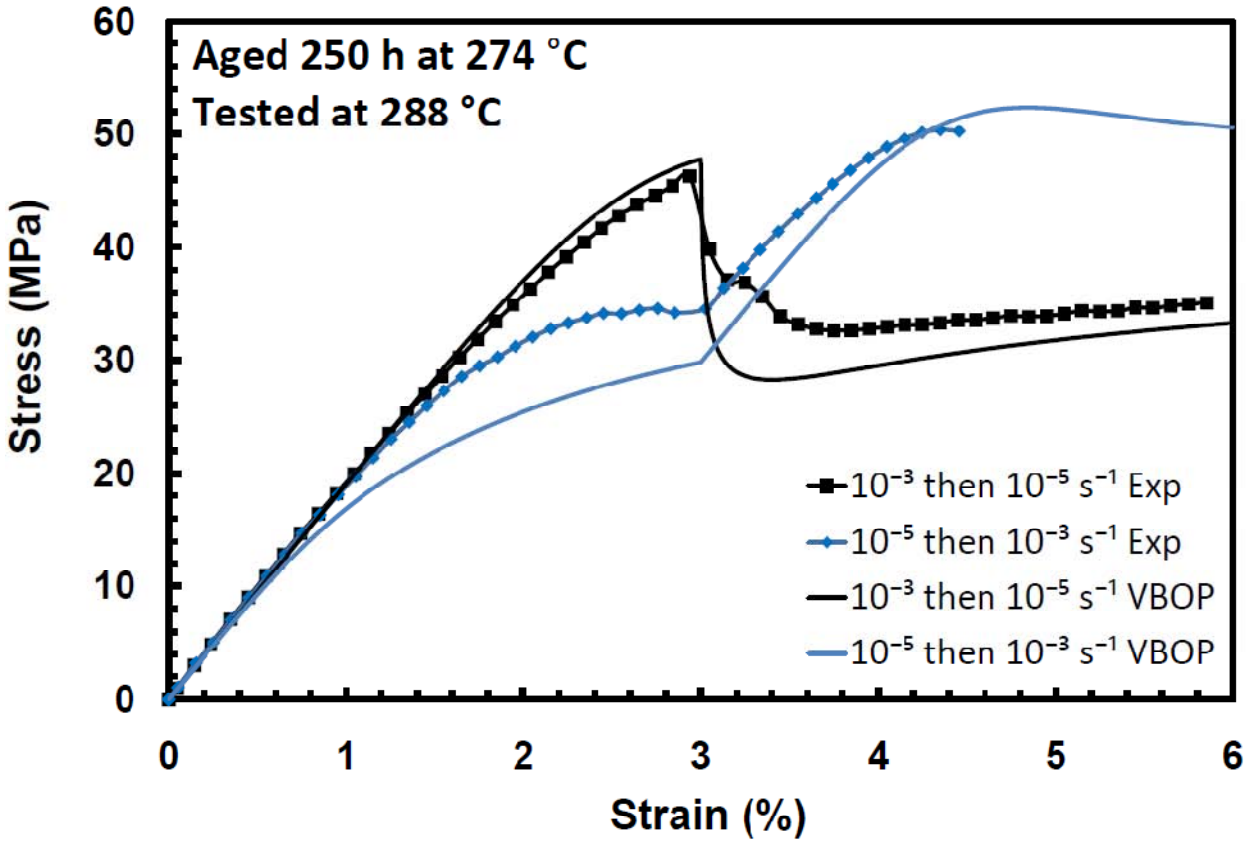

Figure 7.17: A Comparison of Experimental and Predicted Stress-Strain Curves Obtained in Strain Rate Jump Tests at 288 °C for PMR-15 Aged for 250 h at 274 °C in Argon.

Prior Aging for 500 h

Following the VBOP model characterization procedure proposed by McClung [27]. the shape function parameter C_2=1000 MPa was obtained by optimization based on experimental data from monotonic tension to failure tests. The C_2=1000 MPa was lower than the C_2 values obtained for either the 100-h or the 250-h aging groups. Hence the experimental data from the monotonic loading portion of the stress-strain curve preceding relaxation were added to the optimization routine used to determine C_2. By using this larger sample group the optimal value C_2 = 1130 MPa was found. Simulations of strain-controlled monotonic loading generated with the two different values of C_2 are compared with the experimental data in Figure 7.18. It is seen that the simulations produced with the C_2 = 1130 MPa better represent the observed behavior. Based upon this analysis the value of C_2 = 1130 MPa was selected and used for all subsequent modeling of this aging group.

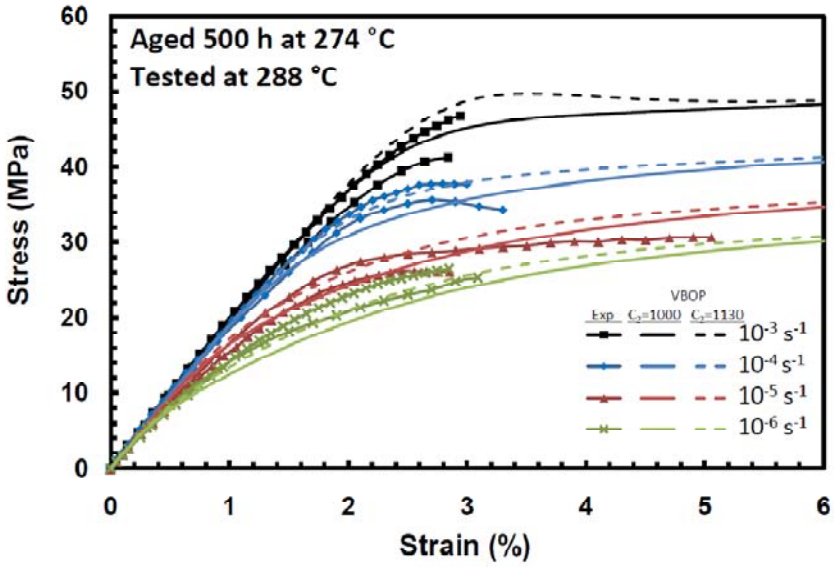

Figure 7.18: A Comparison of Experimental and Simulated Monotonic Tensile Stress-Strain Curves Obtained at 288 °C for PMR-15 Aged for 500 h at 274 °C in Argon. Stress-Strain Curves Simulated by VBOP with Different Values of the Parameter C_2.

The VBOP model parameters obtained at 288 ° for PMR-15 aged for 500 h at 274 °C in argon are summarized in Table 7-4.

Table 7-4: VBOP Model Parameters at 288 °C for PMR-15 Neat Resin Subjected to 500 h of Prior Aging at 274 °C in Argon.

Moduli	E = 1940 MPa, E_t = 61.8 MPa
Isotropic Stress	A = 24.6 MPa
Viscosity Function	k_1 = 1.15e+04 s, k_2 = 29.8 MPa, k_3 = 12.7
Shape Function	C_1 = 100 MPa, C_2 = 1130 MPa, C_3 = 10.0

The effects of prior strain rate on relaxation behavior are well represented by the VBOP as shown in Figure 7.19. The model simulations are in excellent agreement with the experimental data for the prior strain rates of 10^{-4} and 10^{-5} s^{-1}. In the case of other prior strain rates, the simulations are also very close to experimental results.

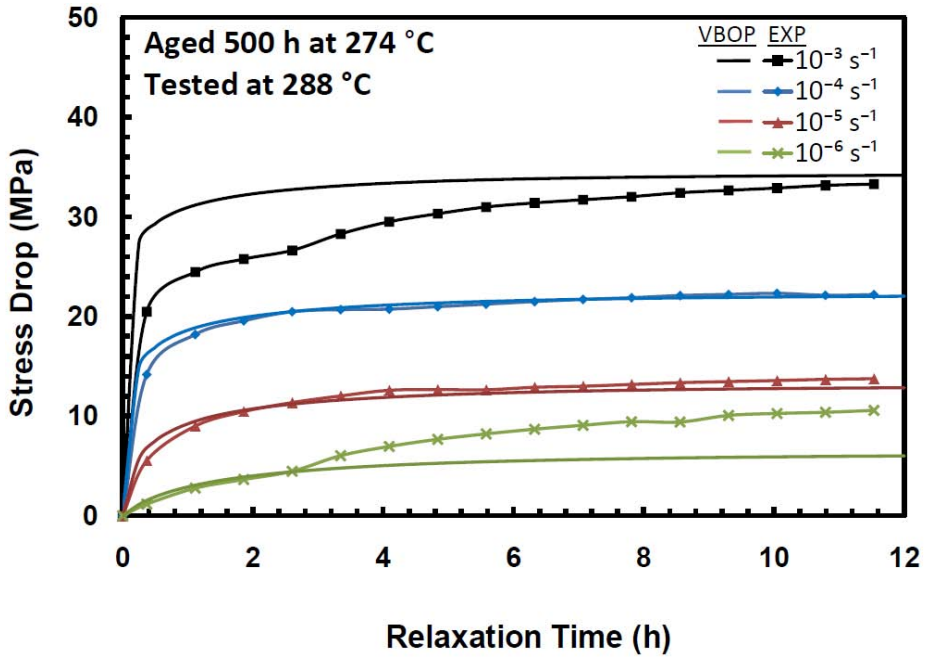

Figure 7.19: A Comparison of Experimental and Simulated Stress Decrease vs. Relaxation Time Curves Obtained at 288 °C for PMR-15 Aged for 500 h at 274 °C in Argon.

Figure 7.20 compares predictions of the loading and unloading at different constant strain rates with the experimental data. It is seen that the loading stress-strain behavior is predicted accurately at strain rates except at the strain rate of 10^{-6} s^{-1}, which produced uncharacteristically high stress levels in experiment. As noted earlier, the unloading stress-strain behavior was not modeled accurately.

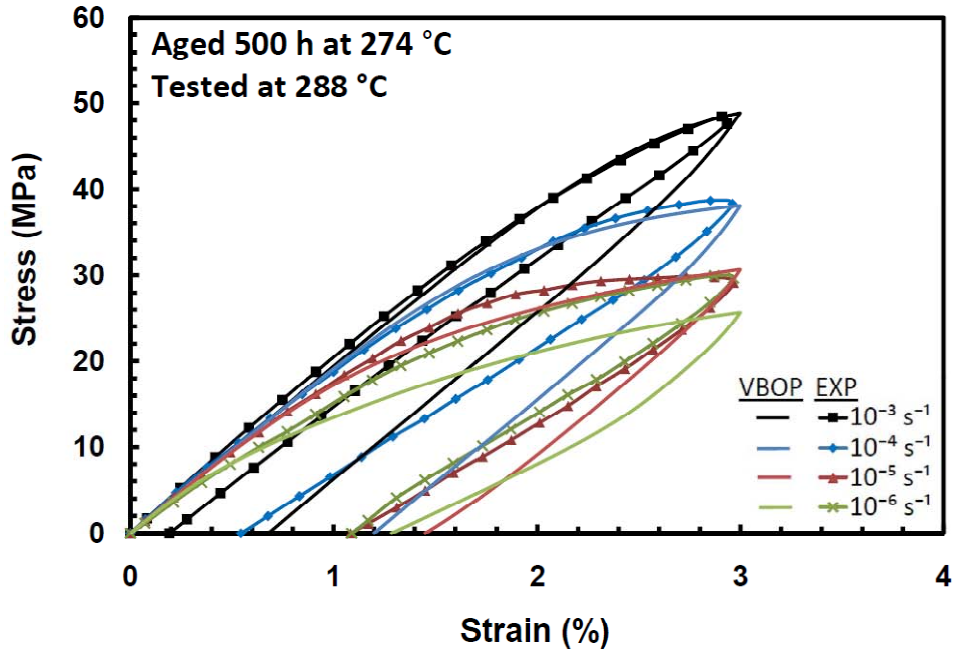

Figure 7.20: A Comparison of Experimental and Predicted Stress-Strain Curves Obtained in Loading and Unloading at 288 °C for PMR-15 Aged for 500 h at 274 °C in Argon.

As seen in Figure 7.21 the VBOP over predicts strains produced in creep tests at 21 MPa preceded by strain-controlled loading at 10^{-4} s^{-1} and at 10^{-6} s^{-1}.

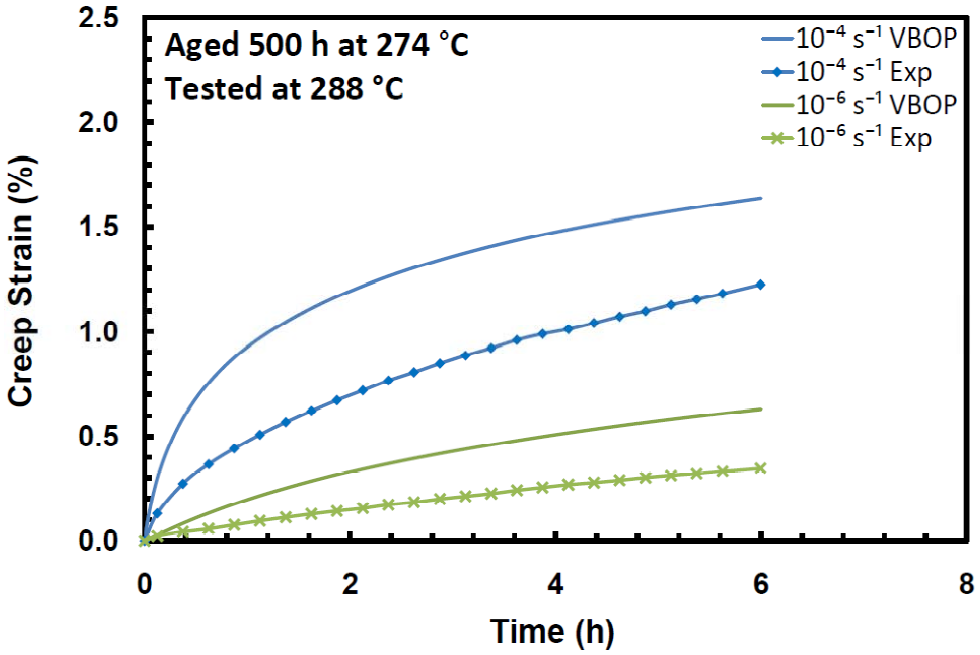

Figure 7.21: A Comparison of Experimental and Predicted Creep Strain vs. Time Curves Obtained at 21 MPa and 288 °C for PMR-15 Aged for 500 h at 274 °C in Argon.

The prediction of the strain rate jump test is compared with the experimental results in Figure 7.22. Initially the prediction diverges from the test results. However, the model represents the change in stress in response to the change in strain rate.

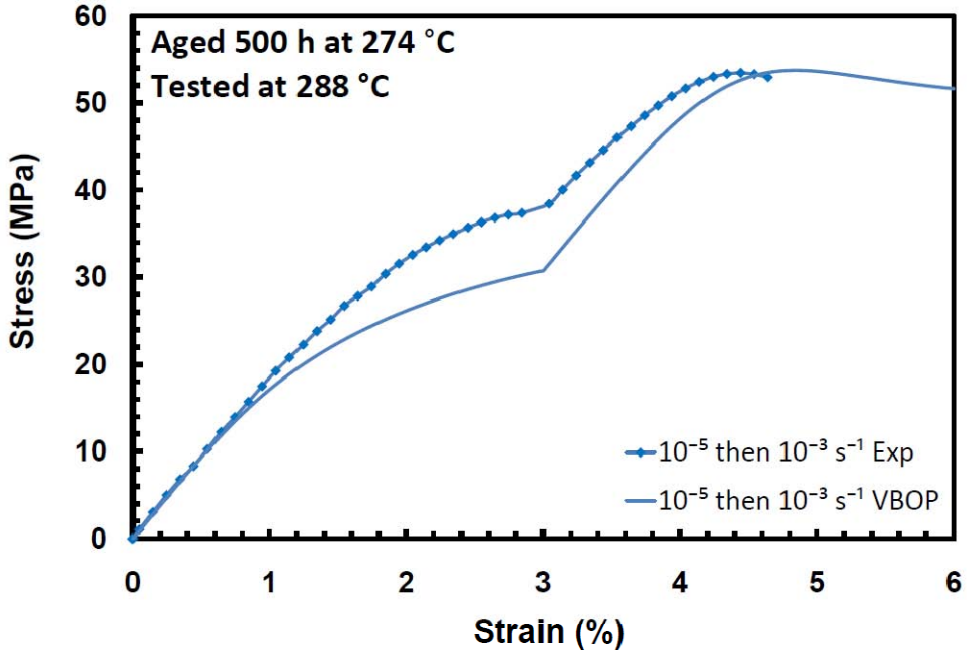

Figure 7.22: A Comparison of Experimental and Predicted Stress-Strain Curves Obtained in Strain Rate Jump Tests at 288 °C for PMR-15 Aged for 500 h at 274 °C in Argon.

Prior Aging for 1000 h

Due to increased brittleness only three specimens in this aging group were subjected to the monotonic test with the relaxation period at the strain of 3%. Based on the stress levels at the end of relaxation isotropic stress A=28 MPa was determined. However, using VBOP with this value of isotropic stress generated unacceptable simulations of the monotonic tension to failure tests. Numerical experiments with several lower values of isotropic stress A were performed. Based on the results, a value of isotropic stress A=26 MPa was selected for this

aging group. The VBOP model parameters obtained at 288 ° for PMR-15 aged for 1000 h at 274 °C in argon are summarized in Table 7-5.

Table 7-5: VBOP Model Parameters at 288 °C for PMR-15 Neat Resin Subjected to 1000 h of Prior Aging at 274 °C in Argon.

Moduli	E = 1990 MPa, E_t = 48.0 MPa
Isotropic Stress	A = 26.0 MPa
Viscosity Function	k_1 = 1.15e+04 s, k_2 = 29.8 MPa, k_3 = 12.7
Shape Function	C_1 = 100 MPa, C_2 = 1160 MPa, C_3 = 10.0

Simulations of the relaxation behavior are compared with the experimental results in Figure 7.23. As noted for other aging groups, the VBOP represents relaxation behavior accurately, only slightly over predicting the stress drop for fast prior strain rates and under predicting the stress drop for slow prior strain rates.

The simulations of the monotonic stress-strain behavior are in good agreement with the experimental results, as seen in Figure 7.24. Initial deformation behavior is modeled well at all but the slowest strain rates and plastic deformation is modeled well at both the fastest and the slowest strain rates. The only discrepancy between simulated and observed stress-strain behavior is seen at the strain rate of 10^{-5} s^{-1}, which may be due to specimen-to-specimen variability.

Predictions of the loading and unloading at various strain rates are compared with the experimental results in Figure 7.25. Stress-strain behavior upon loading path is well represented by the VBOP. Conversely, the stress-strain behavior during unloading at faster strain rates is

modeled poorly. However, at the slowest strain rate the prediction of unloading behavior is remarkably accurate.

Figure 7.26 compares prediction with the experimental results obtained in creep tests preceded by strain-controlled loading to the creep stress level of 21 MPa. As was the case for other aging groups, the VBOP accurately predicts the effect of prior strain rate on creep response, but over predicts the amount of creep strain.

The limited results of the strain rate jump test (SRJT) obtained for this aging group do not provide a reliable basis for model verification. However, Figure 7.27 shows a reasonable agreement between the prediction of the SRJT and the existing experimental results.

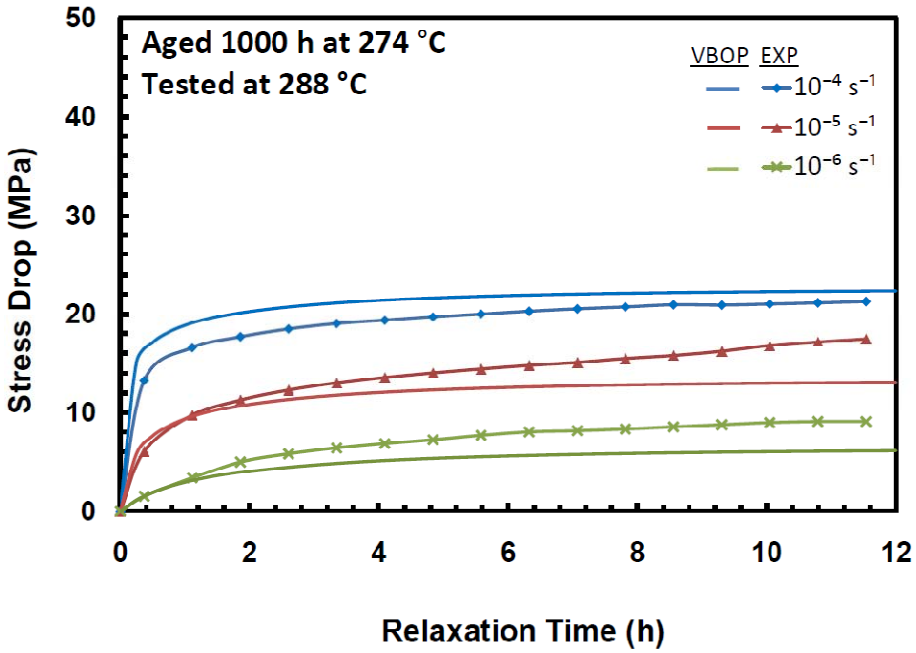

Figure 7.23: A Comparison of Experimental and Simulated Stress Decrease vs. Relaxation Time Curves Obtained at 288 °C for PMR-15 Aged for 1000 h at 274 °C in Argon.

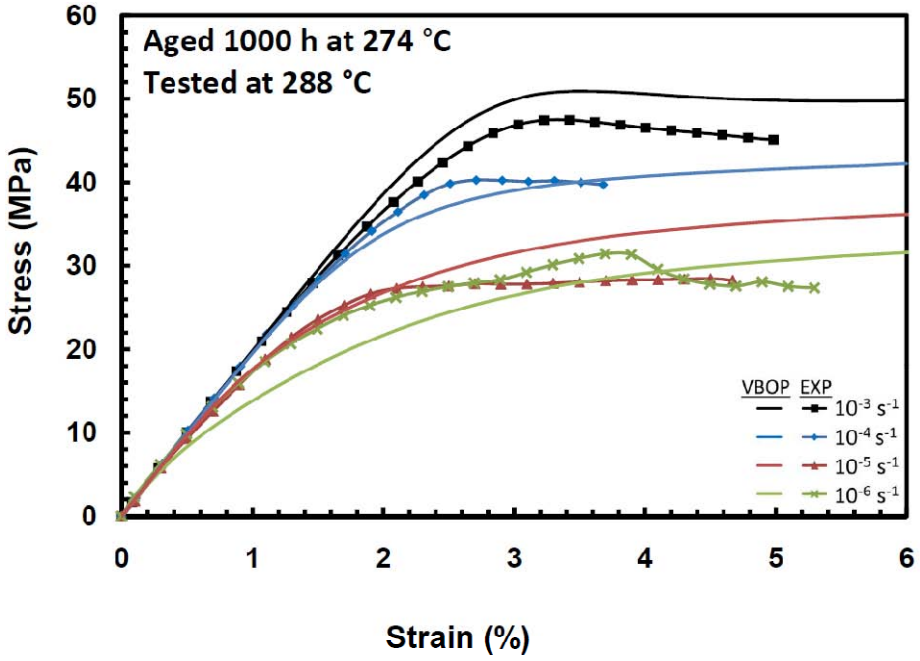

Figure 7.24: A Comparison of Experimental and Simulated Monotonic Tensile Stress-Strain Curves Obtained at 288 °C for PMR-15 Aged for 1000 h at 274 °C in Argon.

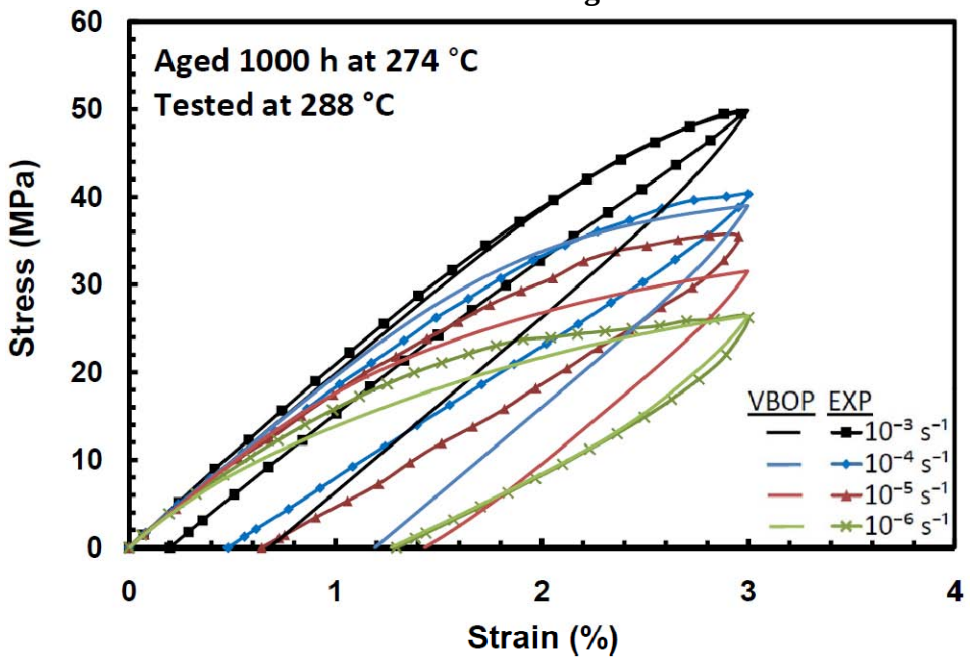

Figure 7.25: A Comparison of Experimental and Predicted Stress-Strain Curves Obtained in Loading and Unloading at 288 °C for PMR-15 Aged for 1000 h at 274 °C in Argon.

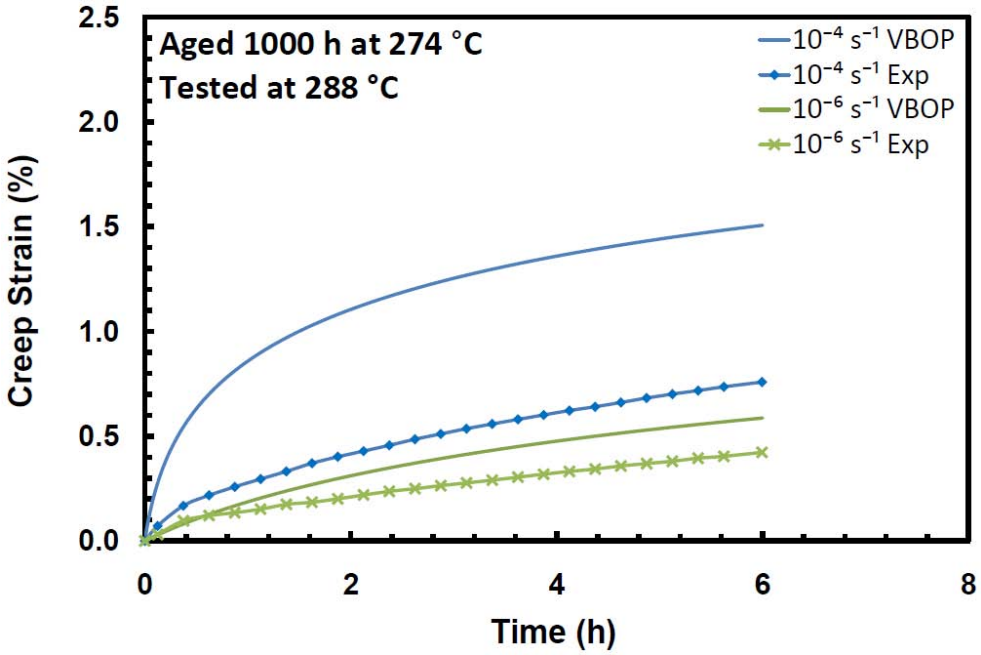

Figure 7.26: A Comparison of Experimental and Predicted Creep Strain vs. Time Curves Obtained at 21 MPa and 288 °C for PMR-15 Aged for 1000 h at 274 °C in Argon.

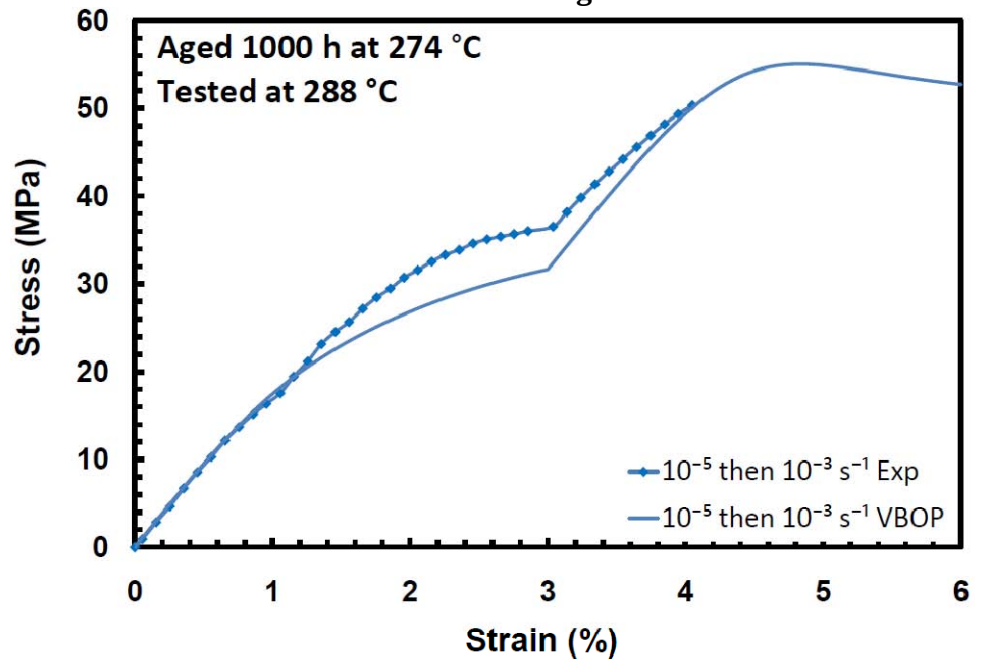

Figure 7.27: A Comparison of Experimental and Predicted Stress-Strain Curves Obtained in Strain Rate Jump Tests at 288 °C for PMR-15 Aged for 1000 h at 274 °C in Argon.

VBOP Model Parameters as Functions of Prior Aging Time

McClung [27] observed that several VBOP model parameters obtained for PMR-15 subjected to prior isothermal aging did not change with aging duration. These were the viscosity function parameters k_1, k_2, k_3 and the shape function parameters C_1 and C_3. All other VBOP parameters used to model the behavior of PMR-15 subjected to prior isothermal aging were functions of aging duration. This research has confirmed that the VBOP is capable of representing behavior of PMR-15 subjected to prior isothermal aging. Furthermore, the only model parameters dependent on prior aging time are E, E_t, A, and C_2.

The elastic modulus as a function of prior aging time is shown in Figure 7.28 for PMR-15 subjected to prior aging at 274 °C. It is seen that the average elastic modulus increases with increasing prior aging time. However, it should be noted that this increase in average elastic modulus is discernable because data for a large number of specimens was available. In contrast to the large number of data points available to calculate the average quasi-elastic modulus, it was necessary to evaluate the average tangent modulus, E_t, from a very limited number of data points. Yet it is still possible to recognize a trend of increasing tangent modulus with increasing prior aging time in Figure 7.29.

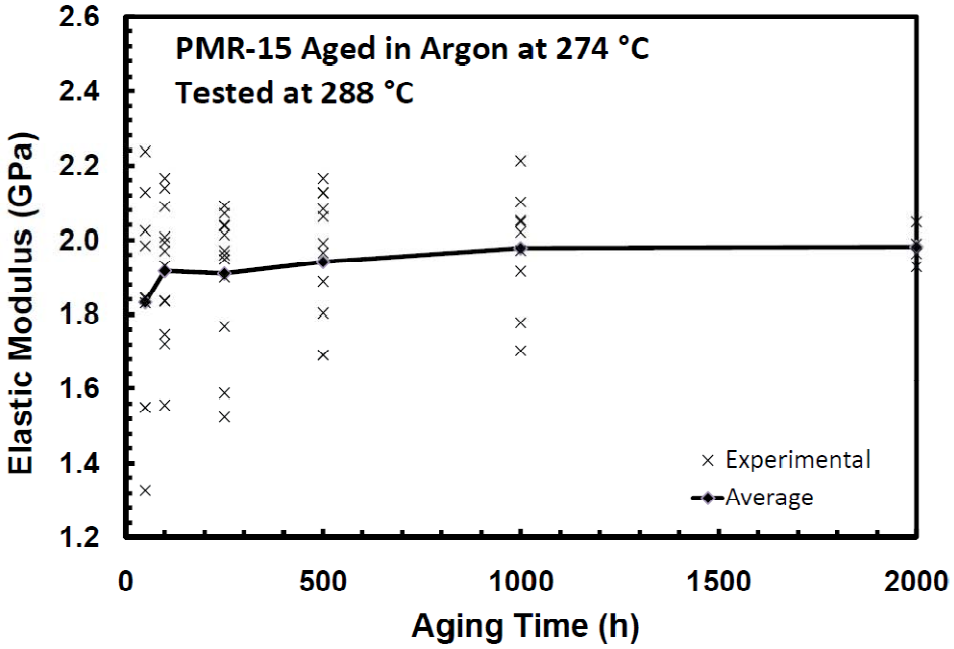

Figure 7.28: Elastic Modulus, E, at 288 °C as a Function of Prior Aging Time at 274 °C in Argon for PMR-15.

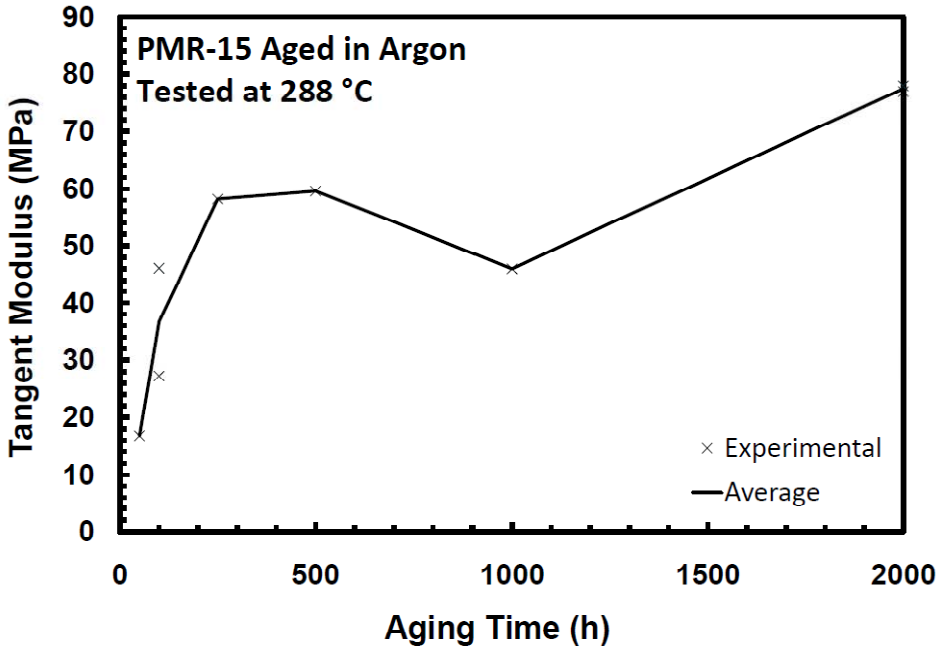

Figure 7.29: Tangent Modulus, E_t, at 288 °C as a Function of Prior Aging Time at 274 °C in Argon for PMR-15.

To predict the behavior of specimens subjected to prior aging times other than those investigated experimentally it is necessary to model the change in the VBOP parameters with prior aging time. This work uses the power law structure proposed by McClung [27] to expand the VBOP parameters into functions of prior aging time. To validate this approach the test results obtained for specimens aged for 50 to 1000 h were used to predict the behavior of the specimens aged for 2000 h. A MATLAB program was used to optimize all power law function parameters based upon the 50-1000 h aging data.

The average values of the elastic modulus are plotted vs. prior aging time in Figure 7.30. Based on these results the elastic modulus is represented as the power law function of the prior aging time,

$$E = 0.0162 \times t_a^{0.356} + 1.80 \qquad (7.8)$$

The power law function in Equation (7.8) is used to predict the elastic modulus for the 2000-h aging group. The predicted elastic modulus is slightly higher than the experimental value. However, because this error is small Equation (7.8) is an appropriate choice for representing the modulus as a function of prior aging time for aging durations up to and including 2000 h.

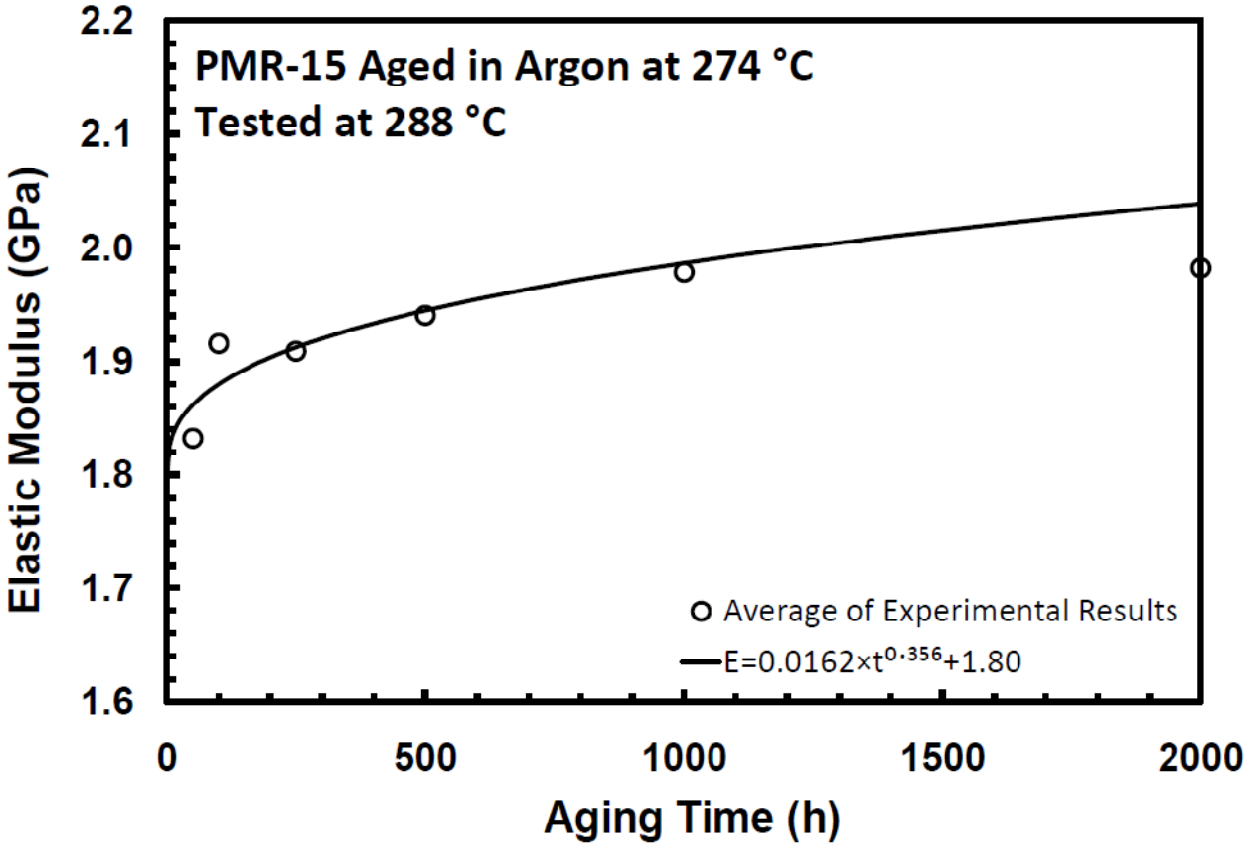

Figure 7.30: Elastic Modulus, E, at 288 °C as a Function of Prior Aging Time at 274 °C in Argon for PMR-15.

The average values of the tangent modulus are plotted vs prior aging time in Figure 7.31. Based on these results the tangent modulus is represented as the power law function of the prior aging time,

$$E_t = 1.33 \times t_a^{0.459} + 24.5 \qquad (7.9)$$

Recall that in the case of all aging groups the tangent modulus was determined based on the limited amount of experimental data. As a result the evaluation of the power law parameters is difficult. Yet the power law function in Equation (7.9) does predict the tangent modulus for the

2000-h group that is within 15% of the experimentally measured value, which is admirable considering the limited amount and high variability of the characterization data.

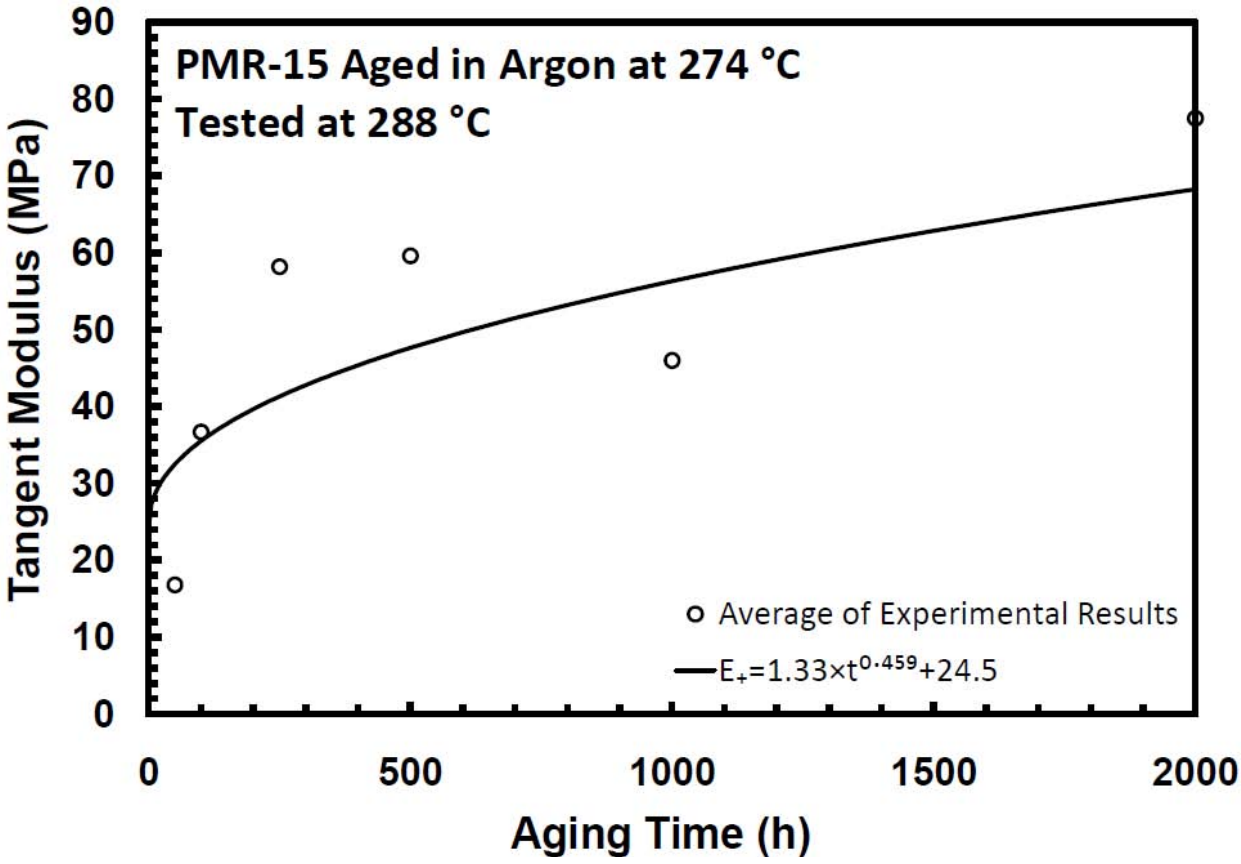

Figure 7.31: Tangent Modulus, E_t, at 288 °C as a Function of Prior Aging Time at 274 °C in Argon for PMR-15.

The isotropic stress A is plotted vs. prior aging time in Figure 7.32. Based on the results shown in Figure 7.32, the isotropic stress is represented as the power law function of the prior aging time,

$$A = 0.6174 \times t_a^{0.329} + 20.0 \qquad (7.10)$$

Equation (7.10) predicts the isotropic stress value for the 2000-h aging group that is within 0.3 MPa of the experiment based value. This result indicates that the power law relationship in

Equation (7.10) is well suited to representing changes in isotropic stress with prior aging time at 274°C.

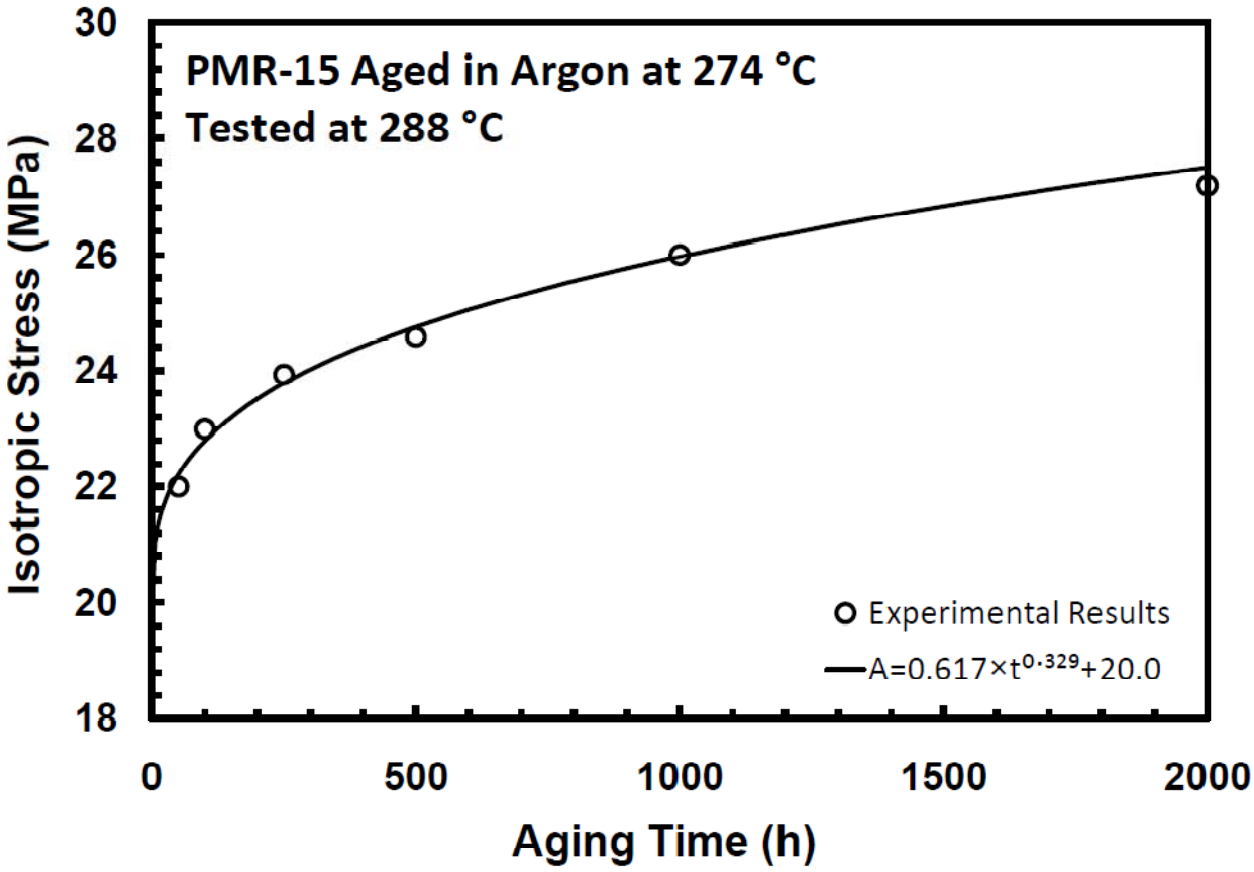

Figure 7.32: Isotropic Stress, A, at 288 °C as a Function of Prior Aging Time at 274 °C in Argon for PMR-15.

The shape function parameter C_2 is plotted vs prior aging time in Figure 7.33. Based on these results the shape function parameter C_2 is represented as the power law function of the prior aging time,

$$C_2 = 0.00280 \times t_a^{0.322} + 0.910 \qquad (7.11)$$

Note that the C_2 value predicted for the 2000-h aging group using Equation (7.11) is 80 MPa higher than the experiment based value.

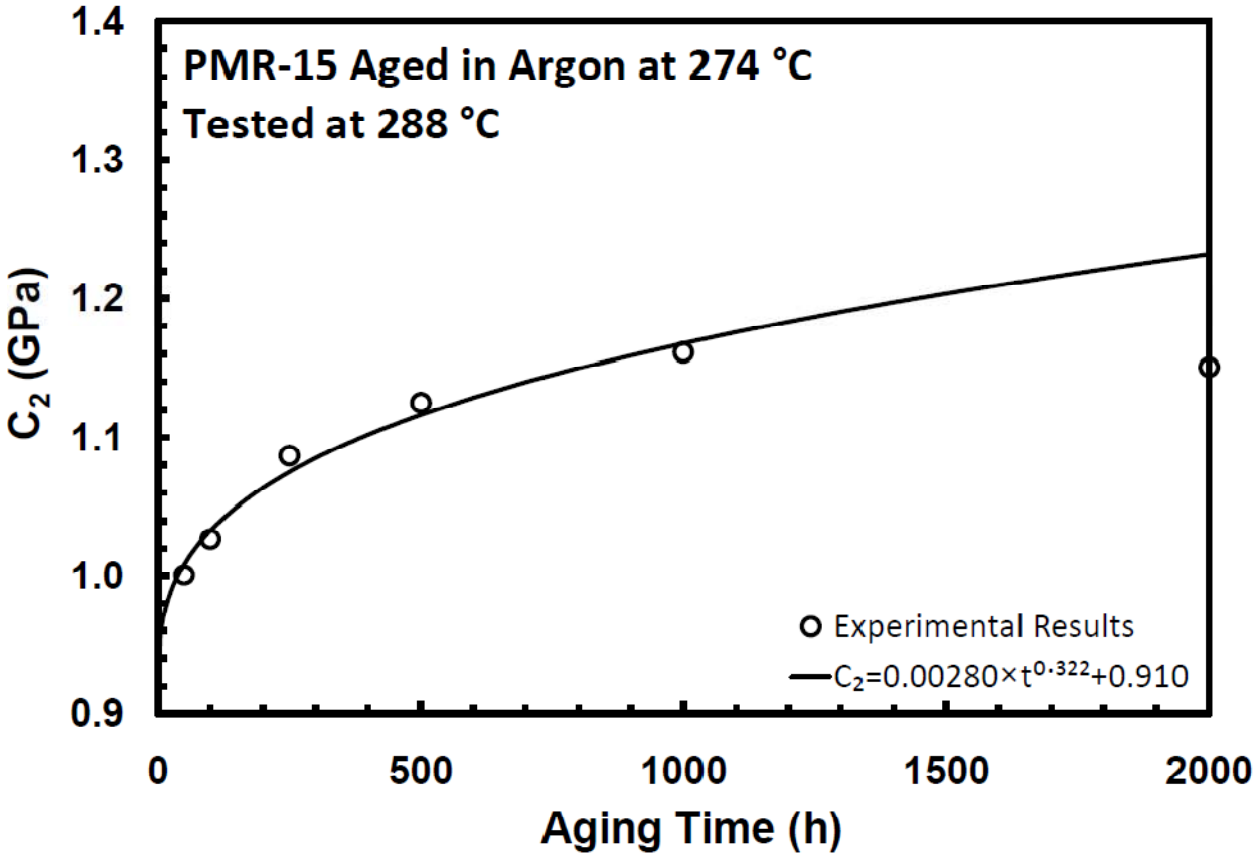

Figure 7.33: Shape Function Parameter C_2 at 288 °C as a Function of Prior Aging Time at 274 °C in Argon for PMR-15.

Predictions of Deformation Behavior for the PMR-15 Neat Resin Subjected to 2000 h of Prior Aging at 274 °C in Argon

Validation of both the VBOP model characterization procedure and the VBOP model extension to include the effects of prior aging was accomplished by comparing model predictions with the experimental data for the 2000-h aging group. The model parameters determined from test data obtained for specimens subjected to prior aging for 50-1000 h were used to predict the VBOP model parameters for specimens subjected to 2000 h of prior aging. The VBOP model parameters calculated at 288 ° for PMR-15 aged for 2000 h at 274 °C in argon are summarized in Table 7-6.

Table 7-6: VBOP Model Parameters at 288 °C for PMR-15 Neat Resin Subjected to 2000 h of Prior Aging at 274 °C in Argon.

Moduli	E = 2030 MPa, E_t = 68.3 MPa
Isotropic Stress	A = 27.5 MPa
Viscosity Function	k_1 = 1.15e+04 s, k_2 = 29.8 MPa, k_3 = 12.7
Shape Function	C_1 = 100 MPa, C_2 = 1240 MPa, C_3 = 10.0

Predictions of the relaxation response are compared with the experimental results in Figure 7.34. The model accurately predicts the relaxation behavior for the prior strain rate of 10^{-6} s^{-1}. Conversely, the relaxation stress drop for the prior strain rate of 10^{-3} s^{-1} is over predicted.

The VBOP predictions of the monotonic stress-strain behavior compare reasonably well with the experimental results (see Figure 7.35). Stress-strain behavior at the strain rate of 10^{-6} s^{-1} is accurately modeled. In contrast, the model over predicts the flow stress for the strain rate of 10^{-5} s^{-1}. Due to early failures experimental results produced at 10^{-3} s^{-1} and at 10^{-4} s^{-1} could not be used for model validation.

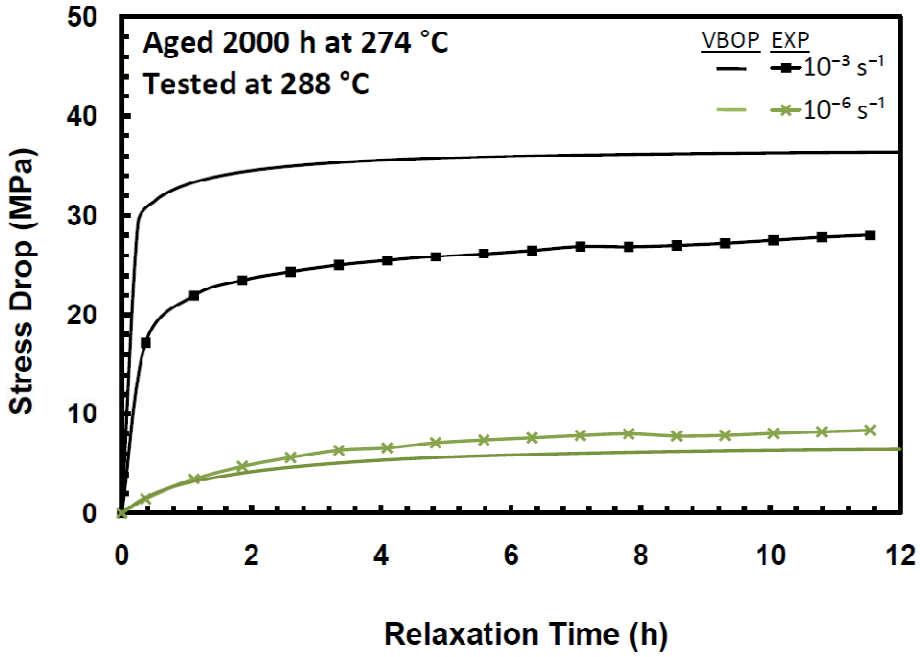

Figure 7.34: A Comparison of Experimental and Simulated Stress Decrease vs. Relaxation Time Curves Obtained at 288 °C for PMR-15 Aged for 2000 h at 274 °C in Argon.

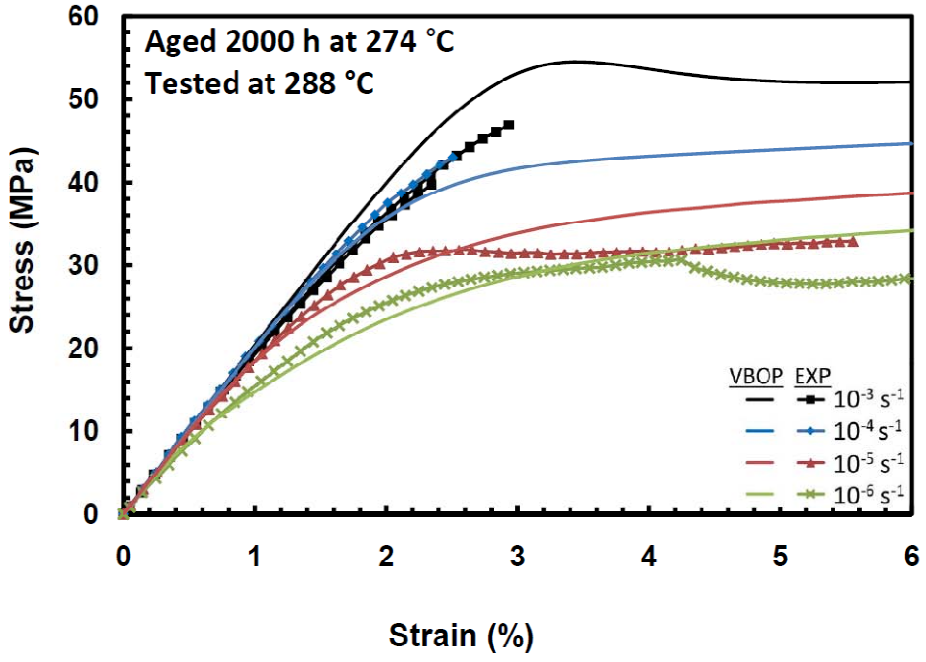

Figure 7.35: A Comparison of Experimental and Predicted Monotonic Tensile Stress-Strain Curves Obtained at 288 °C for PMR-15 Aged for 2000 h at 274 °C in Argon.

Predictions of loading and unloading at various constant strain rates are compared with the experimental results in Figure 7.36. The stress-strain behavior during loading is adequately modeled with some discrepancies likely due to specimen-to-specimen variability. The inability of the VBOP to accurately model the unloading stress-strain behavior is again observed for this aging group.

Figure 7.37 compares predictions with experimental results obtained in creep tests. The VBOP predicts decreasing creep strain accumulation with increasing aging duration. The VBOP also predicts the increasing creep strain accumulation with increasing prior strain rate. However, the model over predicts the creep strain for this aging group.

Because of early specimen failure only limited results of the strain rate jump test were obtained for this aging group. Figure 7.38 shows a reasonable agreement between the prediction of the strain rate jump test and the existing experimental results.

Overall the behavior of the PMR-15 neat resin subjected to 2000 h of prior aging at 274 °C in argon is well represented by the VBOP with the predicted model parameters. The modeling results reveal that the deformation behavior of PMR-15 subjected to prior aging at 274 °C can be adequately modeled with the VBOP by expanding E, E_t, A, and C_2 into power law functions of the prior aging time.

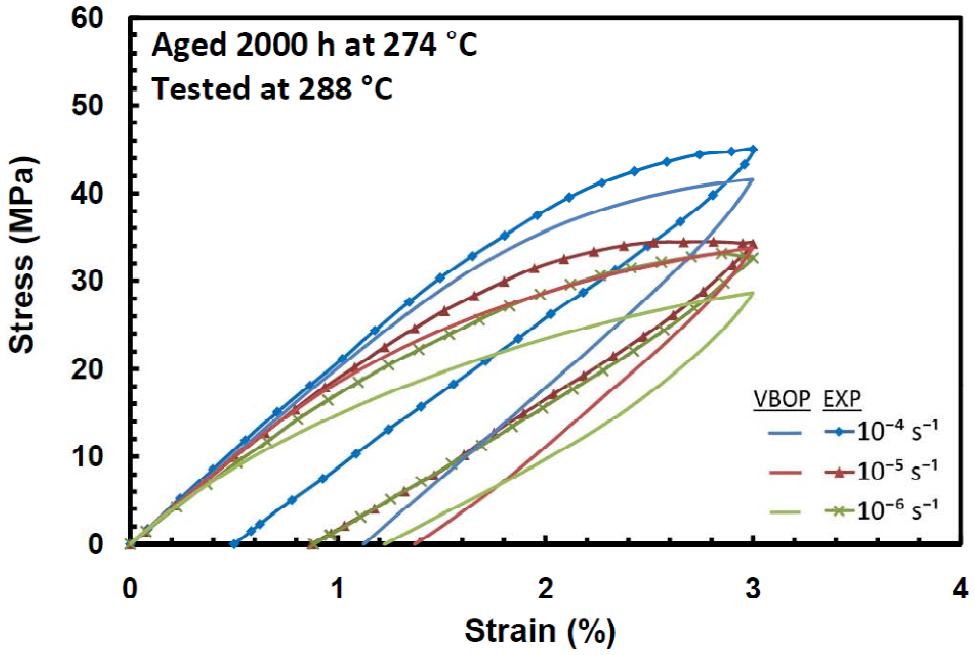

Figure 7.36: A Comparison of Experimental and Predicted Stress-Strain Curves Obtained in Loading and Unloading at 288 °C for PMR-15 Aged for 2000 h at 274 °C in Argon.

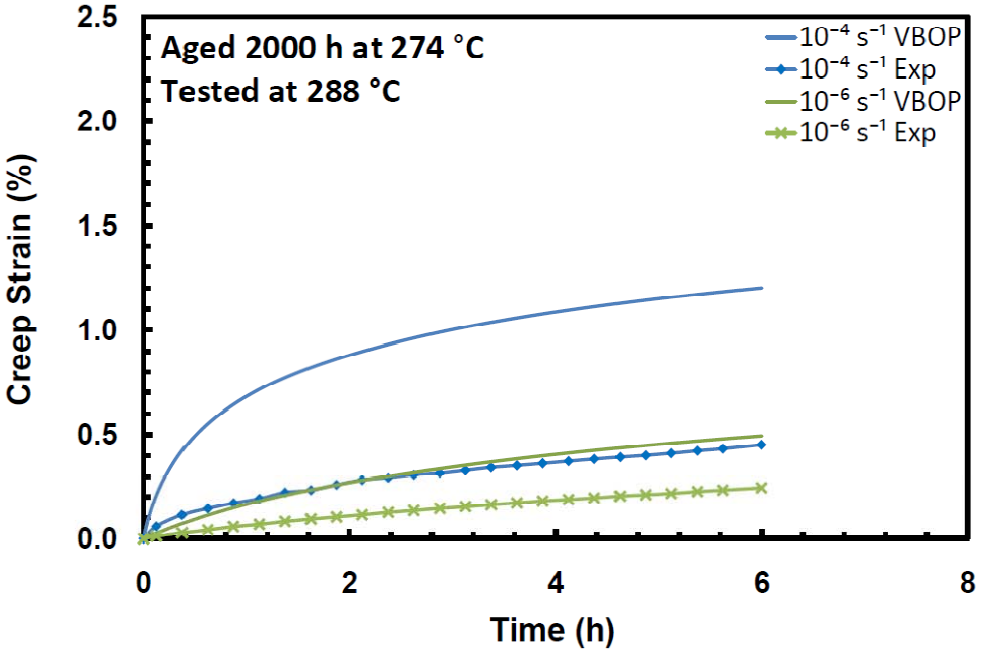

Figure 7.37: A Comparison of Experimental and Predicted Creep Strain vs. Time Curves Obtained at 21 MPa and 288 °C for PMR-15 Aged for 2000 h at 274 °C in Argon.

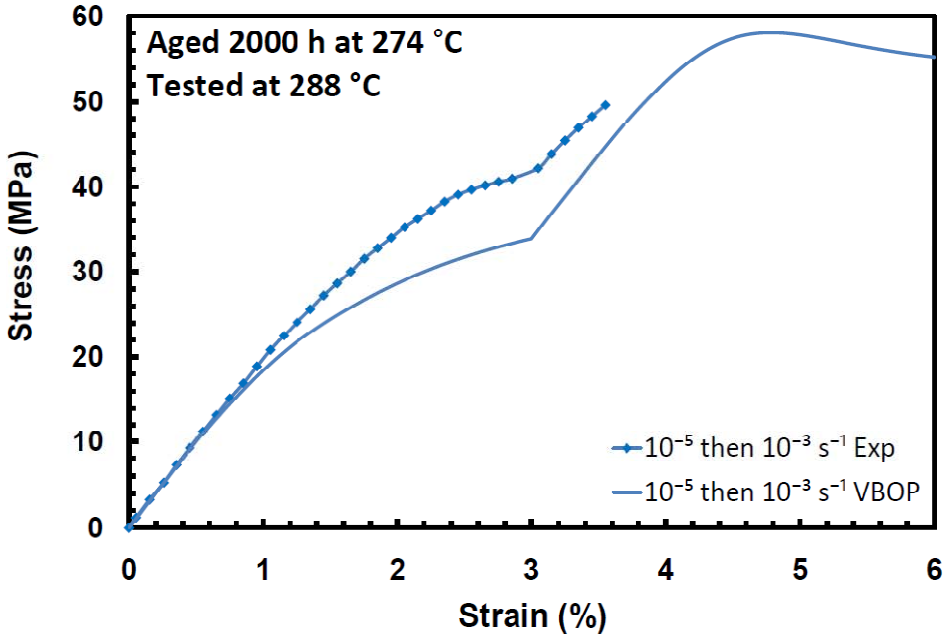

Figure 7.38: A Comparison of Experimental and Predicted Stress-Strain Curves Obtained in Strain Rate Jump Tests at 288 °C for PMR-15 Aged for 2000 h at 274 °C in Argon.

Comparison of VBOP Model Parameters Obtained for PMR-15 Subjected to Prior Aging at 274 °C and 288 °C

A key objective of this research has been to explore and quantify the differences in deformation beahvior at 288 °C resulting from prior aging at different temperatures, i. e. 274 °C and 288 °C. To further this understanding, the evolutions of the VBOP parameters with prior aging time obtained for each aging temperature are compared.

Figure 7.39 compares the calculated and experimental elastic modulus values as functions of prior aging time for the aging temperature of 288 °C and for the aging temprerature of 274 °C. In the case of prior aging temperature of 274 °C, the calculated modulus values are generated using Equation (7.8). In the case of prior aging temperature of 288 °C, the calculated modulus values are generated using Equation (7) from Ref [24]. In order to reduce data scatter, these

results are normalized by the average room temperature modulus value. The evolution in elastic modulus for the two aging temperatures shows verry little difference. It may be noted that there is virtually no change in elastic modulus for the specimens aged for 1000-2000 h at 274 °C, however, the power law equation predicts a modest rise. This may be evidence of a saturation of chain scisions and cross linking for PMR-15 at this temperature. Yet, due to the large ammount of data scatter observed in the elastic modulus (see Figure 7.30) a larger number of tests would be required to draw any firm conclusions.

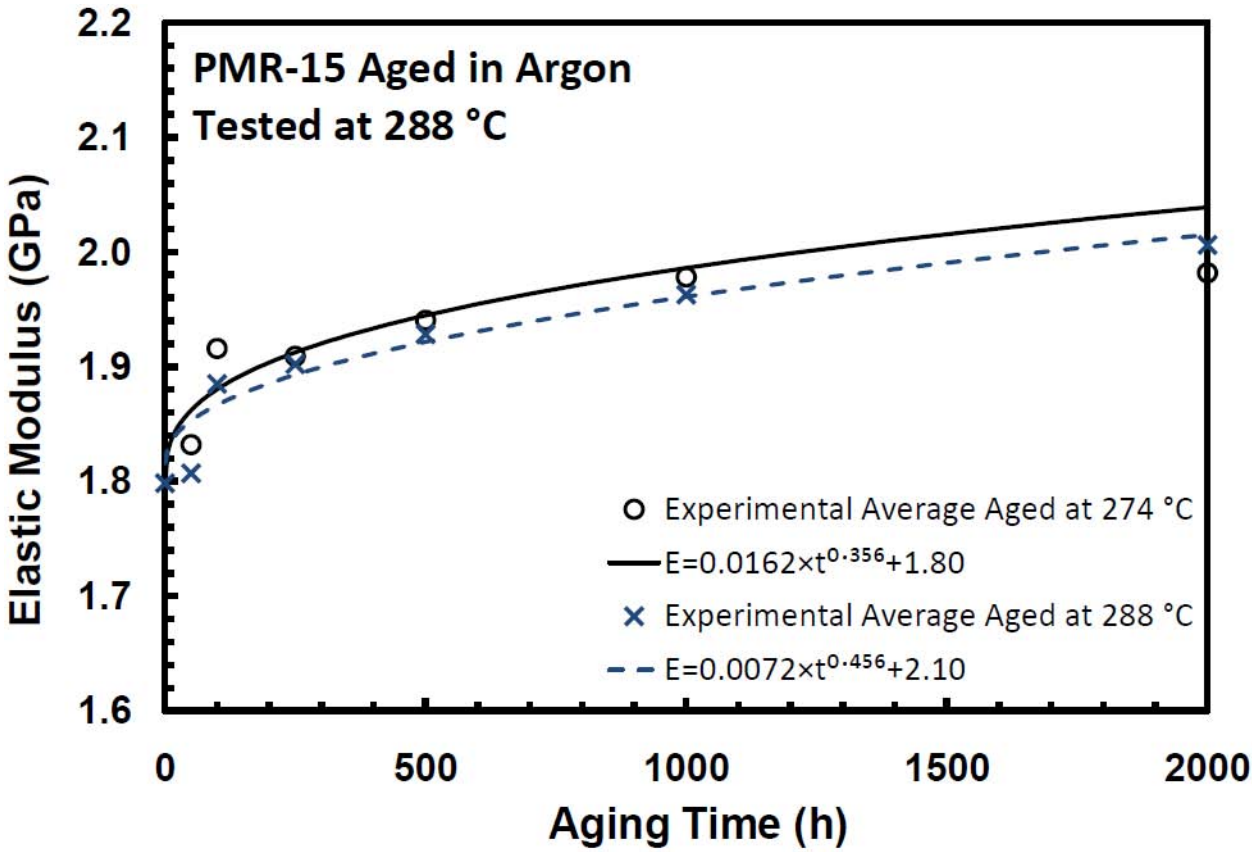

Figure 7.39: Elastic Modulus, E, at 288 °C as a Function of Prior Aging Time at 274 °C in Argon for PMR-15 Polymer, Compared to Elastic Modulus, E, at 288 °C as a Function of Prior Aging Time at 288 °C in Argon for PMR-15 Polymer. Experimental Data at 288 °C from McClung [27].

Figure 7.40 compares the calculated and experimental tangent modulus values as functions of prior aging time for the aging temperature of 288 °C and for the aging temprerature of 274 °C. The evolution in tangent modulus for the two aging temperatures is very similar.

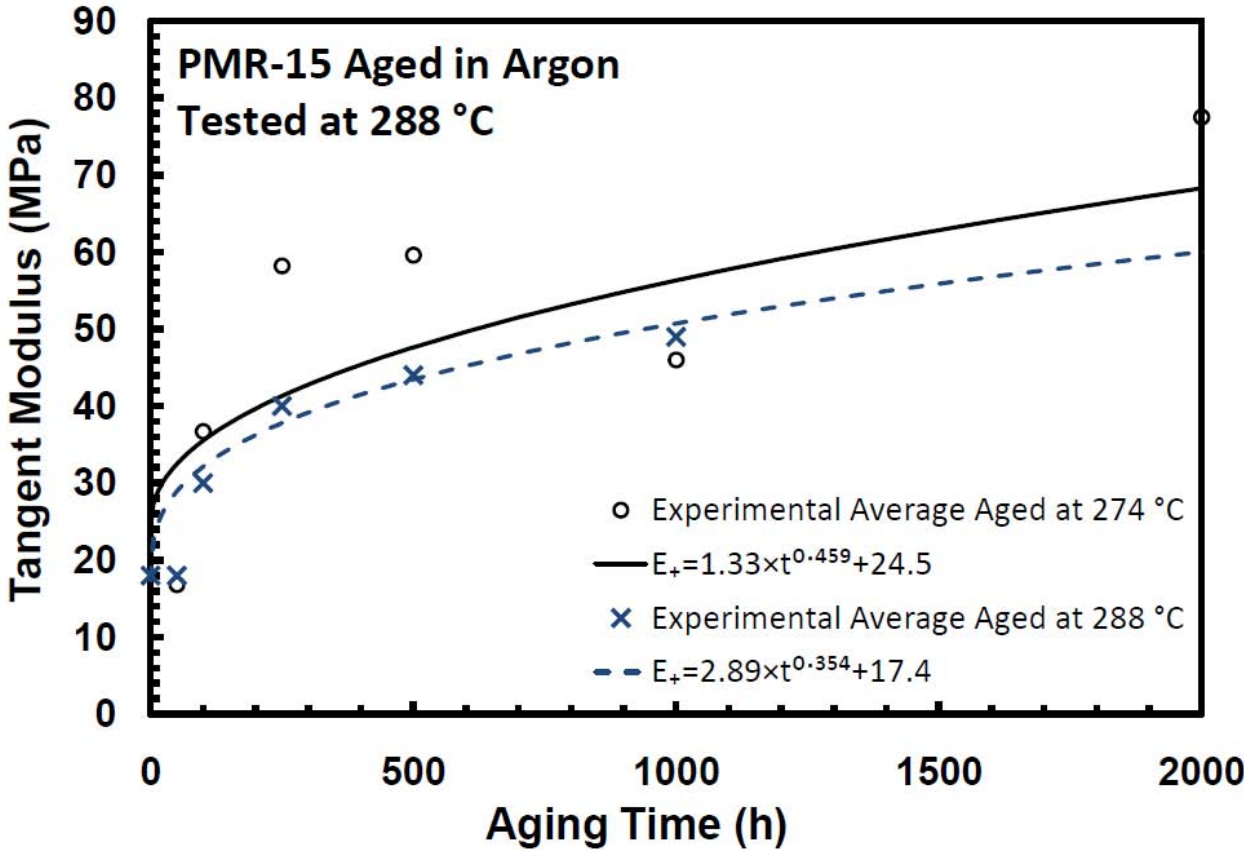

Figure 7.40: Tangent Modulus, E_t, at 288 °C as a Function of Prior Aging Time at 274 °C in Argon for PMR-15 Polymer, Compared to Tangent Modulus, E_t, at 288 °C as a Function of Prior Aging Time at 288 °C in Argon for PMR-15 Polymer. Experimental Data at 288 °C from McClung [27].

Figure 7.41 compares the calculated and experimental isotropic stress values as functions of prior aging time for the aging temperature of 288 °C and for the aging temprerature of 274 °C. The evolution in isotropic stress for the two aging temperatures is very similar.

.

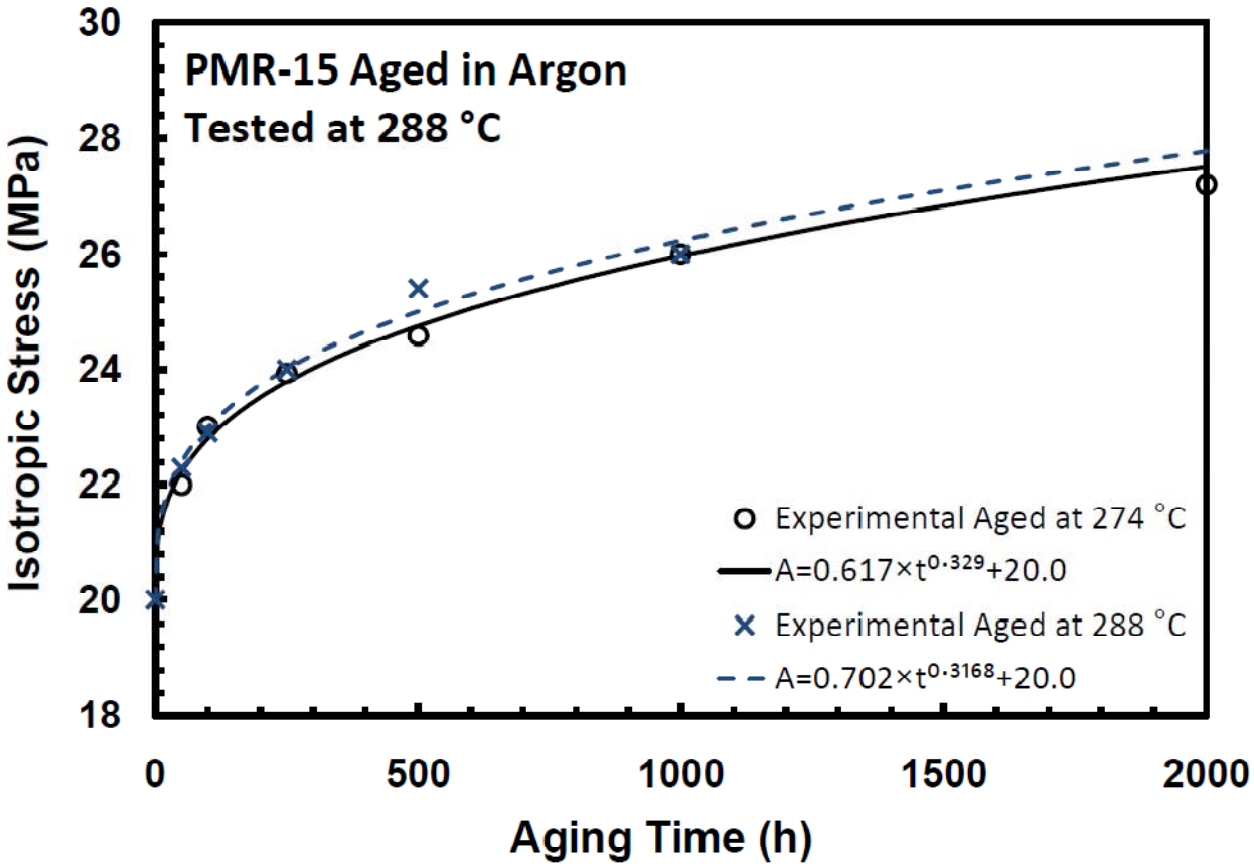

Figure 7.41: Isotropic Stress, A, at 288 °C as a Function of Prior Aging Time at 274 °C in Argon for PMR-15 Polymer, Compared to Isotropic Stress, A, at 288 °C as a Function of Prior Aging Time at 288 °C in Argon for PMR-15 Polymer. Experimental Data at 288 °C from McClung [27].

Figure 7.42 compares the calculated and experimental values of the shape function parameter C_2 as functions of prior aging time for the aging temperature of 288 °C and for the aging temprerature of 274 °C. As seen in Figure 7.42, the shape function parameter C_2 is quantitatively influenced by prior isothermal aging temperature. However, the evolution in the shape function parameter C_2 for the two aging temperatures is qualitative similar. Variation in C_2 with prior aging time for two aging temperatures is represented by nearly parallel power law curves.

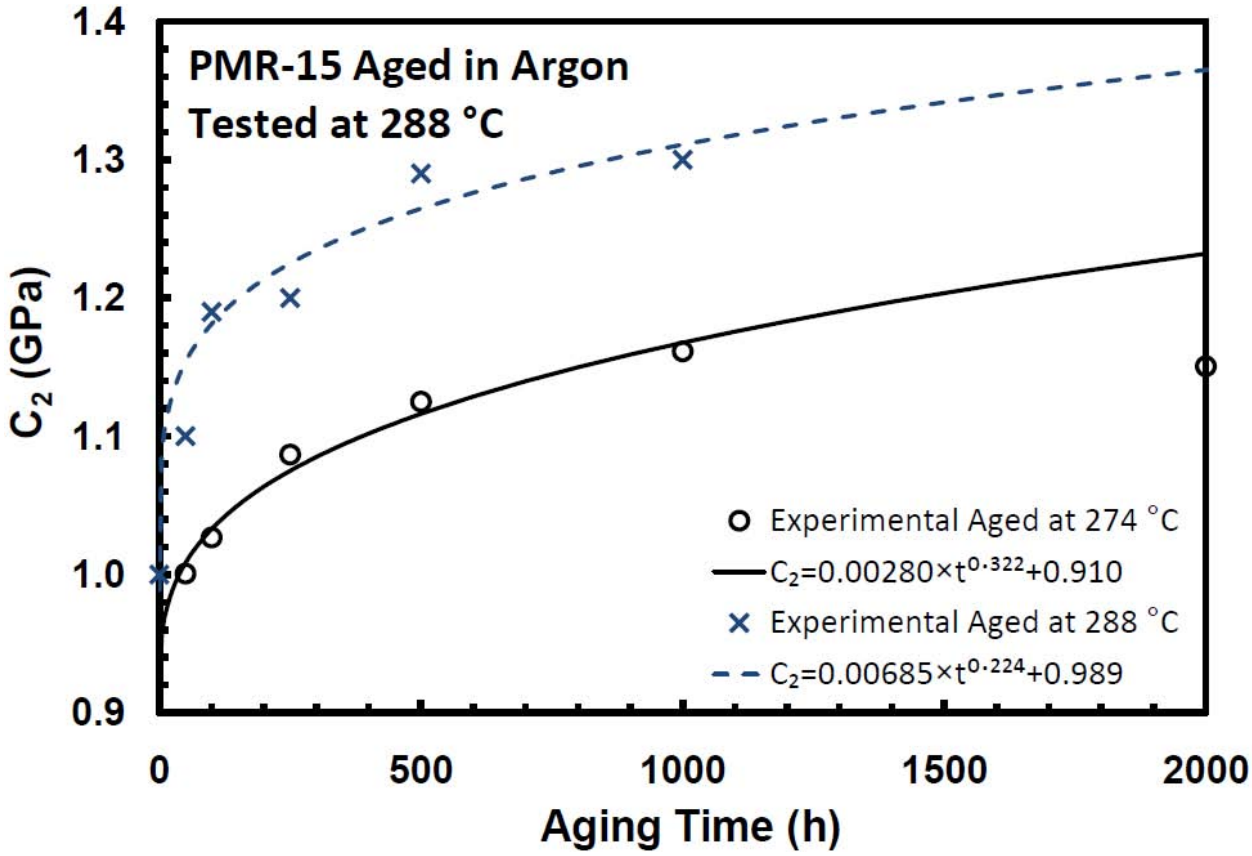

Figure 7.42: Shape Function Parameter, C_2, at 288 °C as a Function of Prior Aging Time at 274 °C in Argon for PMR-15 Polymer, Compared to Shape Function Parameter, C_2, at 288 °C as a Function of Prior Aging Time at 288 °C in Argon for PMR-15 Polymer. Experimental Data at 288 °C from McClung [27].

Additional differences may be noted in the behavior of specimens aged at 274 °C and specimens aged at 288 °C which are not directly modeled by the VBOP. Experimental results reveal that the specimen aged at a lower temperature did not accumulate as much strain in creep as did the specimen aged at a higher temperature. However, it is difficult to draw a conclusion based on a small number of tests. Additional creep tests would have to be performed to make a definitive conclusion. The most marked change in behavior of specimens aged at different temperatures is seen in failure strain. Aging for durations of 1000 hours or longer at 288 °C

resulted in early failures, whereas multiple specimens aged at 274 °C for durations up to 2000 hours produced significant inelastic strains. This is illustrated in Figure 7.43(a) and 7.43 (b), where tensile stress-strain curves obtained at 288 °C for the PMR-15 polymer subjected to prior aging for 2000 h in argon at 274 °C and at 288 °C are shown, respectively. The average failure strain for specimens aged for 2000 hours at 274 °C was 4.3% whereas the average failure strain for specimens aged for 2000 h at 288 °C was only 1.5%. Even though the VBOP model does not have a parameter directly associated with embrittlement, which would account for decreased failure strain, this dramatic difference in material behavior should not be ignored.

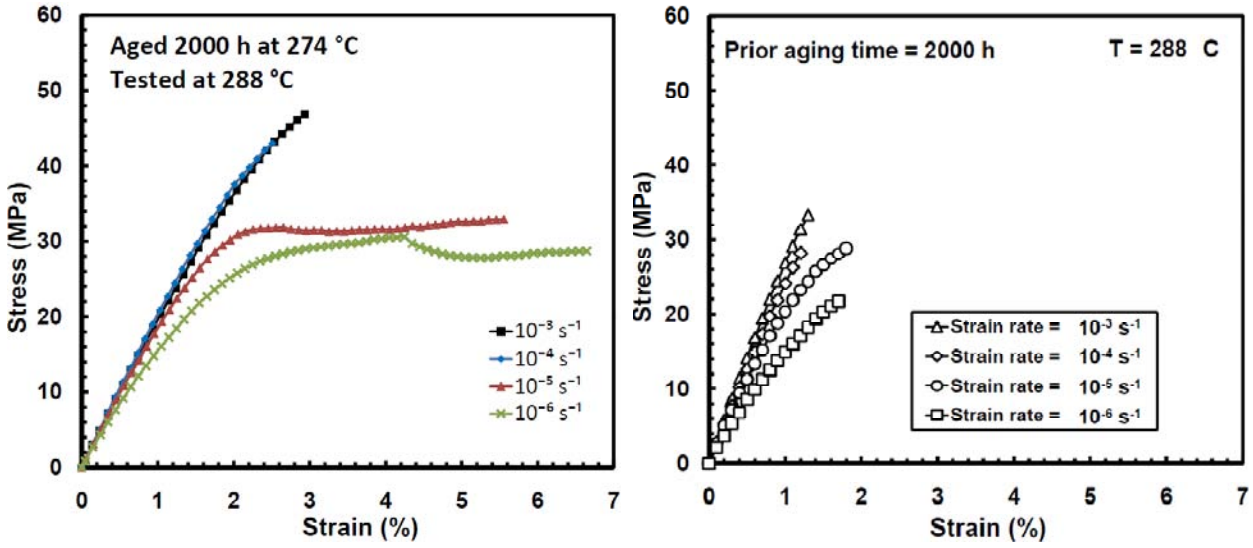

(a) (b)

Figure 7.43: Stress-Strain Curves Obtained at 288 °C for PMR-15 Subjected to Prior Aging for 2000 h in Argon at: (a) 274 °C and (b) 288 °C. Data for PMR-15 aged at 288 °C from McClung [27].

8. Conclusions and Recommendations

Concluding Remarks

Deformation behavior of PMR-15 neat resin subjected to prior aging at 274 °C was investigated at 288 °C. Exploratory tests revealed positive non linear strain rate dependence during both loading and unloading. The flow stress levels increased nonlinearly with increasing strain rate. Additionally, increase in strain rate resulted in more abrupt transitions from elastic to the inelastic region of the stress-strain curve. In loading and unloading tests performed at constant strain rate magnitudes the strain measured immediately upon unloading to zero stress decreased with increasing strain rate magnitude. Effects of prior strain rate were observed in both the relaxation and creep tests. Results of the relaxations tests revealed that an increase in prior strain rate caused increased stress drop during relaxation. Creep tests demonstrated that larger creep strains were accumulated in creep tests preceded by loading at a faster strain rate. Results of the strain rate jump tests performed in this study also demonstrated that the material did not exhibit the strain rate history effect.

The following effects of prior aging at 274 °C on the inelastic behavior at 288 °C were identified:

- Elastic modulus increased with prior aging time
- Tangent modulus increased with prior aging time
- The knee of the tensile stress-strain curve became increasingly more pronounced with increasing prior aging time
- Flow stress increased with prior aging time

- Creep strain accumulation decreased with increasing prior aging time
- Progressive embrittlement with increasing prior aging time

Notably the relaxation behavior was little affected prior aging at 274°C. Likewise the specimens aged for various durations exhibited similar lack of the strain rate history effect.

The experimental results presented here strongly suggest the usefulness of the overstress concept in the modeling inelastic deformation at 288 ºC of the PMR-15 neat resin subjected to prior aging at 274 °C. Hence the VBOP constitutive model was selected to simulate and predict the observed deformation behaviors. A systematic model characterization procedure developed by McClung [27] was used to determine the VBOP model parameters based on the results of the strain-controlled experiments obtained for the PMR-15 specimens aged for 50, 100, 250, 500, and 1000 h. To account for the effect of prior aging at 274 °C in argon on the inelastic behavior at 288 °C using the VBOP it was sufficient to make the elastic modulus, the tangent modulus, the isotropic stress, and the shape function parameter C_2 dependent on the prior aging time. The viscosity function and the C_1 and C_3 parameters of the shape function showed no dependence on prior isothermal aging history. The modified VBOP model was validated by comparing predictions with the experimental results for the stress and strain-controlled experiments that differ in kind from those used for model characterization.

Model parameters used to represent the deformation behavior at 288 °C of the PMR-15 aged at 274 °C for 2000 h were predicted from experimental data obtained for specimens aged at 274 °C for 50 to 1000 h. The VBOP model predictions obtained for the 2000-h aging group were in good agreement with the experimental results. The VBOP was able to accurately represent loading stress-strain behavior, relaxation response, and strain rate jump behavior for all

aging groups. Modeling of the stress-strain behavior during unloading and creep response produced results which were qualitatively correct but were quantitatively inaccurate in many cases.

The effects of prior aging at 274 °C and 288 °C on deformation behavior at 288 °C were compared. All but one of the VBOP model parameters used to represent the behavior of PMR-15 at 288 °C were insensitive to the change in aging temperature. The model parameter C_2 experienced considerably greater growth due to aging at 288 °C as opposed to aging at 274 °C. Additionally, prior aging temperature had a marked effect on the capacity of the specimens to accumulate inelastic strain. This was particularly evident in the behavior of specimens subjected to long aging durations. Specimens aged at 274 °C for up to 2000 h produced substantial inelastic strains, while the specimens aged at 288 °C for over 500 h rarely produced strains outside the quasi elastic region.

Recommendations

Further research is needed to thoroughly understand and quantify the effects of aging temperature on the deformation behavior of high-temperature polymers. Investigation of the deformation behavior at a single temperature (i.e. 288 °C) for specimens subjected to prior aging at various temperatures will provide means to isolate and identify the effects of prior aging temperature. Subsequent study of aging temperatures both above 288 °C and below 274 °C will be required. Additionally, testing of un-aged specimens at various temperatures will provide data necessary to understand and model the effects of temperature on the deformation behavior.

Combining the results of these two directions of research will allow for independent selection of test temperature, aging temperature, and aging duration when predicting material behavior.

Bibliography

1. Baker, Alan, S. Dutton and D. Kelly, *Composite Materials for Aircraft Structures.* 2nd Edition. Reston: American Institute of Aeronautics and Astronautics, 2004.

2. Bordonaro, C.M. and E. Krempl. "A state Variable Model for High Strength Polymers." *Polymer Engineering and Science* 35.4 (1995): 310-316.

3. Bordonaro, Christine Marie. *Rate Dependent Mechanical Behavior of High Strength Plastics: Experiment and Modeling.* Rensselaer Polytechnic Institute. Troy, NY, 1995.

4. Bowles, K. J., et al. "Longtime Durability of PMR-15 Matrix Polymer at 204, 260, 288, and 316 °C." TM 210602 2001.

5. Broeckert, J. L. and M.B. Ruggless-Wrenn. "Effects of Prior Aging at 288 °C in Air and in Argon Environments on Creep Response of PMR-15 Neat Resin." *Journal of applied Polymer Science* 111 (2009): 228-236.

6. Broeckert, Joseph L. *Effects of Prior Aging at Elevated Temperature in Air and in Argon Environments onCreep Response of PMR-15 Neat Resin at 288 °C.* Master's thesis. Air Force Institute of Technology. Wright-Patterson Air Force Base, Ohio, 2007.

7. Cernocky, E.P. and E. Krempl. A Theory of Viscoplasticity Based on Infinitesimal Total Strain. Contract RPI CS 78-3, Rensselaer Polytechnic Institute, May 1978.

8. Chuang, K. "Development of DMBZ-15 High-Glass-Transition-Temperature Polyimides as PMR-15 Replacements Given R&D 100 Award." (n.d.).

9. Daniel, I.M. and O Ishai. *Engineering Mechancis of Composite Materials.* Oxford: Oxford University Press, 1994.

10. Diedrick, Bradley K. *Effects of Prior Aging at 260 °C in Argon on Inelastic Deformation Behavior of PMR-15 Polymer at 260 °C: Experiment and Modeling.* Master's Thesis. Wright Patterson AFB, OH: Department of Aeronautics and Astronautics, Air Force Institute of Technology, 2010.

11. Falcone, C. M. and M. B. Ruggles-Wrenn. "Rate Dependence and Short-Term Creep Behavior of a Thermoset Polymer at Elevated Temperature." *Journal of Pressure Vessel Technology* 131 (2009).

12. Falcone, Christina. *Some Aspects of the Mechanical Response of PMR-15 Neat Resin at 288 °C: Experiment and Modeling.* Master's Thesis. Air Force Institute of Technology. Wright-Patterson Air Force Base, Ohio, 2006.

13. Ho, K. *Application of the Viscoplasticity Theory Based on Overstress to the Modeling of Dynamic Strain Aging of Metals and to the Modeling of the Solid Polymers, Specifically to Nylon 66.* Ph.D. Thesis. Rensselaer Polytechnic Institute. Troy, NY, 1998.

14. Ho, Kwangsoo. “Modeling of Nonlinear Rate Sensitivity by Using an Overstress Model”. CMES, 2(3):351–364, 2001.

15. Ho, Kwangsoo and Erhard Krempl. “Extension of the Viscoplasticity Theory Based on Overstress (VBO) to Capture Non-Standard Rate Dependence in Solids”. International Journal of Plasticity, 18:851–872, 2002.

16. Kelley, Anthony and Carl Zweben, *Comprehensive Composite Materials.* New York: Elsevier, 2000.

17. Khan, Fazeel and Erhard Krempl. “Amorphous and Semi-crystalline Solid Polymers: Experimental and Modeling Studies of Their Inelastic Deformation Behaviors”. J Eng Mater Technology, Trans ASME, 128:64–72, 2006.

18. Krempl, E, J.J. McMahon and D. Yao. "Viscoplasticity Based on Oversterss with a Differential Growth Law for the Equilibrium Stress." *Nonlinear Constitutive Relations for High Temperature Application-1984 Symposium Proceedings.* Cleveland, OH: NASA Conference Publication 2369, 1984. 25-50.

19. Krempl, E. "Cyclic Creep: An Interpretive Literature Survey." *Weld. Res. Counc. Bull.* no. 195 (1974): pp. 63-123.

20. Krempl, E. *Unified Constitutive Laws of Plastic Deformation.* San Diego: Academic Press, 1996.

21. Krempl, Erhard and F. Khan. "Rate (time)-Dependent Deformation Behavior: An Overview of some Proiperties of Metals and Solid Polymers." *International Journal of Plasticity* 19 (2003): 1069-1095.

22. Krempl, Erhard. "From the Standard Linear Solid to the Viscoplasticity Theory Based on Overstress." *Proceedings of the International Conference on Computational Engineering science.* Ed. S.N. Atluri, G. Yagawa and T.A. Cruse. Hawaii: Springer, 1995. 1679-1684.

23. Krempl, Erhard. "The Role of Aging in the Modeling of Elevated Temperature Deformation." *Proceedings of the International Conference.* Ed. Wilshire B. and D. R. J. Owen. Swansea, Wales: Pineridge Press, 1981. 201-211.

24. McClung, A. J. W. and M. B. Ruggles-Wrenn. "Effects of Prior Aging at 288 °C in Argon environment on Time-Dependent Deformation Behavior of a Thremoset Polymer at Elevated Temperature, Part 2 Modeling with Viscoplasticity Theory Based on Overstress: " *Journal of Applied Polymer Science 3389* (2009).

25. McClung, A. J. W. and M. B. Ruggles-Wrenn. "Strain Rate Dependence and Short-Term Relaxation Behavior of a Thermoset Polymer at Elevated Temperature: Experiment and Modeling." *Journal of Pressure Vessel Technology* 131 (2009).

26. McClung, A. J. W. and Ruggles-Wrenn M. B. "The Rate (Time)-Dependent Mechanical Behavior of the PM-15 Thermoset Polymer at Elevated Temperature." *Polymer Testing* 27 (2008): 908-914.

27. McClung, Amber J. W. *Extension of Viscoplasticity Based on Overstress to Capture the Effects of Prior Aging on the Time Dependent Deformation of a High-Temperature Polymer: Experiments and Modeling.* PhD Dissertation. Air Force Institute of Technology. Wright-Patterson Air Force Base, Ohio, 2008.

28. Ozmen, Ozgur. *Effects of Prior Aging at 316 °C in Argon on Inelastic Deformation Behavior of PMR-15 Polymer at 316 °C: Experiment and Modeling.* Master's Thesis. Wright Patterson AFB, OH: Department of Aeronautics and Astronautics, Air Force Institute of Technology, 2009.

29. Ozmen, O. and M. B. Ruggles-Wrenn. "The Rate (Time)-Dependent Mechanical Behavior of the PMR-15 Thermoset Polymer at 316 °C: Experiments and Modeling" *Journal of Pressure Vessel Technology* 132 (2010).

30. Riande, Evaristo et al, ed. *Polymer Viscoelasticity: Sterss and strain in Practice.* Marcel Dekker, Inc, 2000.

31. Schapery, R.A. "On the Characterizatin of Nonlinear Viscoelastic Materials." *Polymer Engineering and Science* 9 (1969): 295-310.

32. Tsuji, L.C., H. L. McManus and K. J. Bowles. "Mechanical Properties of Degraded PMR-15 Resin." TM 208487 1998.

33. Westberry, Candice M. *Rate Dependence and short-Term reep Behavior of PMR-15 Neat Resin at 23 and 288 °C.* Master's Thesis. Air Force Institute of Technology. Wright-Patterson Air Force Base, Ohio, 2005.

REPORT DOCUMENTATION PAGE

Form Approved
OMB No. 0704–0188

1. REPORT DATE (DD–MM–YYYY)	2. REPORT TYPE	3. DATES COVERED *(From — To)*
23-12-2010	Master's Thesis	Sept 2009 – Dec 2010

4. TITLE AND SUBTITLE

Effectsof Prior Aging at 274 °C in Argon on Inelastic Deformation Behavior of PMR-15 Polymer at 288 °C: Experiment and Modeling

5a. CONTRACT NUMBER

5b. GRANT NUMBER

5c. PROGRAM ELEMENT NUMBER

6. AUTHOR(S)

Joseph A. Wahlquist, Capt, USAF

5d. PROJECT NUMBER

5e. TASK NUMBER

5f. WORK UNIT NUMBER

7. PERFORMING ORGANIZATION NAME(S) AND ADDRESS(ES)
Air Force Institute of Technology
Graduate School of Engineering and Management (AFIT/ENY)
2950 Hobson Way
WPAFB OH 45433-7765

8. PERFORMING ORGANIZATION REPORT NUMBER

AFIT/GAE/ENY/10-D03

9. SPONSORING / MONITORING AGENCY NAME(S) AND ADDRESS(ES)

Dr. Joycelynn Harrison
Air Force Office of Scientific Research (AFOSR)
875 N Randolph St. Suite 325 Rm. 3112
Arlington, VA 22203
DSN: 426-6225 E-MAIL: Joycelyn.Harrison@AFOSR.AF.MIL

10. SPONSOR/MONITOR'S ACRONYM(S)
AFOSR

11. SPONSOR/MONITOR'S REPORT NUMBER(S)

12. DISTRIBUTION / AVAILABILITY STATEMENT

APPROVED FOR PUBLIC RELEASE; DISTRIBUTION UNLIMITED

13. SUPPLEMENTARY NOTES

14. ABSTRACT

The inelastic deformation behavior of PMR-15 neat resin, a high-temperature polymer, was investigated at 288 °C. The experimental program was designed to explore the influence of strain rate on loading and unloading behaviors. In addition, the effect of prior strain rate on creep, relaxation, and recovery responses was evaluated. The material exhibits positive, nonlinear strain rate sensitivity in monotonic loading. The creep, relaxation, and recovery responses are significantly influenced by prior strain rate. The experimental data were modeled using the Viscoplasticity Based on Overstress for Polymers (VBOP) theory. The effects of prior aging in argon at 274 °C on the time (rate)-dependent behavior of the PMR-15 polymer were evaluated in a series of stress and strain controlled experiments. Several of the VBO material parameters were expanded as functions of prior aging time. The resulting model was used to predict the behavior of PMR-15 subjected to prior aging at 274 °C for 2000h. The effects of aging at 274 °C were compared to previous research in which aging was conducted at 288 °C.

15. SUBJECT TERMS

Polymer, PMR-15, creep, recovery, relaxation, prior strain rate, nonlinear viscoplastic theory, aging

16. SECURITY CLASSIFICATION OF:			17. LIMITATION OF ABSTRACT	18. NUMBER OF PAGES	19a. NAME OF RESPONSIBLE PERSON
a. REPORT	b. ABSTRACT	c. THIS PAGE	UU	189	Marina B. Ruggles-Wrenn, PhD
U	U	U			19b. TELEPHONE NUMBER (Include Area Code) (937)255-3636, ext 4641